

This electronic thesis or dissertation has been downloaded from the King's Research Portal at <https://kclpure.kcl.ac.uk/portal/>



Human Papillomavirus-Mediated Response of Head and Neck Cancer Cells to Therapeutic Agents

Ayaz, Bushra

Awarding institution:
King's College London

The copyright of this thesis rests with the author and no quotation from it or information derived from it may be published without proper acknowledgement.

END USER LICENCE AGREEMENT



Unless another licence is stated on the immediately following page this work is licensed

under a Creative Commons Attribution-NonCommercial-NoDerivatives 4.0 International

licence. <https://creativecommons.org/licenses/by-nc-nd/4.0/>

You are free to copy, distribute and transmit the work

Under the following conditions:

- Attribution: You must attribute the work in the manner specified by the author (but not in any way that suggests that they endorse you or your use of the work).
- Non Commercial: You may not use this work for commercial purposes.
- No Derivative Works - You may not alter, transform, or build upon this work.

Any of these conditions can be waived if you receive permission from the author. Your fair dealings and other rights are in no way affected by the above.

Take down policy

If you believe that this document breaches copyright please contact librarypure@kcl.ac.uk providing details, and we will remove access to the work immediately and investigate your claim.

**Human Papillomavirus-Mediated
Response of Head and Neck Cancer
Cells to Therapeutic Agents**

**A thesis presented for the degree of
Doctor of Philosophy
King's College London
2016**

**By
Bushra Ayaz**

Abstract

The dramatic increase in oropharyngeal squamous cell carcinomas (OPSCC) over the past few decades is attributable to oncogenic types of human papillomaviruses (HPV). The presence of HPV in OPSCC has important clinical significance since patients with HPV-positive OPSCC tumours have improved response to conventional therapeutic agents such as radiation and cisplatin compared to those with HPV-negative tumours. The overall aim of this study was to investigate potential mechanisms of improved therapeutic response of HPV-positive OPSCC.

Following confirmation of HPV status in a panel of five HPV-positive and two HPV-negative head and neck cancer cell lines, an *in vitro* model of relative sensitivity to conventional therapeutic agents was established. All HPV-positive cells were more sensitive to radiation and cisplatin compared to HPV-negative cells. Stabilisation of functional p53 tumour suppressor protein was observed following treatment of HPV-positive cells to radiation and cisplatin. Attenuation of p53 in HPV-positive cells increased resistance to these agents indicating sensitivity of these cells to conventional therapeutic agents *in vitro* is p53-dependent. Furthermore, abrogation of the HPV oncogene E6 also caused stabilisation of p53 and slightly sensitised cells to radiation and cisplatin. The functional role of E6 was further explored by expressing this protein in p53

mutant HPV-negative cells. Interestingly, expression of E6 increased sensitivity of HPV-negative cells to radiation and slightly to cisplatin.

This study went on to evaluate the response of the aforementioned panel of cells to targeted and novel therapeutic agents. By contrast to conventional therapeutic agents, HPV-positive cells were more resistant to cetuximab (an inhibitor of the Epidermal Growth Factor Receptor, EGFR) and Tumour Necrosis Factor-related Apoptosis-Inducing Ligand (TRAIL). Expression of EGFR protein in HPV-negative cell lines was consistently high whereas there was variable protein expression in HPV-positive cells; response to cetuximab corresponded to the EGFR protein levels in the latter. An inverse correlation between HPV status and EGFR protein expression was also present in formalin-fixed paraffin embedded OPSCC tissue samples, but EGFR protein levels did not provide additional prognostic value beyond HPV status in the study cohort.

The current study provides an *in vitro* model of relative sensitivity in HPV-positive OPSCC and possible supportive mechanisms to explain this observation. This study also raises the possibility that HPV-positive OPSCC may be relatively resistant to EGFR-targeted and TRAIL therapies.

Acknowledgements

I would first like to thank my supervisor, Dr SelvamThavaraj who was always there whenever I ran into difficulty or had questions about my research or writing. He consistently offered his invaluable assistance and steered me in the right direction whenever he thought I needed it. I could not have imagined having a better advisor and mentor for my PhD study. Sincere thanks to my second supervisor, Professor MahvashTavassoli for providing me with all necessary facilities, valuable support and guidance.

I would also like to extend my gratitude to Professor Agamemnon Grigoriadis for being ever so kind to show interest in my research and for giving his precious and kind advice throughout. I am grateful to Commonwealth Scholarship Commission, UK for the financial support, which allowed me to complete my PhD at King's College London.

I must express my very profound gratitude to my family especially my husband Ayaz for providing me with unfailing support and continuous encouragement throughout my years of study and through the process of researching and writing this thesis. This accomplishment would not have been possible without him.

Special thanks also to my laboratory members, especially ZuraizaZaini, NinaRaulf, JessicaBullenkamp, HersiHersi, Yae-EunSuh, Radien Al-Attar, Angela Stokes and DurdanaRahman for their support and guidance.

Table of Contents

Abstract	2
Acknowledgements	4
Table of Contents	5
List of Figures and Tables	14
List of Abbreviations	18
CHAPTER 1 - General Introduction	23
1.1 Head and Neck Squamous Cell Carcinoma	24
1.1.1 Site distribution and associated risk factors of HNSCC.....	24
1.1.2 Molecular characterisation of HNSCC.....	25
1.1.3 Epidemiology.....	26
1.1.3.1 Global incidence of HNSCC	26
1.1.3.2 Changing trends in HNSCC.....	27
1.1.4 Evidence for HPV as the cause for increase in OPSCC.....	28
1.2 HPV	30
1.2.1 Classification of HPV	30
1.2.2 Structure of HPV	33
1.2.3 HPV proteins	35
1.2.3.1 E1 and E2.....	35
1.2.3.2 E4	36
1.2.3.3 E5	36

1.2.3.4	E6	37
1.2.3.5	E7	42
1.2.3.6	L1	42
1.2.3.7	L2	43
1.2.3.8	LCR	43
1.2.4	Role of HPV in carcinogenesis	43
1.2.5	Epidemiology of HPV-associated OPSCC	47
1.3	HPV detection methods.....	49
1.3.1	HPV DNA	50
1.3.2	HPV RNA	50
1.3.3	HPV proteins	51
1.4	Clinical and pathological features of HPV-associated OPSCC.....	52
1.5	Genetic distinctiveness of HPV-positive OPSCC	56
1.6	Improved survival of HPV-positive OPSCC	58
1.6.1	Putative mechanisms of improved outcome in HPV-associated OPSCC	59
1.6.1.1	Role of p53	60
1.6.1.2	Other cell cycle regulatory mechanisms	60
1.6.1.3	DNA damage response	61
1.6.1.4	Lack of field cancerisation	62
1.6.1.5	Tumour microenvironment.....	62
1.7	Management of HNSCC.....	63

1.8	Management of HPV-positive OPSCC	69
1.9	Rationale, aim and objectives of this study.....	72
Chapter 2 - Materials and Methods		74
2.1	Materials.....	75
2.1.1	Plastics.....	75
2.1.2	Chemicals and solutions	75
2.1.3	Antibodies	84
2.1.3.1	Antibodies used for Western Blotting.....	84
2.1.3.2	Antibodies used for Immunohistochemistry	85
2.1.4	Primers.....	86
2.1.4.1	Primers used for Standard PCR	86
2.1.4.2	Primers used for RT- PCR.....	87
2.1.5	Lentiviral and Retroviral shRNA constructs	88
2.1.5.1	shRNA scrambled controls	88
2.1.5.2	shRNA constructs	89
2.1.5.3	HPV16 E6 forced expression.....	90
2.2	Methods.....	91
2.2.1	Cell culture	91
2.2.1.1	Cell lines	91
2.2.1.2	Culture and maintenance of cell lines	94
2.2.1.3	Thawing of cell lines	94
2.2.1.4	Mycoplasma testing.....	94
2.2.1.5	Sub-culture of cell lines.....	95
2.2.1.6	Freezing of cells	95

2.2.1.7	Cell counting	95
2.2.1.8	Cell counting for growth curves	96
2.2.1.9	Standard Polymerase chain reaction (PCR)	96
2.2.1.10	Reverse transcription polymerase chain reaction (RT-PCR).....	97
2.2.1.11	Radiation	99
2.2.1.12	Chemotherapy	100
2.2.1.13	MTT cell viability assay.....	100
2.2.1.14	Clonogenic Assay	101
2.2.2	Immunohistochemistry and DNA in-situ hybridisation	102
2.2.2.1	Paraffin embedded cell pellets.....	102
2.2.2.2	Immunohistochemistry (IHC) staining and scoring	103
2.2.2.3	HPV DNA in situ hybridisation (ISH).....	105
2.2.3	Western blotting	105
2.2.3.1	Preparation of cell pellets	105
2.2.3.2	Preparation of total cell lysates and protein extraction	105
2.2.3.3	Bradford assay	106
2.2.3.4	SDS-PAGE (sodium dodecylsulfate polyacrylamide gel electrophoresis)	106
2.2.3.5	Transfer of proteins	108
2.2.3.6	Probing of membrane with antibodies	108
2.2.3.7	Detection by enhanced chemiluminescence (ECL)	109
2.2.4	Lentivirus methods	109
2.2.4.1	Bacterial transformation.....	110
2.2.4.2	Plasmid extraction	111

2.2.4.3	Lentivirus production	111
2.2.4.4	Lentivirus infection	112
2.2.4.5	Generation of stable knockdown cell lines.....	112
2.2.5	Retrovirus methods	112
2.2.6	Survival analysis.....	114
2.2.7	Statistical analysis	114

Chapter 3 - Characterisation of cell lines and differential response of HPV-positive and HPV-negative HNSCC cells to conventional therapy <i>in vitro</i>.....	115
3.1 Introduction.....	116
3.2 Results	117
3.2.1 Confirmation of HPV status	117
3.2.1.1 Polymerase chain reaction	117
3.2.1.1.1 Consensus PCR	117
3.2.1.1.2 Genotype-specific PCR.....	119
3.2.1.2 HPV DNA in-situ hybridisation	120
3.2.2 Growth rates of cell lines	122
3.2.3 Response to therapeutic agents.....	124
3.2.3.1 Cell viability following radiation	124
3.2.3.2 Clonogenic survival following radiation	126
3.2.3.3 Cell viability following cisplatin.....	129
3.3 Discussion	131
3.3.1 Characterisation of HPV-positive and HPV-negative cell lines.....	131

3.3.2 Response of HPV-positive and HPV-negative cell lines to conventional therapeutic agents.....	132
3.3.2.1 Radiosensitivity.....	132
3.3.2.2 Chemosensitivity (cisplatin)	136
3.4 Limitations.....	138
3.5 Conclusion.....	141
 Chapter 4 - The role of p53 and HPV-16 E6 in the response of head and neck cancer cell lines to conventional therapeutic agent.....	 142
4.1 Introduction.....	143
4.2 Results	145
4.2.1 Baseline expression of p53	145
4.2.2 p53 stabilisation.....	149
4.2.2.1 p53 stabilisation in response to radiation.....	150
4.2.2.2 p53 stabilisation in response to cisplatin.....	152
4.2.3 Effect of p53 attenuation to radiation and cisplatin	154
4.2.3.1 Attenuation of p53 in HPV-positive cells.....	154
4.2.3.2 Growth rate of p53 attenuated cells.....	158
4.2.3.3 Cell viability of p53 attenuated cells following radiation ...	160
4.2.3.4 Clonogenic survival of p53 attenuated cells following radiation.....	163
4.2.3.5 Cell viability of p53 attenuated cells following cisplatin	165
4.2.4 Response of HPV-16 E6 attenuation to radiation and cisplatin	168
4.2.4.1 Attenuation of E6 in HPV-positive cells.....	168

4.2.4.2	Growth rate of E6 attenuated cells	173
4.2.4.3	Cell viability of E6 attenuated cells following radiation.....	174
4.2.4.4	Clonogenic survival of E6 attenuated cells following radiation.....	175
4.2.4.5	Cell viability of E6 attenuated cells following treatment with cisplatin	176
4.2.5	HPV-16 E6 expression in HPV-negative cell line	178
4.2.5.1	Expression of HPV-16 E6 in HPV-negative cell line	178
4.2.5.2	Growth rate of HPV-16 E6 expressed cells	180
4.2.5.3	Cell viability of HPV-16 E6 expressed cells following radiation.....	182
4.2.5.4	Cell viability of HPV-16 E6 expressed cells following cisplatin	184
4.3	Discussion	186
4.3.1	Baseline expression of p53	187
4.3.2	Role of p53 in increased sensitivity of HPV-positive cells to radiation and cisplatin.....	188
4.3.3	Attenuation of HPV-16 E6	190
4.3.4	Expression of HPV-16 E6.....	193
4.4	Limitations	198
4.5	Conclusion.....	200

Chapter 5 - Differential response of HPV-positive and HPV-negative HNSCC cells to targeted therapy <i>in vitro</i> and association of EGFR with HPV status.	201
5.1 Introduction.....	202
5.2 Results	203
5.2.1 Response to targeted therapy	203
5.2.1.1 Cell viability following cetuximab treatment	203
5.2.1.2 Cell viability following cetuximab treatment in E6-attenuated cells	205
5.2.1.3 Cell viability of E6 expressed cells following cetuximab	207
5.2.2 Association of EGFR with HPV status.....	209
5.2.2.1 Baseline EGFR expression.....	209
5.2.2.1.1 Immunohistochemistry	209
5.2.2.1.2 Western Blot	211
5.2.2.2 EGFR expression in patient tumour samples	213
5.2.3 Survival analysis.....	220
5.2.3.1 Overall survival by HPV status	220
5.2.3.2 Overall survival analysis by EGFR status.....	222
5.2.3.3 Overall survival by HPV and EGFR status.....	224
5.2.4 Response to novel therapeutic agent -TRAIL.....	226
5.2.4.1 Cell viability following TRAIL treatment	226
5.2.4.2 Cell viability in response to TRAIL following attenuation of E6.....	228
5.2.4.3 Cell viability of E6 expressed cells following TRAIL.....	230

5.3 Discussion	232
5.3.1 Response of cell lines to cetuximab	232
5.3.2 Association of EGFR with HPV status in OPSCC tissue specimens	235
5.3.3 Survival analysis.....	236
5.3.4 Impact on management of OPSCC	238
5.3.5 Response of cell lines to TRAIL	239
5.4 Limitations	241
5.5 Conclusion.....	243
CHAPTER 6 - Conclusions and Future Work	244
6.1. Summary and Conclusions.....	245
6.2 Future Work.....	246
Bibliography	248
Appendix- Publication arising during thesis.....	285

List of Figures and Tables

Figure 1.1. The evolutionary genera of HPV.....	32
Figure 1.2. Genome organization of Human papillomavirus type 16.....	34
Figure 1.3. Summary of key oncogenic functions of HPV-16 E6.....	41
Figure 1.4. Schematic view of the roles of HPV-16 E6 and E7 in HPV infection of a mucosal cell.	46
Figure 1.5. Representative photomicrograph of normal tonsil.....	53
Figure 1.6. Comparative histomorphology of HPV-positive and HPV-negative OPSCC.....	55
Figure 1. 7. Schematic representation of the extrinsic pathway.....	68
Table 1: SDS Polyacrylamide Gels.....	82
Table 2: Antibodies used for Western Blotting	84
Table 3: Antibodies used for Immunohistochemistry.....	85
Table 4: Primers used for standard PCR	86
Table 5: Primers used for RT-PCR	87
Table 6: shRNA control plasmids.....	88
Table 7: shRNA plasmids	89
Table 8: E6 expression vectors.....	90
Figure 3.1. Conventional PCR for DNA in of HPV-negative and HPVpositive cell lines cell lines.....	118

Figure 3.2. Standard PCR for HPV-16 E6 DNA in of HPV-negative and HPVpositive cell lines cell lines.	119
Figure 3.3. DNA in situ-hybridisation and immunohistochemistry.	121
Figure 3.4. Cell lines growth rates.....	123
Figure 3.5. Cell viability of HPV-negative and HPVpositive cell lines following radiation.	125
Figure 3.6. Representative photograph of clonogenic survival following radiation.	127
Figure 3.7. Cell survival of HPV-negative and HPVpositive cell lines following radiation.	128
Figure 3.8. Cell viability of HPV-negative and HPVpositive cell lines following cisplatin.	130
Figure 4.1. p53 immunohistochemistry.	147
Figure 4.2. p53 baseline expression by western blot.	148
Figure 4.3. Stabilisation of p53 following radiation.	151
Figure 4.4. Stabilisation of p53 following cisplatin.....	153
Figure 4.5. Attenuation of p53 in HPV-positive cells.	155
Figure 4.6. p53 stabilisation in p53shRNA cells following cisplatin.	157
Figure 4.7. Growth rate of UPCI-SCC 090 p53shRNA cells.	159
Figure 4.8. Cell viability of UPCI-SCC 090 p53shRNA cells following radiation..	161
Figure 4.9. Cell viability of UPCI-SCC 089 p53shRNA cells following radiation..	162
Figure 4.10. Cell survival of UPCI-SCC 090 p53shRNA cells following radiation.	164
Figure 4. 11. Cell viability of UPCI-SCC 090 p53shRNA cells following cisplatin.	166

Figure 4. 12. Cell viability of UPCI-SCC 089 p53shRNA cells following cisplatin.	167
Figure 4.13. Attenuation of E6 in HPV-positive cell lines.	170
Figure 4.14. p53 stabilisation in UPCI-SCC 090 E6shRNA cells following cisplatin.....	172
Figure 4.15. Growth rate of UPCI-SCC 090 E6shRNA cells.	173
Figure 4.16. Cell viability of UPCI-SCC 090 E6shRNA cells following radiation.	174
Figure 4.17. Cell survival of UPCI-SCC 090 E6shRNA cells following radiation.	175
Figure 4.18. Cell viability of UPCI-SCC 090 E6shRNA cells following cisplatin. .	177
Figure 4.19. RT-PCR of HPV-16 E6 expressed HPV-negative cells.....	179
Figure 4.20. Growth rate of HPV-16 E6 expressed UPCI-SCC 089 cells.	181
Figure 4.21. Cell viability of E6 expressed UPCI-SCC 089 cells following radiation.	183
Figure 4.22. Cell viability of E6 expressed UPCI-SCC 089 cells following cisplatin.....	185
Figure 5.1. Cell viability HPV-negative and HPV-positive cell lines following cetuximab.	204
Figure 5.2. Cell viability of UPCI-SCC 090 E6shRNA cells following cetuximab.	206
Figure 5.3. Cell viability of E6 expressed UPCI-SCC 089 cells following treatment with cetuximab.	208
Figure 5.4. EGFR Immunohistochemistry.	210
Figure 5.5. Western blot analysis of baseline expression of EGFR.	212
Table 9: Summary of patient characteristics. Gender, site, disease stage and treatment modality of 93 patients with OPSCC.	214

List of Figures and Tables

Figure 5.6. Photomicrographs of EGFR (3C6) immunohistochemistry.	215
Figure 5.7. Photomicrographs of EGFR (5B7) immunohistochemistry.....	216
Figure 5.8. Dot over box-and whisker plot of EGFR.....	218
Figure 5.9. Photomicrograph of an OPSCC with EGFR (3C6) immunohistochemistry.	219
Figure 5.10. Kaplan–Meier survival plot for overall survival by HPV status.	221
Figure 5.11. Kaplan–Meier survival plot for overall survival by EGFR status.	223
Figure 5.12. Overall survival Kaplan-Meier plots for HPV+ and HPV- patients at incremental EGFR C36 and EGFR 5B7 H-scores.	225
Figure 5.13. Cell viability of HPV-negative and HPV-positive cell lines following TRAIL.....	227
Figure 5.14. Cell viability of UPCI-SCC 090 E6shRNA cells following TRAIL.	229
Figure 5.15. Cell viability of E6 expressed UPCI-SCC 089 cells following TRAIL.	231

List of Abbreviations

°C	Degree centigrade
µg	Microgram
µg/ml	Microgram per millilitre
µl	Microliter
µM	Micromolar
%	Percentage
ATP	Adenosine triphosphate
bp	Base Pairs
BSA	Bovine Serum Albumin
Ca ²⁺	Calcium
cDNA	Complementary Deoxyribonucleic Acid
CDK	Cyclin Dependent Kinase
CDKN2A	Cyclin Dependent Kinase Inhibitor 2A
CCND1	Cyclin D1
CDK4	Cyclin Dependent Kinase 4
CRT	Chemo-radiation Therapy
CIS	Carcinoma in Situ
DFS	Disease-Free Survival
DISC	Death Inducing Signalling Complex
DMEM	Dulbecco's Modified Eagles Medium
DMSO	Dimethyl Sulfoxide

List of Abbreviations

DNA	Deoxyribonucleic Acid
dNTP	Deoxynucleotide Triphosphate
ECOG	Eastern Cooperative Oncology Group
ECL	Enhanced Chemiluminescence
EDTA	Ethylene Diamine Tetraacetic Acid
EGF	Epidermal Growth Factor
EGFR	Epidermal Growth Factor Receptor
EGTA	Ethylene Glycol Tetra Acetic Acid
E6AP	E6 Associated Protein
Et al	Et alia (and others)
FADD	Fas-Associated Protein with Death Domain
FBS	Foetal Bovine Serum
FFPE	Formalin Fixed Paraffin Embedded
G	Gram
hADA3	Human ADA3 a part of histone acetyltransferase complexes
H & N	Head and Neck
HNC	Head and Neck Cancer
HNSCC	Head and Neck Squamous Cell Carcinoma
H ₂ O	Water
HCl	Hydrogen Chloride
HNSCC	Head and Neck Squamous Cell Carcinoma
HPV	Human Papilloma Virus
hTERT	Human Telomerase Reverse Transcriptase
Hrs	Hours

List of Abbreviations

IAP	Inhibitor of Apoptosis
IARC	International Agency for Research on Cancer
IHC	Immunohistochemistry
IMRT	Intensity-Modulated Radiation Therapy
IFN β	Interferon Beta
IRF3	Interferon Regulatory Factor-3
IR	Ionising Radiation
ISH	In-situ Hybridisation
kDa	Kilodaltons
LB	Luria-Betani
LCR	Long Control Region
LSB	Laemmli Sample Buffer
M	Molar
mA	Milliampere
min	Minute
ml	Millilitre
mm	Millimeter
mM	Millimolar
MgCl ₂	Magnesium Chloride
Mg/ml	Microgram per millilitre
miRNA	Micro Ribonucleic Acid

List of Abbreviations

mRNA	Messenger Ribonucleic Acid
MSCV	Murine Stem Cell Virus
MTT	(3-[4,5-Dimethylthiazol-2-yl]-2,5-diphenyltetrazolium bromide)
mTOR	Mammalian Target of Rapamycin
NaCl	Sodium Chloride
NaOH	Sodium Hydroxide
NaH ₂ PO ₄	Sodium Dihydrogen Phosphate
nm	Nano Meter
OC	Oral Cancer
OPSCC	Oropharyngeal Squamous Cell Carcinoma
OPC	Oropharyngeal Cancer
OPG	Osteoprotegerin
OD	Optical Density
ORF	Open Reading Frame
OSCC	Oral Squamous Cell Carcinoma
PD-1	Programmed Cell Death-1
p53	Tumour Suppressor Protein 53
PCR	Polymerase Chain Reaction
PDZ	Post synaptic density protein (PSD95)/Drosophila disc large tumour suppressor (Dlg1)/ zonula occludens-1 protein (zo-1)
PI3K	Phosphoinositide 3-kinase
pRb	Retinoblastoma Tumour Suppression Protein
PTEN	Phosphate and Tensin Homolog
RPM	Revolutions per minute

List of Abbreviations

RTOG	Radiation Therapy Oncology Group
RT-PCR	Reverse transcriptase-PCR
RT	Room Temperature
RT	Radiation Therapy
RNA	Ribonucleic Acid
SCC	Squamous Cell Carcinoma
Taq	Thermusaquaticus
TBST	Tris-Buffered Saline-Tween 20
TERT	Telomerase Reverse Transcriptase
TRAIL	Tumour Necrosis Factor-Related Apoptosis-Inducing Ligand
TNF	Tumour Necrosis Factor
TNFR1	Tumour Necrosis Factor Receptor-1
UBE3A	Ubiquitin-Protein Ligase E3A
UPCI	University of Pittsburgh Cancer Institute
UK	United Kingdom
USA	United States of America
URR	Upstream Regulatory Region
VEGF	Vascular Endothelial Growth Factor
w/v	Mass/Volume
XIAP	X-linked Inhibitor of Apoptosis Protein

CHAPTER 1 - General Introduction

1.1 Head and Neck Squamous Cell Carcinoma

Head and neck cancer (HNC) is a collective term defined on an anatomical-topographical basis to describe the malignant tumours of the upper aero-digestive tract, including the nasal cavity and paranasal sinuses, nasopharynx, hypopharynx, larynx, oral cavity and oropharynx.¹ Numerous types of cancers effect the head and neck region but the vast majority arise from the stratified squamous epithelium of the upper aero-digestive tract and are therefore collectively termed as head and neck squamous cell carcinomas (HNSCC).²

1.1.1 Site distribution and associated risk factors of HNSCC

HNCs are a heterogeneous group, consisting of cancers of the oral cavity (ventral surfaces and posterolateral border of tongue, gingiva, floor of mouth and hard palate), pharynx (oropharynx, nasopharynx, and hypopharynx), sinonasal tract and larynx. Tongue cancer is described as the most common site for oral cancer worldwide, with most tumours arising on the ventral surfaces and posterolateral border.^{3,4}

HNSCCs are associated with variable risk factors. Tobacco smoking and chewing habits and alcohol intake are considered the most important aetiological agents.^{5,6} The use of tobacco in combination with alcohol together demonstrate a greater risk of developing HNSCC compared to use

of tobacco or alcohol alone.^{4,7} In addition to tobacco and alcohol, Human Papillomavirus (HPV), primarily types 16 and 18, have been acknowledged as a common aetiological agent in some HNCs.⁸

1.1.2 Molecular characterisation of HNSCC

A plethora of oncogene activation and/or tumour suppressor gene inactivation has been reported as being important in driving head and neck carcinogenesis. However, several genes including p53, cyclin dependent kinase inhibitor 2A (CDKN2A or p16), epidermal growth factor receptor (EGFR) and cyclin D1 (CCND1) are consistently altered and will be discussed in further depth for the purpose of this introduction.⁹⁻¹¹

Loss of chromosome region 17p13 encoding the tumour suppressor gene TP53 is mutated in up to 70% of HNSCC.^{9,12} p53 is a nuclear phosphoprotein involved in DNA synthesis, repair, apoptosis and cell cycle control.¹³ Activation of p53 results in the formation of p53 tetramers, which can then act as a transcription factor.¹⁴ One of the functions of the p53 tetramer is to induce expression of the CDK inhibitor p21^{CIP}, which negatively regulates cyclin A/CDK1, cyclin B/CDK1 and cyclin E/CDK2 complexes, preventing cell cycle progression.^{15,16} p53 mutations have been associated with a decreased overall survival, thus establishing its significance in HNSCC progression.^{12,17} 9p21-22 is a frequent chromosomal region, which is lost in HNSCCs. Genes included in this region include p16^{INK4a} (p16) and p14^{ARF} at the CDKN2A locus.¹⁸ The p16 gene (also

known as cyclin-dependent kinase inhibitor 2A, CDKN2A) acts as a tumour suppressor gene. The p16 protein, by binding to cyclin dependent kinase 4 (CDK4) or CDK6, inhibits phosphorylation of the retinoblastoma protein (pRb) thus impeding G1 to S phase transition of the cell cycle.¹⁹ Loss of its function, either through mutations, deletion or hypermethylation is common in HNSCC.^{20,21} In addition, the overexpression of cyclin D1 (encoded by CCND1) due to amplification of chromosome 11q13, is found in over 80% of cases.²² There is evidence that overexpression of cyclin D1 serves as a rate-limiting controller of G1 phase progression and is associated with a more aggressive tumour phenotype.²³

Epidermal growth factor receptor (EGFR) is a glycoprotein cell surface receptor composed of an extracellular ligand-binding domain, transmembrane domain and cytoplasmic tyrosine kinase (TK) domain. EGFR is present in normal epithelia, it plays a vital role in cell growth, apoptosis and angiogenesis and is overexpressed in several types of carcinomas. EGFR is highly expressed (42%–80%) in HNC and its expression is associated with poor outcome.^{24,25,26}

1.1.3 Epidemiology

1.1.3.1 Global incidence of HNSCC

HNSCC is the sixth most common cancer worldwide, with approximately 680,000 new cases diagnosed and 370,000 deaths recorded in 2012 by

Global Burden of Cancer Study (Globocan).^{27,28} Males are affected more than females with a ratio ranging from 2:1 to 4:1.²⁹

In the United States (US), HNC accounts for 3% of malignancies, with almost 60,000 Americans developing these tumours annually and 12,000 dying from the disease.³⁰ In Europe approximately 250,000 cases (estimated 4% of the cancer incidence) and 63,500 deaths were reported in 2012.³¹ There is considerable geographical variation in the incidence of HNSCC; for example, in the United Kingdom (UK) in 2008 there were 11,682 reported HNCs, which constituted 3.73% of all cancers compared to 200,000 cases of HNCs in India, accounting for over 30% of all cancers in the latter.^{27,32,33}

Despite the fact that advances have been made in diagnosis and treatment of HNC, mortality rates have only marginally decreased over the last decades and the 5-year survival rate currently ranges between 40%–60%.³⁴

1.1.3.2 Changing trends in HNSCC

Over the past 30 years there has been a marked increase in the incidence of HNSCC in several countries including North America (United States³⁵ and Canada³⁶), Western Europe (Denmark,³⁷ Netherlands,³⁸ Norway,³⁹ Sweden,⁴⁰ the UK⁴¹) and Australia.⁴² The incidence rose from 16.3% during 1984 to 1989 to 71.7% during 2000 to 2004 in the US.³⁵ This trend was

observed in parallel with a reduction in the incidence of other smoking related cancers such as Non-small cell lung cancer (NSCLC) of lung.⁴³

Subsite analysis of the increase in incidence demonstrated that the rise in HNC was due to the exponential increase in the cancers of the oropharynx (faucial tonsils, base of tongue and soft palate).^{44,45} The marked increase in oropharyngeal squamous cell carcinoma (OPSCC) was seen in parallel with a decrease in incidence of other HNCs including that of the larynx and oral cavity. The latter observation may be explained by the reduction in tobacco smoking over the same period, while the increase in OPSCC is attributed to HPV.^{46,47}

1.1.4 Evidence for HPV as the cause for increase in OPSCC

Evidence for a causal involvement of HPV in the pathogenesis of OPSCC comes from epidemiologic and molecular studies. The earliest suggestion of a possible link between HPV and squamous cell carcinomas of the oral cavity (OSCC) was made by Syrjänen *et al* (1983) where the group observed that some of these tumours have morphological and immunohistochemical features indicative of HPV infection.⁴⁸ Subsequent studies have supported the predilection of the virus for oropharyngeal cancers (OPC). In two case series (1996 and 1997), 50% and 60% of tonsillar carcinomas were HPV positive, respectively, in comparison to 6% and 10% of tumours at other oral sites.^{49,50} Additionally, Gillison *et al* (2000)

and Stransky *et al* (2011) confirmed that the only HNC subsite with a demonstrated carcinogenic role for HPV was the oropharynx.^{21,51}

The mechanism of initial phases of HPV infection in oropharyngeal mucosa remains largely unknown. To date, there is lack of any functional evidence for the predilection of high-risk HPV for the oropharyngeal mucosa. The lamina propria of the oropharynx, particularly the palatine (faucal) tonsil and base of tongue comprise lymphoid tissue invaginated by epithelial-lined crypts. The epithelium is of reticulated crypt type and forms a loose network infiltrated by lymphocytes (Figure 1.5, page 55). Some authorities liken this epithelium to that of the cervical transformation zone, but there is currently insufficient evidence to support either structural or functional similarity.^{52,53} The reticulated crypt epithelium is infiltrated by lymphocytes to form a complex lymphoepithelial structure, which is the site of antigen trafficking to the underlying lymphoid tissue.⁵⁴ Immune escape, together with increased permeability of the reticulated crypt epithelium, may be the source of persistent HPV infection and subsequent carcinogenesis. This theory is supported by the observation that HPV-associated OPSCC originates within the crypts of this lymphoepithelial region.^{55,56}

Temporal studies have supported HPV as the causative role in the increase of OPSCC. Nasman *et al* (2009) analysed the increased incidence of tonsillar cancer in the Stockholm area between 1970 and 2007. They showed that the percentages of tonsillar cancers that were HPV-positive was 23%, 29%, 57% and 79% during the 1970s, 1980s, 1990s and

2000–2007, respectively.⁵⁷ Similarly, in the UK, Scachee *et al* (2011) demonstrated an increase in the prevalence of HPV positivity in OPSCC 14% to 57% in the period between 1998 and 2009.⁵⁸ In the United States, Chaturvedi *et al* (2011) confirmed the temporal increase in the proportion of OPSCC that were HPV positive from 20% in 1988 to more than 70% in 2004.^{59,60}

The last 25 years has seen an exponential growth in the literature surrounding this field, and there is now a strong and consistent molecular evidence base for a causal role of HPV in OPSCC. Indeed, in 2009 HPV was authoritatively recognised as a causal agent in the development of OPSCC.⁶¹

1.2 HPV

1.2.1 Classification of HPV

HPV is an epitheliotropic virus with an average size of approximately 8000 base pairs (bp).⁶² More than 100 different types of HPV have been identified by DNA sequence analysis.⁶³ HPV subtypes can generally be divided into low- and high-risk groups. Low-risk groups, for example HPV-6 and HPV-11, are associated with benign lesions such as cutaneous or genital warts and laryngeal papillomas. There are approximately 15 high-risk types, so called because of their association with malignant neoplasm. The most common high-risk types are HPV-16 and HPV-18.⁶³

There are several evolutionary genera of HPV (Figure 1.1). The main groups are the Alpha and Beta papillomaviruses. Classification of papillomaviruses is based on the nucleotide sequence of the major capsid protein, L1, which categorises viruses into genera.⁶⁴ These account for approximately 90% of the known HPV subtypes. The Alpha papillomaviruses make up the largest group that contains the high-risk mucosal subtypes responsible for both cervical carcinomas and OPSCC. HPV-16 is the most common high-risk subtype in the general population from alpha papillomaviruses, and is responsible for approximately 70% of cervical carcinomas and 85-90% of HPV associated OPSCC.^{8,65-67} Beta papillomaviruses are usually associated with benign cutaneous infections. However, in immunocompromised patients, these infections can be associated with the development of non-melanoma skin cancer. The remaining types of HPV belong to the Gamma, Mu and Nu genera. These cause cutaneous warts (verruccous and palmar warts) and are not associated with malignancy.⁶⁸

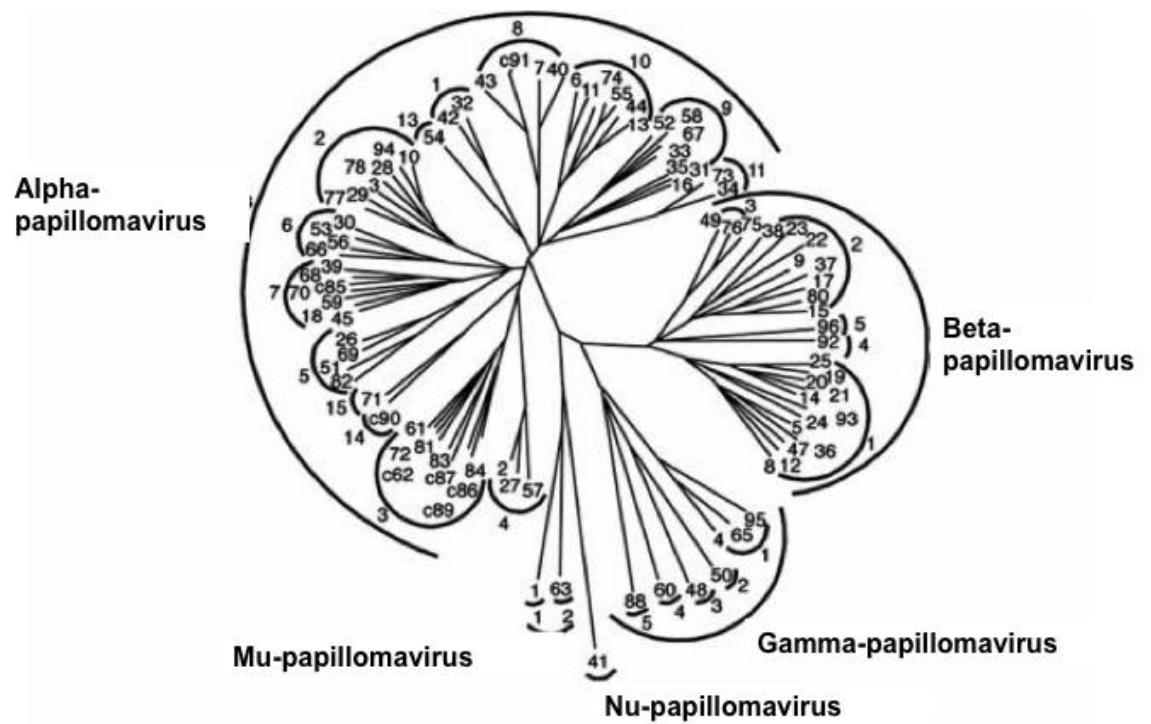


Figure 1.1. The evolutionary genera of HPV.

Phylogenetic analysis based on the L1 open reading frame (ORF) sequences of HPV types.⁶⁸

1.2.2 Structure of HPV

HPV is a small (50-55 nm in diameter), non-enveloped circular double stranded DNA virus with an icosahedral capsid coat.⁶² The viral genome can be considered as having three distinct regions (Figure 1.2).

1. A non-coding upstream regulatory region of 400 to 1000 bp, also called the long control region (LCR, 10%), or the upper regulatory region (URR), located between the L2 and E6 open reading frames.
2. An early region (50%), consisting of ORFs E1, E2, E4, E5, E6, and E7, which are involved in viral replication and oncogenesis.
3. A late region (40%), which encodes the L1 and L2 structural proteins for the viral capsid.⁶⁹

The three regions in all papillomaviruses are separated by two polyadenylation (pA) sites; early pA (A_E) and late pA (A_L) sites.⁷⁰

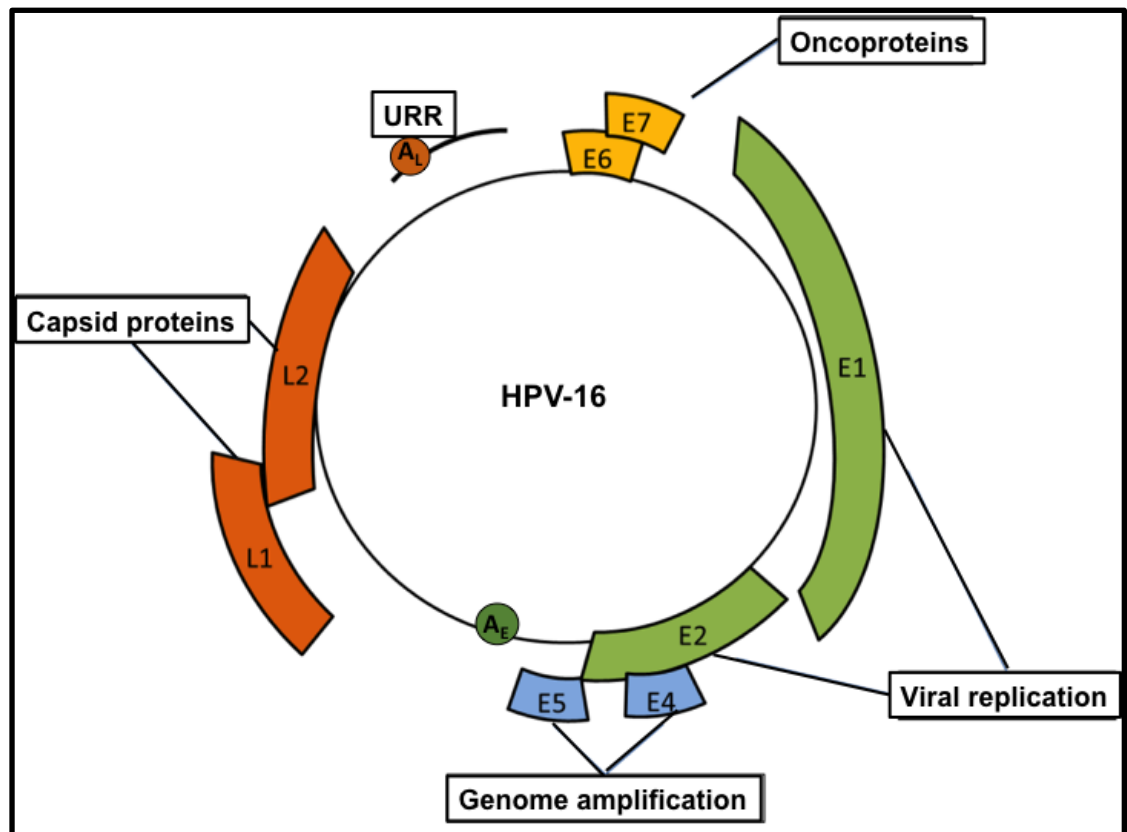


Figure 1.2. Genome organization of Human papillomavirus type 16.

Schematic representation of the HPV-16 genome showing the location and functions of the early (E) and late genes (L1 and L2) adapted from Malik H *et al.*⁷¹

1.2.3 HPV proteins

1.2.3.1 E1 and E2

E1 and E2 are involved in viral DNA replication and the regulation of early transcription. E2 binds to the non-coding region of the viral genome and forms a complex with E1, thus bringing E1 into approximation with the origin of replication.⁷²

In lesions containing HPV in the nucleus as episomes (circular extrachromosomal element), the E2 protein directly represses the expression of other early genes as a mechanism to regulate the copy number. The relative abundance of E2 proteins within the cell is an important factor regulating papillomavirus DNA replication. It is suggested that the viral copy number remains relatively constant in HR-HPV-positive cells, which indicates that regulatory circuits are active to control copy number.⁶² In addition to full-length-form of E2, several papillomaviruses (PV) express a spliced mRNA which links a splice donor site in E1 to the major splice acceptor site in the E2/E4 region. This transcript encodes an E8^{E2C} (or E8/E2) protein which consists of the E8 gene product fused to the C-terminal half of E2, which mediates sequence-specific DNA binding and dimerization of E2 proteins.^{73,74} Genetic analyses have revealed that E8^{E2C} is a potent inhibitor of the genome replication.⁷⁵ Hence E2's prime function for viral DNA replication is to enhance E1 binding to the origin and recruitment of cellular proteins that contribute to viral DNA replication.⁷⁶

Integration of the HPV genome in the host cell chromosome usually disrupts E2 expression, causing a deregulated expression of early viral genes, including E6 and E7, and this event can favour the transformation of human cells and the transition into a malignant state as the integrated viral transcripts confer stronger transforming capacity than those derived from episomes, due to longer half-life of transcripts. However, unlike models of HPV-induced cervical carcinogenesis, an integration event does not appear to be a necessary step for oropharyngeal carcinogenesis.^{77,78}

1.2.3.2E4

The 17 kDa E4 is a cytoplasmic protein. Although expressed at low levels during the early phase of viral infection, expression of E4 increases dramatically during the late phase of infection, when viral particles are produced and released, hence it is a facilitator of viral genome packing and maturation of the viral particles and is expressed together with the capsid proteins in the upper layers of the epithelium.^{72,79} The mRNA encoding E4 is the most abundant and it has been proposed that the HPV E4 protein can account for up to 20-25% of the cell's total protein content.⁸⁰

1.2.3.3 E5

The 8-10 kDa E5 protein is a small hydrophobic peptide, approximately 83 amino acids in size that localises primarily to the endoplasmic reticulum. When expressed alone, HPV E5 has weak oncogenic properties. However, HPV E5 can enhance the transforming activity of E6 and E7, suggesting that

it may have a supportive role in tumour progression.^{72,81,82} It has also been suggested that E5 increases cellular proliferation in the presence of EGFR and increases its activation.^{83,84} The coding sequence for this protein is frequently deleted or disrupted in the process of viral DNA integration in established or later infection, leading to the presumption that its persistent expression is not a fundamental requirement or necessity for ongoing oncogenesis.⁸⁵

1.2.3.4E6

The 16-18 kDa E6 is a main transforming protein.^{72,86,87} It is a 151 amino acid protein in length containing four cysteine arrays comprising two relatively large zinc fingers, which together are needed for full function.⁸⁸ The E6 oncogene is expressed as full-length or as alternate transcripts designated E6*I and E6*II. Alternate E6* expression has been implicated in oncogenesis and may be related to viral integration and/or loss of regulation by E2.⁸⁹ The sequences of the E6*I and E6*II proteins are almost identical, differing only in the last two to five amino acids. Thus, it appears likely that the carboxy-terminal region of E6*I is important in mediating some of its effects.⁹⁰

Intriguingly, E6 protein has very limited enzymatic activities and nearly all of the activities are induced by protein–protein interactions (Figure 1.3).⁹¹ E6 associated protein (E6AP), is an enzyme that in humans is encoded by the ubiquitin-protein ligase E3A (UBE3A) gene. This enzyme is involved in targeting proteins for degradation within cells. E6AP is one of the initial and

most common proteins to interact with E6.⁹² p53 is one of the key targets of E6 protein.⁹³ E6 binds directly to E6AP causing the degradation of p53 through the ubiquitin proteasome pathway and removes the cell cycle checkpoint control (G1/S and G2/M) usually provided by p53, preventing apoptosis and promoting the replication of viral DNA.⁹⁴ Studies have suggested that E6AP is not involved in the regulation of p53 levels in cells that do not contain E6.^{95,96} Advances have been made at blocking E6AP activity, either by the use of antisense oligonucleotides or dominant negative mutants, resulting in increased levels of p53 in HPV-positive, but not in HPV-negative cells, confirming that E6AP plays an essential role in E6-directed degradation of p53 protein.^{95,96}

However, under stress conditions, e.g. radiation and drugs, the expression of E6 oncoprotein is suppressed, the degradative pathway is inhibited and p53 is both stabilised and activated.⁹⁷

The binding of E6 to p53 varies between low and high-risk HPV types.⁹⁸ Although low risk HPV E6 can bind to p53, it does so with reduced affinity and is largely unable to bind to E6AP or induce p53 degradation.^{99,100} E6 can also inhibit the transcriptional activities of p53 independently of E6AP.¹⁰¹ Three different mechanisms have been proposed to explain E6AP-independent p53 inactivation.

1. The inhibition of p53 binding to its target sequence in the genome.^{102,103}

2. E6 may be able to inhibit p53 signalling by maintaining it within the cytoplasm.¹⁰⁴
3. E6 with the histone acetyltransferases p300, CREB binding protein (CBP) and ADA3, transcriptional co-activators essential for cell growth and differentiation prevents p53 acetylation (Ac), inhibiting the transcription of p53-responsive genes.^{105,106} However, unlike p300, E6 interaction with hADA3, a transcriptional co-activator protein (part of histone acetyltransferase complexes) results in hADA3 degradation suggesting a mechanism for inhibiting p53 activation by blocking the p14/ARF pathway.¹⁰⁷

Several functions of high-risk E6 enable inhibition of apoptosis in a p53 independent manner. HPV-16 E6 oncoprotein interacts with the extrinsic apoptotic pathway by binding to and altering the functions of upstream signalling molecules. It can bind to the TNF receptor-1 (TNFR1) and subsequently inhibit TNFR1 induced apoptosis.¹⁰⁸ E6 also interacts with the adaptor protein FAS-associated protein with death domain (FADD) and caspase 8 to block cell death in response to FAS and TRAIL. E6 can also interfere with induction of the extrinsic and intrinsic (mitochondrial) apoptotic pathways through interactions with the pro-apoptotic Bcl2 members BAK and BAX and down-regulates caspase dependent apoptotic cascade.^{109,110}

E6 also inhibits the immune response by interacting with host interferon regulatory factor-3 (IRF3). E6 inhibition of IRF-3 transcriptional activity impairs the induction of interferon beta (IFN β) in response to viral

infection.¹¹¹ The interaction of HPV-16 E6 with IRF-3 and the inhibition of its transactivation function could contribute to the ability of the virus to disrupt the cellular antiviral response.¹¹¹

High-risk E6 also stimulates cellular immortality. In normal somatic cells, each cell division results in shortening of telomere length, a system of cellular ageing. The interaction of E6 with transcription factor SP1 also known as specificity protein, myelocytomatosis oncogene cellular homolog (Myc), a nuclear transcription factor, X box-binding protein-123 (NFX123) and E6AP activates telomerase reverse transcriptase (TERT) and telomerase, preventing telomere shortening in response to persistent proliferation and in turn promoting immortalisation.¹¹²

Unlike low-risk HPV, high-risk HPV-16 E6 contains a PDZ domain.¹¹³ PDZ domain or binding motif is an abbreviation combining the first letters of three proteins, post synaptic density protein (PSD95), drosophila disc large tumour suppressor (Dlg1), and zonula occludens-1 protein (zo-1), which were first discovered to share the domain. On account of this motif, E6 is capable of interrelating with a large number of cellular proteins that contain PDZ domains that are mostly involved in regulation of processes associated with the control of cell attachment, cell proliferation, cell polarity and cell signalling.¹¹⁴ The targeted degradation of PDZ domain-containing cellular proteins results in cellular transformation owing to loss of cell-cell contact and loss of polarity, and may play a role in tumour metastasis by interrupting

normal cell adhesion.¹¹⁵ The key oncogenic functions of HPV-16 E6 are summarised in Figure 1.3.

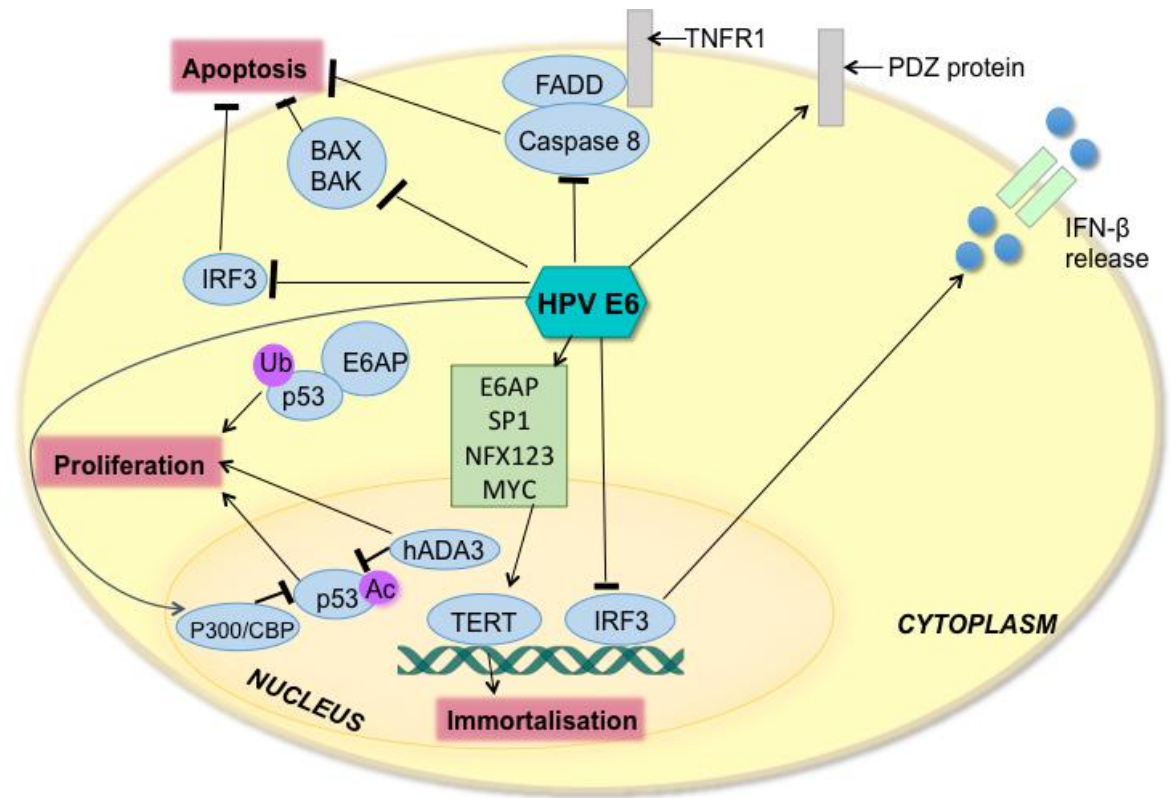


Figure 1.3. Summary of key oncogenic functions of HPV-16 E6.

High-risk E6 proteins inhibit p53-dependent growth arrest and apoptosis in response to aberrant proliferation through several mechanisms, resulting in the induction of genomic instability and the accumulation of cellular mutations. Formation of an E6–E6AP–p53 trimeric complex results in p53 degradation, and the interaction of E6 with p300, CBP and ADA3 prevents p53 acetylation (Ac), inhibiting the transcription of p53-responsive genes. E6 also inhibits apoptotic signalling in response to growth-suppressive cytokines through interaction with the tumour necrosis factor (TNF)- α receptor TNFR1, FADD and caspase 8, and through the degradation of pro-apoptotic BAX and BAK. E6 interaction with SP1, MYC, NFX123 and E6AP activates telomerase reverse transcriptase (TERT) and telomerase, promoting immortalisation. E6-mediated degradation of PDZ proteins leads to loss of cell polarity and induces hyperplasia. E6 subverts the interferon (IFN) response through interaction with IRF3.

1.2.3.5 E7

Another major transforming protein, E7, is a small 11kDa protein with a role both in immortalisation and cellular transformation.^{72,116} The primary function of E7 protein is that it binds with cullin 2 ubiquitin ligase complex and causes ubiquitination of the retinoblastoma tumour suppressor protein (pRb) through proteosomal degradation.¹¹⁷ When E7 binds to pRb, the transcription factor E2F is released from the latter and this stimulates the transcription of the vital cyclins and cyclin dependent kinases for G1-S phase transition.¹¹⁸ E7 also interacts with pRb-related pocket proteins, p107 and p130, and the cyclin dependent kinase inhibitors (CDK) having a further inhibitory effect on cell cycle arrest.¹¹⁰

Functional inactivation of pRb by E7 also induces an up-regulation of p16^{INK4A} (p16) expression. Overexpression of p16 has often been used as an important marker for HPV E7 activity.¹¹⁸ In addition, E7 can also interact with cyclin A, cyclin E and histone deacetylases.^{119,120} The expression of cyclins A and E, regulatory subunits of CDK2, is induced by E2F and thus is increased by E7.¹²¹

1.2.3.6 L1

This major capsid protein is the major determinant for attachment to cell surface receptors.¹²² It is highly immunogenic and has conformational epitopes that stimulate the production of neutralising type-specific antibodies against the virus.¹²³

1.2.3.7L2

As a minor capsid protein, L2 contributes to the binding of the virion to the cell receptor (Kap β 2 and Kap β 3), supporting its uptake, transference to the nucleus, and delivery of viral DNA to replication centers. L2 with L1 helps the packaging of viral DNA into the capsids.^{124,125,126}

1.2.3.8 LCR

LCR is a segment of about 850 bp, has no protein-coding function and is the origin of replication and regulation for HPV gene expression. It is only expressed in squamous epithelial cells which are terminally differentiated.¹²⁷

1.2.4 Role of HPV in carcinogenesis

Much of what is known of the initial phases of HPV infection has been determined using models of cervical cancer and pre-cancer. In the context of cervical carcinogenesis, the HPV life cycle originates with infectious virion particles acquiring entry to epithelial basal lamina possibly through micro-abrasions in the epithelial layer, permitting approach to the basal layer where the virus infects basal cells. Within the HNC, the virus favours the highly specialised reticulated crypt epithelium in lymphoepithelial tissue of Waldeyer's ring.¹²⁸ These sites lie deep within complex crypts and as such are not readily reachable to surface trauma. Therefore, micro-abrasion, as suggested, as the initial phase of HPV-associated cervical oncogenesis is not likely to play a comparable role the oropharyngeal carcinogenesis; the mechanism of initial phases of HPV infection in oropharyngeal mucosa

remains largely unknown, but may be associated to the distinctive presence of transitional mucosa in the oropharynx, predominantly found in the tonsillar tissue and which demonstrates histological similarities to the cervical mucosa.^{52,53} Another possibility lies within the genetic features of HPV 16, which accounts for more than 90-95% of all HPV associated oropharyngeal cancers, as it may facilitate survival in the tonsillar crypt epithelium.^{55,56} It is also possible that the invagination of the mucosal surface of the tonsil may favour virus capture and maintenance by promoting its access to basal cells.⁵⁴

Entrance of virions into the basal epithelial cells is an active process. It is suggested that heparin sulphate proteoglycans, and in particular syndecan-1, play a role in the preliminary attachment and that a secondary receptor (beta 6 integrin) is then essential for complete infection.^{129,130} Subsequent to receptor binding, HPV particles enter the cell via endocytosis. They are then disassembled in lysosomes and the genome is moved to the nucleus, the L2 capsid protein enables the progression. The viral genome is established within the nucleus of the host cell as an episome, i.e. the viral genome is not integrated with that of the host cell, once a cell is infected. This stage progresses with the assistance of viral proteins E1 and E2, resulting in augmented number of infected cells and multiple copies, resulting in the establishment of 20 to 100 copies of the viral episome within each basal cell.¹³¹

Replication of the HPV genome is highly dependent on the reproductive cellular processes of the host and exclusively occurs in dividing cells.¹³² As the HPV-infected keratinocytes travel toward the epithelial surface upon differentiation, distinctive viral genes are expressed, allowing high viral genome amplification and the expression of the late region genes (L1 and L2) that encode the viral capsid proteins. As the cells get to the surface, the HPV episomes are packed within the capsids for final viral assembly and release of mature infectious virions.¹³¹

Frequently, the infection becomes latent and no infectious virus is produced, although HPV DNA can be detected in desquamated cells. A large proportion of the healthy population is infected with high risk- HPV (HR-HPV) but malignant transformation is comparatively rare, and transient infection is usually cleared by immunological mechanisms within 1-2 years.^{133,134} However, in some individuals, rare malignant transformation occurs where viral persistence, arguably the most important factor in malignant progression, with HPV E6 and E7 oncogenes increasing cellular proliferation in the basal and supra basal levels by pushing the cells into S-phase. Integration events can disrupt E2, allowing up-regulation of the HPV E6 and E7 oncogenes, which then further promotes growth promotions and genomic instability by binding and targeting p53 and Rb proteins for degradation, respectively (Figure 1.4).¹³⁵

Nevertheless, it should be emphasised that much of what is known about HPV-induced malignant transformation has been determined in models of

cervical carcinogenesis and may not directly apply to virus-associated oropharyngeal oncogenesis.

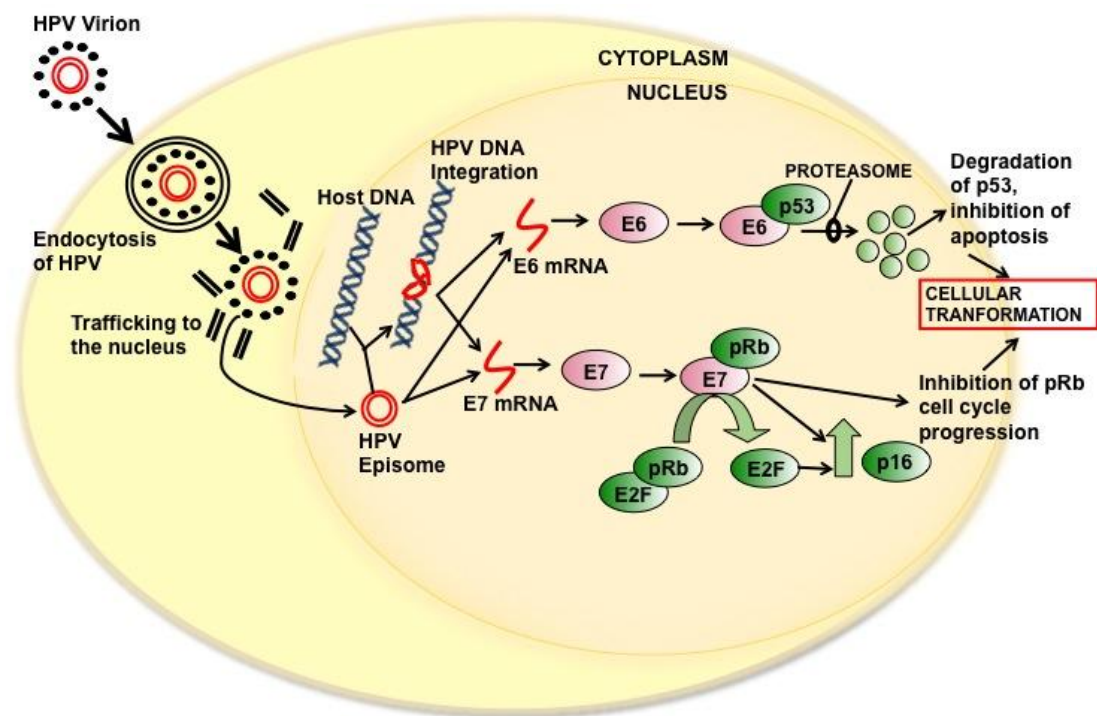


Figure 1.4. Schematic view of the roles of HPV-16 E6 and E7 in HPV infection of a mucosal cell.

Both viral episome or integrated forms of the viral DNA are capable of expressing viral oncoproteins such as E6 and E7 that are able to degrade p53 and inhibit pRb, respectively. E7 oncoprotein with dissociation of pRb and E2F causes a successive up-regulation of p16INK4A. The figure is modified from Allen *et al* (2010).¹³⁶

1.2.5 Epidemiology of HPV-associated OPSCC

There appears to be a significant geographic variation in the prevalence of HPV in OPSCC. A systematic review by Kreimer *et al* (2005) reported that the proportion of OPSCC attributable to HPV was 35.9%, with 47% in North America, 46% in Asia, 36% in South/Central America, Australia and Africa, and 26% in Europe.⁸ Other reports have indicated variation between countries within a given region. In Europe, prevalence rates range from 20% in the Netherlands (1997–2002),¹³⁷ to 41% in Switzerland (1998–2003),¹³⁸ 55% in Germany (1997–2005)¹³⁹ and 62% in France (1987–2005).¹⁴⁰ In the United States, prevalence rates are higher, varying from 64% in Texas (2002–2005)¹⁴¹ to 72% in Maryland (2000–2006).¹⁴² Recently Mehanna *et al* (2013) showed a sharp rise in the proportion of HPV-positive OPSCC over the last decade and a higher rate was observed in Europe compared to North America (73.1% versus 69.7 %, respectively). The group showed a significant increase in the overall prevalence of OPSCC from 40.5% before 2000, to 64.3% between 2000 and 2004 and 72.2% between 2005 and 2009.¹⁴³

The reason of the rapid increase in prevalence of HPV positive OPSCCs remains elusive. One of the explanations may be a change in sexual behaviour, i.e., increasing practice of oral sex and increasing numbers of lifetime sex partners.¹⁴⁴ The reason of the rapid increase in prevalence of HPV positive OPSCCs remain has been attributed to change in sexual behaviour, namely, increasing practice of oral sex and increasing numbers of lifetime sex partners.¹⁴⁴ Others have surmised that the reduction in

prophylactic tonsillectomies increases the reservoir of excess lymphoepithelial tissue to persistent HPV infection. Nevertheless, these are still observational studies, which lack any interventional evidence. It is, however, unlikely this rise is due to more sensitive detection methods, borne out by stringent controls adopted in longitudinal studies.¹⁴⁵

1.3 HPV detection methods

Diagnostic techniques differ in virus detection sensitivity, required information (a broad group of high-risk HPV or specific HPV genotypes), available tissue type (fresh frozen tissue, fixed tissue, brush cytology, saliva, serum, fine needle aspiration biopsy), the target molecule (DNA, RNA, and protein), labour intensiveness, complexity of the procedure, and costs.^{146,147}

Persistent expression of high-risk HPV E6/E7 viral oncogene is a fundamental requisite for both the commencement and the continuation of an HPV-driven malignant phenotype. As a result, demonstration of transcriptionally active oncogenic viral infection on samples derived from fresh tissue has been considered to the reference or 'gold standard' test. The practical application of this test is usually by means of quantitative reverse transcriptase polymerase chain reaction (qRT-PCR) amplifying high-risk HPV E6/E7 mRNA transcripts.^{148,149} However, the utility of this reference standard in routine diagnosis is unfeasible for practical reasons; diagnostic procedures are mostly established on the evaluation of formalin-fixed, paraffin-embedded (FFPE) tissue.⁵⁸

In cells and tissue, the virus may be detected at the levels of DNA, RNA and/or protein.

1.3.1 HPV DNA

Target amplification techniques such as consensus (PGMY09/PGMY11, 450 bp or GP5+/GP6+, 150 bp) or type-specific polymerase chain reaction (PCR), have high sensitivity rates but can detect biologically irrelevant HPV, and is prone to contamination resulting in a risk of false positivity.²⁰⁹ DNA in-situ hybridisation (ISH) is a signal amplification test which allows direct visualisation of viral DNA co-localising with the host nucleus. Although ISH has been shown to have a high specificity, its sensitivity limits its use as a single modality test.^{150,151}

1.3.2 HPV RNA

Reverse transcriptase (RT)-PCR for the detection of HPV E6 mRNA in fresh frozen specimens is considered as the reference or 'gold' standard for the presence of biologically active virus. However, its use in routine diagnosis is limited due to reasons of practicality.¹⁵² HPV RNA ISH is a novel technique, which allows direct visualisation of viral transcripts in FFPE sections.¹⁵³ In a study of 196 OPSCC patients, RNA ISH demonstrated a better sensitivity in HPV detection than DNA ISH.¹⁵⁴ However it's a novel technique with limited available data and is currently still awaiting European Union *in-vitro* diagnostic (CE-IVD) approval.¹⁵³

1.3.3 HPV proteins

No commercially available viral protein detection method is currently available. However, p16 immunohistochemistry (IHC) is widely used in the diagnostic laboratory as a surrogate marker for HPV infection in OPSCC.¹⁴¹ The inactivation of pRb determined by HPV E7 is associated with up-regulation of CDKN2A with consequent rise in p16. The test is highly sensitive, suitable on FFPE material and easy to interpret, it provides proof of transcriptional activity of the oncoprotein, easily available commercially, accessible to most laboratories and cost effective. However it has low specificity (79-82%) due to false positive staining in the absence of HPV infection.^{155,156}

No single standard detecting technique for testing or interpretation of HPV is available, each assay have technical limitations with none of the methods offering optimal sensitivity and specificity levels. In order to overcome this problem, stepwise algorithms that combine different HPV tests have been suggested as an approach to counteract the limitations of individual tests. Two diagnostic algorithms, applicable in FFPE samples, are considered as clinically adequate by several studies and trials. With p16 as a first-line assay, groups combined different techniques in order to obtain guaranteed results, for instance Smeetet *al* (2007) used p16 followed by PCR (GP5+/6+), for HPV-DNA detection, Singhiet *al* (2010) utilised type-16 specific ISH and Rietbergenet *al* (2013) used E6/E7 mRNA transcripts (RT-PCR).^{150,157,158}

1.4 Clinical and pathological features of HPV-associated OPSCC

The oropharynx comprises the tonsillar fossa with the faucial tonsil, glossotonsillar sulci, soft palate, uvula, lateral and posterior pharyngeal walls, vallecula and base of tongue. The squamous mucosa of the oropharynx differs from other areas within the head and neck region in that lamina propria of the former is composed of lymphoid tissue. Collectively, the lymphoid-rich mucosa of the faucial tonsils, base of tongue and adenoids are termed Waldeyer's ring. Furthermore, the surface of the faucial tonsils and base of tongue extend down at regular intervals to form crypts. The crypts are lined by a loose network of lymphoepithelial tissue known as the reticulated crypt epithelium (Figure 1.5). HPV-positive OPSCC originates within the crypts rather than surface epithelium.^{128,159} Within the oropharynx, HPV-positive OPSCC is most prevalent in the faucial tonsils, followed by the base of tongue.^{34,40}

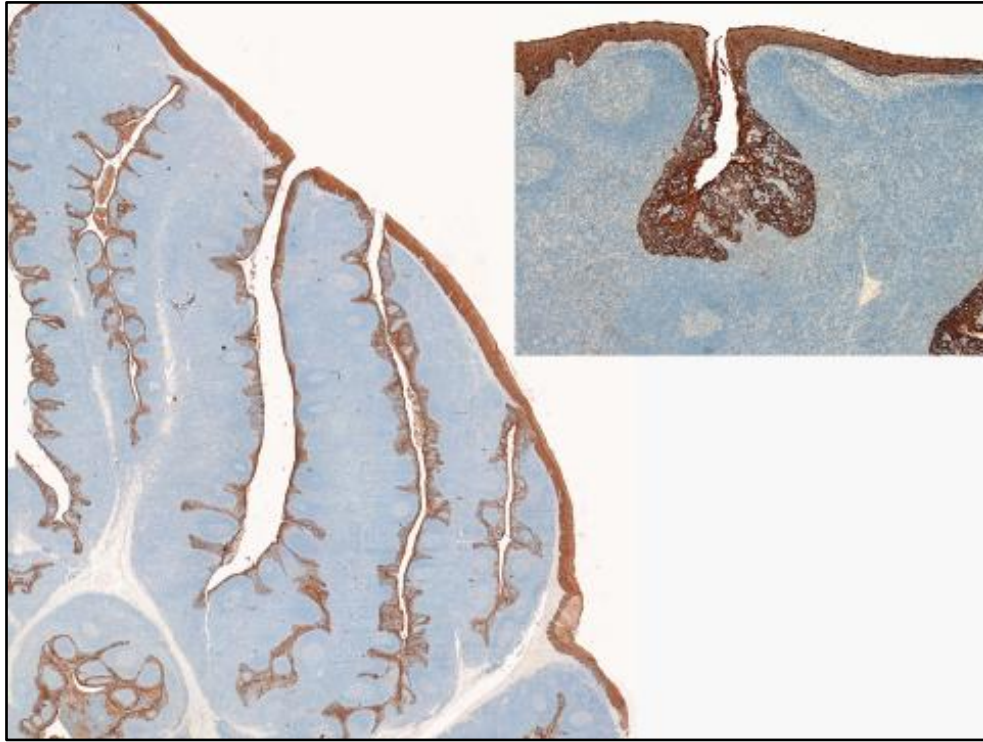


Figure 1.5. Representative photomicrograph of normal tonsil.

Photomicrograph of low-power (left) and high-power (right) views of normal tonsil immunohistochemically stained for pan-cytokeratin demonstrating the greater integrity of the surface stratified squamous epithelium in comparison to the crypt epithelium.

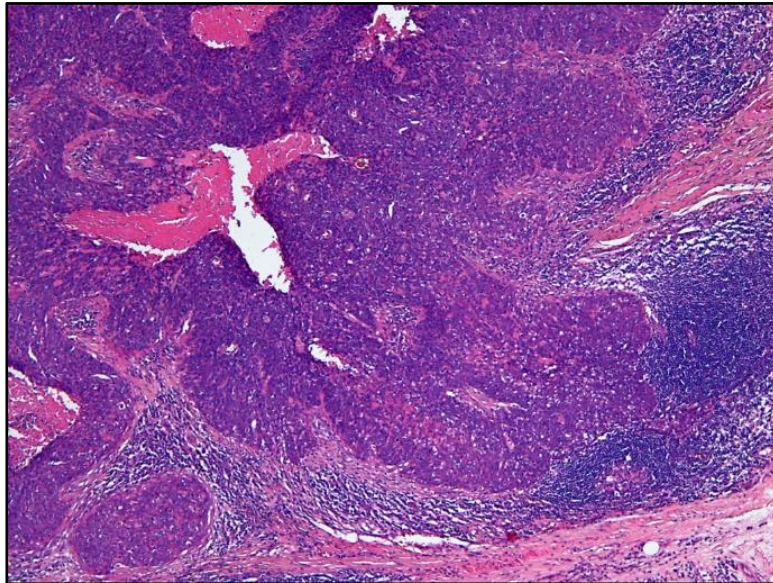
Further to a strong predilection for lymphoepithelial tissue, HPV-positive OPSCC also demonstrates several distinct clinico-demographic features.

Patients with HPV-positive OPSCC:

1. Are likely to present with early nodal involvement; approximately 60% of these patients present with stage III–IV tumours at diagnosis.¹⁶⁰
2. Tend to be slightly younger with a median age of diagnosis of 54 years.¹⁶¹
3. Have a history of minimum exposure to tobacco and alcohol.^{40,162,163}
4. Hail from higher socioeconomic and educational backgrounds.¹⁶⁴
5. Are three times more likely to be male rather female.¹⁵²
6. More likely to be of White rather than Black or Asian ethnicity^{163,165,166}

HPV-positive OPSCC has distinct histological features exhibiting a mainly non-keratinising morphology in contrast to HPV-negative HNSCC where significant keratinisation is usually seen (Figure 1.6).¹⁶⁷ The reticulated crypt epithelium, in its normal state, is non-keratinised. Therefore, the non-keratinising phenotype of HPV-associated OPSCC may be explained by its recapitulation of the reticulated crypt epithelium. It is also possible, that the non-keratinising characteristic of the reticulated crypt epithelium renders it more susceptible to persistent HPV infection.¹⁶⁸

HPV-positive



HPV-negative

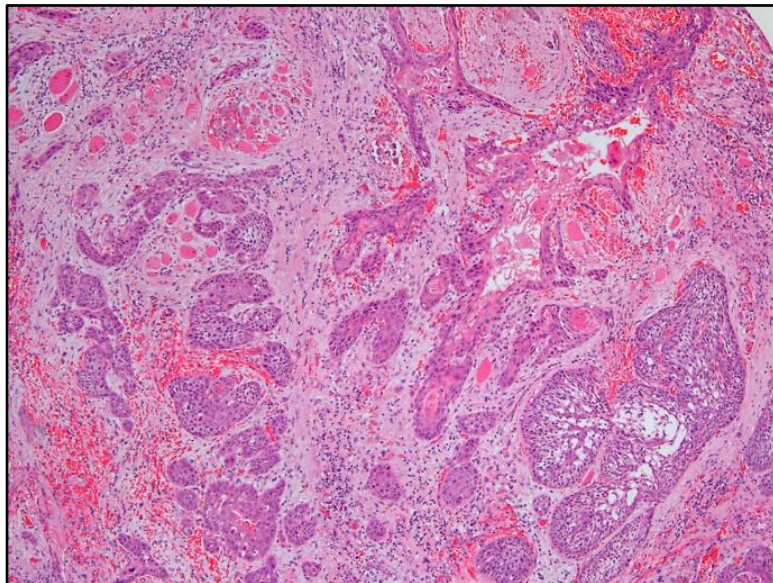


Figure 1.6. Comparative histomorphology of HPV-positive and HPV-negative OPSCC.

Comparative histomorphology of HPV-positive (top, non-keratinising) and HPV-negative (bottom, keratinising) OPSCC. H&E original magnification x 40.

1.5 Genetic distinctiveness of HPV-positive OPSCC

In general, HPV-positive OPSCC contain fewer and distinct genetic mutations compared to HPV-negative tumours. Despite these indications that HPV status is associated with molecular and clinical differences, all HNSCCs are clinically managed irrespective of their HPV status. Understanding of genetic differences between HPV-positive and HPV-negative HNSCC tumours might allow to develop biomarkers for early detection or recurrence surveillance, to identify therapeutic targets, and to begin individualisation of treatment based on the biology of these tumours.

Combined data from four independent studies, namely Agarwal *et al* (2011)²⁰, Stransky *et al* (2011)²¹, Lechner *et al* (2013)¹⁶⁹ and Seiwert *et al* (2014)¹⁷⁰ indicate that HPV-positive HNSCC harbor fewer gene mutations HPV-negative OPSCC. However, there appears to be several consistent gene mutations in HPV-positive tumours. For instance phosphatidylinositol-4,5-bisphosphate 3-kinase catalytic subunit alpha (PIK3CA) was the most commonly mutated gene found in HPV-positive cancer cells (24% in HPV-positive HNSCC versus 8% in HPV-negative HNSCC) followed by E1A binding protein (EP300), a gene that plays an essential role in regulating cell growth and division, prompting cellular differentiation, and preventing the growth of cancerous tumours (6% in HPV-positive HNSCC versus 3% in HPV-negative HNSCC). Fibroblast growth factor receptor 3 (FGFR3) (7% in

HPV-positive HNSCC versus 3% in HPV-negative HNSCC), V-Ki-ras2 Kirsten rat sarcoma viral oncogene homolog (*KRAS*), a gene that performs an essential function in normal tissue signalling (6% in HPV-positive HNSCC versus 2% in HPV-negative HNSCC). On the other hand TP53 was mutated in HPV-negative tumours with the highest rate of 79% (84 of 107) compared to 4% (3 of 83) of HPV-positive samples. Mutation rate of NOTCH1 was lower in HPV-positive (8%) compared to HPV-negative HNSCC samples (16%). CDKN2A was only found in 11% of the HPV-negative samples, none in HPV-positive samples.

Braakhuis *et al* (2004) following determining presence of HPV DNA and E6/E7 mRNA by PCR in 143 consecutively treated HNSCCs correlated HPV status with mutations in the gene encoding p53 (TP53) and loss of heterozygosity (LOH) in a number of chromosomes generally found to be affected in HNSCC. The group observed that HPV-positive tumours had generally lower levels of LOH with significantly lower levels of p53 mutations than HPV-negative tumours. In the HPV-negative tumours, most LOH was found on chromosomes 3p (encodes several tumour suppressor genes), 9p (encodes CDKN2A) and 17p (encodes TP53).¹³⁷

In addition to fewer mutations per tumour, HPV-positive OPSCCs also have been reported to demonstrate distinct DNA gains and losses when compared to HPV-negative tumours. Dahlgren *et al* (2003) investigated the pattern of DNA losses and gains in 25 tonsillar tumours, of which 60% were HPV-positive. Eleven of 15 HPV-positive samples (73%) had gains at

chromosome 3q (encodes human telomerase gene), compared to 4/10(40%) in HPV-negative tumours ($p=0.049$).¹⁷¹ By contrast, gains at 7q and amplification of 11q13 (encodes cyclin D1) were more common in HPV-negative tumours and were independently associated with poorer outcome.¹⁷¹

1.6 Improved survival of HPV-positive OPSCC

It is now well established that HPV-related OPSCC not only represents a distinct subtype of HNC but is also associated with a better prognosis. In a retrospective study, Gillison *et al* (2000) were among the first authors to identify a positive survival benefit in patients harbouring the virus HPV in their tumours. There was a 59% reduction in disease-specific death compared to HPV-negative patients.⁵¹ Other early work in support of Gillison *et al* resulted from a study in Sweden that showed increased overall survival in HPV-associated tonsillar SCC (65.3%) compared to HPV-negative counterparts (31.5%).¹⁷² Similarly in the Eastern Cooperative Oncology Group (ECOG) protocol 2399, confirmed improved survival outcomes for patients with HPV-positive HNSCC in retrospective survival analyses.^{173,174} A systematic review investigating cancer-specific survival in HPV-related HNSCCs demonstrated a 72% reduction in OPSCC specific mortality.¹⁷⁵

Since then, several other retrospective studies showed similar findings, and there is now significant evidence that HPV-positive tumours have greatly improved survival compared to HPV-negative HNSCC regardless of

treatment modality (radiation, chemotherapy, surgery or concurrent radio-chemotherapy).^{138,176} Moreover, there is robust evidence demonstrating a lower degree of treatment failure and recurrence in HPV-positive tumours, accounting for improved survival rates.¹⁷⁷ The improved survival of these patients has stimulated the formulation of clinical trials in both North America (RTOG 1016) and Europe (De-escalate-HPV) to test the feasibility of de-escalation of therapy to reduce acute and late toxicities.^{143,178}

1.6.1 Putative mechanisms of improved outcome in HPV-associated OPSCC

The mechanisms for improved survival in patients with HPV-associated OPSCC are yet to be fully elucidated. Improved survival may be caused by a combination of several factors including a slightly younger age at diagnosis, an inverse correlation with tobacco smoking and exposure to alcohol and good performance status with absence of significant comorbidities.¹⁵² However, there is an increasing body of evidence indicating that the favorable outcome and increased survival of HPV-positive OPSCC could be due to inherent sensitivity of these carcinomas to chemotherapy and/or radiotherapy.¹⁷⁹ In general, there are fewer somatic molecular alterations in HPV-positive cancers compared to HPV-negative counterparts, the latter containing greater numbers of activating mutations of oncogenes and/or inactivating alterations in tumour suppressor genes acting to confer a more resistant phenotype.^{141,180}

1.6.1.1 Role of p53

At the molecular level, it has been observed that p53 tumour suppressor pathways in HPV-positive cancer cells are intact but dormant, controlled by E6.^{181,182} High-risk HPV-16 E6 proteins are able to bind wild-type p53 and mediate p53 degradation in vitro through the ubiquitin–proteasome pathway.¹⁸² Although HPV-positive OPSCC have reduced p53 levels due to abrogation by E6, p53 mutations are rare in this group, possibly due to reduced exposure to tobacco, and it is possible that any remaining p53 is still functionally able to exert its effects on abnormal cells.^{4,183} In a comparative study by Westraet *al* (2008) none of the HPV16-positive tonsillar carcinomas showed disruptive p53 mutations compared to presence of disruptive p53 mutations in HPV-negative HNSCC (0% versus 57%; $p=0.008$).¹⁸³ In HPV-positive tumours p53 is generally present in low levels and in an inactive state, cellular stress promotes an increase in p53 protein levels. When triggered, p53 functions to activate pathways for DNA repair, cell cycle arrest and/or apoptosis, depending upon the nature and degree of damage.⁹⁷

1.6.1.2 Other cell cycle regulatory mechanisms

In general, cells undergoing mitosis are more susceptible to radiation-induced death while cells in late S-phase appear to be relatively radio-resistant. To this effect, several groups have demonstrated that, following radiation, HPV-positive cells showed prolonged G2-M cell-cycle arrest compared to HPV-negative cells.¹⁸⁴⁻¹⁸⁶ The greater propensity for cell cycle arrest is critically, regulated by checkpoint kinases 1 and 2 (Chk1/2).¹⁸⁷

There is a growing body of evidence indicating a trend towards inverse correlation between HPV status and EGFR expression.^{188,189} Phosphorylation of EGFR is an upstream event in mitogen activated protein kinase (MAPK) and phosphatidylinositol-4,5-bisphosphate 3-kinase/protein kinase B/mammalian target of rapamycin (PI3K/AKT/mTOR) pathways.^{190,191} Since both these pathways are known to be important positive regulators of cell proliferation and growth, it is also possible that the relative lower EGFR expression may be important in the less aggressive phenotype demonstrated by HPV-positive OPSCCs.¹⁸⁸

1.6.1.3 DNA damage response

Evidence from *in vitro* studies suggest that HPV-positive OPSCC cells have a decreased capacity for genomic repair following exposure to DNA-damaging agents such as radiation, thereby inducing cell death. Rieckman *et al* (2013) showed increased mitotic catastrophe in HPV-positive cells as a result of residual double-strand breaks (DSBs), as demonstrated by γ -H2AX staining.¹⁸⁶ Furthermore, E7-induces a reduction in sub-lethal DNA damage thereby directing HPV-positive cells towards cell death following treatment.¹⁹² Interestingly, increased cell death may be also explained by HPV-induced p16 over-expression. Dok *et al* (2014) showed p16 interferes with RAD51-associated homologous recombination-associated DNA repair, by down regulating cyclin D1 protein expression. The end result is failure or misrepair of DSBs with resultant cell death.¹⁹³

1.6.1.4 Lack of field cancerisation

Patients with HPV-positive OPSCC demonstrate a lower incidence of local-regional recurrences (LRRs) and second primary tumors (SPTs). The decreased frequency might be explained by the absence of ‘field cancerisation’ effect, which is a crucial aspect of LRRs and SPTs in HPV-negative HNSCC patients.¹⁹⁴ Field cancerisation in HPV-negative tumors is defined as the existence of a single or more mucosal fields approximating a tumour that comprises of epithelial cells having tumor-associated genetic or epi-genetic modifications.^{195,196} Rietbergen *et al* (2014) showed absence of transcriptionally active HPV in 91 out of 97 resection mucosal margins surrounding an HPV-positive tumour of 20 HPV-positive OPSCC patients, suggesting absence of a field cancerisation.¹⁹⁷ Similarly Begum *et al* (2005) showed that HPV integration is tightly coupled to the neoplastic process and did not occur outside of the field of phenotypically altered cells.¹⁵⁹ Other studies have also shown discrete boundaries of p16-immunostaining in HPV-positive tonsillar carcinomas that distinguish tumor from adjacent uninvolved mucosa.^{198,199}

1.6.1.5 Tumour microenvironment

It is also suggested that HPV-positive HNSCCs are less hypoxic than the negative counterparts and that this apparent lack of hypoxia in HPV -positive tumors could be linked to the superior prognosis observed.^{200,201} As HPV-associated OPSCC appears in the lymphoid tissue of the tonsils and the base of the tongue the tumours can generally be characterised by infiltration

of lymphocytes in the stroma and tumour nests.²⁰² A possible account for survival advantage may be the tumour-infiltrating T lymphocytes (TILs) that infiltrate many HPV-positive OPSCC and generate a defensive effect by an adaptive host immune response conducted against viral antigens such as E6 and E7.^{203,204} HPV-16-specific CD8-positive T cells have been identified in the blood of HPV-positive OPSCC patients and lately, isolated from tumours, implicating a role in the anti-tumour response.²⁰⁴⁻²⁰⁶

1.7 Management of HNSCC

Numerous treatment modalities including surgery, radiotherapy, chemotherapy and/or a combination of these exist for HNSCC. For practical purposes, HNC is divided into three clinical stages: early, loco-regionally advanced, and metastatic or recurrent.²⁰⁷ The clinical management assessments for HNSCC are based on the evaluation of the tumour size, regional nodal status and distant metastasis (TNM).²⁰⁸ The TNM status is classified into tumour stage where patients at stages I or II can be categorised into early and stages III or IV as advanced, taking into account metastatic or recurrent disease.²⁰⁸ Treatment approaches can vary depending on the disease stage. In general, patients with early stage disease experience a more satisfactory prognosis,²⁰⁹ whereas those with advanced stage disease have a notably poorer clinical outcome.²¹⁰ Factors that influence the choice of treatment include primary site, stage at presentation, age and co-morbidities. For example, the preferential treatment option for tumour stages I and II of the oral cavity is surgery with or without

post-operative radiation (RT) or chemo-radiation therapy (CRT) when indicated.²¹¹ For HNSCC located in the pharynx, early stage patients are treated with RT alone and more advanced disease (stages III and IV) are treated with CRT.^{208,212}

Radiation therapy is the use of high-energy x-rays or other particles to induce cancer cell death. A radiation therapy regimen usually consists of a specific number of treatments given over a set period of time. It can be as a single modality treatment, or as adjuvant treatment following surgery, depending on stage, nodal and margin status. Radiation results in DNA damage in the form of, intra- and inter-strand cross-links and single and double strand breaks (DSBs). Unrepaired DSBs are thought to be the main cytotoxic lesions.²¹³ The interaction of radiation with tissues results in the production of free radicals. Free radicals are short-lived but their half-life is increased in the presence of oxygen, which is said to fix the radicals and increase the chances of interacting with DNA. Hypoxia is associated with production of fewer radiation-induced free radicals, reducing their overall interaction with DNA thereby causing less radiation-induced DNA damage and a reduction in tumour cell killing.²¹⁴

Probably the most commonly used single chemotherapeutic agent, in HNSCC is cisplatin. It can be administered as first line therapy, neoadjuvant or induction (prior to surgery and/or RT), concurrent chemo-radiotherapy (administered at the same time as RT) or as an adjuvant therapy following surgery or radiation.²¹⁵ Cisplatin acts via crosslinking DNA and making its

repair impossible, thus activating apoptosis in quickly dividing cells.²¹⁶ Because of its different spectrum of toxicity, methotrexate, carboplatin and oxaliplatin have also been used in cases of recurrent and metastatic HNSCC.^{217,218,219}

In order to improve patient outcome and minimise the toxic side effects of less specific cytotoxic agents such as cisplatin, increasing emphasis is being placed on targeting malignant cells while sparing healthy normal cells from toxic therapeutic effects. Prospective targeted therapies in HNSCC principally aim at cellular pathways of carcinogenesis.^{220,221} One such molecular target includes EGFR.²⁴ EGFR is a type 1 transmembrane receptor tyrosine kinase (RTK) that is involved in numerous aspects of HNSCC pathogenesis. It is one member of a superfamily of such receptors, including c-erbB-2 (human epidermal growth factor receptor 2(Her-2/neu)), c-erbB-3, and c-erbB-4. The EGFR is activated by ligand binding followed either by homodimerisation, or heterodimerisation with another member of the EGFR superfamily.^{190,222} Anti-EGFR agents including monoclonal antibodies against the EGFR (cetuximab) and EGFR tyrosine kinase inhibitors (TKIs, Gefitinib and Erlotinib) are currently used for the management of various types of cancer.²²³ Cetuximab is a chimeric monoclonal antibody that attaches with high affinity at the endogenous ligand-binding site of EGFR preventing dimerisation, internalisation, and autophosphorylation, thereby inhibiting downstream signalling cascades involved in cellular proliferation. Furthermore, it has also been shown that cetuximab promotes EGFR degradation, and has antibody-dependent

cell-mediated cytotoxicity effects.²²⁴ In combination with radiotherapy, cetuximab improved survival of HNSCC patients to 49 months compared to 29.3 months for radiotherapy alone.²²⁵ Several studies have confirmed that EGFR inhibition sensitises HNSCC to the effects of radiation therapy.²²⁶⁻²²⁸ In recent years, the novel targeted therapeutic agent tumour necrosis factor-related apoptosis-inducing ligand (TRAIL) has been evaluated for its potential in the management of several types of cancer. It is an increasingly attractive therapeutic option because of its relatively restricted expression on tumor cells and its ability to act in concert with various chemotherapeutic agents to promote tumor cell death.²²⁹ Although the efficacy of recombinant TRAIL for the treatment of HNSCC is yet to be determined, this agent has been tested in clinical trials for a wide variety of epithelial derived cancers such as breast, colon, renal and lung cancers.²³⁰ TRAIL is a tumour necrosis factor (TNF) receptor family ligand that initiates apoptosis through the extrinsic pathway by binding itself to the death receptors (DR4 and DR5). This leads to oligomerisation of the death receptors and formation of the death inducing signalling complex (DISC) followed by recruitment of the adaptor molecule, Fas-associated protein with death domain (FADD) and procaspase-8. DISC assembly stimulates the auto-cleavage and activation of caspase-8 resulting in activation of the effector caspase (caspase-3) that eventually leads to apoptotic cell death (Figure 1.2).²³¹⁻²³⁴

The major current limitation of TRAIL therapy is the development of resistance to this agent in cancer cells through a variety of mechanisms.

1. TRAIL interacts with two agonistic receptors, namely TRAIL-R1 (DR4) and TRAIL-R2 (DR5) both capable of signalling apoptosis. TRAIL is also able to bind to three antagonistic (non-signalling decoy) receptors TRAIL-R3 (DcR1), TRAIL-R4 (DcR2) and osteoprotegerin (OPG) that may function by sequestering TRAIL extracellularly.²³⁵⁻²³⁸ In some cases, increased expression of these decoy receptors has been correlated with TRAIL resistance in tumour cells.²³⁹
2. Other mechanisms that inhibits TRAIL signalling includes increased expression of inhibitors such as cellular FLICE-inhibitory protein (c-FLIP), it has sequence homology to caspase-8, but lack protease activity, therefore it is suggested that the recruitment of c-FLIP to the DISC in place of caspase-8 blocks their activation and consequently confers TRAIL resistance.²⁴⁰
3. The anti-apoptotic function of family of inhibitor of apoptosis proteins (IAPs) that comprises a number of members like X-linked inhibitor of apoptosis protein (XIAP), cellular IAP (cIAP1 and cIAP2) have been shown to prevent activation of caspases-3, -7 and -9 via direct or indirect binding thereby exerting protection against TRAIL-mediated cell death.^{241,242}

High-risk HPV is known to drive the oncogenic process by attenuating component of the extrinsic apoptotic pathway. In particular, HPV-16 E6 has been shown to interact with FADD thereby inhibiting the binding and activation of caspase-8. There is also evidence to suggest that HPV-16 E6 causes enhanced degradation of caspase-8.^{243,244} Other HPV oncoproteins

are also known to cause preferential inhibition of FasL- and/or TRAIL-mediated apoptosis.²⁴⁵

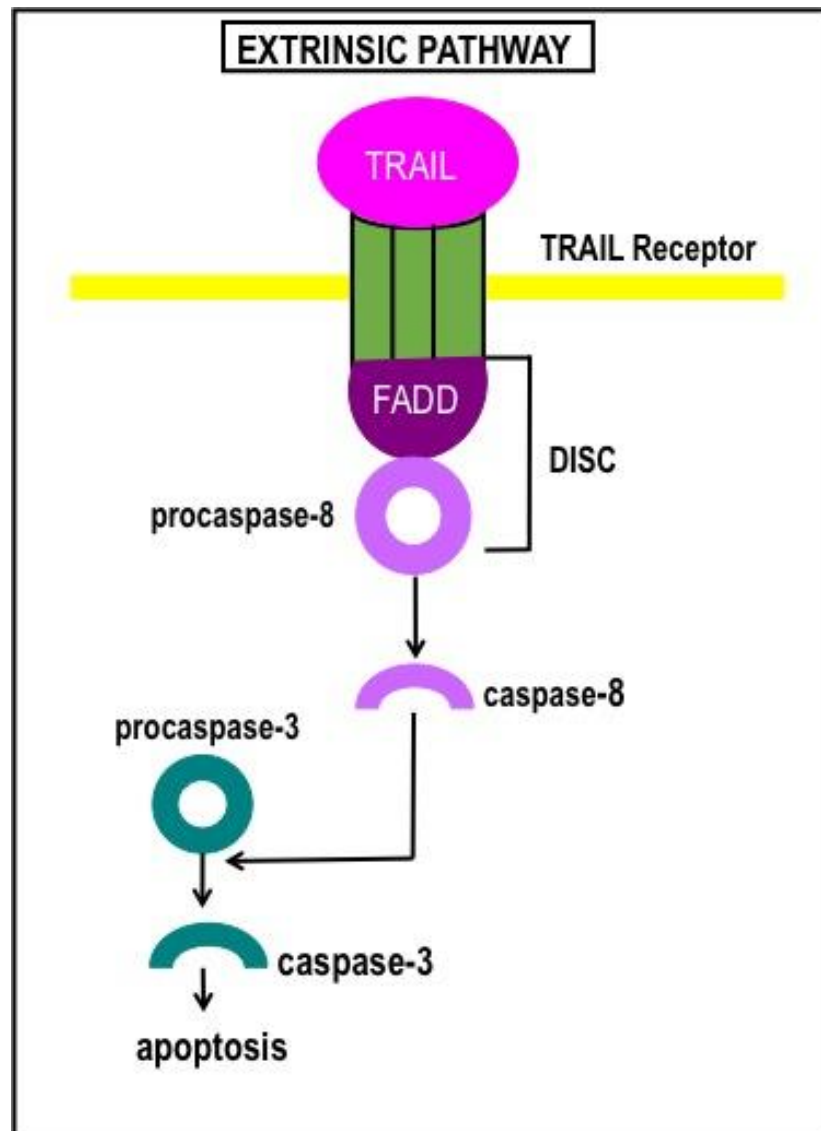


Figure 1. 7. Schematic representation of the extrinsic pathway.

Binding of TRAIL and trimerisation of TRAIL death receptors leads to the recruitment of FADD, and procaspase-8. Together these comprise the DISC. This initiates the activation of initiator caspase 8, once active it propagates apoptosis via direct cleavage of caspase 3.

1.8 Management of HPV-positive OPSCC

Currently, radiotherapy is the most commonly used single modality in patients with early-stage OPSCC (stage I/II).^{246,247} The treatment of patients with locally advanced or stage III/IV OPSCC disease involves combination of surgery, radiotherapy and chemotherapy.²⁴⁸ For instance, surgery with adjuvant radiation or chemo-radiation with chemotherapy being added for high-risk pathologic features found from the surgical specimen,²⁴⁹⁻²⁵² or radiotherapy with concomitant chemotherapy.²⁵³⁻²⁵⁵

The increase in the incidence of HPV-associated OPSCC over the past decade has been paralleled with the observation that there is significant overall- and disease-free survival (DFS) advantage for patients with these tumours compared to HPV-negative counterparts.^{51,141} Despite the survival advantage, HPV-positive and HPV-negative OPSCCs are treated using similar traditional standard treatment modalities resulting in possible avoidable toxicities and decreased quality of life in HPV-positive patients.²⁵⁶ This has led to some authorities to suggest the possibility of offering different treatment regimens for HPV-positive and HPV-negative tumours. Although there is currently insufficient evidence to support the modification of treatment based on HPV status alone, several clinical trials are in progress towards de-escalation of treatment intensity in HPV-positive OPSCC with the intent to reduce toxicity and thereby improve the long-term quality of life, while maintaining efficacy and without compromising outcomes. Possible de-escalation options include reducing radiotherapy dosages, withholding

chemotherapy or replacing chemotherapy with targeted therapies such as the EGFR monoclonal antibody, cetuximab.

Current on-going de-intensification trials include Eastern Cooperative Oncology Group (ECOG)1308, Radiation Therapy Oncology Group (RTOG 1016), De-ESCALaTE HPV, NCT1088802/J0988, Trans-Tasman Radiation Oncology Group-TROG 12.01, quarterback trial, ADEPT, ECOG 3311 and PATHOS.

These de-escalation trials are mainly based on reduction in radiotherapy intensity (from 70Gy down to 54Gy) or on the substitution of cisplatin with cetuximab in concurrent chemotherapy regimens.²⁵⁷⁻²⁶⁵ Many of the de-escalation trails for instance RTOG 1016, TROG 12.01 and De-ESCALaTE are focused on reducing toxicity by replacement of cisplatin with cetuximab.²⁶⁶

Preliminary results from ECOG 1308 appear to suggest it may be possible to safely reduce radiotherapy dose in a selected cohort of HPV-positive OPSCC patients, however the final data on progression free survival and overall survival are pending.²⁵⁷

HPV-positive OPSCC may achieve specific targeting of HPV-positive tumour cells due to the unique expression of E6 and E7 oncoproteins. For example, suppression of cellular E6 and E7 protein levels by short hairpin RNA is able to restore p53 and pRb function and induce apoptosis in cell line studies.²⁶⁷ As a consequence, small molecule inhibitors that inhibit the protein-protein interaction of the viral oncoproteins E6 and E7 are actively being investigated, which may sensitize tumor cells to other therapies.²⁶⁸ For instance small molecules could inhibit E6 from binding to procaspase 8 and

FADD and in turn would restore the normal functioning of the apoptosis pathway.²⁶⁹

Tumor expression of E6 and E7 may also provide the possibility of inducing or enhancing cell-mediated immunity against tumor cells.²⁷⁰ Harvesting, expanding and re-administering tumor-infiltrating lymphocytes to patients with HPV-associated OPSCC in order to enhance the cytotoxic anti-tumoural immune response to these tumours may also be potential treatment strategy.²⁷¹

Another advancement creating interest in the field of oncology is the inhibition of programmed cell death-1 (PD-1) or its associated ligand (PD-L1).²⁷² PD-1, functions as an immune checkpoint and plays a significant role in down regulating the immune system by inhibiting the activation of T-cells.²⁷³

Significant expression of PD-L1 has been shown on HPV-associated HNCs.²⁷⁴ A recent study has suggested a role for PD-1–PD-L1 interaction in the initial HPV infection and subsequent immune resistance of HPV-associated tonsillar cancer.²⁷⁴ Initial reports of single agent PD1 monoclonal antibody (mAb), MK3475 (MK-3475 is a highly selective, humanised IgG4/kappa isotype mAb designed to block PD-1 interaction with its ligands PD-L1 and PD-L2) used for checkpoint inhibition and reactivation of the immune system, from the Keynote-012 trial have been very promising, with a significant percentage of patients with recurrent and metastatic HNSCC demonstrating PD-L1 positivity and with >50% of patients demonstrating objective responses to treatment.²⁷⁵

These approaches have the intrinsic benefit of using physiologic anti-tumoural responses as a treatment modality that theoretically carries decreased risk and morbidity otherwise seen in conventional treatments with substantial toxicities.

1.9 Rationale, aim and objectives of this study

In parallel to the ‘epidemic’ rise of HPV-associated OPSCC, there is robust evidence to indicate a significantly improved disease-specific and overall survival outcome following treatment in these patients compared to HPV-negative HNCs.⁴ The mechanisms for improved outcome in HPV-positive OPSCC is still poorly understood. The overall aim of this study is elucidate potential mechanisms of improved response to therapeutic agents in HPV-associated HNC. In the longer term, it is anticipated that identification of potential mechanisms of improved response in HPV-positive HNC cells may be exploited to improve survival outcomes in all HNC patients.

Specific objectives of this study were to:

1. Develop an *in vitro* cell line model for increased relative sensitivity to conventional (radiation and cisplatin) and targeted (cetuximab and TRAIL) therapeutic agents in HPV-positive HNC.
2. Evaluate the functional role of p53 and HPV16-E6 in the differential response of these cells to radiation, cisplatin, cetuximab and TRAIL.

3. Determine whether response to cetuximab *in vitro* correlates with EGFR protein expression.
4. Compare HPV status and EGFR protein expression in the cell line model with OPSCC tissue specimens and correlate overall survival in the latter.

Chapter 2- Materials and Methods

2.1 Materials

2.1.1 Plastics

Plastics used in tissue culture were purchased from Griener Bio-one, UK (6, 12, 24 and 96 well plates; 5, 10 and 25ml pipettes; cell scrapers and cryovials) and PAA (T25 and T75 flasks, 15 and 50 ml Falcon tubes, 10 cm dishes). 0.2µm and 0.45µm filters were purchased from Fisher Scientific, UK. Cell culture media were stored at 4°C. Solutions and Buffers were stored at room temperature unless specified.

2.1.2 Chemicals and solutions

All chemicals were purchased from PAA, Sigma-Aldrich and SLS, UK unless stated otherwise.

Agarose

Agarose 100g (Sigma-Aldrich, A9539-100G). 1% (w/v) solution of agarose was made up in 100ml 1x TAE (Tris-acetate-EDTA) and boiled to dissolve the powder entirely. The solution was cooled down to 32-45°C and ethidium bromide (fluorescent tag-nucleic acid stain) was added to a final concentration of 0.5µg/ml.

Albumin from bovine serum (BSA)

1mg/ml of BSA (SLS, A9647-50G).

Ammonium persulfate (APS)

10% APS solution was made up in dH₂O and stored at 4°C for a maximum of two weeks.

Blocking buffer for western blotting

5 or 10% (w/v) Marvel milk powder (purchased from Sainsbury's supermarket) added in Tris-Buffered Saline-Tween20 (TBST).

Cell Lysis Buffer

2mM MgCl₂, 25mM HEPES KOH pH 7.4 and 2mM EGTA (ethylene glycol tetra acetic acid), cell lysis buffer was diluted 1:1 in 2% Triton X-100 and the following components were added: protease inhibitors aprotinin and leupeptin both at a final concentration of 1 µg/ml and PMSF at a final concentration of 100 µg/ml.

Coumaric acid

90mM p-coumaric acid in Dimethyl Sulfoxide (DMSO), stored at -20°C.

Cisplatin

Cisplatin 1mg/ml (TEVA UK Ltd) provided by Guy's Hospital Pharmacy stored at room temperature.

Dimethyl sulfoxide (DMSO)

DMSO from VWR International (317275).

Dulbecco's Modified Eagle Medium (DMEM)

Purchased from PAA (E15-810) and supplemented before use with 50ml of a final concentration of 10/15% fetal bovine serum (FBS) (Sigma-Aldrich,

F7524), 1ml 100 x Penicillin/Streptomycin (PAA Laboratories, P11-010) and 5 ml of 1mM sodium pyruvate (Sigma-Aldrich, UK) in 500 ml of medium.

EDTA buffer

0.5mM disodium ethylenediaminetetraacetic acid (EDTA) was made up in dH₂O, pH was adjusted to 8.0 with NaOH (sodium hydroxide), the solution was sterilised by autoclaving and the solution was stored at 4°C.

Enhanced chemiluminescence (ECL) buffer

100mM Tris-HCL (tris [hydroxymethyl] aminomethane hydrochloride) pH 8.5, stored at 4°C. 10ml of ECL buffer was mixed with 3 µl hydrogen peroxide, 25 µl of 90 mM coumaric acids and 50 µl of 250mM luminol before use for western blots.

Freezing medium for cell culture

10% Dimethyl sulfoxide (DMSO), 20% fetal bovine serum (FBS) and 70% Dulbecco's modified eagle medium (DMEM) / Modified eagle medium (MEM) with Earle's salts. The cells were stored at -80°C for a week or two before transferring them to the liquid nitrogen tanks.

IZ-TRAIL

Recombinant human isoleucine zipper trimerised TRAIL [(TNF)-related apoptosis-inducing ligand] was a kind gift from Professor Henning Walczak, University College London. Stock solution of 1mg/ml was made up and stored at -70°C.

Isopropanol

Isopropanol extra pure (Fisher scientific, 38971).

Laemmli sample buffer (LSB)

Buffer comprised of 62 mM Tris base (2-amino-2[hydroxymethyl] propane-1, 3, diol[tris]) pH 6.8, 10% glycerol, 2% SDS and 5% β-mercaptoethanol. The buffer was made up in dH₂O and stored at -20°C. Before use: protease inhibitors aprotinin and leupeptin both at a final concentration of 1µg/ml, PMSF at a final concentration of 100µg/ml and 200 µl of 1% saturated bromophenol blue were added.

Luminol

250mM luminol in DMSO, stored at -20°C.

Luria-Bertani (LB) - agar plates

1.5%(w/v) agar in LB medium, sterilised by autoclaving were cooled to 50°C and appropriate antibiotic was added.

MEM with Earle's Salts (Lonza, BE12-611F)

50ml of a final concentration of 10% FBS, 5ml of 100 x non-essential Amino Acids (PAA Laboratories, M11-003), 5ml of 200mM L-Glutamine (PAA Laboratories, M11-004) and 550µl of Gentamicin (PAA Laboratories, P11-004) were added into 500ml of medium prior to use.

Midi prep solutions

Plasmid Midi Kit (QIAGEN, 12143).

MTT (3-(4,5-dimethylthiazolyl-2)-2,5-diphenyltetrazolium bromide) stock

5mg/ml MTT (Calbiochem, 475989) was prepared in phosphate buffered saline (PBS), sterilised by filtering through a 0.2µm filter and stored at -20°C protected from light.

MTT Solubilisation Solution

50% dimethylformamide (Sigma-Aldrich, 33120), 0.2% glacial acetic acid (Sigma-Aldrich, 338826), 20mM HCl, 20% SDS, the solution was made up in dH₂O.

Page ruler pre-stained protein ladder

Page Ruler pre-stained protein ladder ready to use (Thermo Scientific, 26616).

Penicillin/Streptomycin

100x Penicillin/Streptomycin (PAA, P11-010).

Phenylmethylsulfonyl fluoride (PMSF)

10mM PMSF was made up in isopropanol and stored at -20°C.

Phosphate-buffered saline (PBS)

140mM NaCl (sodium chloride), 2.7mM KCl (potassium chloride), 8mM Na₂HPO₄(disodium hydrogen phosphate), 1.5mM KH₂PO₄(potassium dihydrogen phosphate).The solution was made up in dH₂O and sterilised by autoclaving.

Protogel 30% Acrylamide Mix

Protogel 30% Acrylamide Mix (37.5:1 acrylamide to bis-acrylamide stabilised solution) was purchased from National Diagnostics(EC-890).

Puromycin

Puromycin 10mg/ml (InvivoGen, ant-pr).

Running/Transfer buffer (10x) for Western Blotting

250mM Tris base, 2.5M glycine and 1% SDS, made up in dH₂O.

Running buffer (1x) for Western Blotting

10% of 10xrunning/transfer buffer in 90% of dH₂O.

sh-RNA Reagents

- **pMD2.G**(Lentivirus)envelope plasmid from Addgene (Plasmid #12259)
- **pCMV-dR8.91**(Lentivirus) packaging plasmid, Department of Salivary and mucosal research, King's College London.
- **VSVG**(Retrovirus) envelope plasmid from Dr Ulrich Maurer, Institute of molecular medicine and cell research, University of Freiburg, Germany.
- **HIT60** (Retrovirus) packaging plasmid from Dr Ulrich Maurer, Institute of molecular medicine and cell research, University of Freiburg, Germany.

10% sodium dodecyl sulphate (10% SDS)

A 10% (w/v) solution of SDS was made up in dH₂O, heated to 68°C to dissolve and the pH was adjusted to 7.2 with concentrated hydrochloric acid (HCl).

SDS Polyacrylamide Gels

Table 1: SDS Polyacrylamide Gels

Resolving gel	10%	12%	15%	Stacking gel	4%
1.5mM Tris pH 8.8	5.0 ml	5.0 ml	5.0 ml	1.0mM Tris pH 6.8	750 µl
30% Acrylamide	6.7 ml	8.0 ml	10.0 ml	30% Acrylamide	1.0 ml
ddH₂O	7.9 ml	6.6 ml	4.6 ml	ddH₂O	4.1 ml
10% SDS	200 µl	200 µl	200 µl	10% SDS	60 µl
10% APS	200 µl	200 µl	200 µl	10% APS	60 µl
TEMED	8 µl	8 µl	8 µl	TEMED	6 µl

Tris-acetate-EDTA buffer (10x TAE buffer)

1 L of 10x solution was made up by adding 48.5g Tris (Trizma, T1503), 11.4ml glacial acetic acid (Sigma, 537020) and 20ml 0.5M EDTA (pH 8.0)(Sigma,03690) in deionised water.

Tris-buffered saline TBS (10x)

250mM Tris base (VWR, 103157P), 1.5M NaCl (SLS, L4509) made up in dH₂O, pH adjusted to 7.4 with concentrated HCl and sterilised by autoclaving.

1x Tris-buffered saline-Tween 20 (1x TBST)

0.1% Tween 20 in 1x TBS.

Tris/EDTA buffer

10mM Tris base and 1mM EDTA made in dH₂O, the pH was adjusted to 9.0 and stored at 4°C.

Tris-EDTA (TE)

10mM Tris-HCl pH 8.0, 1mM EDTA pH 8.0 made in dH₂O.

Transfer buffer (1x)

10% of 10x running/transfer buffer, 20% methanol and 70% dH₂O.

Trypsin (1x)

10% 10xTrypsin (Sigma, T4549).

Versene

0.270mM EDTA pH 8.0 made up in 1x PBS and sterilised by autoclaving.

2.1.3 Antibodies

2.1.3.1 Antibodies used for Western Blotting

Table 2: Antibodies used for Western Blotting

Targets	Species	Clone	Dilution	Supplier	Catalogue Number
β-Actin	Mouse	AC-7	1:5000	Sigma-Aldrich	A5441
EGFR	Mouse	F4	1:1000	*Gift	
p21	Mouse	DCS60	1:1000	Cell Signalling	2946
p53	Mouse	DO-7	1:2000	Novacastra Laboratories	NCL-L
Mouse-HRP-IgG	Goat-anti-mouse	Fc	1:4000	Sigma-Aldrich	A0168

*

Gift from Prof. William Gullick, Department of Bioscience, University of Kent at Canterbury, UK.

2.1.3.2 Antibodies used for Immunohistochemistry

Table 3: Antibodies used for Immunohistochemistry

Targets	Species	Clone	Dilution	Supplier	Catalogue Number
Cyclin-D1	Mouse	A12	1:400	Santa Cruz	sc-8396
EGFR (extracellular domain)	Mouse	C36	1:100	Ventana	790-2988
EGFR (intracellular domain)	Rabbit	5B7	1:100	Ventana	790-4347
p16	Mouse	E6H4	1:40	Ventana	725-4713
p53	Mouse	DO-1	1:100	Santa Cruz	sc-126
p63	Mouse	4A4	1:500	Santa Cruz	sc-8431
Mouse-HRP-IgG	Goat- anti- mouse	FITC	1:100	Santa Cruz	sc-2031
Goat anti-rabbit IgG-B	Goat anti- rabbit	IgG-B	1:100	Santa Cruz	sc-2040

2.1.4 Primers

2.1.4.1 Primers used for Standard PCR

Table 4: Primers used for standard PCR

Primers	Sequence	Supplier
GP5+ GP6+	Forward 5'-TTTGTTACTGTGGTAGATACTAC-3 Reverse 5'-GAAAAATAAACTGTAAATCATATTC-3'	Eurofins
HPV16-E6	Forward 5'-ATGCACCAAAAGAGAACTGC-3' Reverse 5'-TTACAGCTGGGTTTCTCTAC-3'	Eurofins
β-Actin	Forward 5'-CATCTAAGTTGCTATCCAGGC-3' Reverse 5'-CTCCTTAATGTCACGCACGAT-3'	Eurofins

2.1.4.2 Primers used for RT- PCR

Table 5: Primers used for RT-PCR

Primers	Sequence	Supplier
HPV-16 E6	Forward 5'-ATGCACCAAAAGAGAACTGC-3' Reverse 5'-TTACAGCTGGGTTTCTCTAC-3'	Eurofins
GAPDH	Forward 5'-TTGCCATCAATGACCCCTTCA-3' Reverse 5'-CGCCCCACTTGATTTTGGA-3'	Sigma-Aldrich

2.1.5 Lentiviral and Retroviral shRNA constructs

2.1.5.1 shRNA scrambled controls

Table 6: shRNA control plasmids

Plasmids	Description	Supplier
Control E6 shRNA	Negative control shRNA lentiviral plasmid- A. Commercially available. Puromycin was used for selection. https://www.scbt.com/scbt/product/control-shrna-plasmid-a	Santa Cruz (sc-108060)
Control p53 shRNA	3 rd generation lentiviral plasmid- Human (empty backbone). Puromycin was used for selection. Sequence available at: http://www.addgene.org/8453/sequences/	Addgene (8453)
Control E6 forced expression	MSCV-N GFPFLAGHA tagged- mammalian expression, retroviral plasmid. Puromycin was used for selection. Sequence available at: http://www.addgene.org/37855/sequences/	Addgene (37855)

2.1.5.2 shRNA constructs

Table 7: shRNA plasmids

Plasmids	Description	Supplier
E6 shRNA	HPV-16 E6 lentiviral plasmid. Commercially available. Puromycin was used for selection.	Santa Cruz (sc-156008-SH)
p53 shRNA	pLKO-p53shRNA-427, lentiviral plasmid-human. Puromycin was used for selection. Sequence available at: http://www.addgene.org/25636/sequences/	Addgene (25636)
	pLKO-p53shRNA-941, lentiviral plasmid-human. Puromycin was used for selection. Sequence available at: http://www.addgene.org/25637/sequences/	Addgene (25637)
	pLKO.1puro. 3rd gen lentiviral plasmid-human. Puromycin used for selection. Sequence available at: https://www.addgene.org/19119/sequences	Addgene (19119)

2.1.5.3 HPV16 E6 forced expression

Table 8: E6 expression vectors

Plasmids	Description	Supplier
E6 forced expression	MSCV-C terminal on backbone, FLAGHA tagged- mammalian expression, retroviral. Puromycin was used for selection. Sequence available at: https://www.addgene.org/37876/sequences	Addgene (37876)
	MSCV-N terminal on backbone, FLAGHA tagged- mammalian expression, retroviral. Puromycin was used for selection. Sequence available at: https://www.addgene.org/37875/sequences	Addgene (37875)

2.2 Methods

2.2.1 Cell culture

2.2.1.1 Cell lines

Five HPV-positive and two HPV-negative cell lines were obtained from various sources; UPCI-SCC 089, 072, 090, 152 and 154 were a gift from Professor S. Gollin, University of Pittsburgh. UD-SCC2 was a gift from Professors H. Bier, University of Munich and 93-VU-147T was a gift from Dr Steenbergen, VU University, Amsterdam.

Cell lines currently available limited this study. All cell lines were obtained from external laboratories and none were generated locally in this centre due to facility and time limitations. Furthermore, due to its inherent biological properties, primary culture of HPV-positive oropharyngeal squamous cell carcinoma cells is particularly difficult. In this study, two of the cell lines (UPCI-SCC090 and UPCI-SCC154) were derived from the tongue base mucosa. The tongue base and tonsil are functionally and anatomically similar to that of the fauceal tonsil (comprising surface non-keratinising stratified and reticulated crypt squamous epithelium. They were therefore considered suitable as models to study this disease.

UPCI-SCC 089: The UPCI-SCC 089 cell line was derived from a 58-year old Caucasian male smoker and alcoholic patient with primary tumour arising in the tonsil. His tumour was staged as T2N2b M0 according to the 4th Edition

American Joint Committee on Cancer (AJCC) guidelines, with 11q13 gene amplification and HPV status being negative.^{276,277}

UPCI-SCC 072: UPCI-SCC 072 was derived from primary squamous cell carcinoma of tonsils, from a Caucasian 61 year old female. The tumour was staged as T3N2b, with 11q13 gene amplification and HPV status being negative. Tumour DNA showed TP53 missense mutation (14214C>A) with H179N codon change.²⁷⁶⁻²⁷⁸

UPCI-SCC 090: The UPCI-SCC 090 cell line was derived from a 46-year old male who had a history of cigarette and alcohol consumption, with a recurrent oropharyngeal squamous cell carcinoma in the base of tongue. The tumour was staged as T2N1M0 with poorly differentiated invasive tumour comprising basaloid features. The cell line carries integrated HPV type-16 and the TP53 status has been detected as wild type.^{276,279,280}

UPCI-SCC 152: One year later the UPCI-SCC090 patient was diagnosed with a new invasive moderately differentiated squamous cell carcinoma of the hypopharynx termed as UPCI-SCC152, which was staged as T4N2M0. The cells also showed presence of HPV type-16 and wild type TP53.²⁷⁶

UPCI-SCC 154: UPCI-SCC 154 was derived from a 54-year old male smoker and alcoholic patient; the tumour originated from the tongue and was staged as T4N2M0. The cell line also contains integrated HPV-16 and wild type TP53.²⁷⁶

UD-SCC 2: UD-SCC 2 was derived from a 58-year old male smoker and alcoholic patient, tumour occurred in the hypo-pharynx and was staged as T1N3M0. The cell line also contains integrated HPV-16 and wild type TP53.^{281,282}

93-VU-147T: 93-VU-147T cancer cells were isolated from a 58-year old male smoker and alcoholic patient. The tumour stage was T4N2M0 derived from the floor of mouth. Although it has been reported to harbour wild-type p53, it was found to have a heterozygous mutation in TP53 (c.770T>G, p.L257R) in some studies.¹⁸⁴ The cell line also contains integrated HPV-16.²⁸³

2.2.1.2 Culture and maintenance of cell lines

UPCI-SCC 090, UPCI-SCC 154, UPCI-SCC 089, UPCI-SCC 072, UPCI-SCC 152 and UD-SCC 2 were cultured in MEM with Earle's salts supplemented with 5ml L-Glutamine, 550 µl gentamicin, 5 ml non-essential amino acid and 50ml FBS. 93-VU-147T cell line was cultured in high glucose DMEM media supplemented with 50 ml FBS, 1ml penicillin/streptomycin and 5ml sodium pyruvate.

2.2.1.3 Thawing of cell lines

Frozen aliquots of cells were taken out from liquid nitrogen tank and instantly thawed in a water bath at 37°C. Cells from the cryovials were transferred to tubes in 5ml of medium and centrifuged for 5 minutes at 1000x g. The supernatant was discarded and the pellet was re-suspended in 10 ml of fresh medium pre-warmed to 37°C and transferred to 10 cm dishes or 75 cm² flasks, incubated at 37°C and 5% CO₂.

2.2.1.4 Mycoplasma testing

Cell lines were regularly tested for the presence of mycoplasma using a PCR-based detection kit according to the manufacturer's instructions (AppliChem, A3744).

2.2.1.5 Sub-culture of cell lines

Cells in 75cm² flasks were sub-cultured every 3 to 5 days once the cells were 70-80% confluent. After removal of the medium the flasks were washed with 5ml or 10 ml of versene and the cells were incubated with 1ml of 1x trypsin at 37°C for several minutes. After detachment from the base of the flask cells were re-suspended in fresh medium and seeded in fresh flasks according to desired density (1:5/ 1:10) and kept in the incubator at 37°C and 5% CO₂.

2.2.1.6 Freezing of cells

As described above the cells were trypsinised and centrifuged for 5 minutes at 1000 x g, after removal of the supernatant the cells were re-suspended in fresh corresponding medium supplemented with 20% FBS and 10% dimethylsulfoxide (DMSO) and transferred to cryovials, These were slowly frozen down at -80°C in an isopropanol bath (Nalgene Cryoware) for at least 2 days before transfer to a liquid nitrogen tank for long term storage.

2.2.1.7 Cell counting

Following trypsinisation and re-suspension in fresh medium, 10µl of cell suspension was pipetted into the haemocytometer (Neubauer chamber from SLS, HAE2118) and cells in the outer four large squares were counted. The cell concentration (number of cells per ml) was determined by using the formula: (counted cells/4) x 10⁴.

2.2.1.8 Cell counting for growth curves

The cell number was determined by the procedure as described above.

Identical number of cells (50,000/well) for all cell lines was seeded in a six well plate in triplicates, incubated for eight days. The triplicate wells were counted after every 24 hours.

2.2.1.9 Standard Polymerase chain reaction (PCR)

DNA was extracted from pellets of the cell lines following the protocol provided with the QIAamp DNA Micro Kit (Qiagen, 56304). DNA concentrations were determined on a NanoDrop 1000 spectrophotometer (Thermo Scientific). Basic PCR procedure was adapted, in order to detect HPV genotype by GP5+/6+ primers and E6 DNA by using E6 primers.

GP5+/6+ and HPV-16 E6

In order to detect presence of HPV in HPV-positive cell lines the standard PCR protocol was adapted. GP5+/6+ and HPV-16 E6 primers²⁷⁹ (Table 4) were used to amplify HPV genotype and E6 DNA in HPV-positive cell lines. β -Actin (Table 4) was used as loading control.

2 μ l of HPV-DNA (approximately 2000 ng/ μ l) was added to a tube along with 2.5 μ l of 10xPCR buffer, 2 μ l of 3.5mM MgCl₂, 0.5 μ l of 5mM dNTPs, 0.5 μ l each of 100 μ M forward and reverse primers, 0.125 μ l of Taq and made up to 15 μ l per tube with 9.77 μ l of nuclease free water. Samples were vortexed

and centrifuged briefly. The mixture was kept on ice. Negative control with no HPV was also added.

The samples were run in the PCR machine (G-storm), DNA was denatured at 94°C for 5 minutes, followed by 40 PCR cycles of, 94°C for 1 minute (denaturation), 60°C for 1 minute (annealing) and 72°C for 2 minutes (extension). An additional extension step of 72°C for 5 minutes was included at the end of the reaction. The PCR amplified DNA was analysed by agarose gel electrophoresis. 3g of agarose (Sigma, A-9539) in 150ml of 1x TAE buffer was heated in a microwave at medium heat until dissolved.

Meanwhile the gel tank was prepared by tightly sealing the sides, a comb was placed and filled with 1xTAE buffer. 5 µl ethidium bromide (Bioatlas, BA01902) was added to the TAE agarose solution before pouring in the tank. After placing the DNA samples in the wells the gel was run for approximately 1 hour at 100 Volts and it was analysed using Gene genius bio-imaging system (Syngene). The images were printed by Sony digital graphic printer UP-D897.

2.2.1.10 Reverse transcription polymerase chain reaction (RT-PCR)

RT-PCR was carried out using complementary DNA (cDNA) as template. Forward and reverse primers (Table 5) were used to assess the expression of HPV-16 E6. GAPDH was used as endogenous control (Table 5).

Preceding making cDNA, using at least 10^6 cells were harvested for the extraction of total RNA, washed with PBS and placed on ice. RNA extraction was carried out according to manufacturer's protocol using RNeasy[®] Mini Kit (Qiagen-74104). Genomic DNA was removed from 2 µg of total RNA using the DNA-free DNA Removal Kit (Ambion- AM1906) according to the manufacturer's protocol.

Master mix for HPV-16 E6 expression was prepared by mixing 5 µl of 10X Dream Taq buffer (Thermo scientific, EP0702), 5 µl dNTP mix (Thermo scientific, R0241), 1.0 µM each of forward and reverse primers, 1 µg of template DNA, 1.25 µl of Dream thermusaquaticus (taq) DNA polymerase and nuclease free water in order to make the final volume up to 50 µl for each reaction. The reactions were placed in a thermal cycler (Veriti[®] Thermal Cycler).

The thermal cycling conditions are outlined below.

1. 95°C - 2 minutes, 1 cycle
2. 95°C - 15 seconds, 40 cycles
3. 60°C – 6 seconds, 1 cycle

To assess the presence of the cDNA, it was separated on 1% (w/v) agarose (NBS Biologicals, UK) gel in 1x TAE containing 0.5 µg/ml Ethidium Bromide (Bio-Rad; 161-0433) at 120V for up to 45 minutes, analysed using Gene

Genius Bio-imaging System Syngene. The images were printed by Sony Digital Graphic printer UP-D897.

2.2.1.11 Radiation

The planning and administration of radiotherapy to the head and neck is a complex process, which takes into account the biological properties of the disease, anatomical structure limitations (such as the spinal cord) and, in cases of adjuvant treatment, the margin of surgical resection. Therapeutic dose is targeted for the tumour with diminishing marginal dose to adjacent structures. Furthermore, the tumour microenvironments, including the stromal cell population and host immune cells, influence tumour response to radiation. The *in vitro* study of radiation effects in cell lines in monolayer therefore cannot entirely recapitulate the clinical situation, but only provide preclinical models to define suitability for further study in animal models and Phase 1 clinical trials.

25cm² flasks were prepared for each dose along with a control flask. Once 70% confluent, the cells were irradiated at doses of 2Gy, 4Gy and 6Gy (gamma radiation, using Nordion GC-1000S v2.09 cell irradiator [SN. 0242]) and incubated overnight. After 24 hours, cells were trypsinised and counted, as described previously. After diluting in culture medium, various cell concentrations, optimised for each cell line (50,000 to 100,000), were seeded in each well of a 96 well culture plate, 6 replicate wells of different radiation doses, together with the untreated controls with 200µl of cell culture

medium. After 7 days of incubation the assay was stopped when the non-radiated cells had undergone four or more doublings from the original plating number. The cell viability was determined using the MTT assay. All experiments were performed in triplicate.

2.2.1.12 Chemotherapy

Varying concentrations of cells, optimised for each cell line (50,000 to 100,000), were seeded in 96 well plates. After 24 hours the cells were treated with either **cisplatin** (diluted in culture medium at the concentrations of 2.5µg/ml, 5µg/ml and 10µg/ml for 24 hours), **TRAIL** (TNF-related apoptosis-inducing ligand, diluted in culture medium at the concentrations of 1.5625ng/ml, 3.125ng/ml, 6.25ng/ml, 12.5ng/ml, 25ng/ml, 50ng/ml and 100ng/ml for 72 hours) or **cetuximab** (diluted in culture medium at the concentrations of 200nM, 400nM, 600nM, 800nM, 1000nM, 1200nM and 1400nM for 48 hours). Cell viability was determined using the MTT assay. All experiments were performed in triplicate.

2.2.1.13 MTT cell viability assay

MTT (3-(4,5-dimethylthiazolyl-2)-2,5-diphenyltetrazolium bromide) assay is a colorimetric assay for measuring the reduction of tetrazolium salts to formazan dyes by the respiratory enzymes in metabolically active cells.²⁸⁴ The intensity of the colour is directly proportional to the metabolic activity of the cells. By measuring the optical density at 570nm wavelength, after solubilisation the number of metabolically active cells can be correlated.

To assess the viability of cell population in response to different treatments, cells were seeded in 96 well plates at a density of $2-4 \times 10^3$ cells in 100 μ l medium/well. After incubation for seven days following radiation and at different time points for chemotherapeutic drugs, 20 μ l of MTT (5mg/ml, in PBS) was added to each well, which already contained 100 μ l of medium, incubated for 2-4 hours at 37°C and 5% CO₂ before adding 150 μ l of solubilisation solution to each well. After further incubation at 37°C and 5% CO₂ for at least 16 hours absorbance of each well was measured at 595nm using a LT-4000 microplate reader (Labtech) and Manta software. The results were calculated after background subtraction by comparing the readings for treated cells in relation to untreated control cells.

2.2.1.14 Clonogenic Assay

Following radiation, cells were counted after 24 hours using same method as described in Section 2.2.1.7. Cell densities for each cell line were calculated and the cells were seeded in a 60mm culture dish. Triplicate dishes for each radiation dose and non-irradiated controls were prepared. The dishes were placed in an incubator and left until cells in control dishes had formed sufficiently large clones of at least 50 cells per colony. The medium was removed from the dishes once the colonies were formed, the cells were washed with versene, 2-3ml of 10% of buffered formalin was added and the dishes were left for 1 hour for fixation, after that the dishes were rinsed again with versene, the colonies were stained with 2ml methylene blue 1% in H₂O

for 1 hour, rinsed and kept overnight at room temperature to dry out. The colonies were counted and expressed relative non-irradiated controls.

2.2.2 Immunohistochemistry and DNA in-situ hybridisation

2.2.2.1 Paraffin embedded cell pellets

Following trypsinisation (at least 1×10^8 cells), cell pellets were re-suspended in 1 ml of 10% buffered formalin and centrifuged at 13,000rpm, the formalin was removed and the pellets were re-suspended in 1 ml of 1xPBS and stored at 4°C until ready for construction of agarose pellets. For preparation of agarose pellets, 50ml of 20% agarose gel in PBS was prepared. The formalin-fixed cells were re-suspended in PBS then centrifuged at 13000 rpm. The supernatant was removed, the pellets were re-suspended in 200µl of 1x PBS and transferred to 1.5ml eppendorf tubes, the tubes were centrifuged and the supernatant was discarded. The pellets were placed in the 60°C water bath and 200µl of agarose gel was added and re-suspended, vortexed briefly and then centrifuged at 13000 x g for 1 minute and the eppendorf tubes were left vertically placed in a rack for at least 1 hour in order to ensure complete setting of the agarose. The agarose pellets were removed from the eppendorf tubes, longitudinally bisected and placed in labelled histology cassettes. Agarose pellets were forwarded to the Department of Oral Pathology for routine processing. Briefly, agarose pellets were further fixed in 10% (v/v) buffered formal saline for 24 hours, processed and embedded in paraffin wax. 5µm sections were cut, mounted on

polylysine-coated slides, deparaffinised in xylene, dehydrated in 100% (v/v) industrial methylated spirit and rinsed in running tapwater. All sections were stained with haematoxylin and eosin (H&E).

2.2.2.2 Immunohistochemistry (IHC) staining and scoring

The paraffin blocks of agarose embedded cell pellets were sectioned at 5µm sections using routine histological procedure on a LEICA-RM2235 microtome. Sections were cut by Biomedical Scientists in the Department of Oral Pathology for routine processing. For IHC, formalin fixed cell monolayers were air-dried overnight at 37°C and dehydrated. After antigen retrieval and inactivation of endogenous peroxidases, the sections were stained with primary antibodies using the avidin-biotin-peroxidase method.

Counterstaining was provided by Mayer's haemalaun. For each block, the sections were stained using four primary antibodies directed against: p53, p63, p16, cyclin D1 and EGFR (3C6 extracellular domain and 5B7 intracellular domain) using methods recommended by manufacturers where available. The sections of the pellets were stained for p16 using a propriety kit (CINtec Histology, mtm Laboratories) on a Ventana Benchmark Autostainer (Ventana Medical Systems). A tonsil squamous cell carcinoma with high p16 expression was used as a positive control and the same section without adding the p16 primary antibody as a negative control.

The distribution, pattern and intensity of IHC staining of all sections were evaluated using a light microscope under various magnifications. The immunohistochemistry staining was interpreted by collective cytoplasmic and nuclear staining considering the staining intensity for stains such as p53, p63, p16 and cyclin D1. For immunohistochemical evaluation of EGFR in tissue samples, two observers independently scored all cases. Where present, the non-dysplastic surface or reticulated crypt epithelium was taken as the referent. An ordinate value of 0-3 was assigned to the intensity of membrane staining. The percentage of each intensity was allotted to the entire tumour within the whole mount tissue section and a product of each intensity value and its percentage stained within the tumour was determined. An 'H-Score' was then determined using the following formula: $[(1 \times \% \text{ cells intensity } 1) + (2 \times \% \text{ cells intensity } 2) + (3 \times \% \text{ cells intensity } 3)]$.

2.2.2.3 HPV DNA in situ hybridisation (ISH)

High risk HPV DNA ISH was carried out using proprietary reagents (Inform HPV III Family 16 Probe (B), Ventana Medical Systems) on a Benchmark Autostainer (Ventana Medical Systems). The inform HPV III Family 16 Probe (B) detects high-risk genotypes HPV16, 18, 31, 35, 39, 51, 56, 58 and 66.

2.2.3 Western blotting

2.2.3.1 Preparation of cell pellets

Cells were collected by trypsinisation in cold 1x PBS and kept on ice. Following centrifuging at 4°C at 1000 rpm for 5 minutes the cell pellets were re-suspended in 1 ml of cold 1x PBS and transferred to 1.5 ml eppendorf tubes. The eppendorfs were centrifuged for 5 minutes at 1000 rpm at 4°C in the microfuge. The supernatant was removed and the pellets were stored at -20°C until protein extraction.

2.2.3.2 Preparation of total cell lysates and protein extraction

Followed by preparation of fresh cell lysis buffer (1ml of fresh lysis buffer contained 50% of cell lysis buffer, 50% of triton x 100 2%, A/L [2µl], PMSF [6µl]), the cells were re-suspended in 50µl of cell lysis buffer (volume was changed depending on the size of the pellet). The cell pellets were incubated on ice for 10 minutes followed by centrifugation at 13000 rpm at 4°C. The supernatant (protein extract) was transferred to newly labelled tubes and the protein extracts were stored at -20°C until used for Bradford assay.

2.2.3.3 Bradford assay

Protein concentrations were determined using the Bradford assay. It is based on the shift of the dye Coomassie from a doubly-protonated red form to an un-protonated blue form with an absorbance maximum at 595nm when binding to proteins in the sample.²⁸⁵ The resulting increase in the absorbance at 595nm is proportional to the protein concentration.

For the assay samples were diluted 1:1000 in dH₂O and the bovine serum albumin (BSA) standards with concentrations ranging between 0 and 20µg/ml were prepared. Of every sample or standard 100µl were mixed on 96-well plate with 100µl of Bradford reagent (AppliChem). The absorbance of each well was measured at 595nm on a LT-4000 microplate reader (Labtech) and the protein concentration in individual samples was calculated based on the BSA standard curve.

2.2.3.4 SDS-PAGE (sodium dodecylsulfate polyacrylamide gel electrophoresis)

This form of gel electrophoresis is used to analyse proteins, which after denaturation by the anionic detergent SDS, are separated by size on a polyacrylamide gel.²⁸⁶ The smaller the proteins, the faster it migrates through the gel matrix driven by an electric current. After separation proteins can be visualised and analysed by different staining or by western blot analysis. For SDS page equal amounts of proteins were re-suspended in 2 x LSB and heated at 95°C for 5 minutes to allow denaturation.

In case the volume exceeds 50µl samples were boiled for a longer time to reduce the volume for loading. Samples were either stored at -20°C or directly used for gel electrophoresis. Depending on the size of proteins of interest different gel percentages, corresponding to the percentage of polyacrylamide cross-linking of the resolving gel, were used.

The vertical gel-casting apparatus was set up according to the manufacturer's instruction (Bio-Rad, Mini PROTEIN II, 165-2940). The resolving polyacrylamide gel solution was prepared accordingly and poured, leaving space for the upper (stacking) gel. A thin layer of isopropanol was added to flatten the surface and avoid evaporation (drying out of the gel). After the gel had set the isopropanol was removed with filter paper, then the gel was washed with dH₂O and was dried with filter paper. The loading gel was prepared and loaded on top and a 10- or 15- well comb was placed to get wells for sample loading. After the gel was set, the comb was removed and the gel was placed in an electrophoresis tank filled with 1 x running buffer. Protein samples were loaded on the gel after boiling for 5 minutes at 95°C with first lane loaded with 4µl of protein molecular weight marker. The tank was connected to the power supply and electrophoresis was started at 80 volts (V) allowing protein migrations through the stacking gel, before the voltage was increased to 100V for up to 2 hours.

2.2.3.5 Transfer of proteins

A transfer sandwich was made by placing the gel on the black side of the transfer cassette after placement of a sponge and 3 pieces of 3mm filter papers (Whatman, 3030917), the nitrocellulose membrane was then put on top of the gel and covered by another 2 pieces of filter papers and a sponge. The cassettes were closed and locked and placed in the transfer module with corresponding colours in the transfer tank (Bio-Rad Mini PROTEIN II) filled with 1x transfer buffer. Transfer was performed at 400 mA for 90 minutes at 4°C or 40mA overnight at room temperature.

2.2.3.6 Probing of membrane with antibodies

After transfer, the membrane was blocked for an hour at room temperature or over night at 4°C in 5% milk in TBS-T followed by incubating the membrane with primary antibody diluted in 5% milk at appropriate concentrations for overnight at 4°C on a shaker. The membrane was washed 3 x 10 minutes with TBS-T. The blot was then incubated with secondary anti-mouse or anti-rabbit antibody diluted in 5% blocking buffer for an hour at room temperature. Lastly the membrane was washed three times with TBS-T for 10 minutes each time.

2.2.3.7 Detection by enhanced chemiluminescence (ECL)

During the last wash of the membrane ECL solution was prepared (10ml ECL buffer with 3µl of H₂O₂, 25µl coumaric and 50µl of luminol). The membrane was incubated with ECL solution for 1 minute, drained, wrapped in cling film, placed in the western blot cassette and exposed to RX autoradiograph film (Fuji) for varying times depending on signal strength. Before re-probing with another primary antibody, the blot was stripped with Re-blot plus strong buffer (Millipore) for 15 minutes and incubated with blocking buffer 2 times for 5 minutes at RT on a shaker.

2.2.4 Lentivirus methods

Lately, retroviral and lentiviral vectors have developed into a fundamental tool for the efficient delivery of nucleic acids to many cell types in a variety of experimental systems. Using lentiviral or retroviral systems allows for the stable, heritable integration of a specific nucleic acid sequence into the target cell's genome.

Retroviral replication involves the covalent integration of the reverse transcribed viral genome into the host cell chromatin. Provirus, an integrated form of the virus, provides a template for viral gene expression. As the provirus is an integral part of the host genome, retroviruses stay in the host for the lifespan of the infected cell.²⁸⁷

Lentiviruses are a subtype of retrovirus. Main distinction between lentiviruses and standard retroviruses is that lentiviruses are capable of infecting non-dividing and actively dividing cell types whereas standard retroviruses can only infect mitotically active cell types. This means that lentiviruses can infect a greater variety of cell types than retroviruses.²⁸⁸

Both lentiviruses and retroviruses use the gag, pol, and env genes for packaging; however, they are different viruses and thus use slightly different isoforms of these packaging components. Therefore, lentiviral vectors may not be efficiently packaged by retroviral packaging systems, and vice versa.²⁸⁸⁻²⁹⁰

2.2.4.1 Bacterial transformation

To amplify plasmids chemically competent *Escherichia Coli* (Mach1™-T1R, Invitrogen or MAX Efficiency® Stbl2™, Invitrogen) were transformed by adding 1 µl of plasmid DNA, leaving them on ice for 30 min followed by a heat shock (30 sec at 42°C) and a cold shock (at least 2 min on ice). Bacteria were then cultured in 250 µl LB medium for 1 hour at 37°C before they were spread on a pre-warmed LB agar plate supplemented with the appropriate antibiotic. The plates were incubated overnight at 37°C and then stored at 4°C. Single colonies were picked and transferred into 5 ml of LB medium with antibiotic and incubated at 37°C while shaking overnight before plasmid extraction.

2.2.4.2 Plasmid extraction

Plasmid DNA was purified from bacterial cultures using a Plasmid Midi Kit (Qiagen) or a Wizard Plus SV Miniprep DNA Purification System (Promega) according to the manufacturer's instructions. DNA concentrations were determined on a NanoDrop 1000 spectrophotometer (Thermo Scientific).

2.2.4.3 Lentivirus production

HEK293T cells were plated on 10cm dishes to reach around 70 to 80% confluency at the time of transfection. For transfection by calcium phosphate precipitation a vector mix of three plasmids was prepared in 250µl sterile dH₂O: 3.5µg of lentiviral construct, 6.5µg of envelope plasmid (pMD2.G) and 10µg of packaging plasmid (pCMV-dR8.91). After addition of 250µl 2.5M CaCl₂ the vector mix was added drop wise to 500µl of 2xHeBS (pH 8.05) while vortexing. After 30 min incubation at room temperature the suspension was slowly added to the cells which were incubated overnight at 37°C and 5% CO₂ before changing the medium. The virus-containing supernatant was harvested at 24 and 48 hours post-transfection, put through a 0.45µm filter and frozen at -70°C for long-term storage or kept at 4°C overnight. 2.5x10⁵ UPCI-SCC 090 and 089 cells were plated on 12-well plates and infected with several dilutions of concentrated virus supernatant in the presence of 5µg/ml polybrene (Santa Cruz Biotechnology).

2.2.4.4 Lentivirus infection

Target cells were plated 24 hours before infection to reach around 80% confluency at the time of infection. Lentivirus stocks were diluted in a minimal amount of medium supplemented with 5µg/ml polybrene was added to the cells. After 24 hours fresh medium was added and cells were collected at the indicated time points for the respective assays.

2.2.4.5 Generation of stable knockdown cell lines

Target cells were plated approximately 24 hours before infection on 6 cm dishes to reach around 80% confluency at the time of infection. Cells were infected using 1ml of viral supernatant supplemented with 5µg/ml polybrene and 2ml of fresh culture medium were added 8 hours after infection. After several days cells were selected depending on their acquired resistance to antibiotics. A control of non-transduced cells was treated in parallel to ensure toxicity of the antibiotic.

2.2.5 Retrovirus methods

According to the methods for bacterial transformation and plasmid extraction described in sections 2.2.4.1 and 2.2.4.2 respectively, for retrovirus production HEK293T cells were plated on 10cm dishes to reach around 60 to 70% confluency at the time of transfection. For transfection by calcium phosphate precipitation, a vector mix of three plasmids was prepared in 250µl sterile dH₂O, 3.5µg of retroviral construct, 6.5 µg of envelope plasmid (VSVG) and 10 µg of packaging plasmid (HIT 60). After addition of 250µl of 2.5M CaCl₂,

the vector mix was added drop wise to 500µl of 2xHeBS (pH 8.05) while vortexing. After 30 min incubation at room temperature the suspension was slowly added to the cells which were incubated overnight at 37°C and 5% CO₂ before changing the medium. Next day sodium butyrate was added to the selection medium for approximately 10 hours and the virus-containing supernatant was harvested at 24 and 48 hours, put through a 0.45µm filter and frozen at -70°C for long-term storage or kept at 4°C overnight. 2.5x10⁵ UPCI-SCC 090 and 089 cells were plated on 12-well plates and infected with several dilutions of concentrated virus supernatant in the presence of 5µg/ml polybrene (Santa Cruz Biotechnology).

Target cells were plated 24 hours before infection to reach around 80% confluency at the time of infection. Lentivirus stocks were diluted in a minimal amount of medium supplemented with 5µg/ml polybrene. After 24 hours fresh medium was added and cells were collected at the indicated time points for the respective assays. Target cells were plated approximately 24 hours before infection on 6 cm dishes to reach around 80% confluency at the time of infection. Cells were infected using 1ml of viral supernatant supplemented with 5µg/ml polybrene and 2ml of fresh culture medium were added 8 hours after infection. After several days cells were selected depending on their acquired resistance to antibiotics. A control of non-transduced cells was treated in parallel to ensure toxicity of the antibiotic.

2.2.6 Survival analysis

Research Ethics Committee (RECreference 10/H070/027) and Research and Development (R&Dreference RJ110/N320) approval has already been granted in relation to immunohistochemical evaluation in OPSCC tumour samples and correlation with survival outcome. Overall survival data was retrospectively obtained from electronic patient records. Kaplan-Meier survival plots were generated at various H-score cut-offs using SPSS statistics software version (IBM corporation, US).

2.2.7 Statistical analysis

All data was analysed using Microsoft Excel, GraphPad Prism 6 software and SPSS statistics software. Bars or data points throughout this study represent mean values of independent results while error bars indicate the corresponding standard error of the mean (SEM). For experiments involving measurement of replicate data such as MTT assays performed in triplicate, replicate values were combined into an average value and considered as one independently obtained result.

Depending on the experimental design several statistical methods were used and analysis were performed. The difference between two groups was tested using an unpaired, two-tailed Student's t test using GraphPad Prism 6. Survival curves were evaluated by the Kaplan-Meier method, and survival distributions were compared using the log-rank test using SSPS software.

Chapter 3 - Characterisation of cell lines and differential response of HPV-positive and HPV-negative HNSCC cells to conventional therapy *in vitro*.

3.1 Introduction

HPV-positive oropharyngeal squamous cell carcinomas (OPSCCs) have a significantly improved outcome in response to treatment compared to HPV-negative OPSCCs.^{65,173} Although the improved clinical response of HPV-positive OPSCC to conventional therapeutic agents is now well established, the biological mechanisms that underpin these observations remain largely unknown. Therefore, in order to evaluate the possible mechanisms of improved response to treatment in HPV-positive OPSCCs, the initial objective of this study was to develop an *in vitro* model of relative sensitivity of HPV-positive cells to therapeutic agents

3.2 Results

3.2.1 Confirmation of HPV status

Five HPV-positive and two HPV-negative HNSCC cell lines were obtained from various external research laboratories as detailed in section 2.2.1.1. Prior to undertaking further work, the HPV status of each of the cell lines was confirmed as follows.

3.2.1.1 Polymerase chain reaction

3.2.1.1.1 Consensus PCR

Using the GP5+/6+ primer sets which target the highly conserved region of the L1 gene of HPV, conventional PCR by agarose gel electrophoresis confirmed the absence of HPV in HPV-negative cell lines (UPCI-SCC 089 and UPCI-SCC 072). By contrast, the presence of HPV DNA was confirmed in the HPV-positive cell lines (UPCI-SCC 090, UPCI-SCC 152, UPCI-SCC 154, UD-SCC 2 and 93-VU-147T, Figure 3.1) as previously reported.^{291,292}

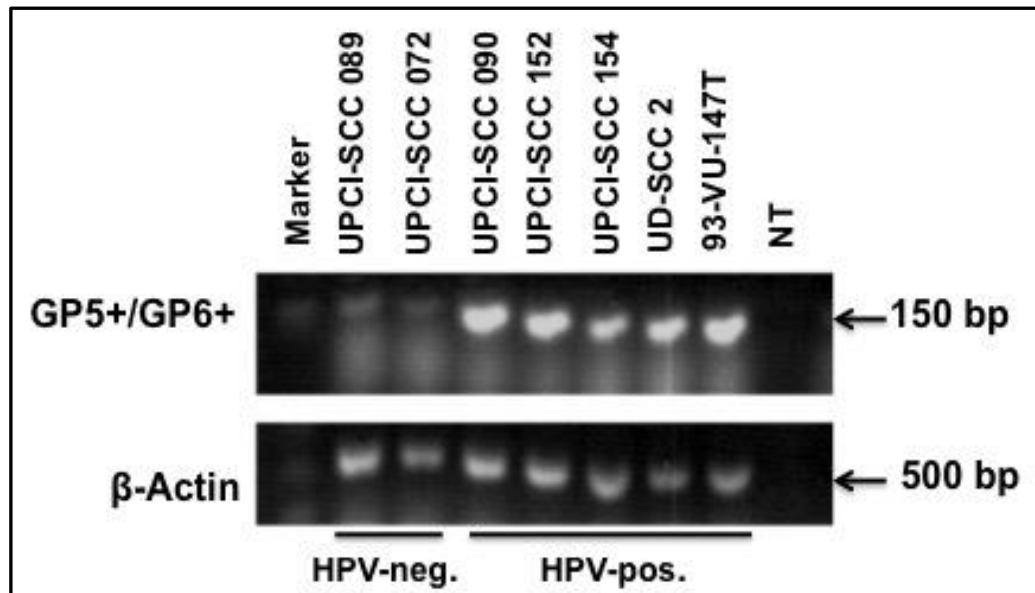


Figure 3.1. Conventional PCR for DNA in of HPV-negative and HPVpositive cell lines cell lines.

Amplification of HPV DNA in HPV-negative (lanes 1 and 2) and HPV-positive cell lines (lanes 3-7) using consensus primers GP5+/6+ (150 bp). Amplification of β -Actin (500 bp) and water (negative template, NT; lane 8) were used as a positive loading and negative controls, respectively.

3.2.1.1.2 Genotype-specific PCR

Following consensus primer PCR, genotype-specific PCR by agarose gel electrophoresis was undertaken using primers against HPV-16 E6 DNA as detailed in section 2.2.1.9. The results confirmed the presence of HPV-16 E6 DNA in all HPV-positive cell lines (Figure 3.2), as previously reported.^{185,186,279}

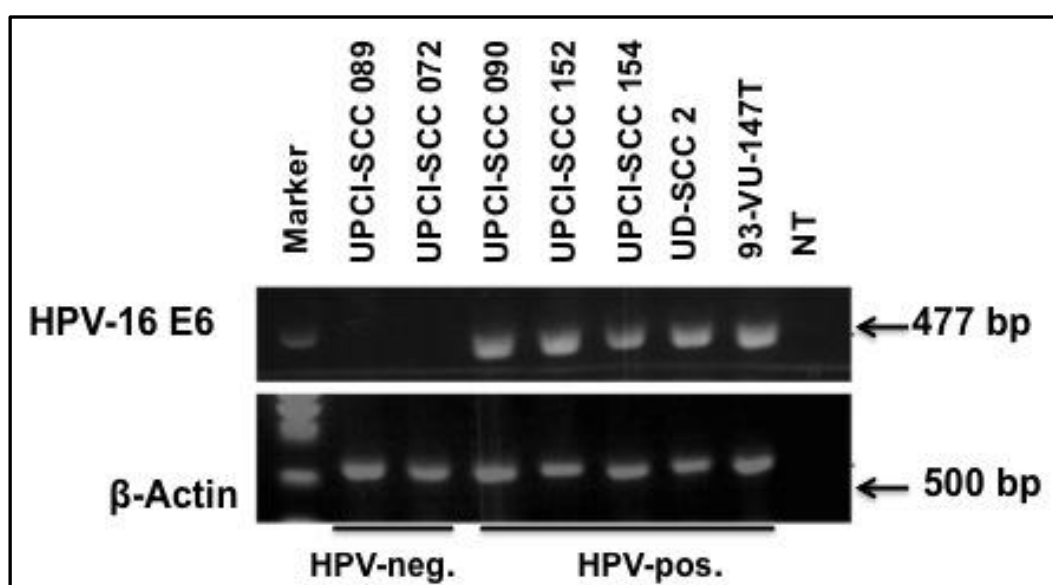


Figure 3.2. Standard PCR for HPV-16 E6 DNA in HPV-negative and HPV-positive cell lines.

Amplification of HPV-16 E6 DNA in HPV-negative (lanes 1 and 2) and HPV-positive cell lines (lanes 3-7) using HPV-16 E6 DNA primers (477 bp). Amplification of β-Actin (500 bp) and water (negative template, NT; lane 8) were used as a positive loading and negative controls, respectively.

3.2.1.2 HPV DNA in-situ hybridisation

Following consensus and genotype specific PCR, a further confirmation of HPV status was undertaken using DNA in-situ hybridisation (ISH). A cocktail of probes against high-risk types (HPV16, 18, 31, 35, 39, 51, 56, 58 and 66) as detailed in section 2.2.2.3 were used. The presence of integrated HPV DNA was confirmed in the HPV-positive cell lines UPCI-SCC 090, UPCI-SCC 152, UD-SCC 2 and 93-VU-147T (Figure 3.3, upper panel) by demonstration of strong punctate signal that co-localised with the nuclei with the exception of UPCI-SCC 154 that demonstrated weak punctate nuclear signal. By contrast, no signal was present in the HPV-negative cells (UPCI-SCC 089 and UPCI-SCC 072, Figure 3.3 upper panel).

The biological significance of the presence of HPV DNA was next evaluated. The viral oncoprotein E7 in high-risk HPV inactivates the retinoblastoma (pRb) tumour suppressor protein leading to overexpression of p16.²⁹³ The overexpression of p16 is a consistent feature of high-risk HPV infection in OPSCC and is therefore used as a sensitive surrogate marker for transcriptionally active virus.²⁹³

Immunohistochemical evaluation of cell lines demonstrated strong and diffuse nuclear and cytoplasmic staining of p16 in all HPV-positive cell lines but was either negative or weak staining in the HPV-negative cell lines (UPCI-SCC 089 and UPCI-SCC 072, respectively, Figure 3.3, lower panel).

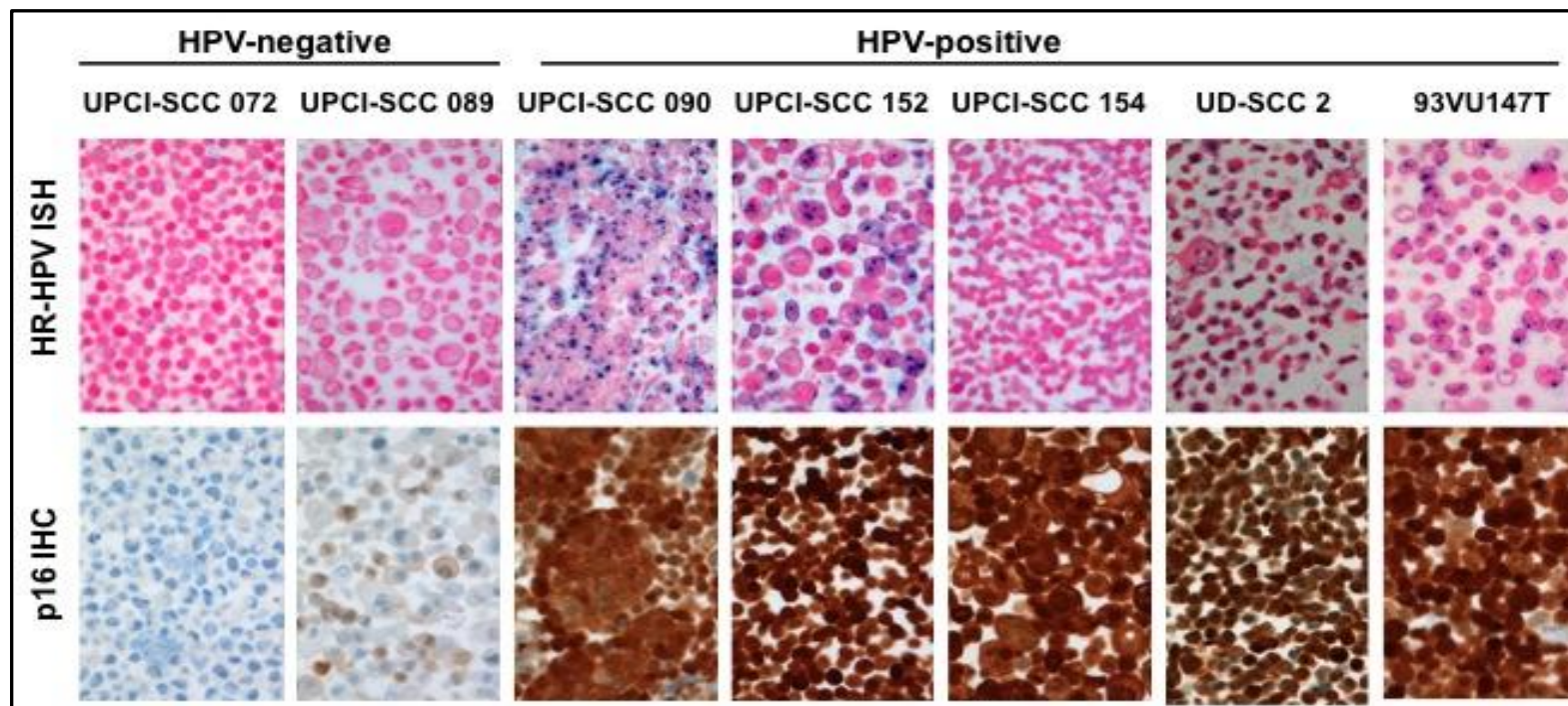


Figure 3.3. DNA in situ-hybridisation and immunohistochemistry.

High-risk HPV DNA in-situ hybridisation (upper panel) showing punctate nuclear staining in the HPV-positive cells (UPCI-SCC 090, UPCI-SCC 152, UPCI-SCC 154, UD-SCC 2 and 93-VU-147T), but lacking any signal in HPV-negative cells (UPCI-SCC 089 and UPCI-SCC 072). p16 immunohistochemistry (lower panel) showing diffuse strong nuclear and cytoplasmic staining in HPV-positive cell lines but is negative or weak in HPV-negative cell lines.

3.2.2 Growth rates of cell lines

Following confirmation of the HPV status, the proliferation rates of the cell lines were determined. This was performed in order to compare HPV-positive and HPV-negative proliferation rates and to determine whether compensatory seeding densities and temporal lag would be necessary for subsequent cell viability and clonogenic assays. The cells were counted for eight days after primary seeding of 5×10^4 cells per well (6-well plate) as detailed in section 2.2.1.8. From day 3 onwards, HPV-negative cell lines (UPCI-SCC089 and UPCI-SCC 072) demonstrated greater increase in growth rates compared to HPV-positive cell lines (UPCI-SCC090, UPCI-SCC152, UPCI-SCC154, UD-SCC2 and 93-VU-147T, Figure 3.4). Grouped comparison of HPV-negative with HPV-positive cell lines following day 3 showed a slower rate in the later group ($p \leq 0.001$, unpaired t-test).

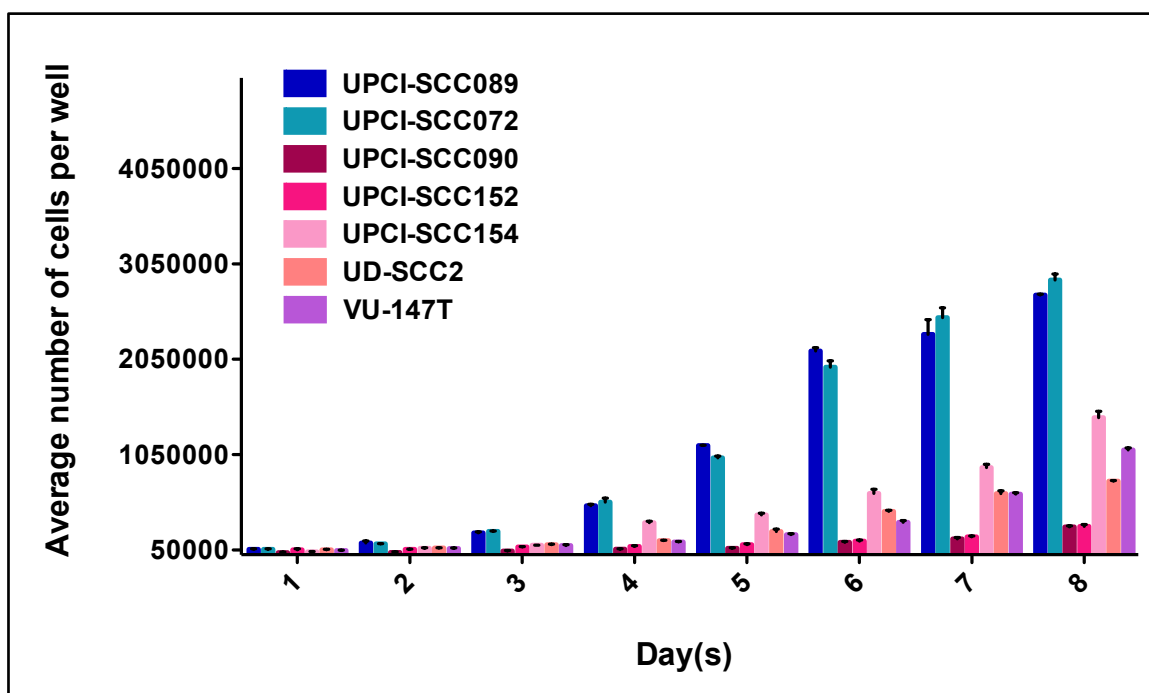


Figure 3.4. Cell lines growth rates.

Bar graph of growth rate analysis of two HPV-negative and five HPV-positive cell lines showing average number of cells per well following seeding of 5×10^4 cells, performed in triplicate, versus time in days. Error bars indicate standard deviation. Graph representative of three independent experiments.

3.2.3 Response to therapeutic agents

It is now generally accepted that patients with HPV-positive OPSCC have improved overall survival and lower incidence of loco-regional recurrence compared to patients with HPV-negative OPSCC.^{162,173} This may be explained at least in part by greater inherent sensitivity to therapeutic agents.²⁹⁴ Having undertaken preliminary characterisation of the cell lines, the next stage of this study was to develop an *in vitro* model of relative sensitivity to conventional therapeutic agents, namely radiation and cisplatin.

3.2.3.1 Cell viability following radiation

Cell viability assays were performed as detailed in section 2.2.1.13. In HPV-positive cells radiation resulted in cell viability ranging from 70%-80%, 60%-65% and 35%-40% at 2, 4 and 6 Gy, respectively. By contrast, HPV-negative cell lines showed cell viability ranging from 78-80%, 65-70% and 60-65% at 2, 4 and 6 Gy, respectively (Figure 3.5). HPV-positive cells demonstrated greater sensitivity to radiation compared to HPV-negative cells at all radiation doses ($p \leq 0.01$ for all HPV-positive versus HPV-negative cells at 2 Gy and all HPV-positive cells versus UPCI-SCC 072 at 6 Gy; $p \leq 0.001$ for all HPV-positive versus HPV-negative cells at 4 Gy and all HPV-positive cells versus UPCI-SCC 089 at 6 Gy, unpaired t-test).

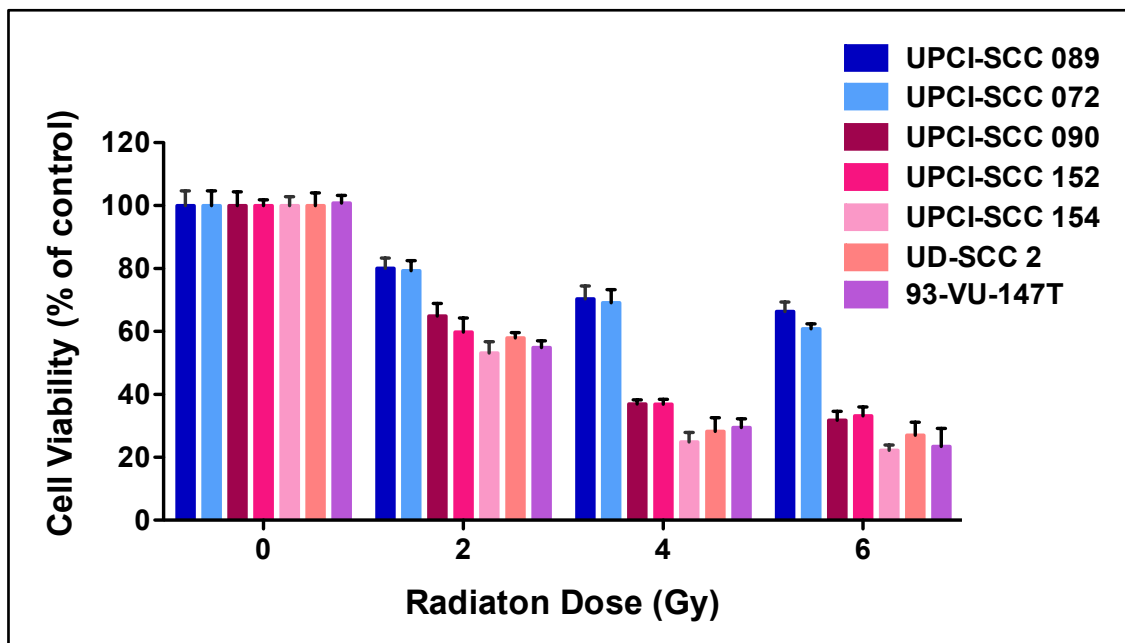


Figure 3.5. Cell viability of HPV-negative and HPVpositive cell lines following radiation.

Bar graph of cell viability expressed relative to control. Radiation was performed in triplicate at 2, 4 and 6 Gy. Cell viability was assessed by MTT assay 7 days following treatment. Bars represent average value from 6 wells normalised to untreated control cells. Error bars indicate standard deviation. This assay is representative of three independent experiments.

3.2.3.2 Clonogenic survival following radiation

Clonogenic survival assay has been considered as the reference standard for measurement of radio-sensitivity *in vitro* because, unlike cell viability assays, it determines the ability of a cell to proliferate indefinitely, thus retaining its reproductive capacity to form a sizeable colony.^{295,296} Therefore, in order to validate the results of Section 3.2.3.1, clonogenic survival assays were performed as detailed in section 2.2.1.14. Figure 3.6 demonstrates representative surviving clones in an HPV-positive (UPCI-SCC 090) and HPV-negative (UPCI-SCC 089) cell line. In HPV-positive cells radiation resulted in cell survival ranging from 50%- 60%, 35%- 40% and 10%- 25% at 2, 4 and 6 Gy, respectively. In contrast, HPV-negative cell lines showed cell survival ranging from 85%- 90%, 70- 85% and 45- 70% at 2, 4 and 6 Gy, respectively (Figure 3.7). HPV-positive cell lines demonstrated greater sensitivity to radiation compared to HPV-negative cell lines at all radiation doses ($p \leq 0.001$ for all HPV-positive versus HPV-negative cells at 2, 4 and 6 Gy, unpaired t-test).

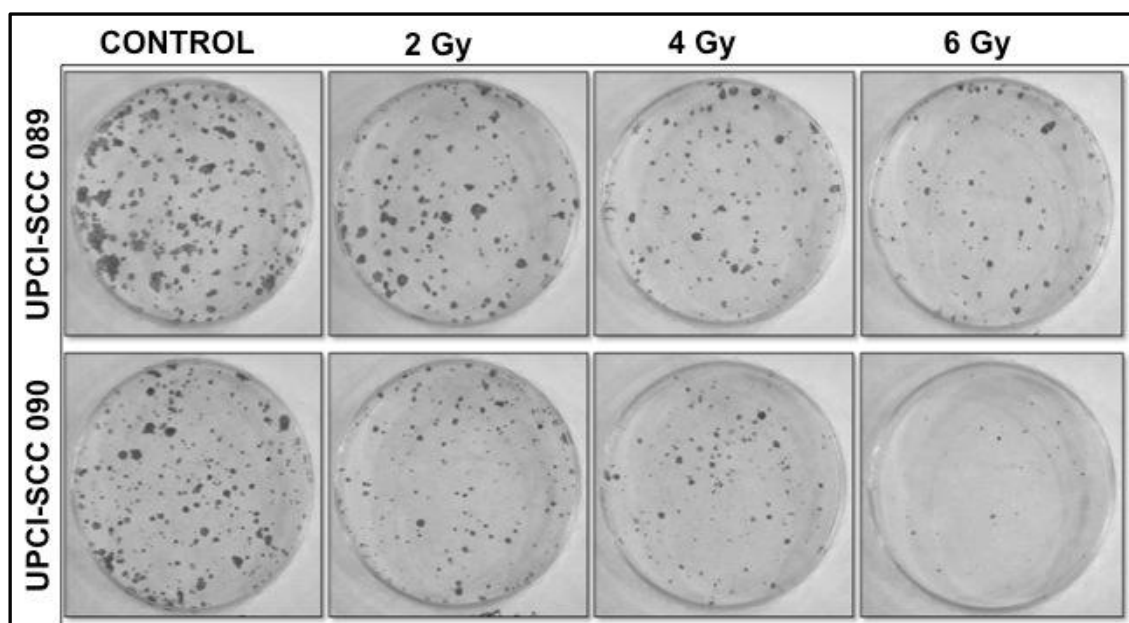


Figure 3.6. Representative photograph of clonogenic survival following radiation.

Representative photograph of colonies of HPV-negative (UPCI-SCC 089) and HPV-positive (UPCI-SCCC 090) cells at 2, 4 and 6 Gy. Controls were seeded without radiation. All dishes were fixed at 15 -25 days following radiation.

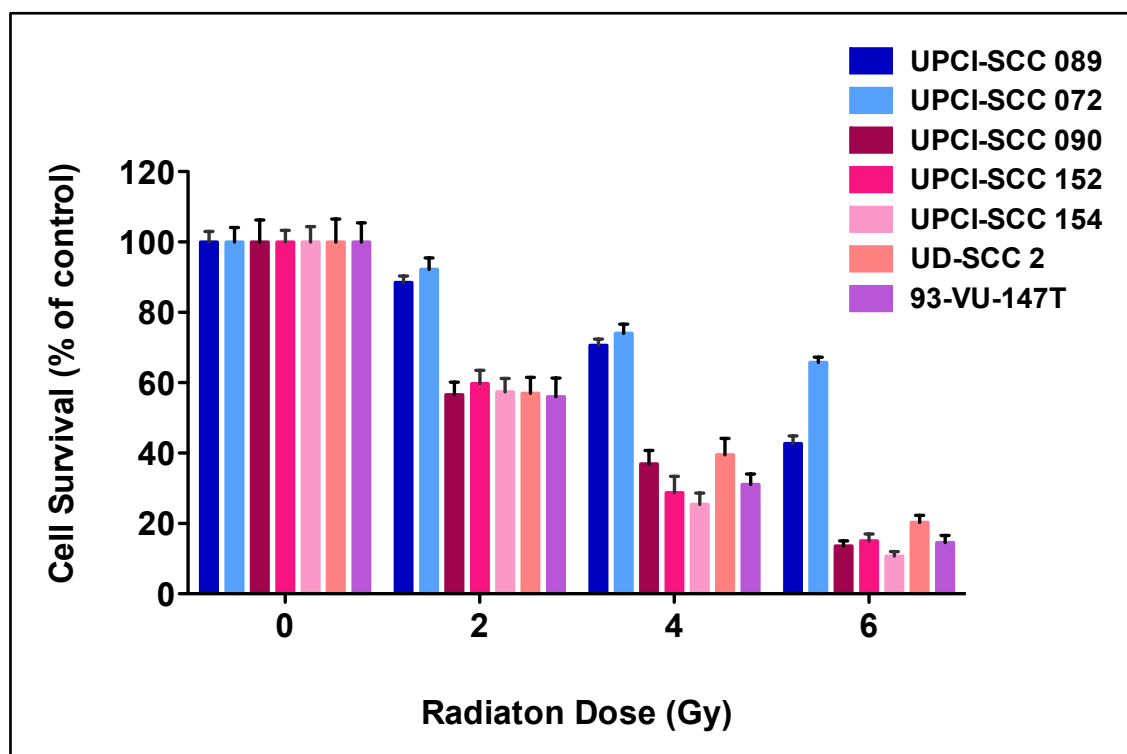


Figure 3.7. Cell survival of HPV-negative and HPVpositive cell lines following radiation.

Bar graph of clonogenic survival expressed relative to control. Radiation was performed in triplicate at 2, 4 and 6 Gy. Cell survival was assessed by clonogenic analysis 15-25 days following treatment. Bars represent average value from 3 dishes normalised to untreated control cells. Error bars indicate standard deviation. This assay is representative of three independent experiments.

3.2.3.3 Cell viability following cisplatin

The results of section 3.2.3.1 and 3.2.3.2 demonstrated HPV-positive cell lines to be more radiosensitive compared to HPV-negative HNC cell lines. Since concomitant chemo-radiation is the current treatment standard for OPSCC, this study also sought to determine whether HPV-positive cells showed similar relative sensitivity to cisplatin. Cell viability assays were performed as detailed in section 2.2.1.13. Cisplatin was used at various concentrations of 2.5, 5 and 10 µg/ml for 24 hours, resulting in cell viability ranging from 60%-85%, 40-50% and 25-30% at 2.5, 5 and 10 µg/ml respectively in HPV-positive cell lines. In contrast, HPV-negative cell lines showed cell viability ranging from 80%-90%, 65- 70% and 55- 60% at 2.5, 5 and 10 µg/ml respectively (Figure 3.8). HPV-positive cell lines demonstrated greater sensitivity to cisplatin compared to HPV-negative cell lines at 5 and 10 µg/ml of cisplatin ($p \leq 0.001$ for all HPV-positive versus HPV-negative cells). At 2.5 µg/ml no significance in survival was observed between UPC-SCC 089 and HPV-positive cell lines however the sensitivity in between UPCI-SCC 072 and HPV-positive cell lines was statistically significant ($p \leq 0.001$, unpaired t-test).

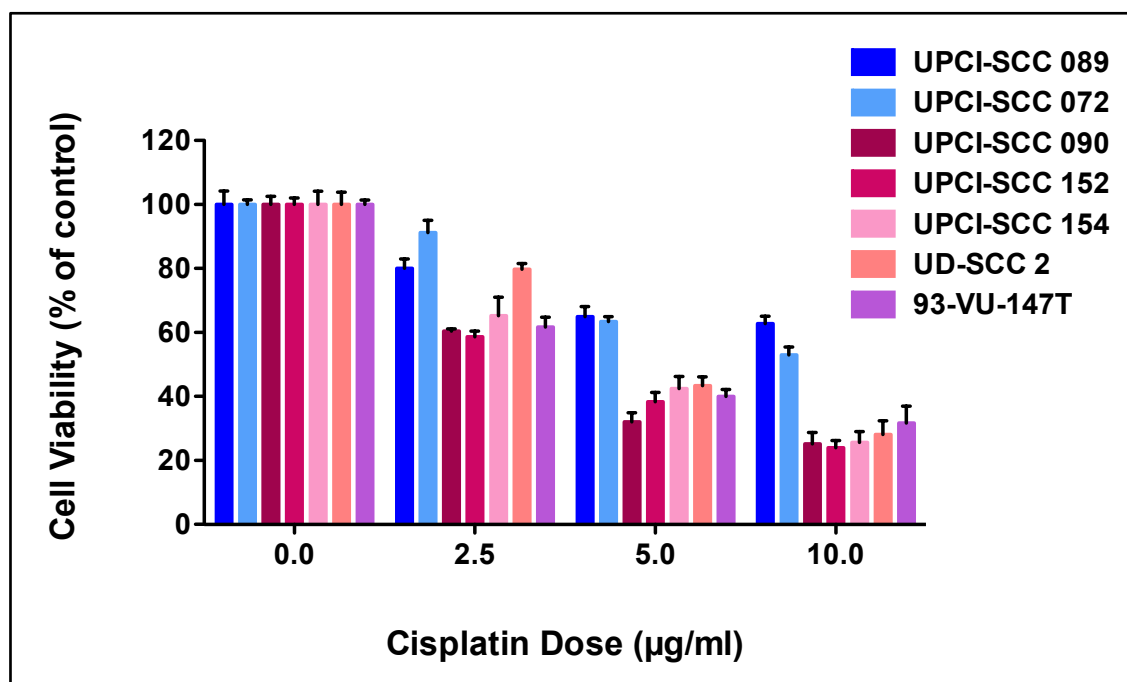


Figure 3.8. Cell viability of HPV-negative and HPVpositive cell lines following cisplatin.

Bar graph of cell viability expressed relative to control. Cisplatin chemotherapy was performed at 2.5, 5 and 10 µg/ml. Cell viability was assessed by MTT assay 7 days following treatment. Bars represent average value from 6 wells normalised to untreated control cells. Error bars indicate standard deviation. This assay is representative of three independent experiments.

3.3 Discussion

There is now robust evidence that patients with HPV-positive OPSCC have a significantly favourable response to chemo-radiation compared to HPV-negative counterparts but the mechanism to explain these observations are largely unknown. Furthermore, there are sparse *in vitro* models available to investigate potential mechanisms, all with variable and sometimes conflicting results.

Therefore, in order to elucidate potential mechanisms of improved response in HPV-positive OPSCC to current therapeutic agents, it was first necessary to develop a reliable and reproducible *in vitro* model.

3.3.1 Characterisation of HPV-positive and HPV-negative cell lines

In this study, all cell lines were obtained from external laboratories, detailed in section 2.2.1.1. Therefore in the first instance, it was necessary to confirm the HPV status of all cell lines. HPV status of all cell lines used in this study was in accordance with previously published reports.^{276,277,281,283} The HPV status of the HPV-positive cell lines was confirmed to contain HPV-16 DNA by PCR and viral integration was confirmed by punctate staining pattern by DNA in-situ hybridization. All HPV-positive cell lines showed increased positivity of integrated HPV DNA with the exception of UPCI-SCC 154, which demonstrated weak punctate staining. The equivocal DNA ISH signal in UPCI-SCC 154 has also previously been observed by fluorescence in-situ hybridisation (FISH) and may be explained by presence of a low viral load (viral load=1) in this cell line compared to a much higher viral load (viral load=739) in UPCI-SCC 090

cells.²⁹⁷ Nevertheless, as with all other HPV-positive cell lines, UPCI-SCC 154 demonstrated p16 over-expression, confirming presence of transcriptionally active high-risk HPV oncogenes despite a low viral copy number.^{193,298}

As part of the characterisation of cell lines and to determine whether it is necessary to compensate for variation in proliferation indices in subsequent experiments, growth rates were evaluated for all cell lines. The current study found increased proliferation rates in HPV-negative cell lines compared to the HPV-positive cell lines, suggesting a link with the clinical observations where HPV-positive tumours are characterised by a higher nodal metastasis rate and lower T-stage, implying a relatively low proliferation rate despite enhanced metastatic capacity.⁶⁵ This study confirms previous findings by Nagel *et al* (2013) who showed similar significantly lower growth rate of HPV-positive HNSCC cell lines compared to HPV-negative HNSCC cell lines.²⁹⁹

3.3.2 Response of HPV-positive and HPV-negative cell lines to conventional therapeutic agents

3.3.2.1 Radiosensitivity

The results of the present chapter demonstrated increased relative radiosensitivity of HPV-positive OPSCC cells compared to site-matched HPV-negative controls, thereby establishing an *in vitro* model that is concordant with clinical observations. Interestingly, although the HPV-positive cell line 93-VU-147T was derived from the floor of the mouth, these cells were also relatively radiosensitive compared to HPV-negative OPSCC cells. There are several

recent studies in the literature in agreement with the current findings.^{179,184-186,193,300-303} While a comprehensive and integrated explanation for these observations is still lacking, emerging data raise the possibility of potential molecular pathways. For example, Gupta *et al* (2009) showed correlation between increased sensitivity to radiation and decreased expression of phosphorylated AKT and increased expression of phosphorylated phosphatase and tensin homolog (PTEN) in HPV-positive HNSCC cell lines. PTEN provides negative regulation of the PI3K-AKT pathway, the pathway is generally upregulated in head and neck cancers.^{304,300} Furthermore, inactivation of mTOR, a downstream target of the PI3K-AKT pathway, in HPV-positive HNSCC cell lines led to further radiosensitivity indicating that an attenuated PI3K-AKT pathway may be, at least in part, responsible for this improved response in HPV-positive HNSCC cells.^{305,306}

Although the capacity of the cell to detect DNA damage and to take over its repair could be responsible for increased radiosensitivity, the tumour's oxygenation status might also be a factor for increased response to radiation.³⁰⁷ The suggestion that HPV-positive HNSCC is less hypoxic compared to HPV-negative counterparts may contribute to increased radiosensitivity of these tumours.²⁰⁰ It has been also shown that under hypoxic conditions HPV-positive HNSCC demonstrate similar upregulation of hypoxia responsive genes and displays increased resistance to radiation similar to HPV-negative tumours regardless of the HPV status.^{301,308,309} Hence, it might be suggested that the improved prognosis of HPV-positive HNSCC may be partly due to differences in hypoxic fraction.

By contrast to the majority of reported studies in the literature demonstrating increased radiosensitivity, there are occasional studies indicating a dissimilar trend, namely HPV-positive HNSCC cell lines being either more resistant or equally radiosensitive to HPV-negative cells.^{299,310,311} This discrepancy may be explained by investigations carried out by groups using cell lines without confirming the presence of integrated HPV DNA in the cells, examining potential cell lines with mixed population of cells exhibiting different biological and genetic properties or by selection of clones with non-viral DNA containing clonogen. Contrary findings could also be explained by loss of viral DNA and the presence of viruses in latent or non-producing state. Other factors may include cell culture contamination, different handling techniques and methodologies used to assess cell lines.¹⁸⁴ A growing body of literature indicated that high passage number affects cell line characteristics and hence the results over time.^{312,313} Moreover, some studies have directly compared HPV-positive oropharyngeal cell lines with non-oropharyngeal HPV-negative counterparts and this may lead to discrepant results since the latter is less likely to be a suitable control.

The tumour microenvironment may also play a part in the relative radiosensitivity of HPV-positive cells. This has been suggested by Spanos *et al* (2009) who showed a dependence of increased radiosensitivity in HPV-positive cells on an intact immune response.³¹⁰ It is also been hypothesised that immune cells produced in reaction to E6 and E7 encoded antigens, have a positive impact on disease outcome in early development of the

tumour.³¹⁴ Further studies are therefore necessary to evaluate the interplay between the

innate tumour characteristics and the tumour microenvironment in the improved clinical outcome of HPV-positive HNSCC.

3.3.2.2 Chemosensitivity (cisplatin)

Cisplatin is currently used as a concomitant therapeutic agent for the management of OPSCC and acts by causing DNA crosslinking leading to apoptosis.³¹⁵ However, data pertaining to the relative response of HPV-positive HNSCC cell lines to cisplatin is scarce and variable.

In accordance with findings of the present study, Chen *et al* (2000) showed an increased sensitivity of HPV-positive cell lines to treatment with cisplatin compared to HPV-negative HNSCC cell lines.³¹⁶ By contrast to this work, Spanos *et al* (2009) and Nagel *et al* (2013) showed increased resistance while Kawakami *et al* (2013) demonstrated no effect to cisplatin in HPV-positive compared to the HPV-negative HNSCC cell lines.^{299,310} Interestingly, Spanos *et al* (2009) showed resistance of HPV-positive cell lines when treated with cisplatin *in vitro* but found that HPV-positive tumour xenografts were more sensitive to the same agent when treated *in vivo*. However, they used very low doses of cisplatin (0.025 -1.0 µg/mL) and counted colonies with more than 15 cell, which may be a cause to explain differences with the present study.³¹⁰

Although Nagel *et al* (2013) used increased dosages of cisplatin (10^{-1} - 10^3 µM) compared to the current study, the differences in observations might be caused by their use of only four HPV-positive cell lines and compared them to a large

panel (fourteen) of non-oropharyngeal cell lines, the latter being a biologically heterogeneous and non-site-matched control group. By contrast, all cell lines in this study were of oropharyngeal origin, with the exception of 93-VU-147T, and controls were therefore likely to be a more suitable comparison group.²⁹⁹ Also in contrast to the current study, Kawakami *et al* (2013) compared response of cisplatin between HPV-positive and HPV-negative oropharyngeal cell lines through clonogenic assay and showed no effect to cisplatin even at higher doses (10^{-1} - $10^3\mu\text{M/L}$) and longer exposure (seventy-two hours), but differences in culture conditions cannot be excluded.

3.4 Limitations

The current study established an *in vitro* model of relative sensitivity to radiation and cisplatin in HPV-positive HNSCC cell lines compared to HPV-negative HNSCC cell lines. However, there are several limitations to the current section of this study.

The currently available repertoire of HPV-positive cell lines and site-matched HPV-negative cell lines was a limitation. Primary culture and generation of immortalised lines is acknowledged as being particularly challenging and may reflect the inherent susceptibility of these tumours to cell death. As such, this study sought to obtain HPV-positive cells from external laboratories. The selected panel of HPV-positive cells included non-orpharyngeal origins, namely hypopharynx, floor of mouth and cervical nodal metastasis. Furthermore, several HPV-positive were derived from patients who were tobacco smokers in contrast to the clinical situation where the majority of HPV-positive OPSCC patients do not smoke. However, until more suitably representative cells become more widely available, all *in vitro* investigations into the mechanisms of HPV-positive HNC are limited to laboratory experiments in these few cell lines. This study utilised two HPV-negative cell lines as controls. Ideally, a similar or greater number HPV-negative cell lines should be used as controls for the five HPV-positive cell lines evaluated in this study. However, after careful searching of the literature and publicly available databases, only two HNC cancer cell lines matched the criterion of having been derived from the oropharynx. The relative paucity of cell lines investigated raises the possibility that the observations of

increased resistance to radiation and cisplatin may be due to cell line variation rather than the inherent biological properties of HPV-negative disease.

Nevertheless, omission of control cell lines not derived from oropharyngeal sites remains a necessity.

The extrapolation of observations from radiation experiments on monolayer of cultured cells is another potential limitation. Evaluation of cells grown in monolayer fails to consider the effects of diminishing margin of target volume of radiation. Furthermore, these experiments do not factor the role of the tumour microenvironment, including stromal and host immune responses following radiation. While the current model provides the initial foundation to study radiation and cisplatin effects in HPV-positive OPSCC, further work is required, namely responses to therapeutic agents of these agents *in vivo* in orthotopic animal models using concomitant and/or induction regimes.

Due to constraints of time and other resources, only limited characterisation of cell lines were undertaken. Ideally, comparative genomic and expression array analysis would have provided more in-depth information of the genotypic differences between HPV-positive and HPV-negative cells used in this study. Downstream cellular responses to radiation and/or cisplatin, including DNA damage pathways, may have been elucidated which may have provided a basis for more tailored investigation of these effects. Similarly, prior to evaluating the effect of targeted therapy described in subsequent chapters it may have been important to characterise the cell lines in relation to death receptor and the ErbB family of receptors.

Effects of radiation and cisplatin in the current study was evaluated using cell viability and clonogenic survival assays. Determination of cell cycle fraction by flow cytometry and the proportion of apoptosis by Annexin V or cleaved caspased-3 assays would have provided more robust data to indicate the possible mechanisms of sensitivity or resistance to radiation or cisplatin.

3.5 Conclusion

In summary, the current study was able to establish an *in vitro* model of relative sensitivity to radiation and cisplatin in HPV-positive HNSCC cell lines compared to HPV-negative HNSCC cell lines. All HPV-positive cell lines (five in total) known to be available at the commencement of the study were utilised to establish this model. Previously published models did not simultaneously test all HPV-positive cells. Since the commencement of this study, several novel HPV-positive cell lines have been reported.^{317,318} Moreover, the control cells used in this study were specifically selected due to their oropharyngeal origin. To my knowledge, no previously published models used site-specific controls.

**Chapter 4 - The role of p53 and HPV-16 E6 in the
response of head and neck cancer cell lines to
conventional therapeutic agent**

4.1 Introduction

The previous chapter detailed the development of an *in vitro* model of relative sensitivity to conventional therapeutic agents in HPV-positive head and neck squamous cell carcinoma (HNSCC) cell lines. HPV-positive HNSCC cell lines were more sensitive to radiation and cisplatin compared to the HPV-negative cells. Having established a suitable model of improved response of HPV-positive HNSCC to conventional therapeutic agents, the next stage of this study was to investigate the possible underlying mechanisms of increased sensitivity.

Two key potential targets were chosen for further evaluation in the current study, namely p53 and HPV-16 E6. p53 was selected because of its central role in regulating cellular responses to stress. Following DNA damage, hypoxia or oncogene activation, several signalling pathways converge on this tumour suppressor gene, which is responsible for the induction of cell cycle arrest, senescence or apoptosis.³¹⁹ p53 has been reported to be mutated in a majority of HNSCC and the existence of mutant p53 in these tumours promotes resistance to cisplatin and radiation treatment.³²⁰ An important clinical finding is that the majority of HPV-16 positive OPSCC tissue samples contain wild-type p53 and it has been proposed that functional p53 may, at least in part, be responsible for the improved response to treatment in these patients.^{321,322}

The p53 tumour suppressor gene is a nuclear phosphoprotein that transcriptionally regulates the expression of a number of target genes including p21.³²³ p21 binds to the G1-S/CDK (CDK4/6, CDK2 and CDK1) complexes (molecules important for the G1/S transition in the cell cycle) inhibiting their activity.³²⁴ When p21 is complexed with CDK2, the cell cannot continue to the next stage of cell division.³²⁵

HPV-16 E6 was selected for further study because of its direct effect of p53 inactivation. The oncoprotein interferes with p53 protein by degrading it via the ubiquitin-proteasome system resulting in disturbance of cell cycle control, which finally leads to increased tumour cell growth.^{326,327} Although high-risk HPV oncoprotein E6 targets p53 for degradation, there is evidence that the latter could be reactivated in response to stress in cells with wild-type p53.^{328,329}

The objective of this part of the study was to evaluate the role of p53 and HPV16-E6 in the increased response of HPV-positive HNSCC cell lines to radiation and cisplatin.

4.2 Results

4.2.1 Baseline expression of p53

The p53 gene is frequently mutated in HNC as a whole.³³⁰ However, almost all HPV-positive OPSCC contain wild type p53.³³¹ Prior to elucidating the functional role of p53 in HPV-positive HNSCC cell lines it was important to initially establish the baseline expression of p53 in the HNSCC cell lines used in this study.

Immunohistochemistry

Immunohistochemical evaluation of cell lines demonstrated negative or weak p53 staining in all HPV-positive cell lines with the exception of 93-VU-147T that showed strong and diffuse p53 staining. On the contrary staining was either intense or moderate in the HPV-negative cell lines (UPCI-SCC 072 and UPCI-SCC 089 respectively, Figure 4.1).

Western Blot

In order to confirm the p53 immunohistochemical staining, protein levels were additionally assessed by western blots. The latter confirmed the immunohistochemistry findings. HPV-negative cells demonstrated moderate (UPCI-SCC 089) and strong (UPCI-SCC 072) p53 protein expression. With the exception of 93-VU-147T, all HPV-positive cell lines showed weak or undetectable p53 protein expression (Figure 4.2 A).

Densitometry quantification of p53 protein expression was undertaken using image J analysis. 93-VU-147T and UPCI-SCC 072 showed increased p53/ β -actin ratio when compared to UPCI-SCC 089 and all other HPV-positive cell lines that showed low or no protein levels (Figure 4.2 B). p -value was determined by unpaired t-test comparing HPV-positive with individual HPV-negative cell lines separately ($p \leq 0.01$ for UPCI-SCC 089 versus UD-SCC 2 cells and $p \leq 0.001$ for each of the HPV-negative cell lines versus UPCI-SCC 090, UPCI-SCC 154, UPCI-SCC 152 UD-SCC 2 and 93-VU-147T). There was no significant difference between UPCI-SCC 072 and 93-VU-147T ($p=0.0568$).

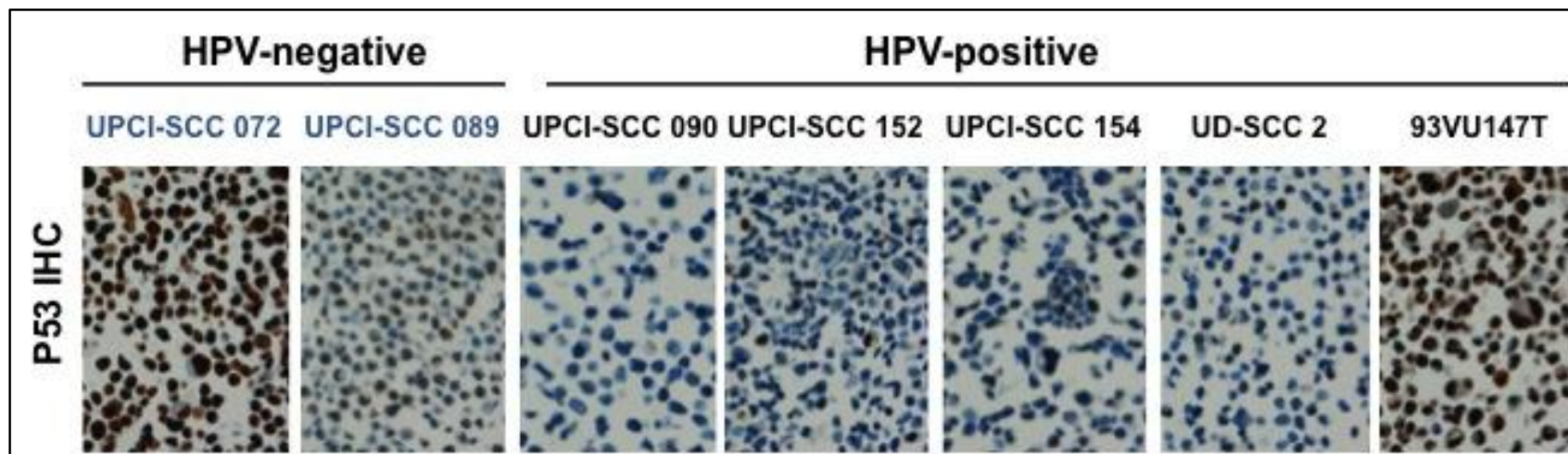


Figure 4.1. p53 immunohistochemistry.

Comparison of p53 immunostaining between HPV- negative (UPCI-SCC 072 and UPCI-SCC 089) and HPV-positive (UPCI-SCC 090, UPCI-SCC 152, UPCI-SCC 154, UD-SCC 2 and 93-VU-147T) on FFPE cell pellet sections. Original magnification x100.

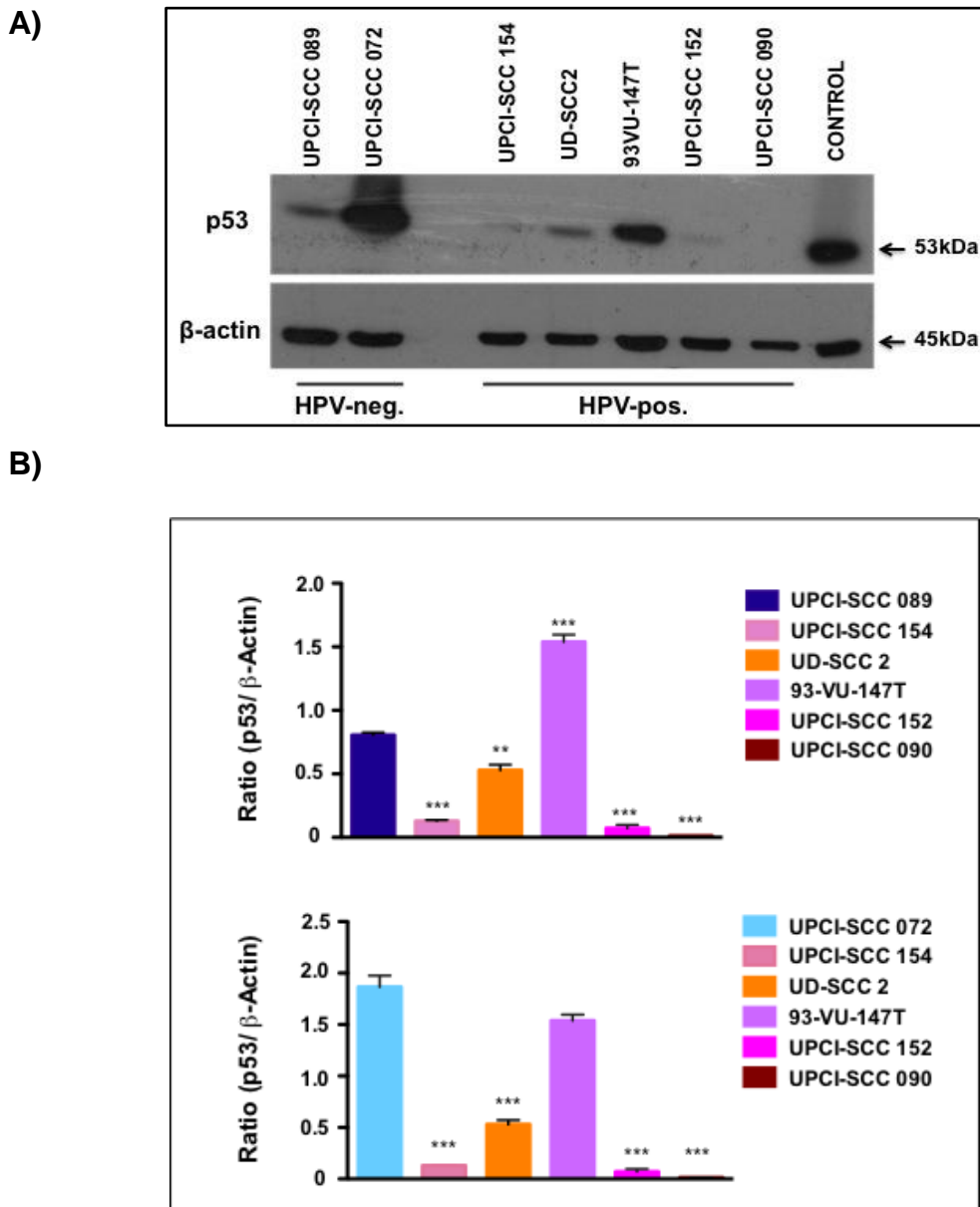


Figure 4.2. p53 baseline expression by western blot.

A) Expression difference of p53 in cells of UPCI-SCC 072 and UPCI-SCC 089 (HPV-negative) and UPCI-SCC 090, UPCI-SCC 152, UPCI-SCC 154, UD-SCC 2 and 93-VU-147T (HPV-positive) cell lines by western blot. Arrows indicate molecular weight of the pre-stained protein ladder. HNSCC cell line HN5 with mutated p53 was used as a positive control. β -actin was used as a loading control. The above is representative of two independent experiments. B) The intensity of the bands shown in western blot (Figure 4.2 A) was quantified by comparing all HPV-positive cell lines with HPV-negative cell line separately in relation to β -actin level using Image J. p -value was determined by unpaired t-test (* p <0.05, ** p <0.01 and *** p <0.001).

4.2.2 p53 stabilisation

In most tobacco and alcohol-related tumours, the tumour suppressor protein p53 is mutated and inactive, while the p53 in HPV-infected tumours is wild-type (wt) and structurally intact. Although, the protein is degraded by the HPV oncoprotein E6,^{249,332} researches indicate that persistent treatment with certain therapeutic agents can suppress E6 oncogenes, allowing the p53 to carry out its normal function.³³³ Therefore, the presence of the wild-type p53 and the lower mutation rate observed in HPV-derived SCC may enable these tumour cells to undergo an intact apoptotic response when treated with radiotherapy and/or chemotherapy, resulting in a greater sensitivity.³³⁴

In order to evaluate the role of p53 in the relative sensitivity of HPV-positive cell lines in the current *in vitro* model, two cell lines i.e. UPCI-SCC 089 (HPV-negative) and UPCI-SCC 090 (HPV-positive) were selected for further study. UPCI-SCC 089 (HPV-negative) was selected because it demonstrated consistent resistance to radiation and cisplatin while being sensitive to TRAIL and Cetuximab. Conversely, UPCI-SCC 090 (HPV-positive) was selected because it demonstrated consistent sensitivity to radiation and cisplatin while being resistant to TRAIL and Cetuximab. Time constraints limited the study to these two cell lines only.

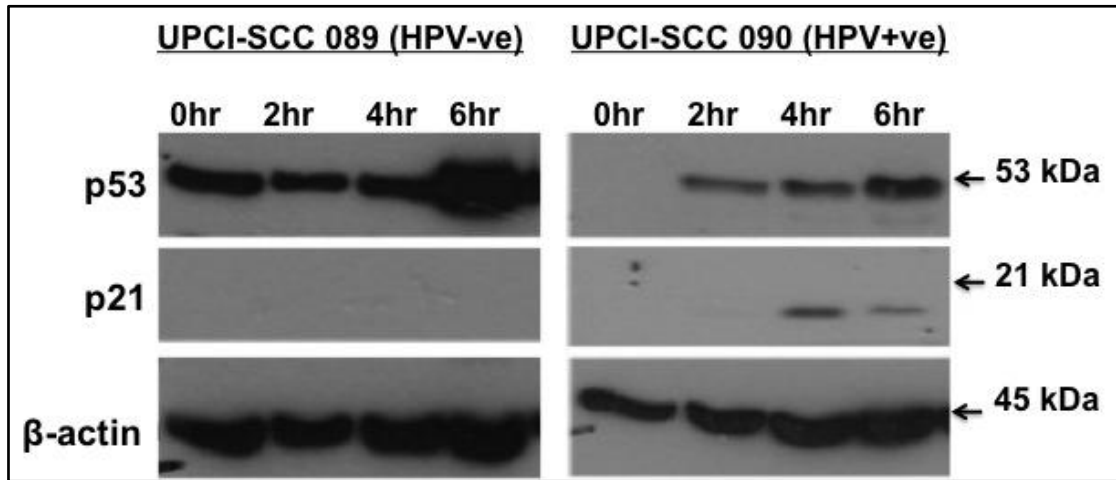
4.2.2.1 p53 stabilisation in response to radiation

UPCI-SCC 089 (HPV-negative) and UPCI-SCC 090 (HPV-positive) cells were treated at 4 Gy and harvested at 2, 4 and 6 hours followed by lysate preparation as described in section 2.2.3.2. Western blot analysis of UPCI-SCC 089 cells following radiation showed almost no alteration in p53 from baseline untreated levels (Figure 4.3 A). By contrast, a time-dependent increase of p53 protein expression was observed in UPCI-SCC 090 cells following radiation.

Furthermore, increased p53 protein expression was accompanied by induction of p21 in HPV-positive cells at 4 and 6 hours after radiation confirming functional activity of p53 (Figure 4.3 A).

Densitometry quantification of p53 protein expression by image J analysis showed that p53 protein levels in UPCI-SCC 089 did not appear to be regulated by radiation therapy at all time points. By contrast HPV-positive cell line (UPCI-SCC 090) showed time dependent increase in p53 and p21/ β -actin ratio compared to the untreated sample (undetectable). *p*-value was determined by unpaired T-test, significant results were appreciated when comparing treated cell lines at different time points with their respective untreated controls (Figure 4.3 B).

A)



B)

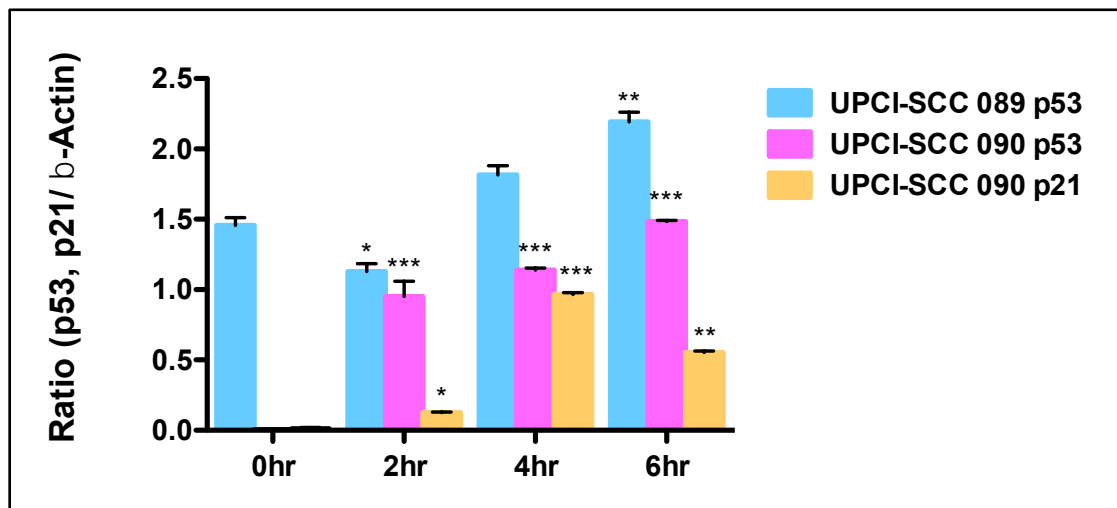


Figure 4.3. Stabilisation of p53 following radiation.

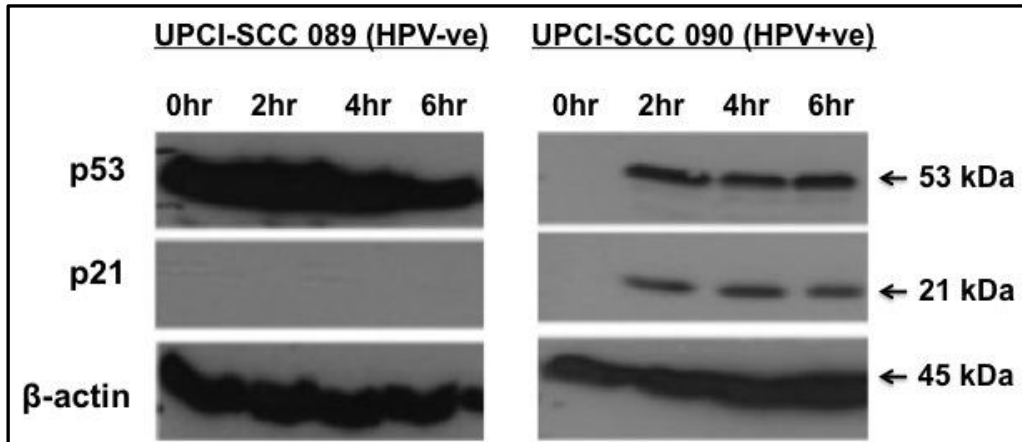
A) Western blot analysis for p53 and p21 in HPV-negative (UPCI-SCC089) and HPV-positive (UPCI-SCC090) cell lines following treatment with radiation (4Gy) at 2, 4 and 6 hours. Arrows indicate molecular weight of the pre-stained protein ladder. Western blot is representative of two independent experiments. B) Quantitative analysis of p53 and p21 induction at indicated times shown in western blot (Figure 4.3 A) after radiation in relation to β -actin level compared to untreated controls using the Image J programme. Error bars indicate standard deviation. p -value was determined by unpaired T-test (* p <0.05, ** p <0.01 and *** p <0.001).

4.2.2.2 p53 stabilisation in response to cisplatin

HPV-negative (UPCI-SCC 089) and HPV-positive (UPCI-SCC 090) cells were treated by 10 µg/ml of cisplatin and harvested at 2, 4 and 6 hours. Lysates were prepared as described in section 2.2.3.2. Western blot analysis of UPCI-SCC 089 cells following treatment showed almost no alteration in p53 from baseline untreated levels. By contrast a time-dependent increase in the levels of p53 was observed in UPCI-SCC 090 following radiation compared to untreated control. Furthermore, increased p53 protein expression was accompanied by induction of p21 at 4 and 6 hours following cisplatin treatment confirming functional activity of p53 (Figure 4.4 A).

Densitometry quantification of p53 protein expression by image J analysis showed that p53 protein levels in UPCI-SCC 089 did not appear to be regulated by cisplatin therapy at all time points. HPV-positive cell line (UPCI-SCC 090) showed time dependent increase in p53 and p21/β-actin ratio compared to the untreated sample (undetectable). *p*-value was determined by unpaired T-test (**p*<0.05, ***p*<0.01 and ****p*<0.001) comparing treated cell lines at different time points with their respective untreated controls (Figure 4.4 B).

A)



B)

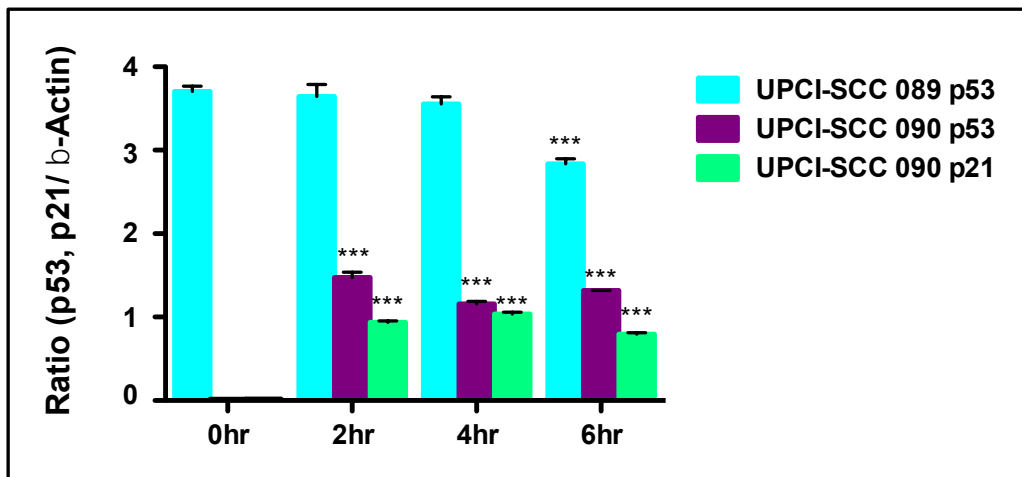


Figure 4.4. Stabilisation of p53 following cisplatin.

A) Western blot analysis for p53 and p21 in HPV-negative (UPCI-SCC089) and HPV-positive (UPCI-SCC090) cell lines following treatment with cisplatin (10μg/ml) at 2, 4 and 6 hours. Arrows indicate molecular weight of the pre-stained protein ladder. Western blot is representative of two independent experiments. B) Quantitative

analysis of p53 and p21 induction at indicated times shown in western blot (Figure 4.4 A) following cisplatin in relation to β-actin level compared to untreated controls using the Image J programme. Error bars indicate standard deviation. *p*-value was determined by unpaired t-test (**p*<0.05, ***p*<0.01 and ****p*<0.001).

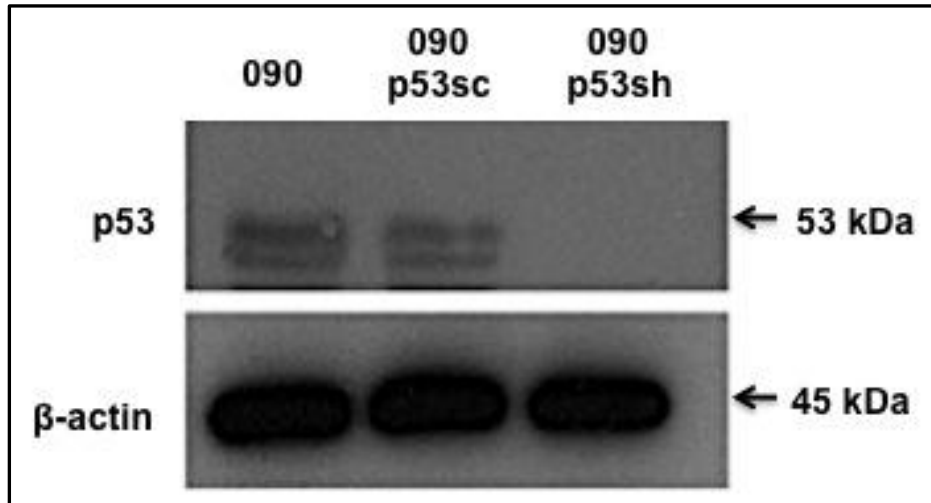
4.2.3 Effect of p53 attenuation to radiation and cisplatin

The results of section 4.2.2 showed stabilisation of p53 protein in HPV-positive cells (UPCI-SCC 090) following treatment with radiation and cisplatin accompanied by the induction of the p53 target protein p21. In order to confirm that the relative sensitivity of HPV-positive cells to radiation and cisplatin is mediated through p53, the functional effect of p53 attenuation was next evaluated.

4.2.3.1 Attenuation of p53 in HPV-positive cells

p53 in HPV-positive cells (UPCI-SCC 090) was attenuated through stable transfection with p53shRNA as detailed in section 2.2.4. p53 protein was undetectable in cells stably transfected with p53shRNA (090 p53sh). By contrast, p53 was detectable in the parental (UPCI-SCC 090) and control cells stably transfected with scrambled control (090 scr control). Unaffected β -actin levels with either construct also established the specificity of p53 reduction (Figure 4.5 A).

A)



B)

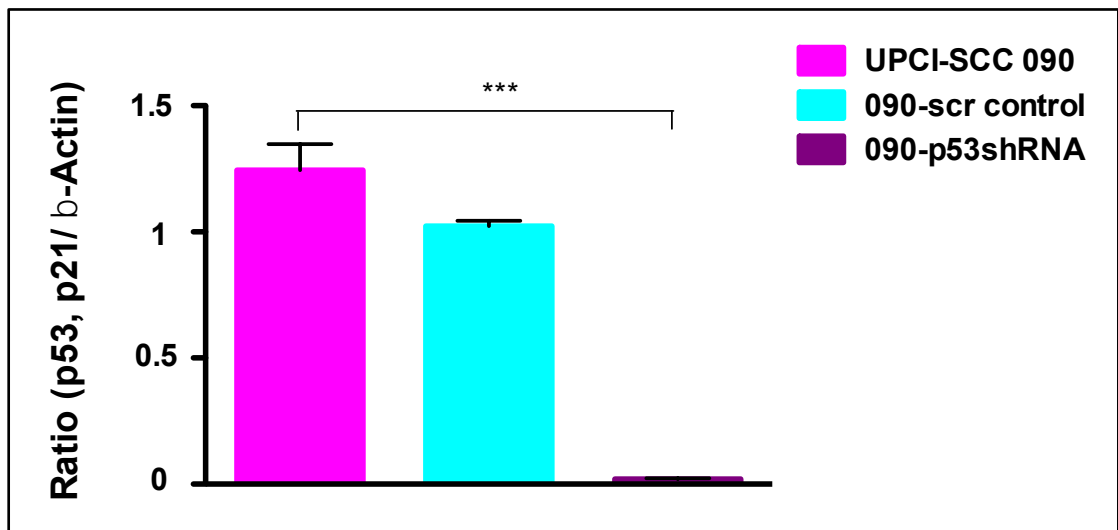


Figure 4.5. Attenuation of p53 in HPV-positive cells.

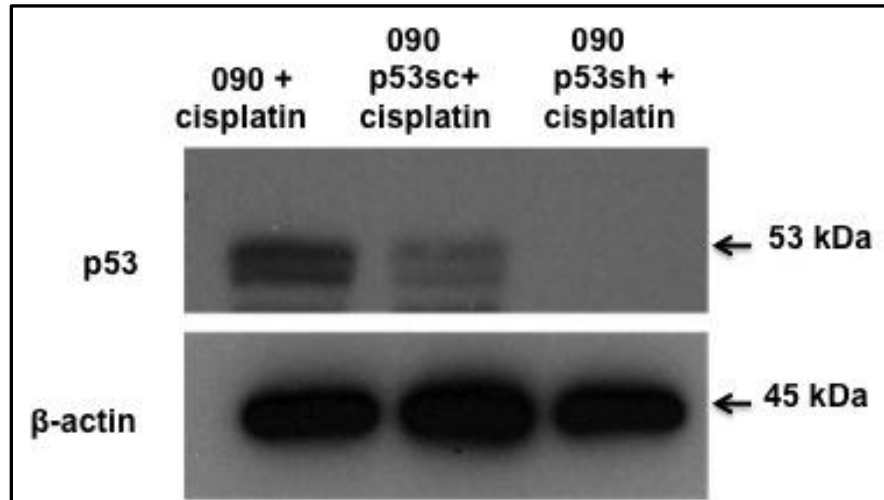
A) Western blot analysis of p53 in HPV-positive cell line UPCI-SCC 090 (090), UPCI-SCC 090 scramble control (090-scr control) and UPCI-SCC 090 p53 attenuated cells (090-p53sh). Arrows indicate molecular weight of the pre-stained protein ladder.

Western blot is representative of two independent experiments. B) Quantitative densitometry of p53 levels following attenuation. Bar represents mean data normalised to β-Actin compared with control. Error bars indicate standard deviation. *p*-value was determined by unpaired t-test (**p*<0.05, ***p*<0.01 and ****p*<0.001).

As described in the previous section (4.2.2.2), cisplatin treatment up-regulated p53 protein levels in UPCI-SCC 090 (HPV-positive) cells compared to untreated controls. In the current section, in order to confirm the functional attenuation of p53, cells stably transfected with p53shRNA and controls were also treated with cisplatin. As expected, following cisplatin treatment UPCI-SCC 090 and scrambled control (090 p53sc + cisplatin) showed up-regulation of p53. By contrast, stably transfected cells (090 p53sh + cisplatin) did not demonstrate p53 stabilisation following cisplatin treatment (Figure 4.6 A).

Densitometry quantification of p53 protein bands correlated with the blots of both pre and post treatment experiments ($p \leq 0.001$ for UPCI-SCC 090 versus 090-p53shRNA and cisplatin treated UPCI-SCC 090 versus cisplatin treated 090-p53shRNA, Figure 4.5 B and 4.6 B respectively).

A)



B)

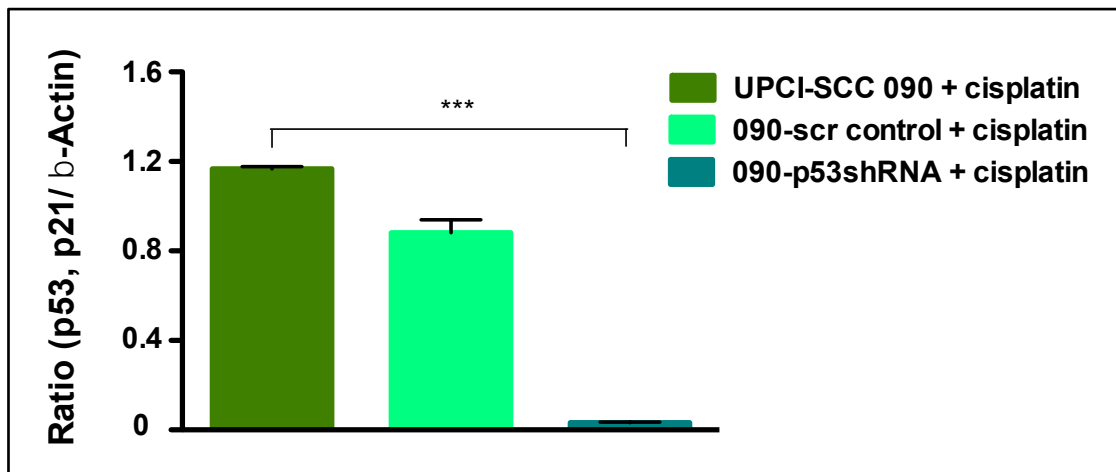


Figure 4.6. p53 stabilisation in p53shRNA cells following cisplatin.

A) Western blot analysis of p53 protein in HPV-positive cell line UPCI-SCC 090 (090), UPCI-SCC 090 scramble control (090-scr control) and UPCI-SCC 090 p53 attenuated cells (090-p53sh) following cisplatin treatment (10 µg/ml) for 6 hours. Arrows indicate molecular weight of the pre-stained protein ladder. Western blot is representative of two independent experiments. B) Quantitative densitometry of p53 levels in transfected cells following cisplatin treatment. Bar represents mean data normalised to β-Actin compared with control. Error bars indicate standard deviation. *p*-value was determined by unpaired t-test (**p*<0.05, ***p*<0.01 and ****p*<0.001).

4.2.3.2 Growth rate of p53 attenuated cells

In order to elucidate the role of p53 on cell proliferation, growth rate assay following p53 attenuation was performed in HPV-positive cells as detailed in section 2.2.1.8.

The results showed increased growth rate of the p53shRNA transfected cells compared to untreated controls particularly after day 3 of seeding (Figure 4.7). p -value was determined by unpaired t-test ($p \leq 0.01$ for UPCI-SCC 090 versus 090-p53shRNA at 4th day and $p \leq 0.001$ for UPCI-SCC 090 versus 090-p53shRNA from 5th to 8th days of growth).

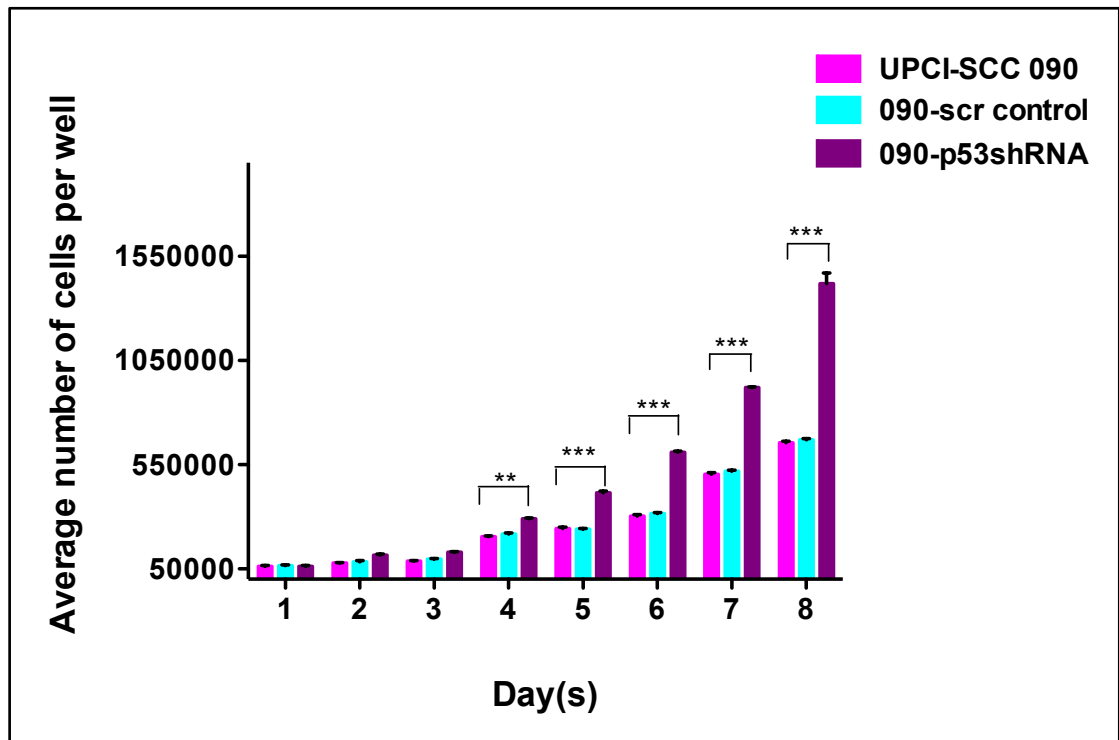


Figure 4.7. Growth rate of UPCI-SCC 090 p53shRNA cells.

Bar graph of growth rate analysis of p53shRNA transfected HPV-positive cells (090-p53shRNA) and the controls (UPCI-SCC 090 and 090-scr control) showing average number of cells per dish versus time in days. Error bars indicate standard deviation. This assay is representative of two independent experiments. p -value was determined by unpaired t-test (* $p < 0.05$, ** $p < 0.01$ and *** $p < 0.001$).

4.2.3.3 Cell viability of p53 attenuated cells following radiation

In order to confirm whether the relative sensitivity of HPV-positive cells to radiation as shown in sections 3.2.3.1 and 3.2.3.2 is mediated through p53, p53shRNA transfected cells, parental cells and cells transfected with control-shRNA were radiated at 2, 4 and 6 Gy and the cell viability was assessed by MTT assay as detailed in section 2.2.1.13. p53shRNA transfected cells showed increased resistance to radiation compared to controls ($p \leq 0.05$ for UPCI-SCC 090 versus 090-p53shRNA at 2Gy, $p \leq 0.01$ for UPCI-SCC 090 versus 090-p53shRNA at 4 Gy and $p \leq 0.001$ for UPCI-SCC 090 versus 090-p53shRNA at 6Gy, Figure 4.8).

Moreover silencing of p53 in HPV-negative cells (089-p53shRA) had no effect on cell viability when treated with radiation at aforementioned doses compared to the parental cell line (UPCI-SCC 089) and the scrambled control (089-scr control, Figure 4.9). No statistical significance was observed comparing treatment response at higher doses ($p=0.6423$ for 089-p53shRA cells versus UPCI-SCC 089 at 2 Gy, $p=0.0760$ for 089-p53shRA cells versus UPCI-SCC 089 at 4 Gy and $p=0.4564$ for 089-p53shRA cells versus UPCI-SCC 089 at 6 Gy; unpaired t-test). Confirming that the p53 mediated therapeutic sensitivity in HPV-positive cells was specific and silencing p53 in HPV-negative cells does not lead to therapeutic resistance.

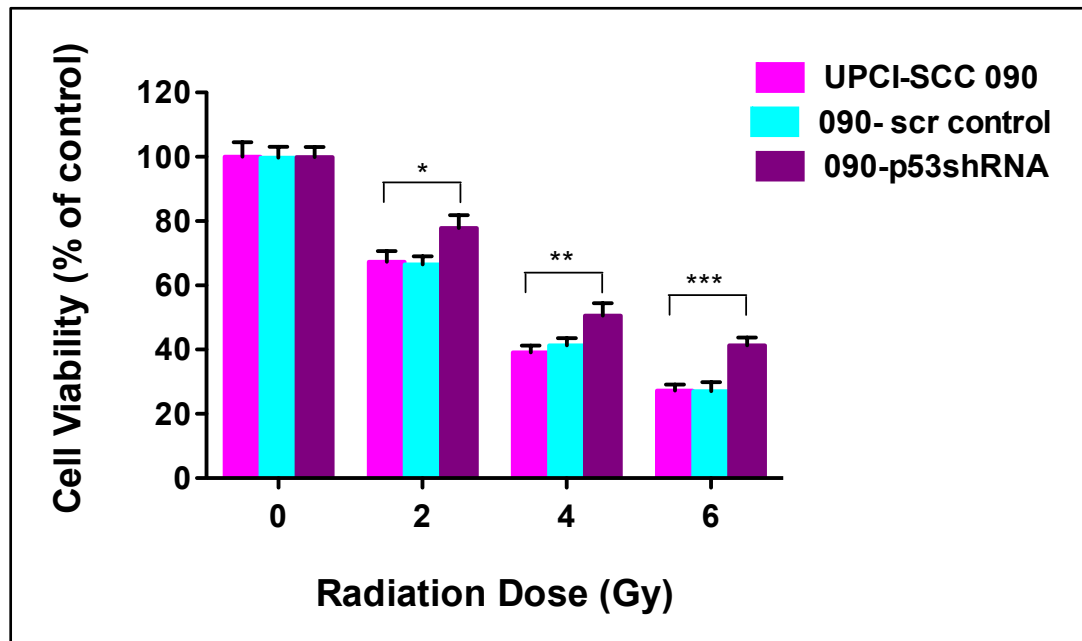


Figure 4.8. Cell viability of UPCI-SCC 090 p53shRNA cells following radiation.

Bar graph of cell viability expressed relative to control. Radiation was performed in triplicate at 2, 4 and 6 Gy. Cell viability was assessed after 7 days of treatment by MTT analysis. Error bars indicate standard deviation. This assay is representative of three independent experiments. *p*-value was determined by unpaired t-test (**p*<0.05, ***p*<0.01 and ****p*<0.001).

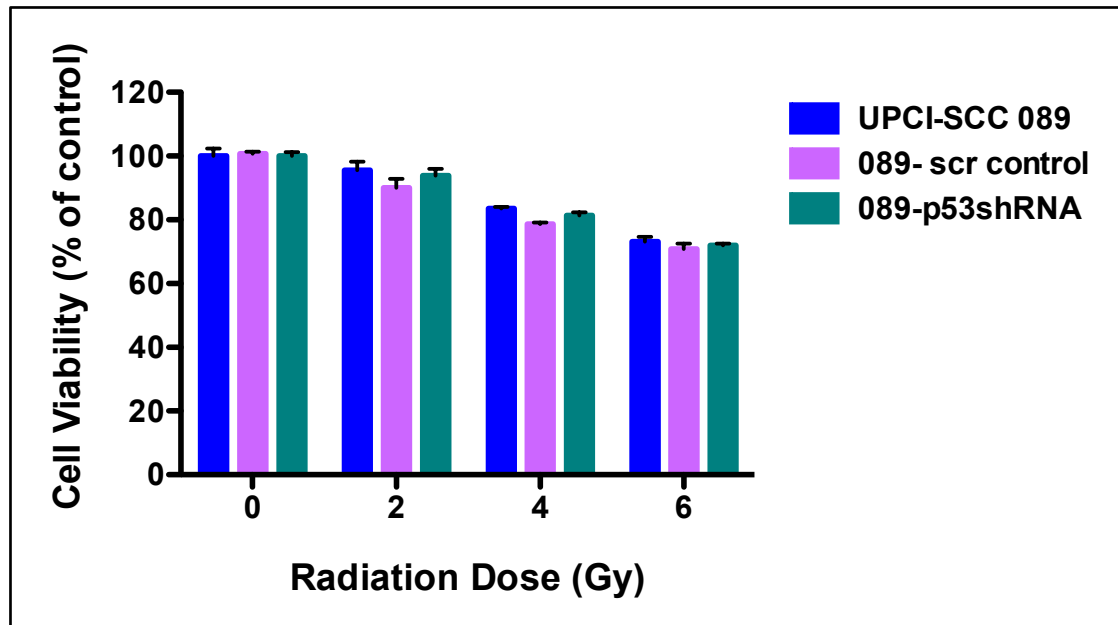


Figure 4.9. Cell viability of UPCI-SCC 089 p53shRNA cells following radiation.

Bar graph of cell viability expressed relative to control. Radiation was performed in triplicate at 2, 4 and 6 Gy. Cell viability was assessed after 7 days of treatment by MTT analysis. Error bars indicate standard deviation. This assay is representative of three independent experiments. *p*-value was determined by unpaired t-test (**p*<0.05, ***p*<0.01 and ****p*<0.001).

4.2.3.4 Clonogenic survival of p53 attenuated cells following radiation

In order to validate results of section 4.2.3.3, clonogenic survival assays were performed as detailed in section 2.2.1.14. Similar to the cell viability assay, p53shRNA transfected HPV-positive cell lines demonstrated significant radio-resistance compared to controls ($p \leq 0.001$ for UPCI-SCC 090 versus 090-p53shRNA at 2, 4 and 6 Gy, Figure 4.10). Taken together, the results (cell viability and cell survival assays) indicate that the relative sensitivity of HPV-positive cells is, at least in part, mediated through endogenous p53.

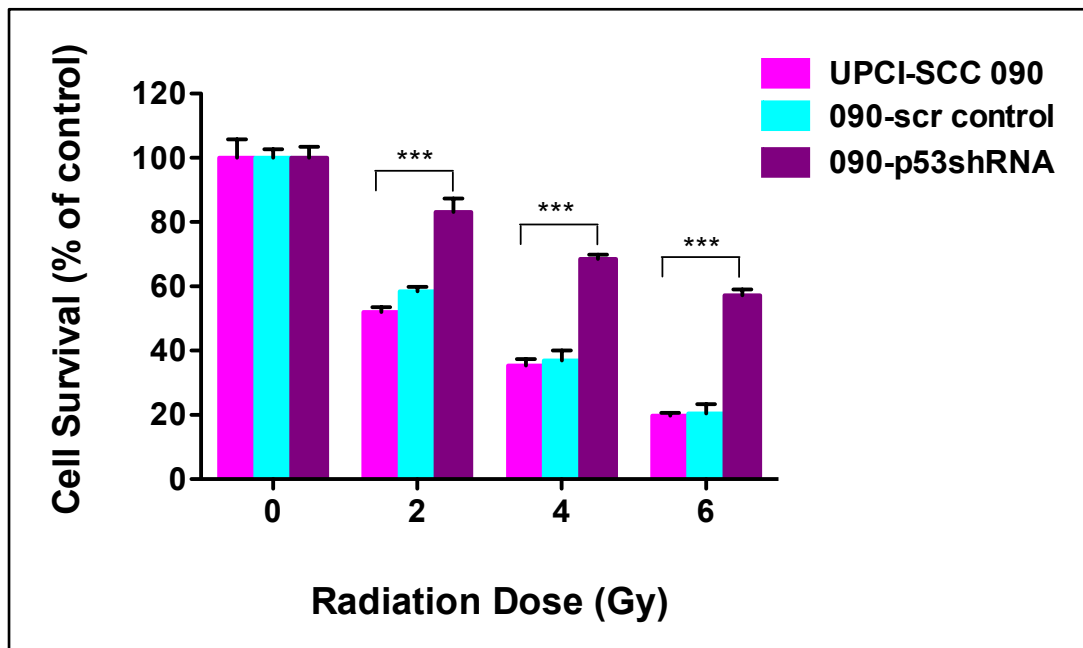


Figure 4.10. Cell survival of UPCI-SCC 090 p53shRNA cells following radiation.

Bar graph of clonogenic survival expressed relative to control. Radiation was performed in triplicate at 2, 4 and 6 Gy. Cell survival was assessed by clonogenic analysis 15-25 days following treatment. Bars represent average value from 3 dishes normalised to untreated control cells. Error bars indicate standard deviation. This assay is representative of three independent experiments. p -value was determined by unpaired t-test (* p <0.05, ** p <0.01 and *** p <0.001).

4.2.3.5 Cell viability of p53 attenuated cells following cisplatin

Having established that the relative sensitivity of HPV-positive cells to radiation was mediated, at least in part, by p53, this study went on to determine whether HPV-positive cells showed similar relative resistance to cisplatin. Cell viability assays were performed as detailed in section 2.2.1.13. p53shRNA transfected cells showed increased resistance to cisplatin compared to controls ($p \leq 0.001$ for UPCI-SCC 090 versus 090-p53shRNA at 2.5 $\mu\text{g/ml}$ and $p \leq 0.01$ for UPCI-SCC 090 versus 090-p53shRNA at 4 and 6 $\mu\text{g/ml}$).

Moreover silencing of p53 in HPV-negative cells (089-p53shRA) had no effect on cell viability when treated with cisplatin at aforementioned doses compared to the parental cell line (UPCI-SCC 089) and the scrambled control (089-scr control, Figure 4.12). No statistical significance was observed comparing treatment response at higher doses ($p=0.0945$ for 089-p53shRA cells versus UPCI-SCC 089 at 2.5 $\mu\text{g/ml}$, $p=0.7597$ for 089-p53shRA cells versus UPCI-SCC 089 at 5 $\mu\text{g/ml}$ and $p=0.8881$ for 089-p53shRA cells versus UPCI-SCC 089 at 10 $\mu\text{g/ml}$; unpaired t-test). Confirming that the p53 mediated therapeutic sensitivity in HPV-positive cells was specific and silencing p53 in HPV-negative cells does not lead to therapeutic resistance.

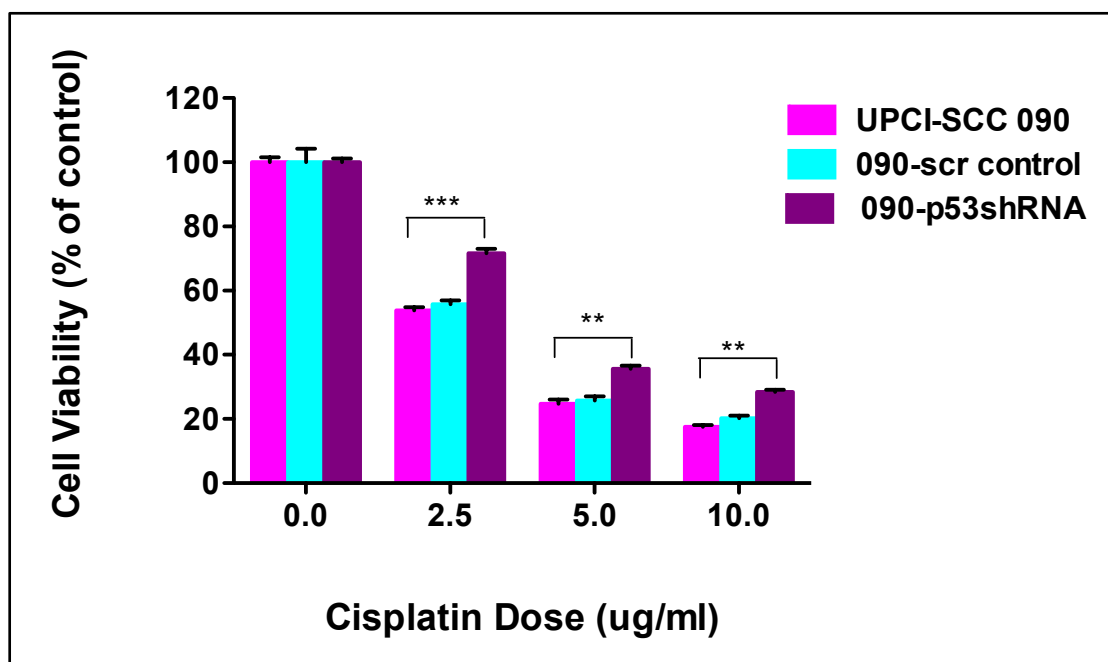


Figure 4. 11. Cell viability of UPCI-SCC 090 p53shRNA cells following cisplatin.

Bar graph of cell viability expressed relative to control. Cisplatin chemotherapy was performed at 2.5, 5 and 10 $\mu\text{g/ml}$. Cell viability was assessed by MTT assay 7 days following treatment. Bars represent average value from triplicate wells normalised to untreated control cells. Error bars indicate standard deviation. This assay is representative of three independent experiments. *p*-value was determined by unpaired *t*-test (**p* < 0.05, ***p* < 0.01 and ****p* < 0.001).

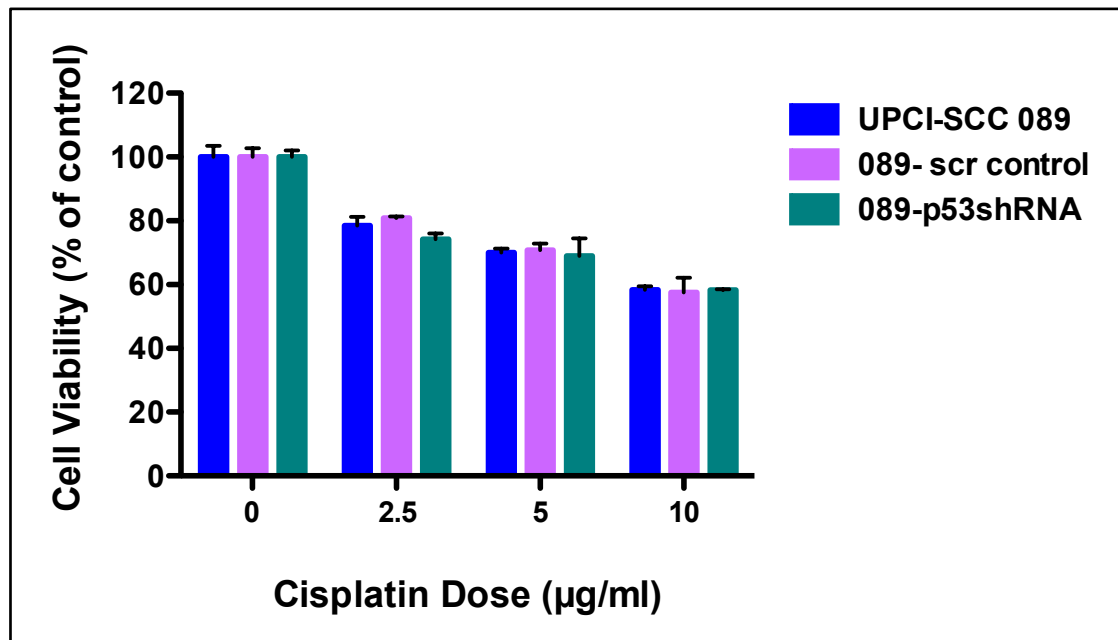


Figure 4. 12. Cell viability of UPCI-SCC 089 p53shRNA cells following cisplatin.

Bar graph of cell viability expressed relative to control. Cisplatin chemotherapy was performed at 2.5, 5 and 10 µg/ml. Cell viability was assessed by MTT assay 7 days following treatment. Bars represent average value from triplicate wells normalised to untreated control cells. Error bars indicate standard deviation. This assay is representative of three independent experiments. *p*-value was determined by unpaired *t*-test (**p*<0.05, ***p*<0.01 and ****p*<0.001).

4.2.4 Response of HPV-16 E6 attenuation to radiation and cisplatin

After establishing that HPV positive cell lines were more sensitive to radiation and cisplatin (chapter 3) and attenuation of p53 mediated increased resistance to radiation and cisplatin in HPV-positive cells (section 4.2.3). The aim of the current section was to determine whether E6 attenuation enhances the sensitivity of HPV-positive cancer cells since it is hypothesised that repression of HPV16 E6 oncogene expression results in stabilisation of the p53 and induction of apoptosis in HPV16-positive OPSCC cell lines.²⁶⁷

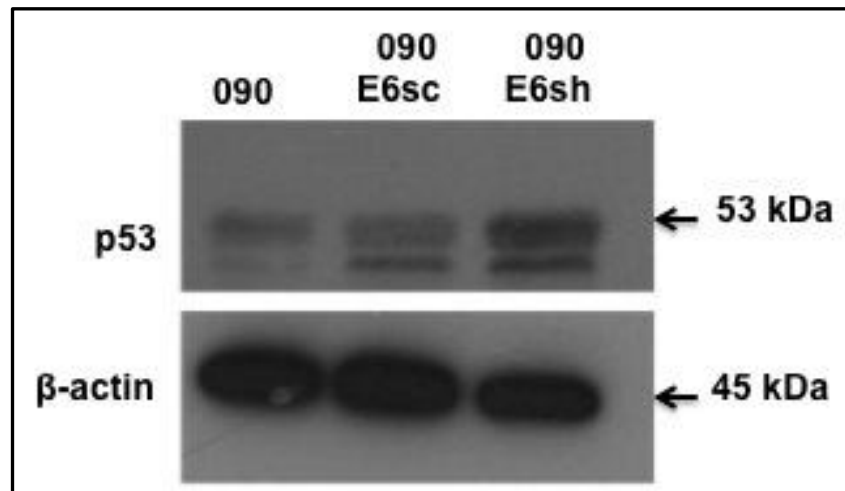
4.2.4.1 Attenuation of E6 in HPV-positive cells

Since the previous section showed that attenuation of p53 caused increased radio- and chemo-resistance in HPV-positive cancer cells, the current section went on to determine whether attenuation of E6 has an effect on endogenous p53 levels and response to radiation and cisplatin. HPV-positive cell line (UPCI-SCC 090) were transfected by E6shRNA through lentivirus detailed in section 2.2.4. There are currently no suitable commercial antibodies against HPV16-E6 for use in Western blot analysis or immunohistochemistry. Therefore, success of E6 knockdown was assessed by evaluating its downstream effects, namely the stabilisation of p53.

Increased p53 expression levels in the E6shRNA transfected cells confirmed reactivation of the protein following transfection with E6shRNA. Densitometry quantification of p53 protein expression by image J analysis showed up to a

fold increase of p53/ β -actin ratio in E6shRNA transfected cells ($p \leq 0.001$ for UPCI-SCC 090 versus 090-E6shRNA, Figure 4.13 B).

A)



B)

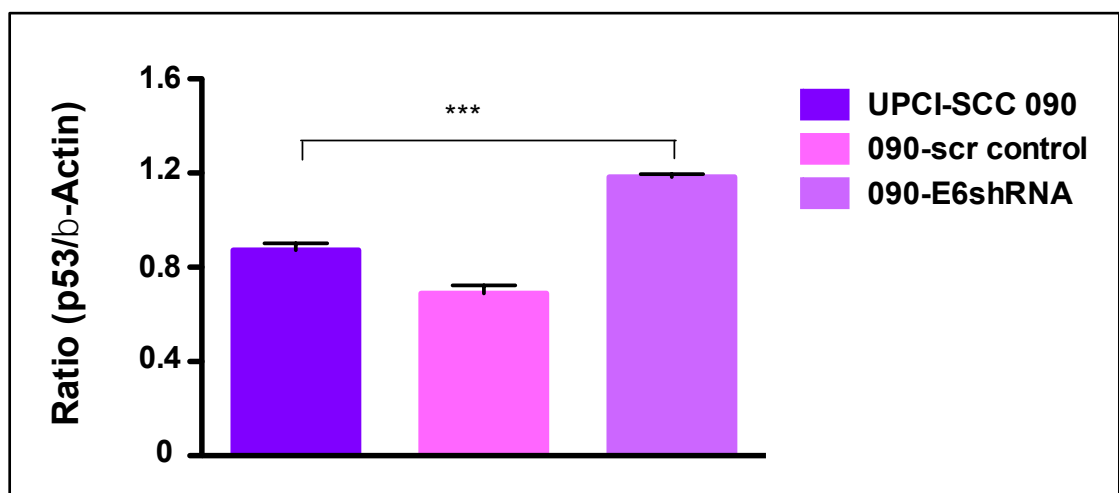
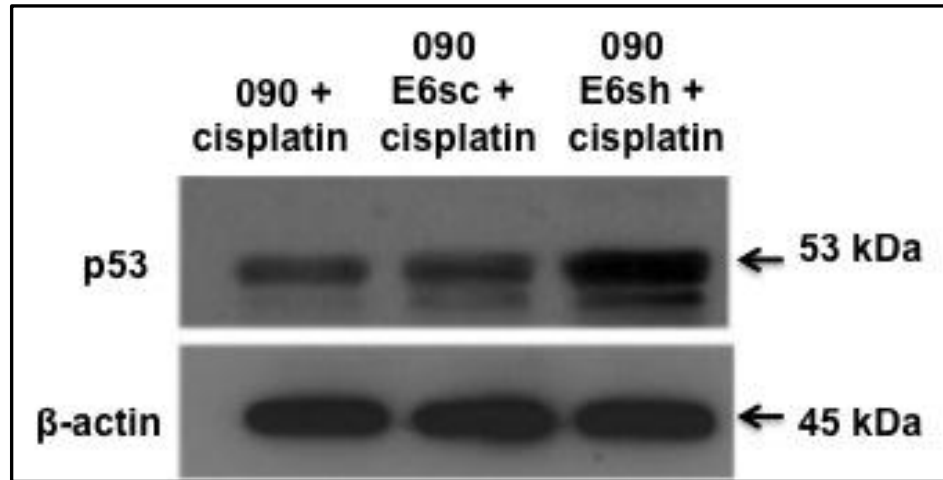


Figure 4.13. Attenuation of E6 in HPV-positive cell lines.

A) Western blot analysis of baseline p53 in HPV-positive cell line (UPCI-SCC 090), UPCI-SCC 090 scramble control (090-scr control) and UPCI-SCC 090 E6 attenuated cells (090-E6shRNA). Arrows indicate molecular weight of the pre-stained protein ladder. Western blot is representative of two independent experiments. B) Quantitative densitometry of p53 levels following attenuation of E6. Bar represents mean data normalised to β-Actin compared to control. Error bars indicate standard deviation. *p*-value was determined by unpaired t-test (**p*<0.05, ***p*<0.01 and ****p*<0.001).

p53 protein levels further increased in the cisplatin treated E6shRNA cells compared to treated controls as well as to untreated samples shown in the previous figure (4.14 A). Densitometry quantification of p53 protein expression by image J analysis showed increase of p53/ β -actin ratio in cisplatin treated E6shRNA transfected cells compared to controls ($p \leq 0.001$ for cisplatin treated UPCI-SCC 090 versus cisplatin treated 090-E6shRNA, Figure 4.14 B).

A)



B)

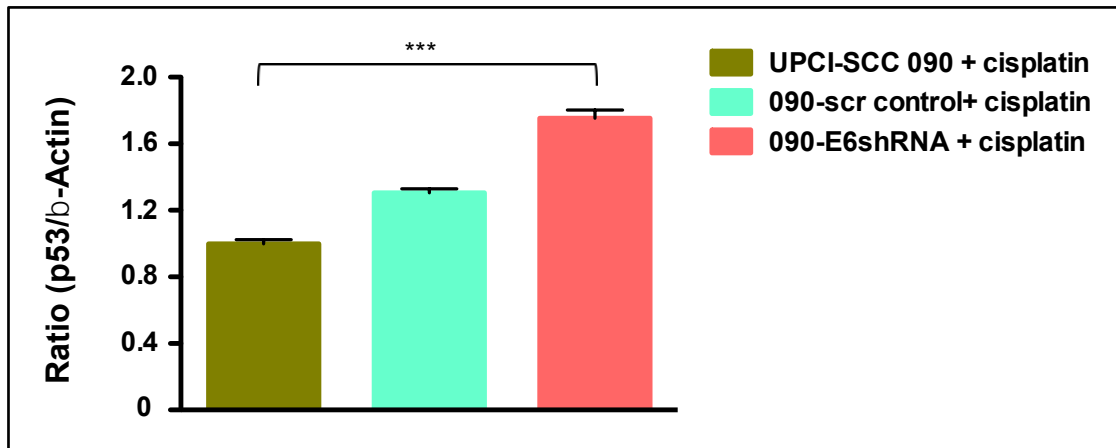


Figure 4.14. p53 stabilisation in UPCI-SCC 090 E6shRNA cells following cisplatin.

A) Western blot analysis of p53 protein in E6 attenuated HPV-positive cell line (090-E6sh), UPCI-SCC 090 scramble control (090-sc) and untreated control (090) following cisplatin treatment. Arrows indicate molecular weight of the pre-stained protein ladder. Western blot is representative of two independent experiments. B) Quantitative densitometry of p53 levels in E6 transfected cells following treatment. Bar represents mean data normalised to β-Actin compared to control. Error bars indicate standard deviation. *p*-value was determined by unpaired t-test (**p*<0.05, ***p*<0.01 and ****p*<0.001).

4.2.4.2 Growth rate of E6 attenuated cells

The results of the previous section (4.2.4.1) demonstrated that attenuation of E6 resulted in up-regulation of p53 protein in HPV-positive HNSCC cells. In order to investigate whether E6 attenuation influence growth rate of the transfected cells, cell proliferation assay was performed as described in section 2.2.1.8.

Results showed slight decrease in the growth rate of the E6shRNA transfected cells compared to controls particularly after day 4 of seeding ($p \leq 0.05$ for UPCI-SCC 090 versus 090-E6shRNA at 5th, 7th and 8th day of cellular proliferation).

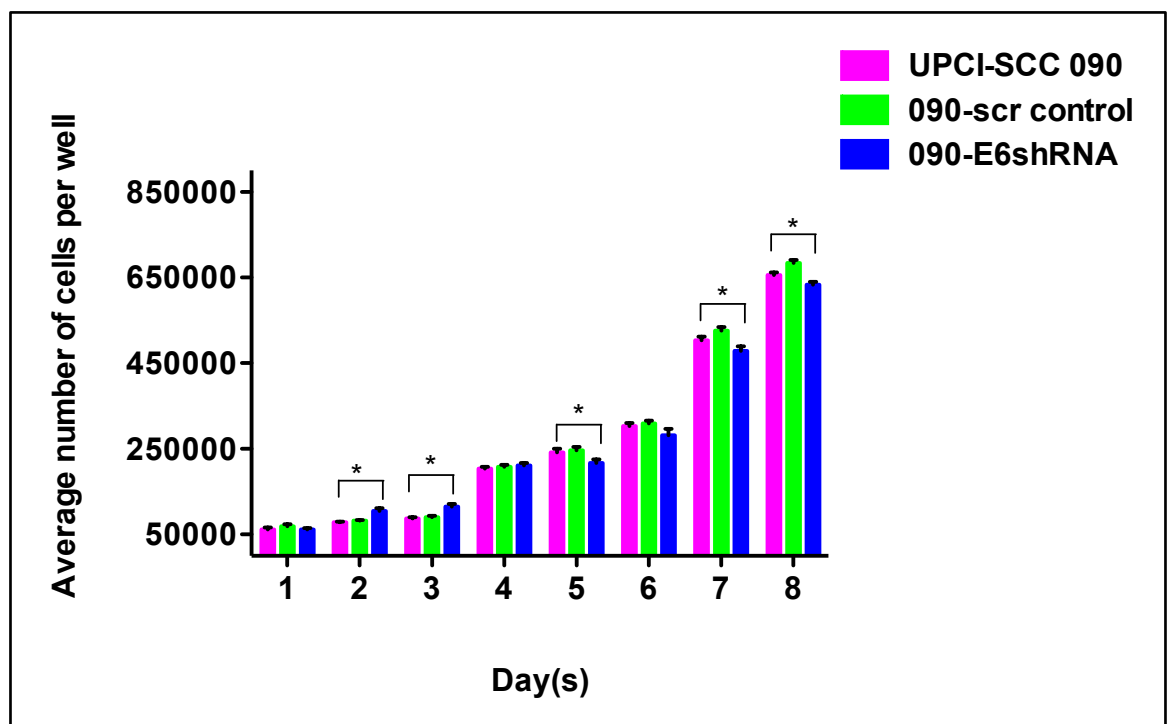


Figure 4.15. Growth rate of UPCI-SCC 090 E6shRNA cells.

Bar graph of growth curve analysis of E6shRNA transfected HPV-positive (090-E6shRNA) and controls (UPCI-SCC 090 and 090-scr control) showing average number of cells per dish versus time in days. Error bars indicate standard deviation. p -value was determined by unpaired t-test (* $p < 0.05$, ** $p < 0.01$ and *** $p < 0.001$).

4.2.4.3 Cell viability of E6 attenuated cells following radiation

In order to investigate the role of E6 attenuation in response to radiation, E6shRNA transfected cells were radiated at 2, 4 and 6 Gy and the cell viability was assessed by MTT assay detailed in section 2.2.1.13. E6shRNA transfected cells showed slight increase in sensitivity to radiation mainly at 4 and 6 Gy compared to the controls (UPCI-SCC 090 and 090-scr control, Figure 4.16). Statistical significance was determined by unpaired t-test ($p < 0.01$ for UPCI-SCC 090 vs. 090-E6shRNA at 6 Gy).

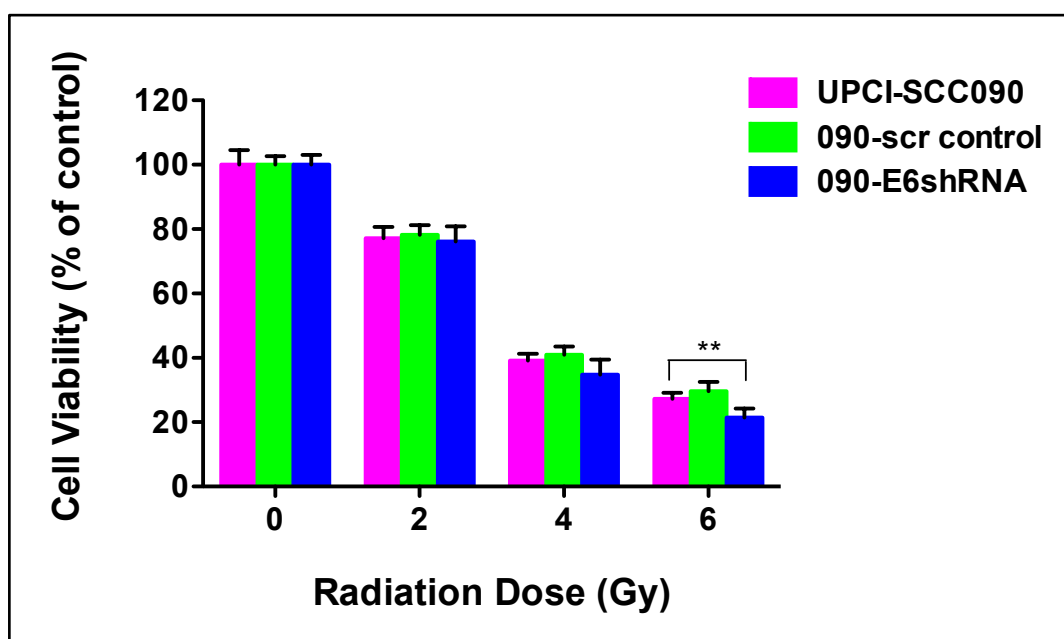


Figure 4.16. Cell viability of UPCI-SCC 090 E6shRNA cells following radiation.

Bar graph of cell viability expressed relative to control. Radiation was performed in triplicate at 2, 4 and 6 Gy. Cell viability was assessed after 7 days of treatment by MTT analysis. Error bars indicate standard deviation. This assay is representative of three independent experiments. p -value was determined by unpaired t-test ($*p < 0.05$, $**p < 0.01$ and $***p < 0.001$).

4.2.4.4 Clonogenic survival of E6 attenuated cells following radiation

In order to validate the results of section 4.2.4.3, clonogenic survival assays were performed as detailed in section 2.2.1.14. Results showed greater sensitivity at 4 and 6 Gy ($p < 0.001$) compared to MTT assay (Figure 4.17) in the E6 attenuated cells. Similar to the results of the cell viability assay, clonogenic cell survival assay also shows that attenuation of HPV-16 E6 in HPV-positive cells increases sensitivity to radiation. Statistical significance was determined by unpaired T test ($p < 0.001$ for UPC-SCC 090 vs. 090-E6shRNA at 4 and 6 Gy).

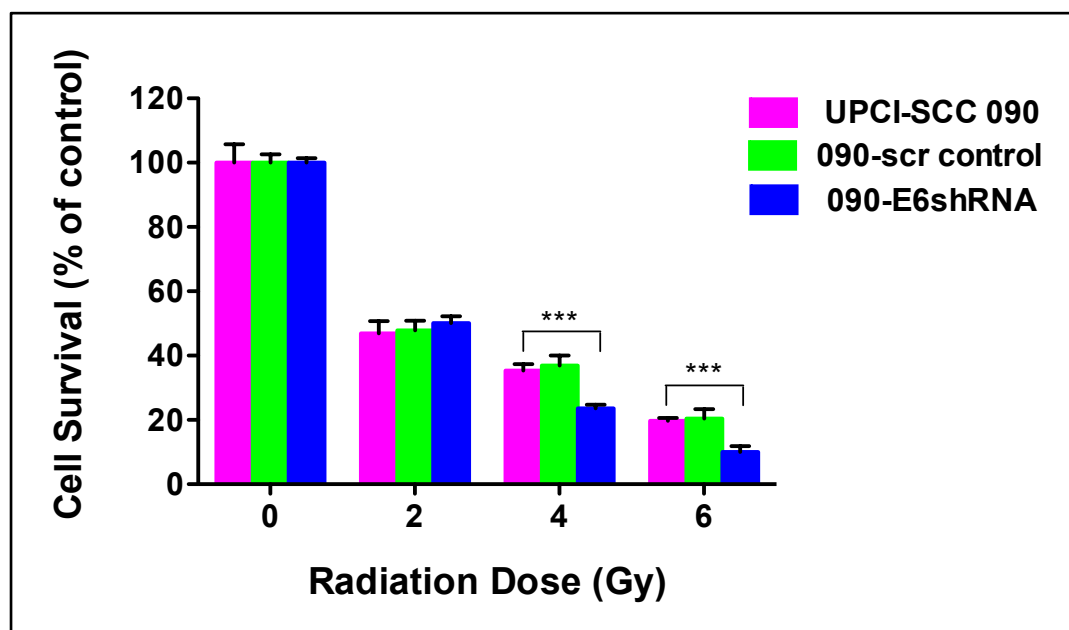


Figure 4.17. Cell survival of UPCI-SCC 090 E6shRNA cells following radiation.

Bar graph of clonogenic survival expressed relative to control. Radiation was performed in triplicate at 2, 4 and 6 Gy. Cell survival was assessed by clonogenic analysis 15-25 days following treatment. Bars represent average value from 3 dishes normalised to untreated control cells. This assay is representative of three independent experiments. Error bars indicate standard deviation. p -value was determined by unpaired t-test ($*p < 0.05$, $**p < 0.01$ and $***p < 0.001$).

4.2.4.5 Cell viability of E6 attenuated cells following treatment with cisplatin

The results of the above sections (4.2.3.3 and 4.2.3.4) demonstrated that attenuation of E6 in HPV-positive cells increased radio-sensitivity compared to controls. In order to determine whether a similar effect, the study went on to determine whether HPV-positive cells showed similar relative sensitivity to cisplatin following E6 attenuation. Cell viability assays were performed as detailed in section 2.2.1.13. Cisplatin was used at various concentrations of 2.5, 5 and 10 µg/ml for 24 hours. There was no significant increase in the relative sensitivity to cisplatin in E6 attenuated cells ($p=0.2$ at 5. µg/ml and $p=0.07$ at 10 µg/ml).

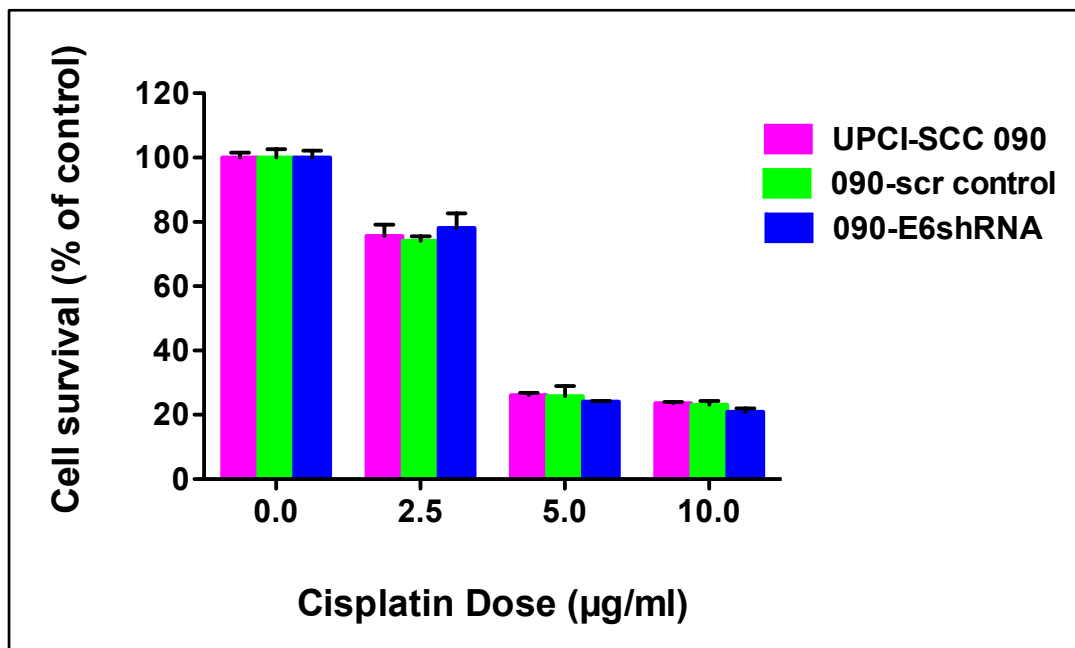


Figure 4.18. Cell viability of UPCI-SCC 090 E6shRNA cells following cisplatin.

Bar graph of cell viability expressed relative to control. Cisplatin chemotherapy was performed at 2.5, 5 and 10 µg/ml. Cell viability was assessed by MTT assay 7 days following treatment. Bars represent average value from 6 wells normalised to untreated control cells. Error bars indicate standard deviation. This assay is representative of three independent experiments.

4.2.5 HPV-16 E6 expression in HPV-negative cell line

The next stage of this study sought to evaluate whether HPV gene products altered sensitivity of HNSCC cells in response to conventional therapeutic agents. In order to determine whether HPV-16 E6 caused increased sensitivity to radiation in a p53-independent manner two HPV-16 E6retroviral constructs, namely E6-75 targeting the C-terminal and E6-76 targeting the N-terminal of E6 gene were stably expressed in one of the HPV-negative cell lines (UPCI-SCC 089) as detailed in section 2.2.5.

4.2.5.1 Expression of HPV-16 E6 in HPV-negative cell line

In order to confirm successful transfection of HPV-16 E6 in the HPV-negative cell line (UPCI-SCC 089), expression of the gene was evaluated by reverse transcription polymerase chain reaction (RT-PCR). The results showed presence of HPV-16 E6 plasmids in the HPV-negative cells compared to the parental cell line (UPCI-SCC 089) and the MSCV-N GFP (089-GFP, Figure 4.19). Further in the study HPV-16 E6 expression vectors will be designated as E6-75 and E6-76 respectively.

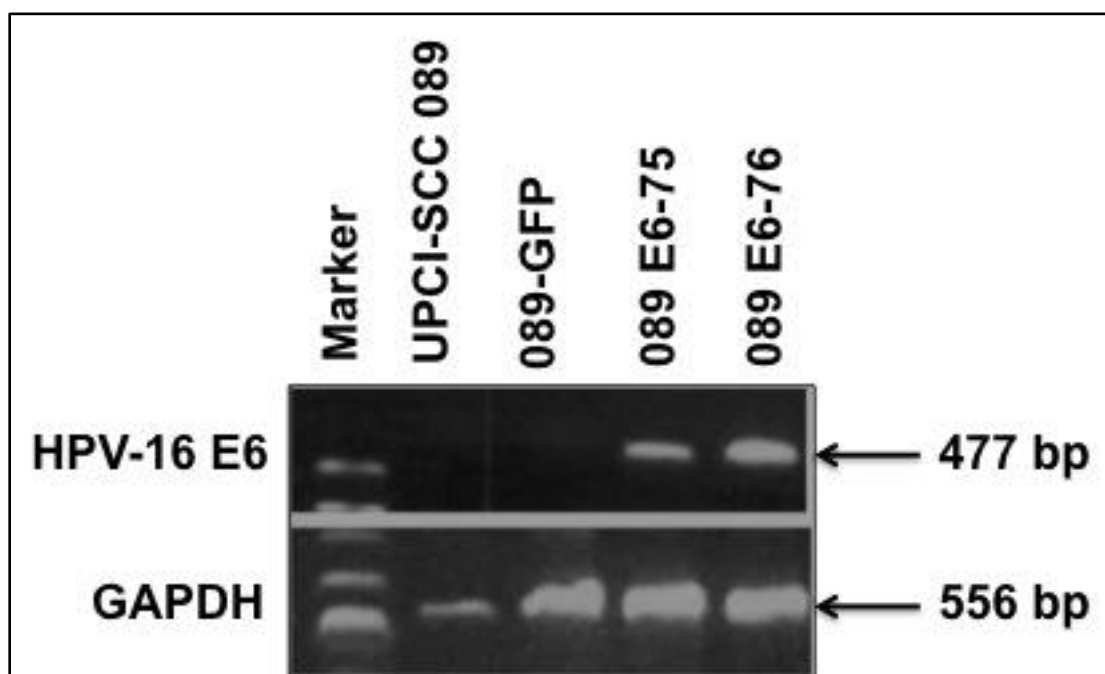


Figure 4.19. RT-PCR of HPV-16 E6 expressed HPV-negative cells.

Amplification of HPV-16 E6 mRNA (477 bp) in HPV-negative cell lines (UPCI-SCC 089), GFP as a control and two expression vectors of E6 (089 E6-75 and 089 E6-76). mRNA of GAPDH was used as a loading control (556 bp).

4.2.5.2 Growth rate of HPV-16 E6 expressed cells

The results of section 3.3.2 showed greater growth rates of HPV-negative cell lines compared to HPV-positive cell lines. This section aimed to determine whether the presence of HPV-16 E6 alters growth rates of HPV-negative cells.

HPV-16 E6 expression in HPV-negative cells resulted in significantly decreased growth rates particularly from third day compared to controls, suggesting possible effect of E6 on growth rate of the cancer cells ($p \leq 0.001$ for UPCI-SCC 089 versus E6-75 and E6-76 at 4th, 5th, 6th, 7th and 8th day of cellular proliferation).

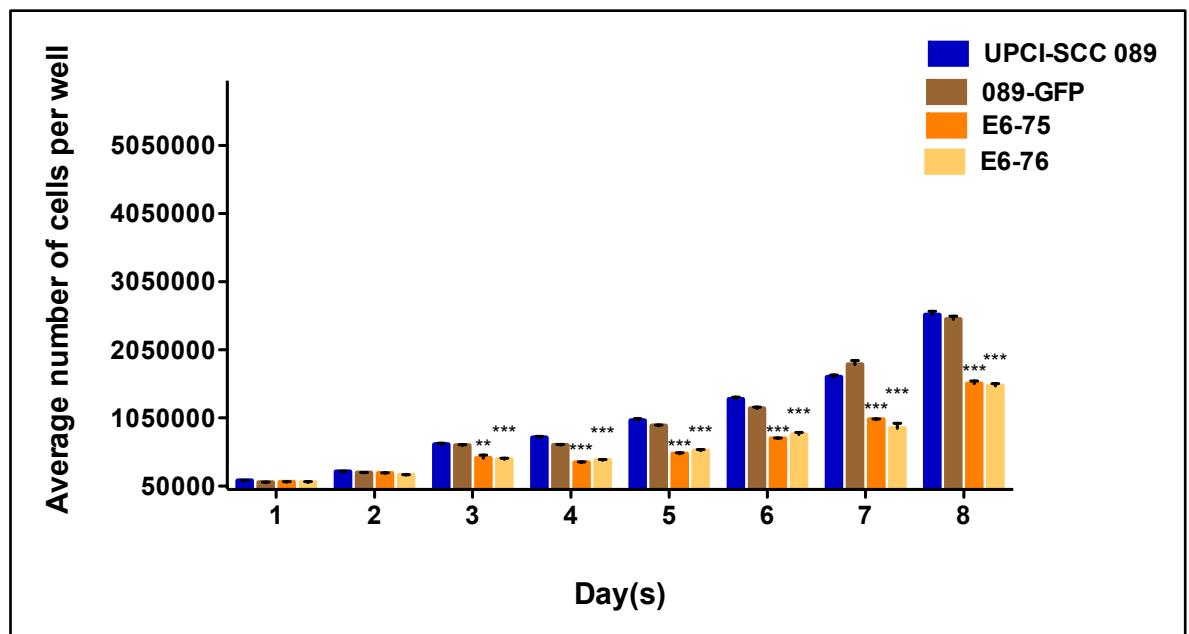


Figure 4.20. Growth rate of HPV-16 E6 expressed UPCI-SCC 089 cells.

Bar graph of growth curve analysis of E6 expression vectors in HPV-negative UPCI-SCC 089 cell lines (E6-75 and E6-76) and controls (UPCI-SCC 089 and 089-GFP) showing average number of cells per dish versus time in days. Error bars indicate standard deviation. p -value was determined by unpaired t-test (* $p<0.05$, ** $p<0.01$ and *** $p<0.001$).

4.2.5.3 Cell viability of HPV-16 E6 expressed cells following radiation

The current section of the study aimed to investigate any effect mediated by HPV-16 E6 oncoprotein, forcefully expressed in HPV-negative OPSCC cells in response to RT. Radiation of HPV-negative cells with forced expression of HPV16 E6 (E6-75 and E6-76) at 2, 4 and 6 Gy showed increased sensitivity compared to the controls ($p<0.05$ for UPCI-SCC 089 versus E6-76 and $p<0.01$ for UPCI-SCC 089 versus E6-76 at 4 Gy; $p<0.001$ for UPCI-SCC 089 versus E6-75 and E6-76 at 6 Gy).

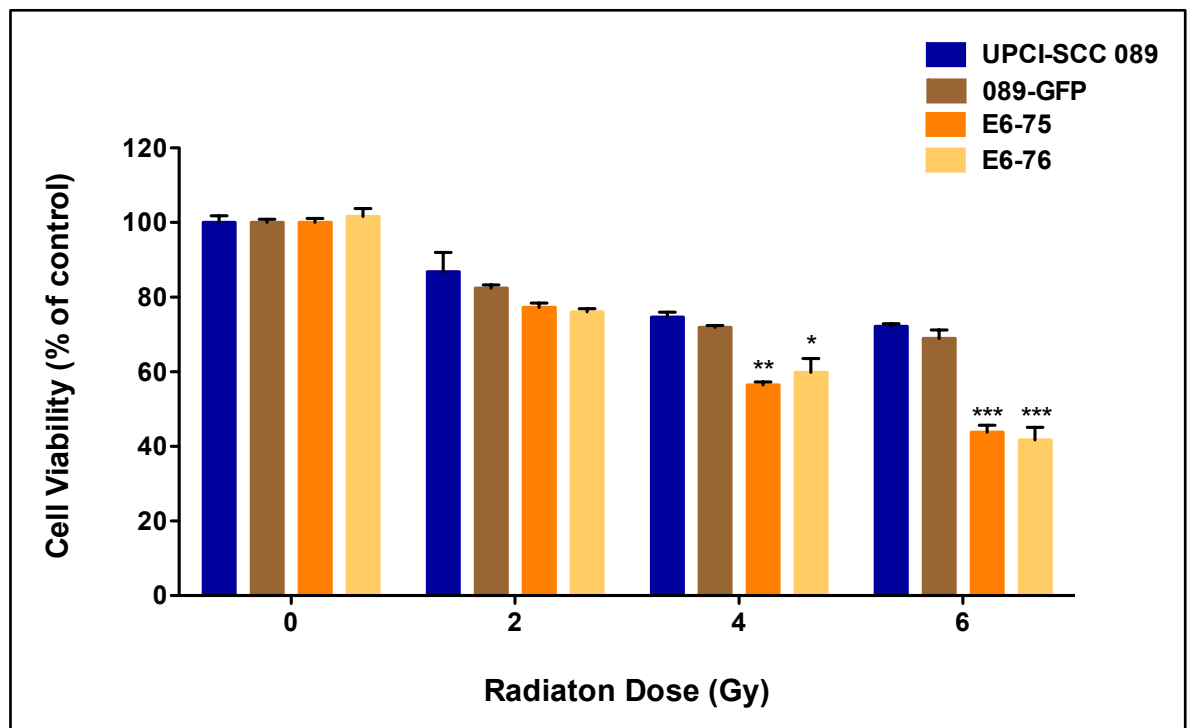


Figure 4.21. Cell viability of E6 expressed UPCI-SCC 089 cells following radiation.

Bar graph of cell viability expressed relative to control. Radiation was performed in triplicate at 2, 4 and 6Gy. Cell viability was assessed after 7 days of treatment by MTT analysis. Error bars indicate standard deviation. This assay is representative of three independent experiments. *p*-value was determined by unpaired t-test (**p*<0.05, ***p*<0.01 and ****p*<0.001).

4.2.5.4 Cell viability of HPV-16 E6 expressed cells following cisplatin

The results of the previous section (4.2.5.3) demonstrated that forced expression of HPV-16 E6 in HPV-negative cells resulted in increased radio-sensitivity. In order to determine whether a similar effect is seen in response to cisplatin treatment, UPCI-SCC 089 cells with E6 were treated with cisplatin at 2.5, 5 and 10 µg/ml doses. Results showed statistically significant sensitivity at all doses ($p<0.05$ for UPCI-SCC 089 versus E6-76 at 5 and 10 µg/ml; $p<0.01$ for UPCI-SCC 089 versus E6-76 and E6-76 at 2.5 µg/ml; $p<0.001$ for UPCI-SCC 089 versus E6-76 at 5 and 10 µg/ml).

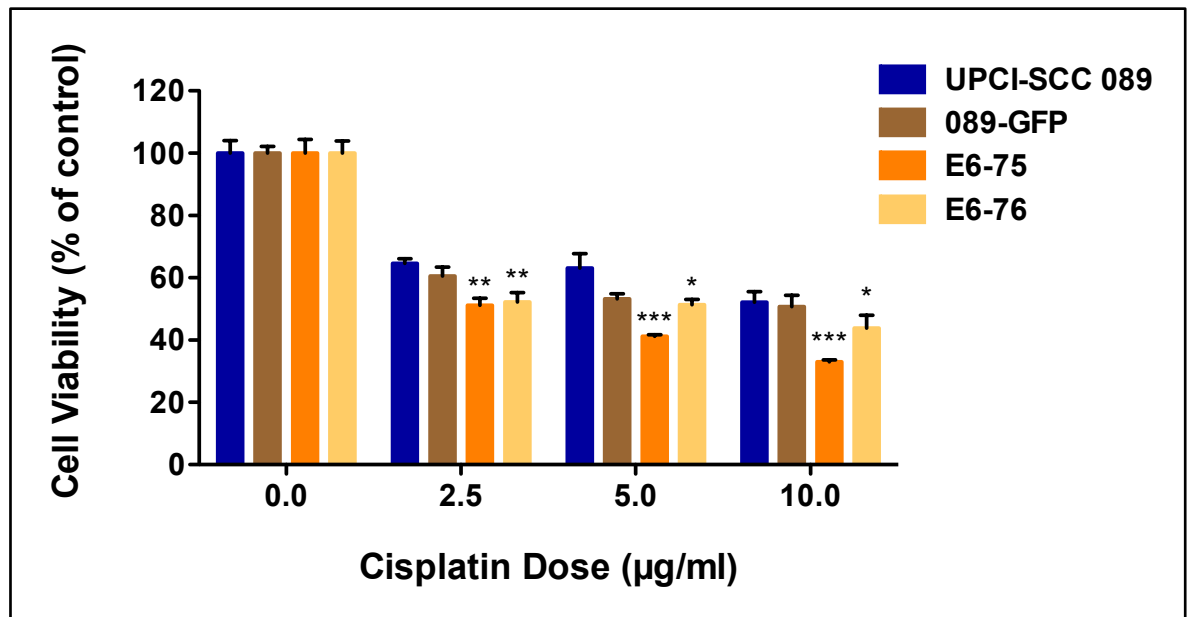


Figure 4.22. Cell viability of E6 expressed UPCI-SCC 089 cells following cisplatin.

Bar graph of cell viability expressed relative to control. Cisplatin chemotherapy was performed at 2.5, 5 and 10 µg/ml. Cell viability was assessed by MTT assay 7 days following treatment. Bars represent average value from 6 wells normalised to untreated control cells. Error bars indicate standard deviation. This assay is representative of three independent experiments. *p*-value was determined by unpaired t-test (**p*<0.05, ***p*<0.01 and ****p*<0.001)

4.3 Discussion

The current chapter focused on elucidating the potential mechanisms of improved response in HPV-positive OPSCC to conventional therapeutic agents, namely radiation and cisplatin. A key cellular protein (p53) and a key viral oncoprotein (E6) were selected for study.

The purpose of selecting p53 was that this tumour suppressor remains one of the single, most important transcription factors governing the genetic circuitry of cells; it has been termed the 'guardian of the genome'. p53 is a unifying factor in the disease because it binds to many regulatory genomic sites and begins production of proteins that halt cell division in order for DNA repair to occur. Alternatively, if the cellular damage is too severe, p53 initiates the process of programmed cell death. Although p53 is the most commonly mutated gene in human cancers, HPV-related OPSCC contain inactive wild-type that is p53 stabilised following cellular stress.³³⁵ If this protein is functional in HPV-positive tumours, p53-induced apoptosis could explain the high response rate of HPV-positive oropharynx tumors to chemotherapy and radiation and be a reason for better response to treatment in patients with this disease.¹⁴¹

The HPV-16 E6 oncoprotein has been appreciated as one of the critical regulators of the viral life cycle and driver of tumourigenesis in high-risk HPV associated OPSCC.³³⁶ In HPV-positive tumours, the E6 interaction with E6AP and p53 results in ubiquitination, export from the nucleus, and proteasomal degradation of p53, thus inhibiting its proapoptotic functions.³³⁶

4.3.1 Baseline expression of p53

p53 in HNSCC caused by traditional risks factors (alcohol and tobacco) is commonly mutated resulting in accumulation of the protein.^{328,329,337} By contrast, HPV-positive OPSCCs are generally associated with wild-type p53.^{137,184,337} The wild-type p53 gene encodes a nuclear phosphoprotein having a very short half-life; consequently this protein does not accumulate in levels high enough to be detected immunohistochemically. However most mutated p53 proteins, exhibit an enhanced stability and prolonged half-life with a high proportion of missense mutation, hence immunohistochemical p53 detection has been considered an appropriate means of detecting p53 mutational alterations.³³⁸⁻³⁴⁰ Although the molecular basis of the prolonged half-life of mutant p53 is not fully known, it could be explained by the inability of mutant p53 to activate Mdm2 (negative regulator of the p53).³⁴¹ Additionally it is reported that p53 protein in an HPV-negative tumour not only is inactive as a tumour suppressor but also can bind and inactivate any remaining wild-type p53 in a tumour cell.³³⁸

In the present study baseline p53 expression by immunohistochemistry (IHC) and western blot *in vitro* showed similar trends. HPV-negative cell lines (UPCISCC 072 and UPCI-SCC 089) showed intense and moderate levels, respectively (Figures 4.1 and 4.2). The intense staining of UPCI-SCC 072 could be related to the presence of missense mutation in the cells (mutation 13214C>A, codon H179N).^{278,342,343} The mutation status of p53 in UPCI-SCC 089 is still not known, but according to the literature it has been used as an HPV-negative control, investigating the response of HPV positive and negative tumours to treatments.³¹¹

The majority of HPV-positive cell lines showed undetectable or weak expressions of p53 protein, which confirm the presence of wild type p53 in accordance with previously published reports. However 93-VU-147T cells showed intense immunohistochemical staining and expression by Western blot. These cells have been reported as harboring both mutated (L257R) as well as wild-type p53. These observations may explain the increased sensitivity to conventional therapeutic agents despite high levels of detectable p53.^{184-186,276,279,344}

In the current study, baseline p53 expression in untreated HPV-positive cells was variable. This observation may be explained by presence of low levels of residual wild-type p53 despite the down-regulating effects of HPV-16 E6.^{181,184} Furthermore, variable baseline p53 expression could also be explained by increased passage numbers and conditional differences of the cultures as cells in culture are under constant environmental and manipulative stress.³¹²

4.3.2 Role of p53 in increased sensitivity of HPV-positive cells to radiation and cisplatin

Cellular stress signals, such as DNA damage, hypoxia, heat shock, and oncogene inactivation induce an increase in the stability of the wild-type p53 protein. The accumulation of p53 is associated with the transcription of a series of p53-responsive genes, including p21 that mediates p53 induction of growth arrest and apoptosis.^{345,346}

p53 in HPV-positive tumours is one of the crucial cellular targets of high-risk HPV-16 E6 oncoprotein. A major strategy employed by the E6 proteins to abrogate p53 functions is to induce its degradation by the ubiquitin-proteasome pathway through E6-associated protein (E6AP).^{92,347} The degradation of p53 by the E6 reduces the net levels of p53 but residual p53 can be activated in response to DNA damage and other cellular stresses.^{182,184,279,348}

In accordance with the findings in the present study, several studies have demonstrated upregulation of p53 protein following treatment with radiation and cisplatin in HPV-positive HNSCC cell lines.^{179,184,279} The results of the current study also showed that stabilisation of p53 was accompanied by induction of p21 (Figure 4.3 and 4.4), a down-stream target of p53 thereby confirming findings in previously published reports.^{179,184} Furthermore, attenuation of p53 by shRNA resulted in increased resistance to radiation and cisplatin thereby indicating a crucial role of this tumour suppressor protein in the response of HPV-positive cells to conventional therapeutic agents.

Although published reports linking p53 to improved treatment response in HPV-positive OPSCC are sparse, the results of the current study confirm the findings by Kimple *et al* (2013). This group utilised the 93-VU-147T cell line and showed that successful silencing of p53 by small interfering RNA (siRNA) resulted in increased radio-resistance of the HPV-positive cells.¹⁸⁴ They postulated that since E6 induces degradation of p53, there is no selective pressure to favour mutation of this tumour suppressor gene in oropharyngeal carcinogenesis; potentially explaining the high prevalence of wt-p53 in OPSCC. The current

study strengthens the evidence that rescue of wt-p53 plays a crucial role in the response of HPV since it utilised a different HPV-positive cell line (UPCI-SCC 090) to that of Kimple *et al.*

It should be noted, however, that near complete silencing of p53, both in this study and by Kimple *et al.* (2013)¹⁸⁴, resulted in only partial resistance to conventional therapeutic agents; HPV-positive cells with attenuated p53 was still relatively sensitive compared to HPV-negative cells. This raises the possibility that while p53 is important, p53-independent mechanism may also play a role in increased radio- and chemo-sensitivity of HPV-positive OPSCC cells.

The observation that p53 stabilisation is important for relative radio- and chemo-sensitivity in HPV-positive cells raises therapeutic implications. Is it possible that agents potentiating p53 stabilisation may form part of multi-modality de-escalation treatment in HPV-positive OPSCC patients. Furthermore, clinical evaluation of the p53 status in tumour samples may also have a possible prognostic and/or predictive role for patients with this disease.

4.3.3 Attenuation of HPV-16 E6

The E6 protein is thought to promote cell proliferation by stimulating degradation of the tumour suppressor p53 protein via the formation of a trimeric complex comprising of E6, p53 and the cellular ubiquitination enzyme E6-AP. E6-stimulated degradation interferes with biological functions of p53; thus

perturbing the control of cell cycle progression, leads to increased tumour cell growth.³²⁶ Since the results of the current chapter showed that sensitivity of HPV-positive cells was p53-dependent, this study went on to postulate that silencing of HPV-16 E6 leads to liberation of functional p53. This would, in turn, result in even greater sensitivity of HPV-positive cell lines to therapeutic agents due to apoptotic and cell cycle arrest functions of p53.

The current study showed shRNA-mediated repression of HPV-16 E6 oncogene expression resulted in activation of the p53 tumour suppressor protein, decrease in cell proliferation and increased sensitivity in HPV16-positive oropharyngeal cancer cells to radiation and slightly but insignificantly to cisplatin (section 4.2.4). In head and neck clinical oncology, chemotherapy as a single modality treatment is not used for therapeutic intent in management of head and neck cancer. Cisplatin, when used, is only an adjunct to radiotherapy; it is therefore only a 'sensitising agent' to radiation. The DNA adducts formed by platinum as a single modality are insufficient to cause cell death. Several clinical trials are now considering the omission of cisplatin in the management of oropharyngeal cancer. However, effects of p53 knockdown on response to cisplatin in this study are preliminary and further work, utilising more cell lines, are necessary.

In accordance to the results of the current study, experimental data from several groups highlight the potential of E6 oncogene repression as a therapeutic strategy in HPV16-positive OPSCC cells since this leads to activation of the p53 tumor suppressor pathways and induction of apoptosis.²⁶⁷

Ferris *et al* (2005) showed p53 restoration in UPCI-SCC 090 cells following E6siRNA transfection of UPCI-SCC 090 cells.²⁷⁹ Rampias *et al* (2009) showed that shRNA mediated silencing of E6 and E7 in HPV-positive oropharyngeal cancer cell line (93-VU-147T and UPCI-SCC 090) resulted in activation of p53 and Rb proteins and induction of increased apoptosis of tumour cells, indicating that the oncoprotein is important in the etiology of HPV-positive oropharyngeal carcinogenesis. The group showed that E6 is key in maintaining resistance to apoptosis since E6shRNA transfection increased the percentage of annexin V–positive cells from 13.4% to 84.3% and 3.3% to 71.2% 93-VU-147T and UPCI-SCC 090 cells, respectively.²⁶⁷ Similarly Adhim *et al* (2013) used the HPV-16-positive UMSCC47 cell line to demonstrate that repression of E6 resulted in recovery of p53 protein with increased induction of apoptosis *in vitro* and reduction of tumour volume *in vivo*.³⁴⁹

All of the above studies showed that siRNA/shRNA-mediated down-regulation of E6/E7 RNA in HPV-positive HNSCC cell lines resulted in p53 up-regulation, while also inducing apoptosis. In addition to this Li *et al* (2013) investigated dependence of apoptosis on p53 and the benefit and impact of liberating wild-type p53. The group used two distinct approaches to liberate p53 in a panel of HPV-positive HNSCC cell lines (UPCI-SCC 090, UD-SCC 2 and UM-SCC-47): Firstly initiated siRNA suppression of E6/E7 RNA and proteasome inhibition with bortezomib. Secondly they used siRNA to prevent p53 up-regulation caused by these approaches, evaluating the role and impact of p53 on apoptosis and cell cycle arrest in the HPV-positive HNSCC cells. The findings

demonstrated that p53 and the p53 targets p21 were up-regulated following E6/E7 suppression or proteasome inhibition. However by preventing p53 expression, apoptosis induced by E6/E7 siRNA or treatment with bortezomib in HPV-positive cells was repressed, confirming that cell death resulting from E6/E7 siRNAs was dependent on p53.³⁵⁰

The results of the current study, and those of previously published reports indicate that silencing of the HPV-16 E6 oncogene does not fully abrogate the malignant phenotype *in vitro*. Nevertheless, these data also suggest that repression of HPV-16 E6 results in liberation of functional p53, which could be a potential therapeutic strategy in future multi-modality management of patients with HPV-positive OPSCC.

4.3.4 Expression of HPV-16 E6

While p53 is an important mediator of HPV-associated sensitivity to chemical- and radiation-induced cell death, several groups have reported p53-independent mechanisms as contributing to increased susceptibility of these cells to conventional therapeutic agents.^{90,303} The current study postulated that HPV gene products, namely HPV-16 E6, may contribute to improved outcome of HPV-positive OPSCC cells to radiation and cisplatin. Interestingly, forced expression of HPV-16 E6 in an HPV-negative cell line (UPCI-SCC 089) resulted in increased sensitivity to radiation and cisplatin (sections 4.2.5.3 and 4.2.5.4), suggesting that the improved outcome in HPV-positive OPSCC patient may be partly due to the direct effect of this viral oncoprotein.

While the status of p53 in UPCI-SCC089 cells is still unknown, baseline expression of this protein by Western blot analysis and immunohistochemistry markedly increased indicating an abrogated pathway, likely mutation resulting in inability for targeted degradation. It was therefore assumed that any effect of forced E6 overexpression in UPCI-SCC 089 cells would be independent of functional p53. Nevertheless, I acknowledge that mutant p53 may have some residual function and the effect of E6 overexpression on mutant forms of this protein should have been evaluated, for example by Western blot analysis.

Increased susceptibility to therapeutic agents in HPV-negative cells by the introduction of E6 has been shown by several other groups.^{90,184} For example, Kimple *et al* (2013) demonstrated increased radiosensitivity in immortalised human tonsillar epithelial (HTE) cells transfected by E6 and this was accompanied by increased apoptosis.¹⁸⁴ However, their report did not proffer any possible explanation for this observation.

Pang *et al* (2011) stably expressed the total open reading frame and an isoform of HPV-16 E6 (E6 total and E6*1, respectively) in two p53 mutant oropharyngeal HPV-negative cell lines (UM-SCC4 and WSU-HN6). UM-SCC4 has severely truncated p53 whereas WSU-HN6 has a H179L substitution in the DNA-binding domain of protein. Their results demonstrated that both E6 total and E6*1 substantially increased the rate of cell death caused by moderate doses of ionizing radiation indicating that the viral oncoprotein conferred sensitivity to

OPSCC cells despite mutant p53.⁹⁰ Following optimisation of wt-p53 in these cells, they showed that while E6 total inhibited p53 transactivation activity, E6*I

was non-inhibitory. This group therefore went on to suggest that E6⁺ sensitized cells to radiation-induced death in a p53-independent manner directing them to either apoptosis or mitotic catastrophe after a delay in G2M upon irradiation.⁹⁰

p53-independent mechanisms involved in increased sensitivity of HPV-positive cells have also been explored by Gubanova *et al* (2012). They showed a decrease levels in suppressor with morphogenetic effect on genitalia (SMG-1), a potential tumor suppressor and often deregulated in cancer, following expression of E6/E7 in HPV-negative cell lines, resulting in increased radio-sensitivity. To confirm their findings, radio-resistance in HPV-positive cells was observed following SMG-1 shRNA or E6shRNA transfection.³⁰³

The mechanisms of radio- and chemo-sensitivity conferred by E6 are still largely unknown. One possible explanation may be the induction of genomic instability by E6. A recent study by Marullo *et al* (2015) showed that chronic oxidative stress is a distinct property of HPV-positive HNSCC cells. The state is due to the induction of reactive oxygen species (ROS) mediated by nicotinamide adenine dinucleotide phosphate oxidases (NOXs) rendering them more susceptible to DNA damage following radiation. The work of this group suggests a distinct mechanism of sustained genomic instability that contributes to the inherent radio-sensitivity of HPV-positive cells.³⁵¹

Hence the apparent contradictions in response E6 knockdown and over expression to radiation and cisplatin may be explained by p53 status. In HPV-

positive cells with wild-type p53, knockdown of E6 abrogates the attenuating effect of p53 by this viral oncoprotein; p53 function is restored and able to induce cell death following radiation. By contrast, E6 was overexpressed in HPV-negative cells with perturbed p53 function where the viral protein has little or no effect on the latter. Under these circumstances, E6 may confer radiosensitivity by mechanisms independent of p53. The mechanisms for E6-induced sensitivity is not known, but possible pathways are discussed above.

The mechanisms of HPV-16 E6-induced sensitivity in HPV-negative cells require further study. Nevertheless, it is a potential avenue of investigation for the improved therapeutic management of HPV-negative HNSCC.

4.4 Limitations

The results of the current show that the increased sensitivity of HPV-positive cells to radiation and cisplatin *in vitro* are p53-dependent. However, there are several limitations to the current study that prevent generalisation and extrapolation to the clinical setting.

The previous chapter described a model of relative sensitivity to radiation and cisplatin in HPV-positive OPSCC using a panel of five HPV-positive cell lines and two HPV-negative cell lines. In the current chapter, due to time and other resource constraints, only two cell lines, namely UPCI-SCC 089 (HPV-negative) and UPCI-SCC 090 (HPV-positive) were selected for further study to determine the mechanism of HPV-associated sensitivity to these therapeutic agents.

Therefore, the data should be interpreted with caution since the role of p53 in the relative sensitivity of HPV-positive cells may be due to cell line variation and should not be generalised to all HPV-positive OPSCCs.

The current study also investigated two targets for further study; one cellular protein (p53) and one viral oncoprotein (E6). These targets were selected because of their key function in HPV-associated carcinogenesis. A more structured method of target selection could have been applied. Key targets from comparative HPV-positive and HPV-negative public genomic and expression array databases could have been interrogated. In addition, expression array analysis of HPV-positive and HPV-negative cells following treatment with radiation or cisplatin could have been obtained. Pathway analysis could have

been undertaken to elucidate important cellular regulators in the differential response of HPV-positive and HPV-negative cells to these therapeutic agents. It is possible that, in addition to p53, other key targets, including those important for cell cycle control, induction of apoptosis and/or DNA damage repair may have been elucidated. Similarly, although the viral oncoprotein E6 was investigated in the current study, the function of other viral proteins such as E5 and E7 may play an important role in the differential response to radiation and cisplatin in these cells.

UPCI-SCC 089 cell line was used to investigate the effects of E6 overexpression in HPV-negative OPSCC. The effectiveness of stable E6 transfection was evaluated by RT-PCR. Since there was intense baseline p53 protein expression in these cells by Western blot analysis and immunohistochemistry, it was assumed that there was functional abrogation of the p53 pathway in these cells. Sequencing of the p53 gene in UPCI-SCC 089 cells, to identify specific mutations, would have provided greater clarity to this study. There is evidence that E6 is able to target mutant p53 degradation.³⁵² Therefore, the effect of E6 overexpression on presumed functionally abrogated p53 in UPCI-SCC 089 cells, both at baseline and following treatment with radiation or cisplatin, would have provided further important information on the role of these proteins to explain sensitivity of HPV-positive and HPV-negative cells to these agents.

4.5 Conclusion

In summary, the results of the current chapter show that, increased sensitivity of HPV-positive cells to radiation and cisplatin *in vitro* is p53-dependent.

Furthermore attenuation of E6 in HPV-positive cells resulted in stabilisation of p53 and a modest increase in sensitivity to radiation and cisplatin. Forced expression of E6 in HPV-negative cells results in increased sensitivity to radiation and cisplatin.

The results of Chapter 4 confirm the findings of some previous reports. However, the literature also suggests some conflicting data, namely HPV-positive cells may be as sensitive or more resistant than HPV-negative cells depending on selection of controls and/or culture conditions. Chapter 4 utilised controls that were site matched while containing mutant p53 (UPCI-SCC072) or likely mutant p53 (UPCI-SCC089). This data suggests that, in HPV-positive cells, wild-type p53 is necessary to confer radiosensitivity. There are therefore clinical implications where, in HPV-positive disease, the determination of p53 status may be of further prognostic value. Furthermore, novel data from this chapter raises the possibility that p53, while playing an important role, may not entirely explain the relative radiosensitivity of HPV-positive cells since overexpression of HPV16-E6 resulted in increased radiosensitivity in HPV-negative cells. While only preliminary, these data is novel and warrants further study of the potential protective effect of this viral oncoprotein.

**Chapter 5 - Differential response of HPV-positive
and HPV-negative HNSCC cells to targeted
therapy *in vitro* and association of EGFR with
HPV status.**

5.1 Introduction

Despite its influence on prognosis, tumour HPV status is still not routinely used to inform therapeutic management. Current OPSCC therapeutic protocols implicate high doses of toxic radiation/chemotherapy, which may prove unnecessary for HPV-positive disease. Short- and long-term complications of current therapeutic protocols significantly impact on quality of life, especially in a younger cohort of patients with a long life expectancy.³⁵³ Subsequently, advancements in molecular research have made the identification of targeted therapies an attractive alternative therapeutic approach due to possible reduced toxicity and improved efficacy.^{354,355}

The results of Chapter 3 demonstrated that HPV-positive HNC cells are relatively more sensitive to conventional therapeutic agents, namely radiation and cisplatin, compared to site-matched HPV-negative cells. In order to determine whether HPV-positive and HPV-negative cells respond in a similar trend to targeted and novel therapeutic agents, this section of the study evaluated the response of these cells to cetuximab and TRAIL, respectively.

Having evaluated the role of p53 and HPV16-E6 in the response of these cells to cetuximab and TRAIL, this study went on to correlate EGFR protein expression with the former. Finally, findings of the *in vitro* association between HPV status and EGFR protein expression levels were correlated in tissue specimens *in vivo*.

5.2 Results

5.2.1 Response to targeted therapy

In relation to targeted therapy, cetuximab was selected since it is a recombinant chimeric monoclonal antibody specifically targeting the extracellular domain of EGFR. This receptor is overexpressed in more than 90% of HNSCC and is associated with poorer prognosis.^{156,356} Cetuximab is the most extensively studied of the anti-EGFR antibodies and is the first and only targeted therapy approved for the treatment of HNC.³⁵⁷⁻³⁵⁹ Furthermore, the impact of cetuximab on response and treatment outcome in HPV-positive OPSCC still remains to be defined. Several currently recruiting clinical trials compare cetuximab with cisplatin as concomitant agents in HPV-associated OPSCCs as part of a de-intensification protocol.^{257-259,261} In relation to this, results from *in vitro* data might be able to inform optimum treatment strategies in this subgroup of patients in future.

5.2.1.1 Cell viability following cetuximab treatment

Cell viability assays were performed as detailed in section 2.2.1.13. In HPV-positive cells treatment with cetuximab resulted in cell viability ranging from 100-90% at all doses from 200-1200nM. By contrast, HPV-negative cell lines showed cell viability ranging from 95-90%, 90-85%, 95-80%, 70-65% and 65-60% at 200, 400, 600, 800, 1000 and 1200 nM, respectively(Figure 5.1). HPV-negative cells demonstrated greater sensitivity to cetuximab compared to HPV-positive cells ($p \leq 0.01$ for HPV-negative cells versus UPCI-SCC 152 and UPCI-

SCC 154 cells at 1000 nM; $p \leq 0.001$ for HPV-negative cells versus UPCI-SCC 090, UD-SCC 2 and 93-VU-147T cells at 1000 nM and all HPV-positive cells at 1200 nM, unpaired t-test).

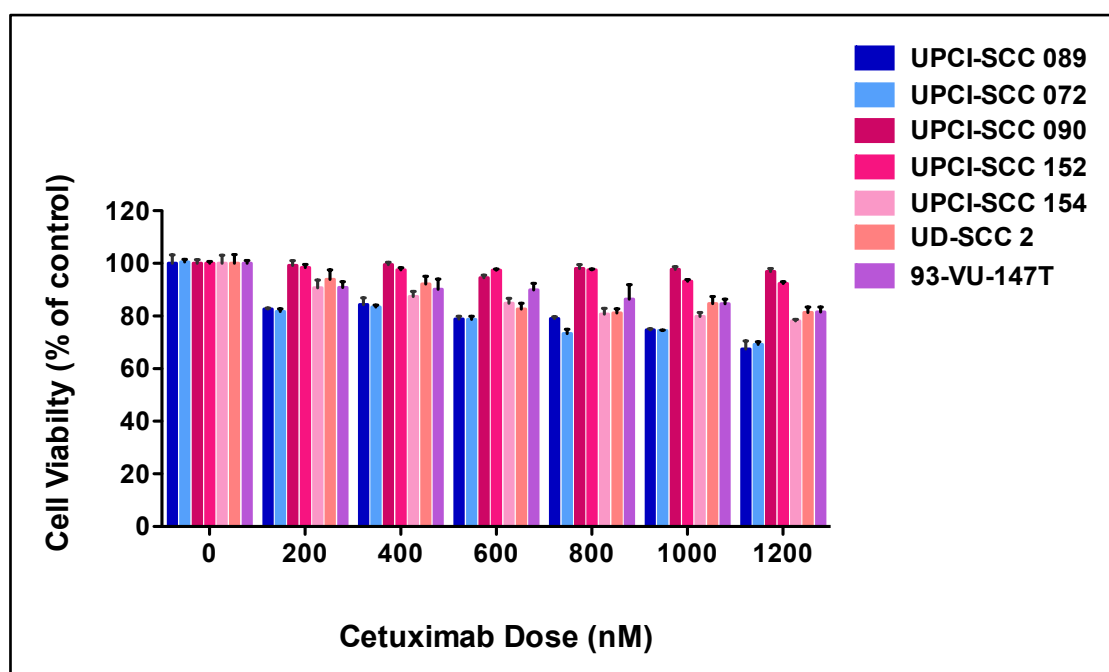


Figure 5.1. Cell viability HPV-negative and HPV-positive cell lines following cetuximab.

Bar graph of cell viability expressed relative to control. Cetuximab chemotherapy was performed at 200, 400, 600, 800, 1000 and 1200 nM. Cell viability was assessed by MTT assay 7 days following treatment. Bars represent average value from 6 wells normalised to untreated control cells. Error bars indicate standard deviation. This assay is representative of three independent experiments.

5.2.1.2 Cell viability following cetuximab treatment in E6-attenuated cells

The results of Chapter 4 showed that shRNA-induced attenuation of E6 expression in HPV-positive cells led to the restoration of p53 protein and greater sensitivity to conventional therapeutic agents. Since HPV-positive cells were resistant to treatment with cetuximab, this study went on to determine whether this observation was due to the oncogenic properties of E6.

The results show that silencing of E6 in HPV-positive cells (090-E6shRA) had no effect on cell viability when treated with cetuximab at aforementioned doses compared to the parental cell line (UPCI-SCC 090) and the scrambled control (090-scr control, Figure 5.2). No statistical significance was observed comparing treatment response at higher doses ($p=0.9854$ for 090-E6shRA cells versus UPCI-SCC 090 at 1000 nM and $p=0.3247$ for 090-E6shRA cells versus UPCI-SCC 090 at 1200 nM, unpaired t-test).

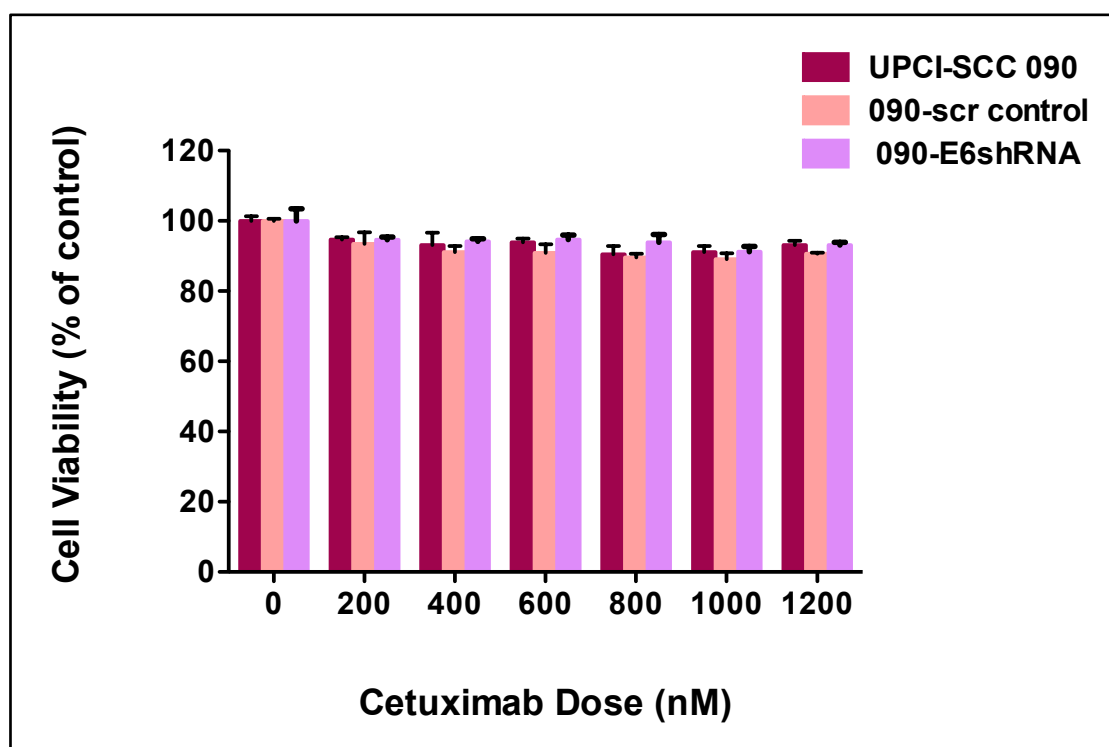


Figure 5.2. Cell viability of UPCI-SCC 090 E6shRNA cells following cetuximab.

Bar graph of cell viability expressed relative to control. Assay was performed in triplicate with 200, 400, 600, 800, 1000 and 1200 nM of cetuximab. UPCI-SCC 090 and scrambled control (090-scr control) were used as negative controls. Error bars indicate standard deviation. This assay is representative of three independent experiments.

5.2.1.3 Cell viability of E6 expressed cells following cetuximab

In order to confirm the findings in section 5.2.1.3, HPV-16 E6 was forcibly expressed in an HPV-negative cell line (UPCI-SCC 089) using two separate HPV16-E6 plasmids (E6-75 and E6-76) by stable transfection. Following treatment with cetuximab, cell viability was assessed by MTT assay. HPV-negative cells expressing E6 or a scrambled control showed similar responses to cetuximab; E6 expressed cells had no effect on cell viability (Figure 5.3). No statistical significance was observed between test and control cells ($p=0.0916$ for E6-75 and $p=0.1441$ for E6-76 versus UPCI-SCC 089 respectively at 1000 nM and $p=0.3694$ for E6-75 and $p=0.3224$ for E6-76 versus UPCI-SCC 089 respectively at 1200 nM, unpaired t-test).

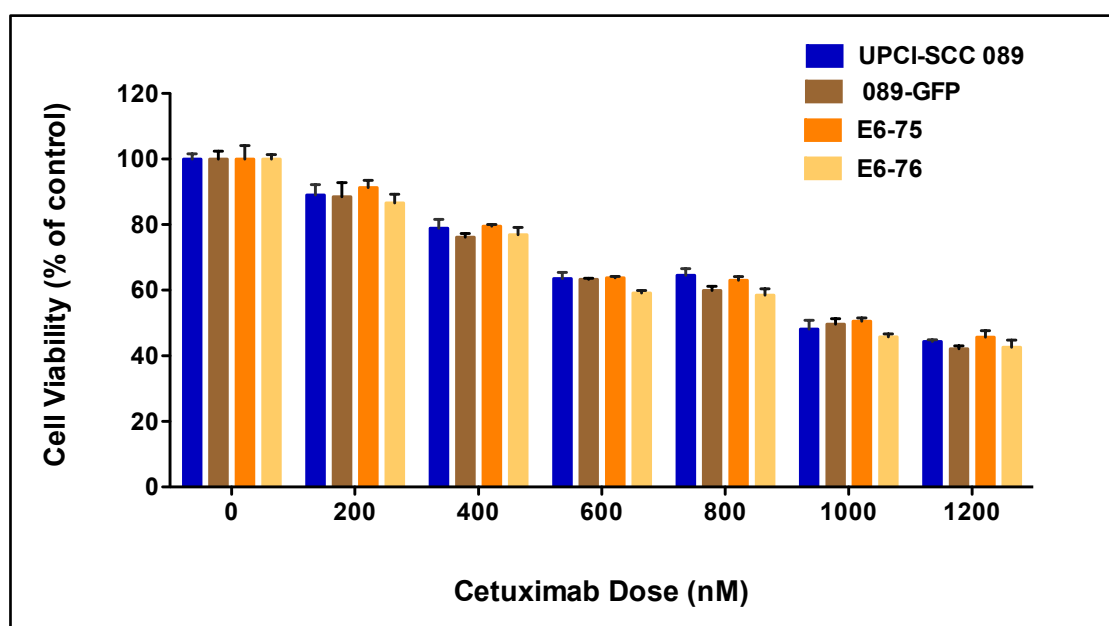


Figure 5.3. Cell viability of E6 expressed UPCI-SCC 089 cells following treatment with cetuximab.

Bar graph of cell viability expressed relative to control. Assay was performed in triplicate. Transfected plasmids of HPV-negative cell line (E6-75 and E6-76) and controls (UPCI-SCC 089 & 089-GFP) were treated at dosages of 200, 400, 600, 800, 1000 and 1200 nM. Error bars indicate standard deviation. This assay is representative of three independent experiments.

5.2.2 Association of EGFR with HPV status

The results of section 5.2.1.1 showed that HPV-positive cells were more resistant to cetuximab treatment *in vitro* compared to HPV-negative cells. In order to determine whether resistance to cetuximab in HPV-positive and HPV-negative cells was associated to baseline expression levels of EGFR, immunohistochemistry and western blot analysis was undertaken on untreated cells.

5.2.2.1 Baseline EGFR expression

5.2.2.1.1 Immunohistochemistry

Immunohistochemical evaluation of cell lines was undertaken using separate antibodies against the external domain (3C6) and internal domain (5B7) of EGFR. HPV-positive cell lines demonstrated variable staining intensity; UPCI-SCC 152 and UPCI-SCC 090 showed weak staining whereas moderate to intense staining was observed in UD-SCC 2, UPCI-SCC 154 and 93-VU-147T. By contrast, both HPV-negative cell lines (UPCI-SCC 072 and UPCI-SCC 089) demonstrated diffuse intense staining (Figure 5.4).

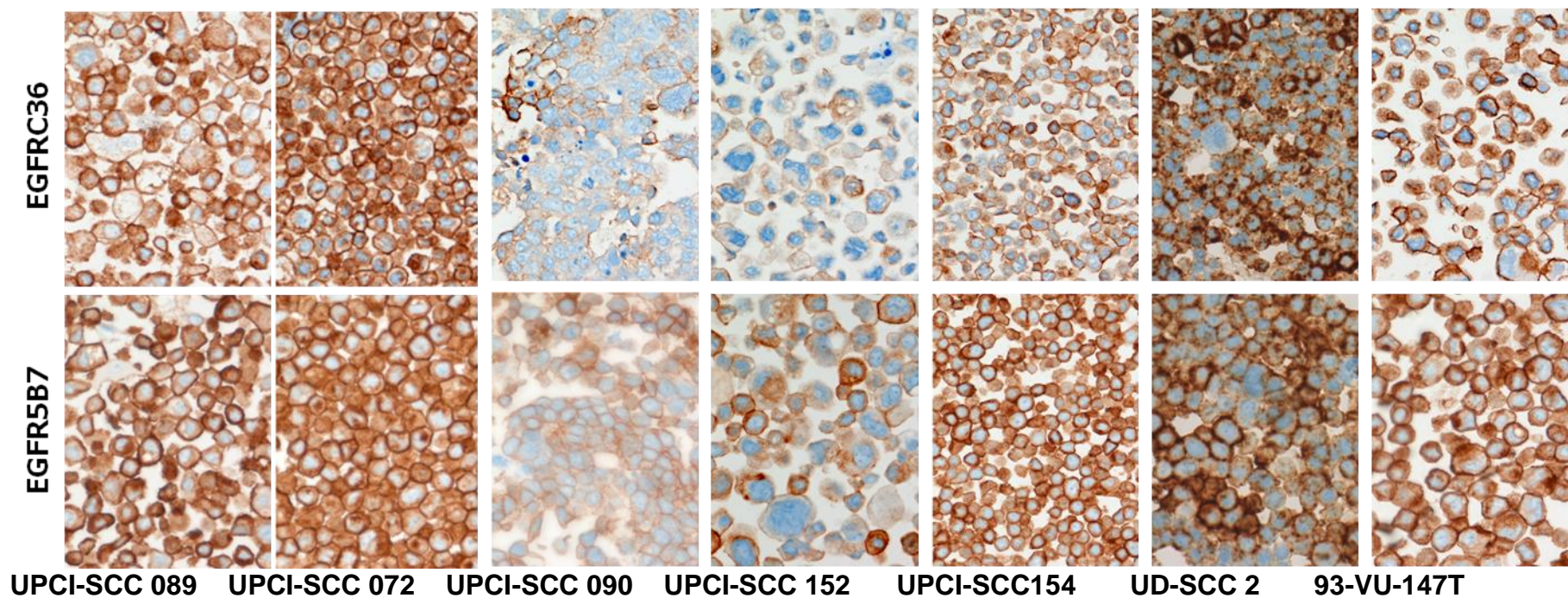


Figure 5.4. EGFR Immunohistochemistry.

Intense EGFR staining in UPCI-SCC 072 and UPCI-SCC 089 (HPV-negative) cell lines. Negative or weak in UPCI-SCC 090, UPCI-SCC 152, UPCI-SCC 154 and UD-SCC 2 and 93-VU-147T (HPV-positive) cell lines. All sections shown are 40 x magnification.

5.2.2.1.2 Western Blot

In order to confirm the EGFR immunohistochemical staining in cell lines, protein levels were additionally analysed by western blot. The latter confirmed the immunohistochemistry findings; namely UPCI-SCC 072 and UPCI-SCC 089 showed increased levels of EGFR. Similarly, in HPV-positive cell lines protein was undetectable in UPCI-SCC 090 and UPCI-SCC152 and weak to moderate in UPCI-SCC 154, UD-SCC 2 and 93-VU-147T (Figure 5.5 A). Quantification of EGFR by image J analysis showed 2-2.5 fold increase in the p53/ β -actin ratio in UPCI-SCC 072 and UPCI-SCC 089 (HPV-negative) cell lines. In contrast to HPV-positive cell lines that showed 0-1 fold increase, ($p \leq 0.001$ for HPV-negative cells versus HPV-negative cells, Figure 5.5 B).

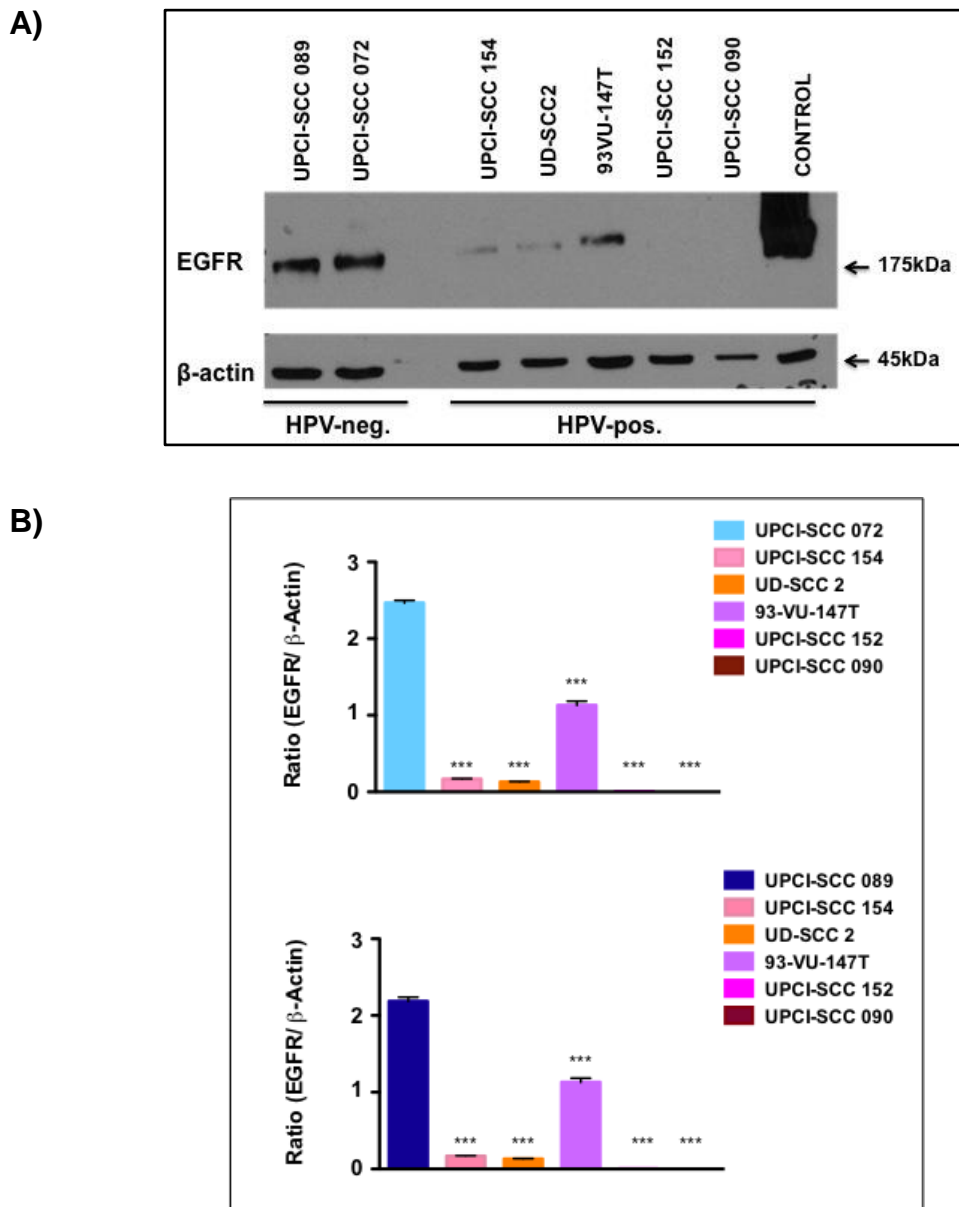


Figure 5.5. Western blot analysis of baseline expression of EGFR.

A) Expression difference of EGFR in cells of UPCI-SCC 072 and UPCI-SCC 089 (HPV-negative) and UPCI-SCC 090, UPCI-SCC 152, UPCI-SCC 154, UD-SCC 2 and 93-VU-147T (HPV-positive) cell lines by western blot. Arrows indicate molecular weight of the pre-stained protein ladder. HN5 cell line was used as positive control for EGFR expression. β -actin was used as a loading control. The above is representative of two independent experiments. B) The intensity of the bands shown in western blot (Figure 5.5 A) was quantified in relation to β -actin level using Image J. p-value was determined by unpaired t-test ($p < 0.001$).

Overall, response of the panel of cell lines to cetuximab broadly corresponded to EGFR protein expression levels with immunohistochemistry and western blot. UPCI-SCC 154, UD-SCC 2 and 93-VU-147T with variable expression of EGFR showed slight sensitivity to cetuximab and UPCI-SCC 090 and UPCI-SCC 152 (HPV-positive), cell lines that showed no expression of EGFR were most resistant to cetuximab. By contrast HPV-negative cell lines, with intense staining were relatively more sensitive (Figure 5.1).

5.2.2.2 EGFR expression in patient tumour samples

The results of section 5.2.2 indicate that there was trend towards an inverse correlation between HPV status and EGFR protein expression in HNSCC cell lines. In order to determine whether this cell line model was an accurate representation of the clinical situation, EGFR immunohistochemistry was carried out OPSCC patient tumour samples.

Tumour samples from 93 OPSCC patients were used (51 HPV-positive, 42 HPV-negative). Clinicopathological features of the patient characteristic e.g. gender, site, disease stage and treatment modality of 93 patients with OPSCC have been summarised in table 9. Two separate EGFR antibodies were used: EGFR (3C6, Figure 5.6), which recognises the external domain, including those with the vIII truncation and EGFR (5B7, Figure 5.7) targeting the intracellular domain. In order to overcome intra-tumour heterogeneity of staining (Figure 5.8), immunohistochemistry was undertaken in on whole sections and a

composite H-score was ascertained (see section 2.2.2.2, materials and methods on H-scoring).

Characteristic	N (%)
Gender	
Male	71 (76.3)
Female	21 (22.6)
Not known	1 (1.1)
Age (years)	
Mean	57
Mode	59
Range	39-80
Site	
Base of tongue	16 (17.2)
Epiglottis	1 (1.1)
Oropharynx, not otherwise specified	14 (15.0)
Soft palate	8 (8.6)
Tonsil	53 (57.0)
Not Known	1 (1.1)
Stage	
I	0 (0)
II	7 (7.5)
III	15 (16.1)
IVa	56 (60.2)
IVb	6 (6.5)
IVc	2 (2.2)
Not known	7 (7.5)
Treatment	
Chemoradiation	62 (66.7)
Radiotherapy	17 (18.3)
Palliative	7 (7.5)
Not known	7 (7.5)

Table 9: Summary of patient characteristics. Gender, site, disease stage and treatment modality of 93 patients with OPSCC.

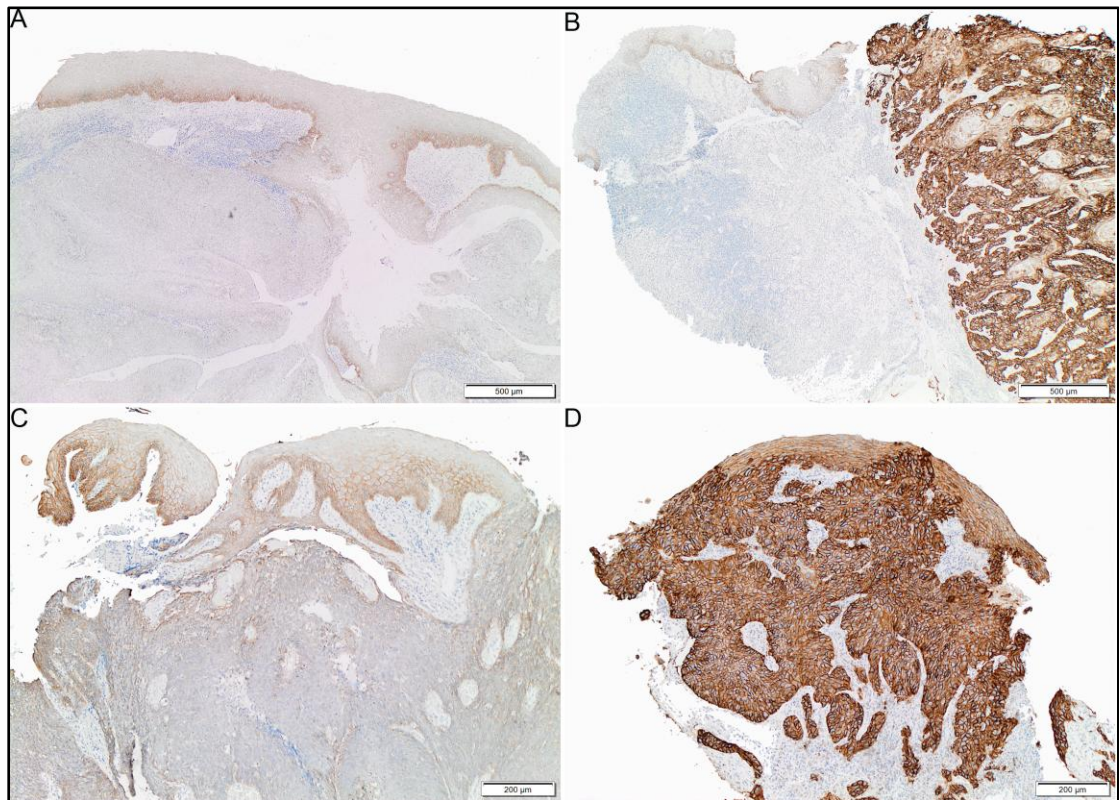


Figure 5.6. Photomicrographs of EGFR (3C6) immunohistochemistry.

Photomicrographs for the extracellular domain of EGFR (3C6) in four separate OPSCC tumour samples (A & B low power view, C & D high power view). A & C were HPV-positive and B & D were HPV-negative. The overall H-score for the tumour samples in A, B, C and D were 100, 300, 90 and 280, respectively. In all cases, the overlying non-dysplastic epithelium served as intra-sectional controls.

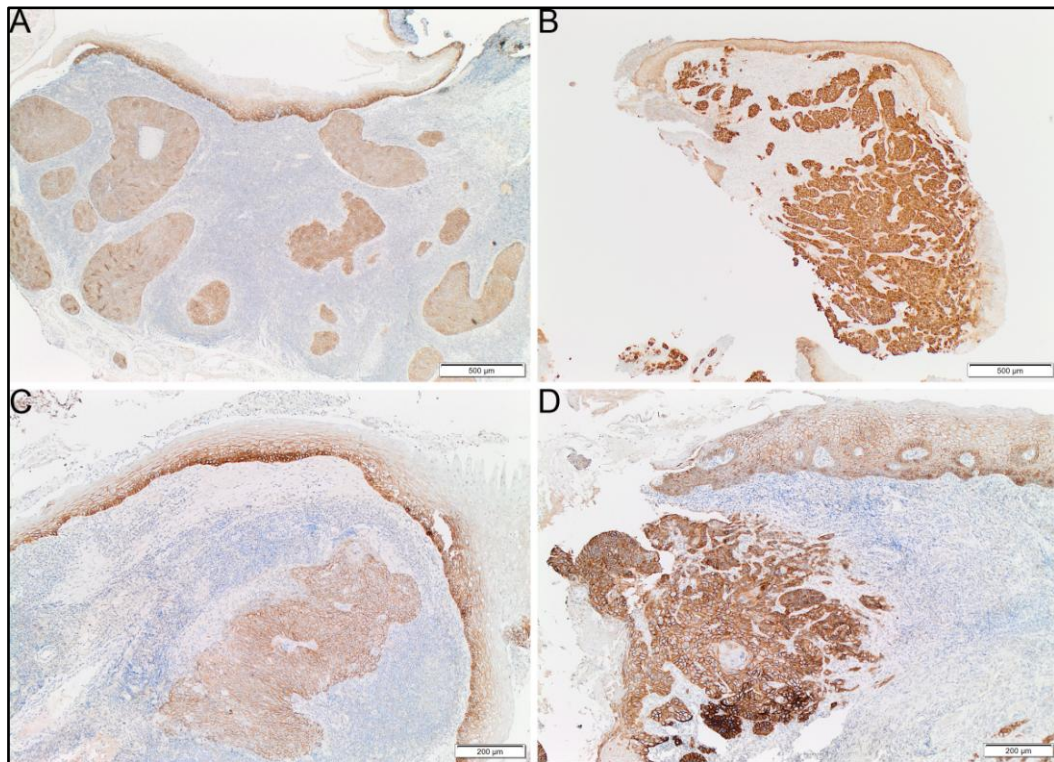


Figure 5.7. Photomicrographs of EGFR (5B7) immunohistochemistry.

Photomicrographs for the intracellular domain of EGFR (5B7) in four separate OPSCC tumour samples (A & B low power view, C & D high power view). A & C were HPV-positive and B & D were HPV-negative. The overall H-score for the tumour samples in A, B, C and D were 100, 300, 90 and 280, respectively. In all cases, the overlying non-dysplastic epithelium served as intra-sectional controls.

Dot over box-and-whisker plots for EGFR (C36) and EGFR (5B7) are shown in Figure 5.8. The mean, mode, median and range for EGFR (3C6) in HPV-positive cases were 63, 45, 50 and 15-230, respectively. By contrast, the mean, mode, median and range for EGFR (3C6) in HPV-negative tumours were 192, 190, 190 and 30-295, respectively. There was an overall trend for lower H-scores in HPV-positive OPSCCs compared to HPV-negative tumours, ($p>0.001$ for EGFR 3C6 and EGFR 5B7, Wilcoxon Signed Rank Test).

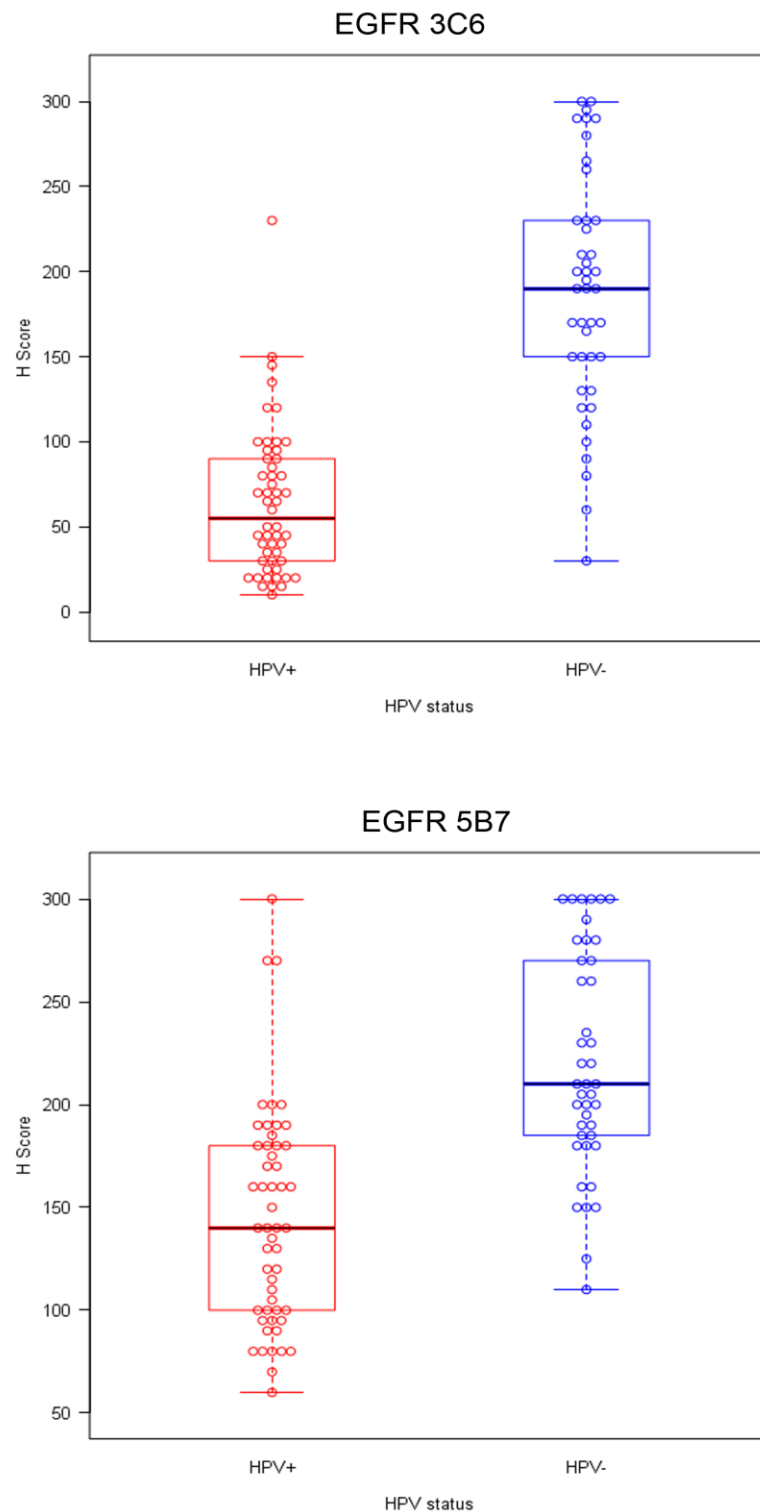


Figure 5.8. Dot over box-and whisker plot of EGFR.

Dot over box-and whisker plot of EGFR H-scores for EGFR (3C6) and EGFR (5B7) in HPV-positive (n=51) and HPV-negative (n=42) OPSCC tumour samples. Median indicated by horizontal bar.

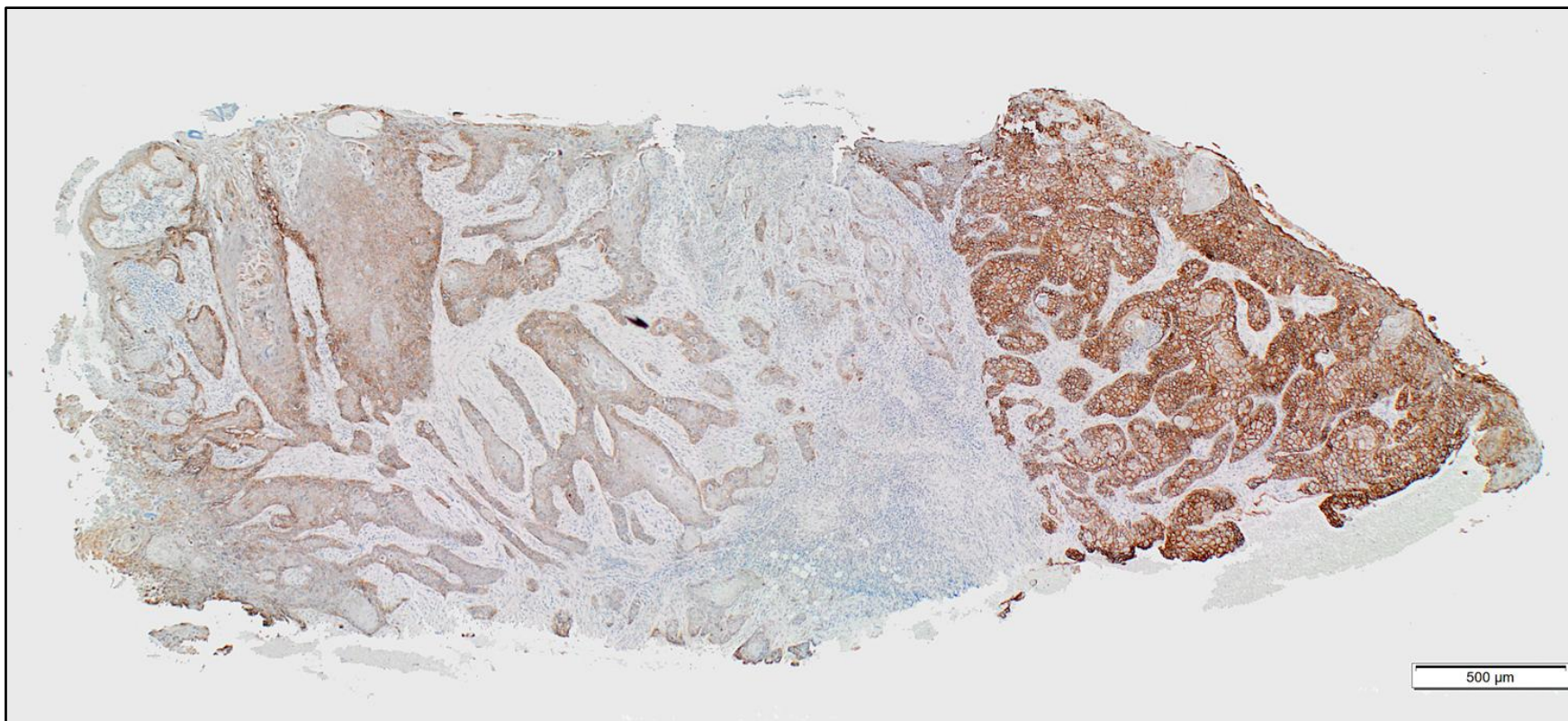


Figure 5.9. Photomicrograph of an OPSCC with EGFR (3C6) immunohistochemistry.

Photomicrograph demonstrating marked intra-tumour heterogeneity for the extra-cellular domain of EGFR (3C6). The overall H-score for this specimen was 200.

5.2.3 Survival analysis

5.2.3.1 Overall survival by HPV status

Figure 5.10 shows the Kaplan–Meier survival plot by HPV status. The mean overall survival for HPV-positive was 107 months (95% confidence interval [CI]= 91-123). By contrast, the mean overall survival for HPV-negative was 40 months (95% CI= 29-50). The overall survival for HPV-positive patients was significantly greater than HPV-negative patients ($p<0.001$, Log Rank). In Kaplan-Meier plots, the term ‘censored’ refers to the event (namely death in the case of overall survival) not having occurred at the time point the data was collected.

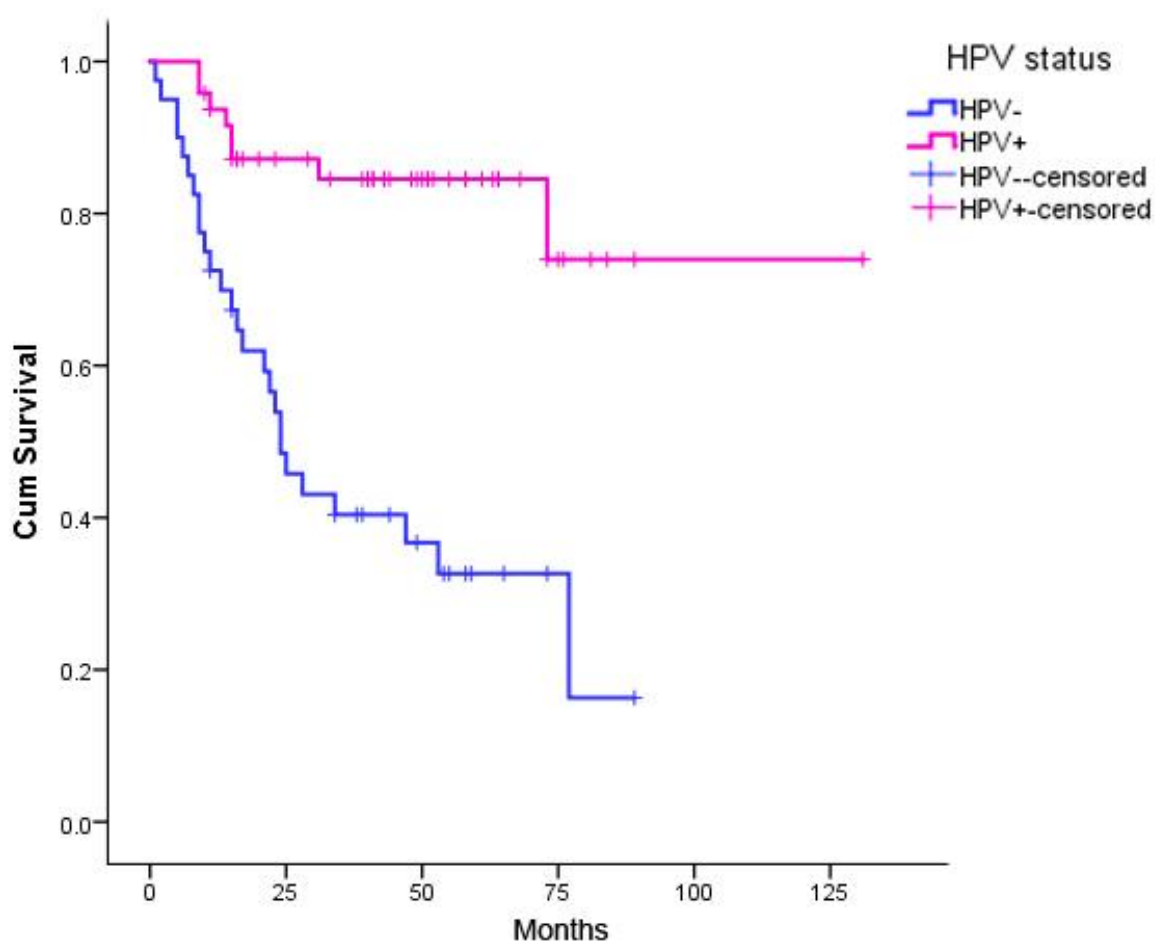


Figure 5.10. Kaplan–Meier survival plot for overall survival by HPV status.

Survival analysis by HPV status. Overall survival curves of HPV-positive (n=51) and HPV-negative (n=42) OPSCC tumour samples were analysed through the Kaplan–Meier method.

5.2.3.2 Overall survival analysis by EGFR status

Figure 5.11 shows the Kaplan–Meier survival plot by EGFR expression levels at various H-score cut-off (50, 100, 150 and 200). The H-scores were calculated as described in section 2.2.2.2. Low EGFR 3C6 levels correlated with improved overall survival for H-score cut-offs of 100, 150 and 200, ($p=0.001$, $p=0.002$ and $p=0.012$, respectively, Log Rank). Low EGFR 5B7 levels correlated with improved overall survival for H-score cut-offs of 100 and 200 ($p=0.008$ and $p=0.001$, respectively, Log Rank).

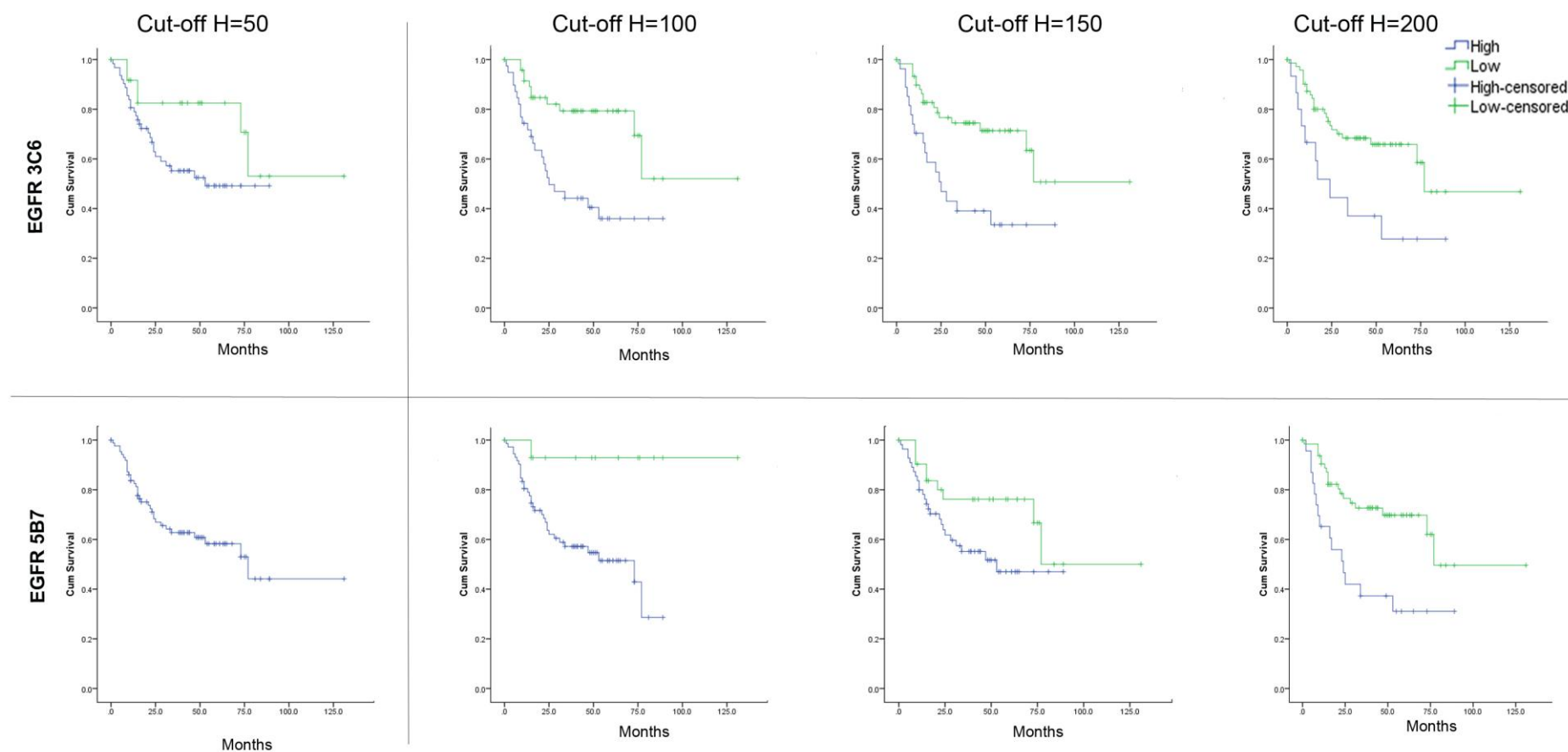


Figure 5.11. Kaplan–Meier survival plot for overall survival by EGFR status.

Survival analysis by EGFR expression. Overall survival of 3C6 and 5B7 curves based on the Kaplan–Meier method were analysed.

5.2.3.3 Overall survival by HPV and EGFR status

The results of the previous two sections indicate that, individually, HPV status and EGFR levels have prognostic utility. In order to determine whether there is prognostic utility in a combination of these two factors, Kaplan-Meier survival plots were undertaken following stratification of patients according to EGFR levels within the HPV-positive (HPV+) and HPV-negative (HPV-) cohorts separately (Figure 5.12). Within the HPV-positive group, there was a trend towards improved survival in the low EGFR 5B7 subgroup at a H-score cut-off of 100, but this was not statistically significant ($p=0.137$, Log Rank). Within HPV-positive and HPV-negative groups, further stratification by EGFR at all other H-score cut-off levels did not show any statistically significant differences in overall survival.

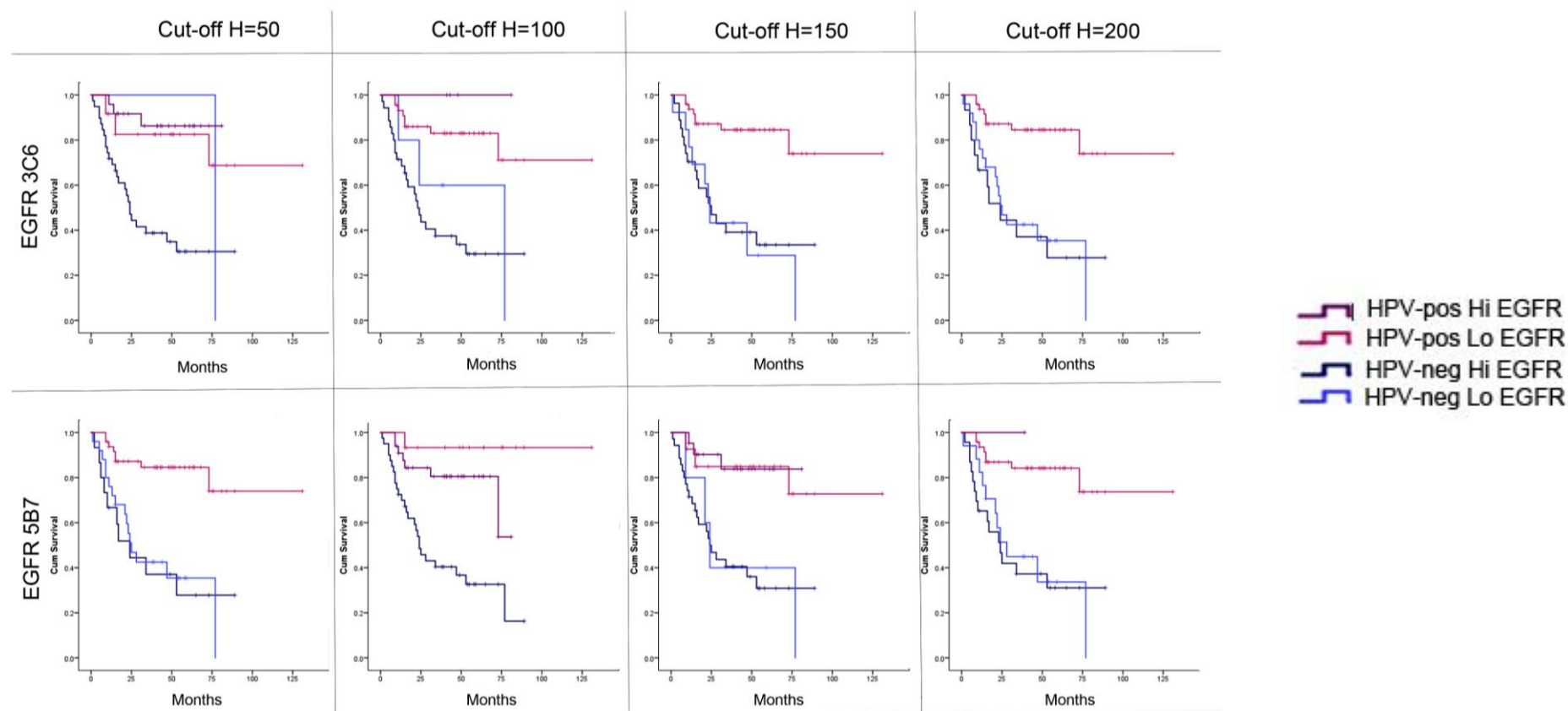


Figure 5.12. Overall survival Kaplan-Meier plots for HPV+ and HPV- patients at incremental EGFR C36 and EGFR 5B7 H-scores.

Survival analysis by HPV and EGFR expression. Overall survival 3C6 (top row) and 5B7 (bottom row) curves based on the Kaplan–Meier method were analysed.

5.2.4 Response to novel therapeutic agent -TRAIL

TRAIL has been shown to demonstrate selective cytotoxicity in several types of malignant cell lines³⁶⁰ and recombinant TRAIL has shown promising results in phase I/II clinical trials for the treatment of patients with advanced tumours.³⁶¹ In HPV-negative HNSCC cell lines, TRAIL has been shown to demonstrate variable death-inducing activity.³⁶² This agent induces apoptosis by activating caspase-8. Since it has been shown that HPV-16 E6 protein has the ability to interact with caspase 8 and target it for degradation,^{363,364} the next stage of this study sought to investigate the relative sensitivity of the current panel of cell lines to TRAIL.

5.2.4.1 Cell viability following TRAIL treatment

Cell viability assays were performed as detailed in section 2.2.1.13. In HPV-positive cells treatment with TRAIL resulted in cell viability ranging from 90-100% at all doses from 3.13 -100 ng/ml. By contrast, HPV-negative cell lines showed cell viability ranging from 5-10%, 20-30%, 20-40%, 25-45%, 30-45 and 50-55 at 3.13, 6.25, 12.5, 25, 50 and 100 ng/ml, respectively (Figure 5.13). HPV-negative cells demonstrated greater sensitivity to TRAIL compared to HPV-positive cells ($p \leq 0.001$ for HPV-negative cells versus all HPV positive cell lines at 50 and 100 ng/ml with the exception of UPCI-SCC 072 versus 93-VU-147T with $p < 0.01$, unpaired t-test).

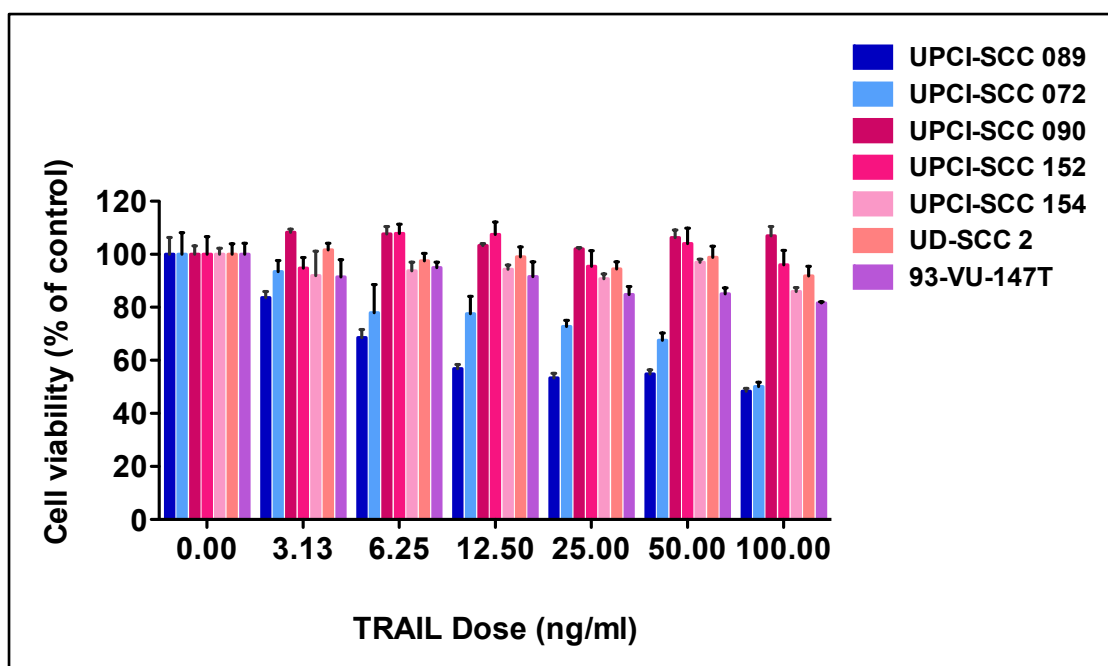


Figure 5.13. Cell viability of HPV-negative and HPV-positive cell lines following TRAIL.

Bar graph of cell viability expressed relative to control. TRAIL chemotherapy was performed for 48 hours at 3.13, 6.25, 12.5, 25, 50 and 100 ng/ml. Cell viability was assessed by MTT assay 7 days following treatment. Bars represent average value from 6 wells normalised to untreated control cells. Error bars indicate standard deviation. This assay is representative of three independent experiments.

5.2.4.2 Cell viability in response to TRAIL following attenuation of E6

In order to determine whether the relative resistance of HPV-positive cells to TRAIL was a direct effect of viral oncoprotein, treatment of these cells were undertaken following attenuation of E6 in HPV-positive cells. There was no effect on cell viability by MTT assay of E6-attenuated cells (090-E6shRA) when treated with TRAIL at aforementioned doses compared to the parental cell line (UPCI-SCC 090) and the scrambled control (090-scr control, Figure 5.14). No statistical significance was observed between test and control cells ($p=0.1969$ for 090-E6shRA cells versus UPCI-SCC 090 at 50 ng/ml and $p=0.3822$ for 090-E6shRA cells versus UPCI-SCC 090 at 100 ng/ml, unpaired t-test).

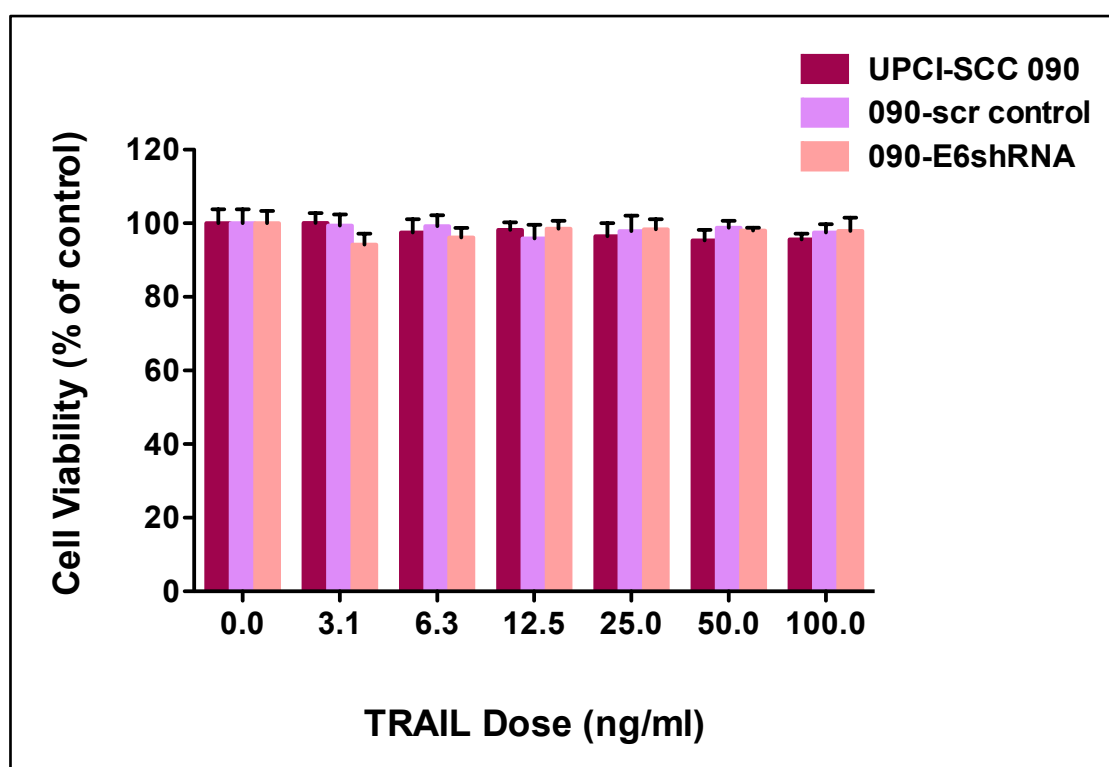


Figure 5.14. Cell viability of UPCI-SCC 090 E6shRNA cells following TRAIL.

Bar graph of cell viability expressed relative to control. Assay was performed in triplicate with 3.13, 6.25, 12.5, 25, 50 and 100 ng/ml of TRAIL through MTT assay. UPCI-SCC 090 and scrambled control (090-scr control) were used as negative controls. Error bars indicate standard deviation. This assay is representative of three independent experiments.

5.2.4.3 Cell viability of E6 expressed cells following TRAIL

To confirm that relative resistance to TRAIL was not a direct effect HVP-16 E6, cell viability MTT assay was undertaken following treatment with this agent of stably expressed HPV-16 E6 HPV-negative cells (E6-75 and E6-76). Cells forcibly expressing E6 or a control vector showed similar responses following treatment with TRAIL; E6 expressed cells had no effect on cell (Figure 5.15). No statistical significance was observed between test and control cells ($p=0.9336$ for E6-75 and $p=0.4284$ for E6-76 versus UPCI-SCC 089 respectively at 50 ng/ml and $p=0.7048$ for E6-75 and $p=0.3674$ for E6-76 versus UPCI-SCC 089 respectively at 100 ng/ml, unpaired t-test).

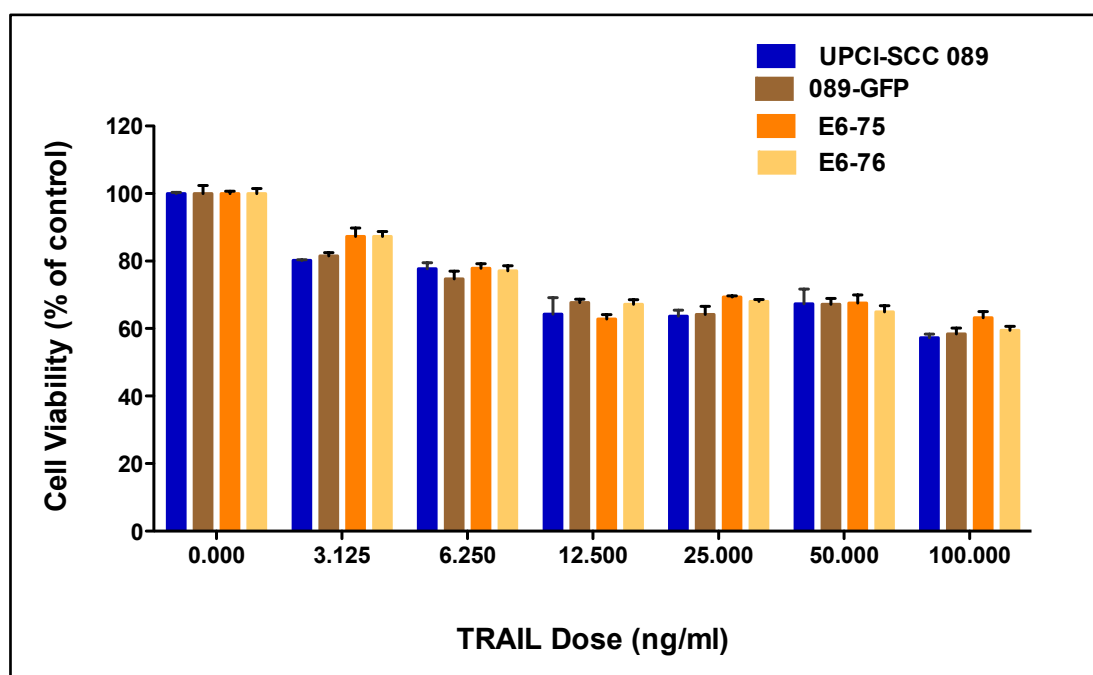


Figure 5.15. Cell viability of E6 expressed UPCI-SCC 089 cells following TRAIL.

Bar graph of cell viability expressed relative to control. Assay was performed in triplicate. Transfected plasmids of HPV-negative cell line (E6-75 and E6-76) and controls (UPCI-SCC 089 & 089-GFP) were treated at dosages of 3.1, 6.3, 12.5, 25, 50 and 100 ng/ml. Error bars indicate standard deviation. This assay is representative of three independent experiments

5.3 Discussion

The results of Chapter 3 indicated that HPV-positive cells demonstrate increased relative sensitivity to radiation or cisplatin compared to site-matched HPV-negative cells. This finding provided a useful *in vitro* model for improved survival in HPV-associated OPSCC since radiation and cisplatin are current mainstay treatment modalities for this disease. Nevertheless, these conventional therapeutic agents are associated with significant toxic effects and there is therefore a trend towards more targeted therapy which maintains current response rates whilst reducing the side effects of treatment. In order to pre-empt clinical studies of the utility of alternatives to radiation and cisplatin, this section of the current study focussed on the *in vitro* response of HPV-positive and HPV-negative HNC cell lines to targeted and novel agents, namely cetuximab and TRAIL, respectively.

5.3.1 Response of cell lines to cetuximab

Cetuximab is a monoclonal chimeric (human/mouse) antibody that targets EGFR with high affinity, and inhibits endogenous ligand binding, thereby blocking receptor dimerisation, tyrosine kinase phosphorylation, and pro-survival signal transduction.^{365,366} This drug, in combination with radiotherapy, is approved for the treatment of HNSCC and there are currently several clinical trials in progress to determine whether cetuximab is an efficacious alternative to cisplatin for the management of this disease.^{258,259,367}

Unlike the relative sensitivity of HPV-positive cells to radiation and cisplatin (Chapter 3), somewhat surprisingly, the results of current study demonstrated that HPV-positive cells were relatively resistant to treatment with cetuximab. Furthermore, modulation of HPV16-E6 (either through attenuation of endogenous E6 in HPV-positive cells, or forced expression in HPV-negative cells) did not significantly alter response to this agent, suggesting a virus-independent role in resistance to cetuximab.

Investigation into the relationship between HPV and EGFR has largely centred on the E5 protein.^{72,81,82} Little is known about the direct relationship between EGFR and E6. Unlike HPV-negative carcinomas where increasing overexpression of EGFR corresponds to stepwise carcinogenesis, EGFR ‘oncogene addiction’ may not to be necessary in HPV-positive disease. Therefore, the inverse relationship between EGFR and HPV may be an epiphenomenon. The relative resistance of HPV-positive cells to cetuximab may be directly related to the quantity of EGFR expression.

Data on the *in vitro* response of HPV-positive cells to cetuximab is sparse. In contrast to the current study, Nagel *et al* (2013) showed no difference in response of HPV-positive and HPV-negative cells to cetuximab.²⁹⁹ The discrepancy with the current study may be partly explained by the lack of site-matched controls and the greater cumulative range of cetuximab dose. Pogorzelski *et al* (2014) also evaluated the effect of HPV on cetuximab-treated cells treatment in HNC cells. They described cell-line variation even among HPV-positive cells (i.e. sensitivity in UPCI-SCC 090 and resistance in

UD-SCC2.³⁶⁸ Furthermore, through enforced transgene activation of E6 and E7, they found that modulation of viral oncoproteins did not significantly affect response to cetuximab. Their results concur with those of the current study where resistance to cetuximab was independent of HPV16-E6.

In a recent report using a similar cell line panel to that of the current study, Gusteret *al* (2014) showed that concomitant cetuximab failed to further radiosensitise HPV-positive cells.³⁶⁹ In support of the findings of the current study their data indicate that the response of HPV-positive cells to cetuximab and radiation are likely to be divergent. To date, there are no reports of a direct mechanistic pathway of HPV proteins in the down-regulation of EGFR. The inverse correlation between HPV and EGFR may also be a function of smoking. Some groups have demonstrated that EGFR expression was significantly higher in current smokers than in past smokers, with never smokers demonstrating lowest levels of the protein.³⁷⁰ Since patients with HPV-associated OPSCC tend to be never, or past smokers, this group of patients are most likely to demonstrate low EGFR levels.

Having determined that HPV-positive cells demonstrated increased resistance to cetuximab, the current study went on to determine whether this may be explained by increased levels of EGFR protein expression. Using immunohistochemistry and western blot analysis, there was a clear correlation between resistance to cetuximab and EGFR protein expression in the panel of cell lines in this study. Since there was a trend towards an inverse correlation between HPV status and EGFR protein expression, this

study went on to determine whether the current panel of cell lines provided a suitable *in vitro* model that reflected the clinical situation. Notwithstanding the possibility that these findings may be explained by cell line variation alone, these data indicate that the current *in vitro* model corresponds to the clinical findings (section 5.2.2), as discussed in the ensuing section (5.3.2).

5.3.2 Association of EGFR with HPV status in OPSCC tissue specimens

The current study demonstrated that EGFR protein levels are significantly downregulated in HPV-positive cells in comparison to HPV-negative cells *in vitro*. Furthermore, this study also demonstrated a similar pattern in patient tissue samples *in vivo*. For semi-quantification by immunohistochemical H-score, EGFR protein levels were evaluated against intra-sectional controls of normal surface and reticulated crypt epithelium (Figure 5.8). Therefore, the downregulation of EGFR in HPV-positive cells are not a result of subsite differences within the head and neck. Nevertheless, the mechanisms of HPV-associated downregulation of EGFR remain largely unknown. In HPV-negative carcinomas, associated with tobacco use and alcohol excess, there is a stepwise increase EGFR protein expression from normal to premalignancy to invasive carcinoma. In these tumours, EGFR is likely to be a necessary driver for carcinogenesis. By contrast, no observable premalignant phase is seen in HPV-positive tumours, raising the possibility that the oncogenic drive may be independent of EGFR. However, further

studies, beyond the scope of this thesis, are necessary to test this hypothesis. The cell line model described above provided a suitable model for evaluating response to cetuximab because it correlated with the findings in OPSCC tissue samples; there was an inverse correlation between HPV status and EGFR protein expression. The inverse correlation was more pronounced for the extracellular domain (EGFR 3C6) compared to the intracellular domain (EGFR 5B7, Figure 5.5). A growing number of previous reports are supportive of this data. Reimers *et al.* (2007) found a trend towards an inverse correlation between EGFR protein expression and p16-positive OPSCC ($p=0.083$).¹⁵⁶ Since then, up to eight independent studies with a combined cohort of 1231 patients have confirmed this inverse relationship.^{128,188,189,370-374} By contrast, Perrone *et al.* (2006) and Rampia *et al.* (2013) did not demonstrate this inverse correlation.^{375,376} Although this discrepancy may be explained by the use of different antibodies, a more likely explanation is the lack of standardised EGFR scoring criteria. Indeed, there are no agreed cut-off with some groups defining EGFR positivity as '*membrane staining of at least moderate intensity of 10% of cancer cells*' while others defining it as '*more than 50% of the cell membranes of the tumour cells*'.^{156,188}

5.3.3 Survival analysis

In the cohort of patients studied, patients with HPV-associated OPSCC demonstrated improved overall survival compared to site and tumour

matched patients. This data add to the pool of already robust findings of improved prognosis in HPV-positive OPSCC patients. Similarly low EGFR 3C6 (H-score cut-offs of 100, 150 and 200) and low EGFR 5B7 (H-score cut-offs of 100 and 200) were also associated with improved overall survival. These results are supported by several previous reports that have shown poorer survival outcome in HNC patients with high EGFR protein expression.^{24,377,378}

Several reports have indicated that a combination of HPV status and EGFR protein levels may have prognostic value.^{188,370,371} The current study failed to demonstrate any further prognostic value when HPV-positive and HPV-negative patients were further stratified into high and low EGFR groups, respectively. There are several possible reasons for this discrepancy. In the current cohort, there was a strong correlation between HPV status and EGFR protein expression; very few HPV-positive OPSCC tumours demonstrated high EGFR levels (Figure 5.9) thereby limiting sub-group analysis. Furthermore, by evaluating H-scores, this current study took into account intra-tumour heterogeneity and therefore, within a single specimen, semi-quantitative evaluation of areas expressing high EGFR intensity levels may have been 'diluted' by foci with low levels of the protein. Nevertheless, further work is necessary, especially in standardising semi-quantitative IHC assessment and cut-offs, to determine whether a combination of HPV and EGFR are useful prognostic indicators in OPSCC.

5.3.4 Impact on management of OPSCC

In light of the fact that HPV-associated OPSCC express less EGFR, the question of importance is, 'is anti-EGFR treatment useful in patients with HPV-positive HNSCC?' Against this background, it is important to highlight that, to date, no study using EGFR inhibitor drugs in HNSCC has shown that EGFR gene copy number or expression level is predictive of clinical tumour response.^{379,380} For example, even amongst those patients with HPV-negative HNSCCs that have high EGFR expression, only 8–13% respond to a single-agent EGFR inhibitor.³⁸¹ In the current study, it was not possible to further evaluate whether pre-treatment expression levels of EGFR impacted on response to cetuximab because only 3 patients within the cohort were treated with this agent as an alternative to cisplatin.

To answer the question above, several clinical trials with cetuximab combined with radiation in an effort to reduce long term side effects of treatment whilst still preserving survival outcomes in HPV-positive patients are in progress. The Radiation Therapy Oncology Group (RTOG) 1016 is a multi-centre based in the United States phase III trial recruiting patients with Stage III or IV p16-positive OPSCC patients with the goal of evaluating the replacement of cisplatin with cetuximab. Patients have been randomised to receive weekly cetuximab or intravenous cisplatin with concurrent accelerated intensity-modulated radiation therapy (IMRT) to 70 Gy.²⁵⁸ Similarly, in the United Kingdom, the De-ESCALaTE HPV trial aims to recruit 304 p16-positive OPSCC patients randomised to conventionally fractionated intensity-modulated radiation therapy (IMRT) with either cetuximab or

cisplatin. The primary outcome measure is rates of long term (i.e. 2-years post treatment) toxic effects, whilst overall survival and disease recurrence are secondary outcome measures.²⁵⁹ Data from these trials, with appropriate follow-up period will not be available for several years. Once available, these results will inform the clinical community whether cetuximab can replace cisplatin for the management of HPV-positive OPSCC with the aim of reducing treatment-related toxicity while maintaining the same cure rates. Furthermore, post-hoc analysis of tissue sample may shed light on whether pre-treatment levels of EGFR are predictive of response to cetuximab.

5.3.5 Response of cell lines to TRAIL

TRAIL is now being considered as a promising anti-tumour approach since it selectively kills several types of malignant cell lines with little effect on normal cells.³⁶⁰ However, to date, there have been no clinical trials evaluating this agent in the management of HNSCC. Pre-clinical investigation has demonstrated HNSCC cell line variation in response to recombinant TRAIL where it appears that high levels of endogenous caspase-8 is associated with sensitivity to this agent.³⁶² Since HPV-16 E6 interferes with caspase-8 activation by accelerating its degradation; this study postulated that HPV-positive cells were likely to be more resistant to TRAIL. Some reports have suggested that small molecules could inhibit E6 from binding to procaspase-8 thereby restoring the apoptotic pathway.²⁶⁹ Although this study demonstrated greater resistance of HPV-positive cells to TRAIL, attenuation of E6 failed to sensitise these cells to the drug. Furthermore, forced

expression of E6 in HPV-negative cells, previously sensitive to TRAIL, did not significantly alter its sensitivity thereby suggesting that HPV-associated resistance to TRAIL may be E6-independent.

The mechanisms of TRAIL resistance in HPV-positive cells is beyond the scope of this thesis. Parallel work within this group has shown that TRAIL resistance in HPV-positive cells is independent of levels of endogenous caspase 3, caspase 8 and XIAP.³⁸² However, larger expression profiling data is necessary to dissect the pathways involved. Nevertheless, from the current study and previous work within this group, it appears that the mechanisms are independent of E6.

5.4 Limitations

The results of the current section of this study demonstrated that HPV-positive cells *in vitro* are more resistant to cetuximab in comparison to HPV-negative cells. Furthermore, the relative resistance to cetuximab *in vitro* is inversely correlated to EGFR protein expression as determined by Western blot analysis. A limitation of the current study is the lack of further characterisation of EGFR status of the cell line panel. Although rare in HNC, missense mutations, truncations and amplifications have been reported.^{2,3} More detailed characterisation of EGFR status is likely to have provided greater accuracy of the utility of this *in vitro* panel as a model that mimics the clinical situation.

As with previous chapters, this section of the study investigated mechanisms of response to therapeutic agents in only one HPV-positive and one HPV-negative cell line. Comparison of therapeutic responses between HPV-positive and HPV-negative cells in a larger panel of cell lines would mitigate against cell line variation independent of viral status. Similarly, this study only evaluated the role of HPV16-E6 in response to novel and targeted therapeutic agents. No significant effect was observed in response to cetuximab or TRAIL when E6 was knocked down in HPV-positive cells, or when the oncoprotein was overexpressed in HPV-negative cells. However, evaluation of the role of E6 alone does not exclude possibility that HPV may still play a role in resistance to therapeutic targeting of EGFR or death receptors. The potential roles of E5 and E7 in resistance to these therapeutic agents still require investigation. Characterisation of these cells in relation EGFR, other ErbB receptor family,

death receptor family and their downstream targets as well as response to EGFR tyrosine kinase inhibitors and a larger panel of death receptor targeting agents are necessary prior to extrapolation to the clinical situation. Parallel *in vitro* studies including response to cetuximab following overexpression of EGFR in HPV-positive cells are also likely to add value to the current study.

This study also demonstrated a trend towards an inverse correlation between HPV status and EGFR protein expression *in vivo* in patient OPSCC tumour samples. However, the study is limited by the small cohort size, which precludes immediate clinical applicability. The high estimated overall survival rate in the HPV-positive group, coupled with the small sample size, may explain the inability of the combination of HPV status and EGFR expression to further refine survival estimates. Multivariate analysis of HPV status, EGFR expression, tumour stage, smoking and alcohol history and therapeutic modality (including equal numbers of patients treated with Cetuximab versus cisplatin combination therapy) is likely to inform translational benefit of this study.

5.5 Conclusion

In summary, the results of the current chapter show that:

1. HPV-positive cells are relatively resistance to treatment with cetuximab compared to HPV-negative cells.
2. Resistance to cetuximab was independent of HPV16-E6, but correlated with EGFR protein expression levels *in vitro*.
3. The *in vitro* cell line model was representative of the clinical tumour samples.
4. As prognostic marker, HPV status and EGFR protein levels demonstrated utility when used separately. However, used in combination, these markers did not demonstrate further refinement of prognostic utility.
5. HPV-positive cells are relatively resistance to treatment with TRAIL compared to HPV-negative cells. Resistance to TRAIL was independent of HPV16-E6.

CHAPTER 6 - Conclusions and Future Work

6.1. Summary and Conclusions

In summary, this thesis describes an *in vitro* model of relative radio- and chemosensitivity, which mirrors clinical observations. Sensitivity to radiation and cisplatin was associated with stabilisation of functional p53 in HPV-positive cells. Forced expression of HPV-16 E6 in HPV-negative, mutant p53 cells, also resulted in sensitivity to radiation and cisplatin. This study therefore describes both p53-dependent and HPV-16 E6-dependent/p53-independent mechanisms of sensitivity of HNC cells to radiation and cisplatin.

By contrast to radiation and cisplatin, HPV-positive cells were relatively resistant to an EGFR-targeted therapeutic agent (cetuximab) and to TRAIL. In inverse correlation between HPV status and EGFR protein expression was demonstrated in cell lines *in vitro* and OPSCC tissue sample *in vivo*, but EGFR protein expression in the later did not confer additional prognostic value beyond HPV status in the latter.

6.2 Future Work

1. Validation of the *in vitro* model of relative radio- and chemo-sensitivity.

Since the development of this model, described in Chapter 3, several novel HPV-positive cell lines have been reported in the literature.^{317,318} Demonstration of the relative sensitivity in these new described HPV-positive cell lines will strengthen the model and overcome the possibility of cell line variation. Furthermore, *in vivo* validation using animal xenografts for the evaluation of tumorigenicity and response to treatment will further validate the current *in vitro* model.

2. E6-mediated induction of radio- and chemo-sensitivity.

The results of Chapter 4 showed that forced expression of HPV-16E6 in HPV-negative HNC cells resulted in increased radio- and chemo-sensitivity in p53-independent manner. The mechanisms to explain this observation are unknown. Investigation of this potential 'protective' effect of HPV16-E6, including the possibility of viral oncoprotein-mediated induction of genetic instability, may have therapeutic implications.

3. Mechanisms of resistance to EGFR-targeted therapy.

The mechanisms for resistance to cetuximab *in vitro* demonstrated in Chapter 5 are still not known. Since there was an inverse correlation between HPV status and EGFR protein expression, an observation confirmed in tissue samples *in vivo*, a clinically important and timely research

question is 'Are pre-treatment levels of EGFR protein expression in OPSCC predictive of response to chemo-radiation?'. This question may be answered by post-hoc evaluation of clinical trial material.

4. Mechanisms of resistance to TRAIL

Further characterisation of the panel of cell lines used in this study in relation to the death receptor (DR)-mediated apoptotic pathway, including caspase-8, FADD and c-FLIP, are likely to explain possible mechanisms of resistance to treatment with TRAIL. Furthermore, evaluation of the possible interaction between HPV-16 E6 and DR pathway genes and proteins will inform whether TRAIL is likely to be a viable therapeutic option in the management of HPV-associated OPSCC.

Bibliography

Bibliography

1. Dobrossy L: Epidemiology of head and neck cancer: magnitude of the problem. *Cancer Metastasis Rev* 24:9-17, 2005
2. Choi S, Myers JN: Molecular pathogenesis of oral squamous cell carcinoma: implications for therapy. *J Dent Res* 87:14-32, 2008
3. Neville BW, Day TA: Oral cancer and precancerous lesions. *CA Cancer J Clin* 52:195-215, 2002
4. Marur S, Forastiere AA: Head and neck cancer: changing epidemiology, diagnosis, and treatment. *Mayo Clin Proc* 83:489-501, 2008
5. Proia NK, Paszkiewicz GM, Nasca MA, et al: Smoking and smokeless tobacco-associated human buccal cell mutations and their association with oral cancer--a review. *Cancer Epidemiol Biomarkers Prev* 15:1061-77, 2006
6. Hashibe M, Boffetta P, Zaridze D, et al: Evidence for an important role of alcohol- and aldehyde-metabolizing genes in cancers of the upper aerodigestive tract. *Cancer Epidemiol Biomarkers Prev* 15:696-703, 2006
7. Hashibe M, Brennan P, Chuang SC, et al: Interaction between tobacco and alcohol use and the risk of head and neck cancer: pooled analysis in the International Head and Neck Cancer Epidemiology Consortium. *Cancer Epidemiol Biomarkers Prev* 18:541-50, 2009
8. Kreimer AR, Clifford GM, Boyle P, et al: Human papillomavirus types in head and neck squamous cell carcinomas worldwide: a systematic review. *Cancer Epidemiol Biomarkers Prev* 14:467-75, 2005
9. Kim MM, Califano JA: Molecular pathology of head-and-neck cancer. *Int J Cancer* 112:545-53, 2004
10. Singh B: Molecular pathogenesis of head and neck cancers. *J Surg Oncol* 97:634-9, 2008
11. Perez-Ordóñez B, Beauchemin M, Jordan RC: Molecular biology of squamous cell carcinoma of the head and neck. *J Clin Pathol* 59:445-53, 2006
12. Poeta ML, Manola J, Goldwasser MA, et al: TP53 mutations and survival in squamous-cell carcinoma of the head and neck. *N Engl J Med* 357:2552-61, 2007

Bibliography

13. Greenblatt MS, Bennett WP, Hollstein M, et al: Mutations in the p53 tumor suppressor gene: clues to cancer etiology and molecular pathogenesis. *Cancer Res* 54:4855-78, 1994
14. Chene P: The role of tetramerization in p53 function. *Oncogene* 20:2611-7, 2001
15. He G, Siddik ZH, Huang Z, et al: Induction of p21 by p53 following DNA damage inhibits both Cdk4 and Cdk2 activities. *Oncogene* 24:2929-43, 2005
16. Satyanarayana A, Hilton MB, Kaldis P: p21 Inhibits Cdk1 in the absence of Cdk2 to maintain the G1/S phase DNA damage checkpoint. *Mol Biol Cell* 19:65-77, 2008
17. Quon H, Liu FF, Cummings BJ: Potential molecular prognostic markers in head and neck squamous cell carcinomas. *Head Neck* 23:147-59, 2001
18. van der Riet P, Nawroz H, Hruban RH, et al: Frequent loss of chromosome 9p21-22 early in head and neck cancer progression. *Cancer Res* 54:1156-8, 1994
19. Stone S, Jiang P, Dayananth P, et al: Complex structure and regulation of the P16 (MTS1) locus. *Cancer Res* 55:2988-94, 1995
20. Agrawal N, Frederick MJ, Pickering CR, et al: Exome sequencing of head and neck squamous cell carcinoma reveals inactivating mutations in NOTCH1. *Science* 333:1154-7, 2011
21. Stransky N, Egloff AM, Tward AD, et al: The mutational landscape of head and neck squamous cell carcinoma. *Science* 333:1157-60, 2011
22. Smeets SJ, Braakhuis BJ, Abbas S, et al: Genome-wide DNA copy number alterations in head and neck squamous cell carcinomas with or without oncogene-expressing human papillomavirus. *Oncogene* 25:2558-64, 2006
23. Freier K, Joos S, Flechtenmacher C, et al: Tissue microarray analysis reveals site-specific prevalence of oncogene amplifications in head and neck squamous cell carcinoma. *Cancer Res* 63:1179-82, 2003

Bibliography

24. Ang KK, Berkey BA, Tu X, et al: Impact of epidermal growth factor receptor expression on survival and pattern of relapse in patients with advanced head and neck carcinoma. *Cancer Res* 62:7350-6, 2002
25. Grandis JR, Tweardy DJ: Elevated levels of transforming growth factor alpha and epidermal growth factor receptor messenger RNA are early markers of carcinogenesis in head and neck cancer. *Cancer Res* 53:3579-84, 1993
26. Ongkeko WM, Altuna X, Weisman RA, et al: Expression of protein tyrosine kinases in head and neck squamous cell carcinomas. *Am J Clin Pathol* 124:71-6, 2005
27. Ferlay J, Soerjomataram I, Dikshit R, et al: Cancer incidence and mortality worldwide: sources, methods and major patterns in GLOBOCAN 2012. *Int J Cancer* 136:E359-86, 2015
28. Torre LA, Bray F, Siegel RL, et al: Global cancer statistics, 2012. *CA Cancer J Clin* 65:87-108, 2015
29. Bray F, Ren JS, Masuyer E, et al: Global estimates of cancer prevalence for 27 sites in the adult population in 2008. *Int J Cancer* 132:1133-45, 2013
30. Siegel RL, Miller KD, Jemal A: Cancer statistics, 2015. *CA Cancer J Clin* 65:5-29, 2015
31. Gatta G, Botta L, Sanchez MJ, et al: Prognoses and improvement for head and neck cancers diagnosed in Europe in early 2000s: The EURO CARE-5 population-based study. *Eur J Cancer*, 2015
32. Ferlay J, Shin HR, Bray F, et al: Estimates of worldwide burden of cancer in 2008: GLOBOCAN 2008. *Int J Cancer* 127:2893-917, 2010
33. Ferlay J, Parkin DM, Steliarova-Foucher E: Estimates of cancer incidence and mortality in Europe in 2008. *Eur J Cancer* 46:765-81, 2010
34. Carvalho AL, Nishimoto IN, Califano JA, et al: Trends in incidence and prognosis for head and neck cancer in the United States: a site-specific analysis of the SEER database. *Int J Cancer* 114:806-16, 2005
35. Chaturvedi AK, Engels EA, Pfeiffer RM, et al: Human papillomavirus and rising oropharyngeal cancer incidence in the United States. *J Clin Oncol* 29:4294-301, 2011

Bibliography

36. Auluck A, Hislop G, Bajdik C, et al: Trends in oropharyngeal and oral cavity cancer incidence of human papillomavirus (HPV)-related and HPV-unrelated sites in a multicultural population: the British Columbia experience. *Cancer* 116:2635-44, 2010
37. Blomberg M, Nielsen A, Munk C, et al: Trends in head and neck cancer incidence in Denmark, 1978-2007: focus on human papillomavirus associated sites. *Int J Cancer* 129:733-41, 2011
38. Braakhuis BJ, Visser O, Leemans CR: Oral and oropharyngeal cancer in The Netherlands between 1989 and 2006: Increasing incidence, but not in young adults. *Oral Oncol* 45:e85-9, 2009
39. Mork J, Moller B, Dahl T, et al: Time trends in pharyngeal cancer incidence in Norway 1981-2005: a subsite analysis based on a reabstraction and recoding of registered cases. *Cancer Causes Control* 21:1397-405, 2010
40. Hammarstedt L, Lindquist D, Dahlstrand H, et al: Human papillomavirus as a risk factor for the increase in incidence of tonsillar cancer. *Int J Cancer* 119:2620-3, 2006
41. Reddy VM, Cundall-Curry D, Bridger MW: Trends in the incidence rates of tonsil and base of tongue cancer in England, 1985-2006. *Ann R Coll Surg Engl* 92:655-9, 2010
42. Hong AM, Grulich AE, Jones D, et al: Squamous cell carcinoma of the oropharynx in Australian males induced by human papillomavirus vaccine targets. *Vaccine* 28:3269-72, 2010
43. Thun MJ, Jemal A: How much of the decrease in cancer death rates in the United States is attributable to reductions in tobacco smoking? *Tob Control* 15:345-7, 2006
44. Paz IB, Cook N, Odom-Maryon T, et al: Human papillomavirus (HPV) in head and neck cancer. An association of HPV 16 with squamous cell carcinoma of Waldeyer's tonsillar ring. *Cancer* 79:595-604, 1997
45. Herrero R, Castellsague X, Pawlita M, et al: Human papillomavirus and oral cancer: the International Agency for Research on Cancer multicenter study. *J Natl Cancer Inst* 95:1772-83, 2003

Bibliography

46. Deschler DG, Richmon JD, Khariwala SS, et al: The "new" head and neck cancer patient-young, nonsmoker, nondrinker, and HPV positive: evaluation. *Otolaryngol Head Neck Surg* 151:375-80, 2014
47. Chaturvedi AK, Anderson WF, Lortet-Tieulent J, et al: Worldwide trends in incidence rates for oral cavity and oropharyngeal cancers. *J Clin Oncol* 31:4550-9, 2013
48. Syrjanen K ea: Morphological and immunohistochemical evidence suggesting human papillomavirus (HPV) involvement in oral squamous cell carcinogenesis. *Int J Oral Surg* 12:418-24, 1983
49. Paz IB CNea: Human papillomavirus (HPV) in head and neck cancer. An association of HPV 16 with squamous cell carcinoma of Waldeyer's tonsillar ring. *Cancer* 79:595–604, 1997
50. DJ H: Human papilloma virus and p53 in head and neck cancer: clinical correlates and survival. *Clin Cancer Res* 2:755–62, 1996
51. Gillison ML, Koch WM, Capone RB, et al: Evidence for a causal association between human papillomavirus and a subset of head and neck cancers. *J Natl Cancer Inst* 92:709-20, 2000
52. Sturgis EM, Ang KK: The epidemic of HPV-associated oropharyngeal cancer is here: is it time to change our treatment paradigms? *J Natl Compr Canc Netw* 9:665-73, 2011
53. Hammarstedt L, Dahlstrand H, Lindquist D, et al: The incidence of tonsillar cancer in Sweden is increasing. *Acta Otolaryngol* 127:988-92, 2007
54. Chu A, Genden E, Posner M, et al: A patient-centered approach to counseling patients with head and neck cancer undergoing human papillomavirus testing: a clinician's guide. *Oncologist* 18:180-9, 2013
55. Klussmann JP, Weissenborn SJ, Wieland U, et al: Prevalence, distribution, and viral load of human papillomavirus 16 DNA in tonsillar carcinomas. *Cancer* 92:2875-84, 2001
56. Joseph AW, D'Souza G: Epidemiology of human papillomavirus-related head and neck cancer. *Otolaryngol Clin North Am* 45:739-64, 2012

Bibliography

57. Nasman A AP, Hammarstedt L, et al.: Incidence of human papillomavirus (HPV) positive tonsillar carcinoma in Stockholm, Sweden: an epidemic of viral-induced carcinoma? *Int J Cancer*. 125:362–366, 2009
58. Schache AG, Liloglou T, Risk JM, et al: Evaluation of human papilloma virus diagnostic testing in oropharyngeal squamous cell carcinoma: sensitivity, specificity, and prognostic discrimination. *Clin Cancer Res* 17:6262-71, 2011
59. Chaturvedi AKE, E. A. Anderson, W. F. Gillison, M. L.: Human Papillomavirus and Rising Oropharyngeal Cancer Incidence in the United States. *J Clin Oncol* 29:4294-301, 2011
60. Chaturvedi AK EE, Anderson WF, et al: Incidence trends for human papillomavirus-related and -unrelated oral squamous cell carcinomas in the United States. *J Clin Oncol* 26:612-619, 2008
61. Bouvard V, Baan R, Straif K, et al: A review of human carcinogens--Part B: biological agents. *Lancet Oncol* 10:321-2, 2009
62. Stubenrauch F, Laimins LA: Human papillomavirus life cycle: active and latent phases. *Semin Cancer Biol* 9:379-86, 1999
63. Bernard HU: The clinical importance of the nomenclature, evolution and taxonomy of human papillomaviruses. *J Clin Virol* 32 Suppl 1:S1-6, 2005
64. Miller DL, Puricelli MD, Stack MS: Virology and molecular pathogenesis of HPV (human papillomavirus)-associated oropharyngeal squamous cell carcinoma. *Biochem J* 443:339-53, 2012
65. Dayyani F, Etzel CJ, Liu M, et al: Meta-analysis of the impact of human papillomavirus (HPV) on cancer risk and overall survival in head and neck squamous cell carcinomas (HNSCC). *Head Neck Oncol* 2:15, 2010
66. Hobbs CG, Sterne JA, Bailey M, et al: Human papillomavirus and head and neck cancer: a systematic review and meta-analysis. *Clin Otolaryngol* 31:259-66, 2006
67. Winer RL, Hughes JP, Feng Q, et al: Condom use and the risk of genital human papillomavirus infection in young women. *N Engl J Med* 354:2645-54, 2006

Bibliography

68. Doorbar J: Molecular biology of human papillomavirus infection and cervical cancer. *Clin Sci (Lond)* 110:525-41, 2006
69. Zheng ZM, Baker CC: Papillomavirus genome structure, expression, and post-transcriptional regulation. *Front Biosci* 11:2286-302, 2006
70. Danos O, Katinka M, Yaniv M: Human papillomavirus 1a complete DNA sequence: a novel type of genome organization among papovaviridae. *EMBO J* 1:231-6, 1982
71. Malik H HN, Khan F: Proteins and Peptides- Re-emergence in Prophylactics and Therapeutics, in Sheikh GMAaIA (ed). USA, OMICS Group eBooks, 2013, pp 4-15
72. zur Hausen H: Papillomavirus infections: A major cause of human cancer., *Infections causing human cancer*. Weinheim, Wiley-VCH Verlag, 2006, pp 145-243.
73. Wang X, Meyers C, Wang HK, et al: Construction of a full transcription map of human papillomavirus type 18 during productive viral infection. *J Virol* 85:8080-92, 2011
74. Doorbar J, Parton A, Hartley K, et al: Detection of novel splicing patterns in a HPV16-containing keratinocyte cell line. *Virology* 178:254-62, 1990
75. Lace MJ, Anson JR, Thomas GS, et al: The E8--E2 gene product of human papillomavirus type 16 represses early transcription and replication but is dispensable for viral plasmid persistence in keratinocytes. *J Virol* 82:10841-53, 2008
76. Stenlund A: Initiation of DNA replication: lessons from viral initiator proteins. *Nat Rev Mol Cell Biol* 4:777-85, 2003
77. Rautava J, Kuuskoski J, Syrjanen K, et al: HPV genotypes and their prognostic significance in head and neck squamous cell carcinomas. *J Clin Virol* 53:116-20, 2012
78. Jeon S, Lambert PF: Integration of human papillomavirus type 16 DNA into the human genome leads to increased stability of E6 and E7 mRNAs: implications for cervical carcinogenesis. *Proc Natl Acad Sci U S A* 92:1654-8, 1995

Bibliography

79. Tsakogiannis D, Ruether IG, Kyriakopoulou Z, et al: Molecular and phylogenetic analysis of the HPV 16 E4 gene in cervical lesions from women in Greece. *Arch Virol* 157:1729-39, 2012
80. Grassmann K, Rapp B, Maschek H, et al: Identification of a differentiation-inducible promoter in the E7 open reading frame of human papillomavirus type 16 (HPV-16) in raft cultures of a new cell line containing high copy numbers of episomal HPV-16 DNA. *J Virol* 70:2339-49, 1996
81. Venuti A, Paolini F, Nasir L, et al: Papillomavirus E5: the smallest oncoprotein with many functions. *Mol Cancer* 10:140, 2011
82. zur Hausen H: Papillomaviruses and cancer: from basic studies to clinical application. *Nat Rev Cancer* 2:342-50, 2002
83. Campo MS, Graham SV, Cortese MS, et al: HPV-16 E5 down-regulates expression of surface HLA class I and reduces recognition by CD8 T cells. *Virology* 407:137-42, 2010
84. Hwang ES, Nottoli T, Dimaio D: The HPV16 E5 protein: expression, detection, and stable complex formation with transmembrane proteins in COS cells. *Virology* 211:227-33, 1995
85. Chung CH, Gillison ML: Human papillomavirus in head and neck cancer: its role in pathogenesis and clinical implications. *Clin Cancer Res* 15:6758-62, 2009
86. Munger K, Scheffner M, Huibregtse JM, et al: Interactions of HPV E6 and E7 oncoproteins with tumour suppressor gene products. *Cancer Surv* 12:197-217, 1992
87. Sun Q, Tang SC, Pater MM, et al: Different HPV16 E6/E7 oncogene expression patterns in epithelia reconstructed from HPV16-immortalized human endocervical cells and genital keratinocytes. *Oncogene* 15:2399-408, 1997
88. Androphy EJ, Hubbert NL, Schiller JT, et al: Identification of the HPV-16 E6 protein from transformed mouse cells and human cervical carcinoma cell lines. *EMBO J* 6:989-92, 1987
89. Romanczuk H, Howley PM: Disruption of either the E1 or the E2 regulatory gene of human papillomavirus type 16 increases viral immortalization capacity. *Proc Natl Acad Sci U S A* 89:3159-63, 1992

Bibliography

90. Pang E, Delic NC, Hong A, et al: Radiosensitization of oropharyngeal squamous cell carcinoma cells by human papillomavirus 16 oncoprotein E6 *I. *Int J Radiat Oncol Biol Phys* 79:860-5, 2011
91. Ristriani T, Nomine Y, Masson M, et al: Specific recognition of four-way DNA junctions by the C-terminal zinc-binding domain of HPV oncoprotein E6. *J Mol Biol* 305:729-39, 2001
92. Huibregtse JM, Scheffner M, Howley PM: A cellular protein mediates association of p53 with the E6 oncoprotein of human papillomavirus types 16 or 18. *EMBO J* 10:4129-35, 1991
93. Funk WD, Pak DT, Karas RH, et al: A transcriptionally active DNA-binding site for human p53 protein complexes. *Mol Cell Biol* 12:2866-71, 1992
94. Huibregtse JM, Beaudenon SL: Mechanism of HPV E6 proteins in cellular transformation. *Semin Cancer Biol* 7:317-26, 1996
95. Beer-Romero P, Glass S, Rolfe M: Antisense targeting of E6AP elevates p53 in HPV-infected cells but not in normal cells. *Oncogene* 14:595-602, 1997
96. Talis AL, Huibregtse JM, Howley PM: The role of E6AP in the regulation of p53 protein levels in human papillomavirus (HPV)-positive and HPV-negative cells. *J Biol Chem* 273:6439-45, 1998
97. Ashcroft M, Vousden KH: Regulation of p53 stability. *Oncogene* 18:7637-43, 1999
98. Havre PA, Yuan J, Hedrick L, et al: p53 inactivation by HPV16 E6 results in increased mutagenesis in human cells. *Cancer Res* 55:4420-4, 1995
99. Zanier K, Charbonnier S, Baltzinger M, et al: Kinetic analysis of the interactions of human papillomavirus E6 oncoproteins with the ubiquitin ligase E6AP using surface plasmon resonance. *J Mol Biol* 349:401-12, 2005
100. Slebos RJ, Kessis TD, Chen AW, et al: Functional consequences of directed mutations in human papillomavirus E6 proteins: abrogation of p53-mediated cell cycle arrest correlates with p53 binding and degradation in vitro. *Virology* 208:111-20, 1995

Bibliography

101. Thomas MC, Chiang CM: E6 oncoprotein represses p53-dependent gene activation via inhibition of protein acetylation independently of inducing p53 degradation. *Mol Cell* 17:251-64, 2005
102. Lechner MS, Laimins LA: Inhibition of p53 DNA binding by human papillomavirus E6 proteins. *J Virol* 68:4262-73, 1994
103. Thomas M, Massimi P, Jenkins J, et al: HPV-18 E6 mediated inhibition of p53 DNA binding activity is independent of E6 induced degradation. *Oncogene* 10:261-8, 1995
104. Isaacs JS, Barrett JC, Weissman BE: Interference of proteins involved in the cytoplasmic sequestration of p53 with human papillomavirus E6-mediated degradation. *Mol Carcinog* 24:70-7, 1999
105. Patel D, Huang SM, Baglia LA, et al: The E6 protein of human papillomavirus type 16 binds to and inhibits co-activation by CBP and p300. *EMBO J* 18:5061-72, 1999
106. Zimmermann H, Degenkolbe R, Bernard HU, et al: The human papillomavirus type 16 E6 oncoprotein can down-regulate p53 activity by targeting the transcriptional coactivator CBP/p300. *J Virol* 73:6209-19, 1999
107. Kumar A, Zhao Y, Meng G, et al: Human papillomavirus oncoprotein E6 inactivates the transcriptional coactivator human ADA3. *Mol Cell Biol* 22:5801-12, 2002
108. Filippova M, Song H, Connolly JL, et al: The human papillomavirus 16 E6 protein binds to tumor necrosis factor (TNF) R1 and protects cells from TNF-induced apoptosis. *J Biol Chem* 277:21730-9, 2002
109. Magal SS, Jackman A, Ish-Shalom S, et al: Downregulation of Bax mRNA expression and protein stability by the E6 protein of human papillomavirus 16. *J Gen Virol* 86:611-21, 2005
110. Ghittoni R, Accardi R, Hasan U, et al: The biological properties of E6 and E7 oncoproteins from human papillomaviruses. *Virus Genes* 40:1-13, 2010
111. Ronco LV, Karpova AY, Vidal M, et al: Human papillomavirus 16 E6 oncoprotein binds to interferon regulatory factor-3 and inhibits its transcriptional activity. *Genes Dev* 12:2061-72, 1998

Bibliography

112. Veldman T, Horikawa I, Barrett JC, et al: Transcriptional activation of the telomerase hTERT gene by human papillomavirus type 16 E6 oncoprotein. *J Virol* 75:4467-72, 2001
113. Pim D, Massimi P, Banks L: Alternatively spliced HPV-18 E6* protein inhibits E6 mediated degradation of p53 and suppresses transformed cell growth. *Oncogene* 15:257-64, 1997
114. Doyle DA, Lee A, Lewis J, et al: Crystal structures of a complexed and peptide-free membrane protein-binding domain: molecular basis of peptide recognition by PDZ. *Cell* 85:1067-76, 1996
115. Watson RA, Thomas M, Banks L, et al: Activity of the human papillomavirus E6 PDZ-binding motif correlates with an enhanced morphological transformation of immortalized human keratinocytes. *J Cell Sci* 116:4925-34, 2003
116. Dyson N, Howley PM, Munger K, et al: The human papilloma virus-16 E7 oncoprotein is able to bind to the retinoblastoma gene product. *Science* 243:934-7, 1989
117. Berezutskaya E, Yu B, Morozov A, et al: Differential regulation of the pocket domains of the retinoblastoma family proteins by the HPV16 E7 oncoprotein. *Cell Growth Differ* 8:1277-86, 1997
118. Vernell R, Helin K, Muller H: Identification of target genes of the p16INK4A-pRB-E2F pathway. *J Biol Chem* 278:46124-37, 2003
119. Funk JO, Waga S, Harry JB, et al: Inhibition of CDK activity and PCNA-dependent DNA replication by p21 is blocked by interaction with the HPV-16 E7 oncoprotein. *Genes Dev* 11:2090-100, 1997
120. Brehm A, Miska EA, McCance DJ, et al: Retinoblastoma protein recruits histone deacetylase to repress transcription. *Nature* 391:597-601, 1998
121. Zerfass K, Schulze A, Spitkovsky D, et al: Sequential activation of cyclin E and cyclin A gene expression by human papillomavirus type 16 E7 through sequences necessary for transformation. *J Virol* 69:6389-99, 1995

Bibliography

122. Chen XS, Garcea RL, Goldberg I, et al: Structure of small virus-like particles assembled from the L1 protein of human papillomavirus 16. *Mol Cell* 5:557-67, 2000
123. Brown DR, Fife KH, Wheeler CM, et al: Early assessment of the efficacy of a human papillomavirus type 16 L1 virus-like particle vaccine. *Vaccine* 22:2936-42, 2004
124. Sapp M, Volpers C, Muller M, et al: Organization of the major and minor capsid proteins in human papillomavirus type 33 virus-like particles. *J Gen Virol* 76 (Pt 9):2407-12, 1995
125. El Mehdaoui S, Touze A, Laurent S, et al: Gene transfer using recombinant rabbit hemorrhagic disease virus capsids with genetically modified DNA encapsidation capacity by addition of packaging sequences from the L1 or L2 protein of human papillomavirus type 16. *J Virol* 74:10332-40, 2000
126. Yang R, Yutzy WH, Viscidi RP, et al: Interaction of L2 with beta-actin directs intracellular transport of papillomavirus and infection. *J Biol Chem* 278:12546-53, 2003
127. Chow LT BT: Papillomavirus DNA replication. *Intervirology* 37:150–158, 1994
128. Kim SH, Koo BS, Kang S, et al: HPV integration begins in the tonsillar crypt and leads to the alteration of p16, EGFR and c-myc during tumor formation. *Int J Cancer* 120:1418-25, 2007
129. Shafii-Keramat S, Handisurya A, Kriehuber E, et al: Different heparan sulfate proteoglycans serve as cellular receptors for human papillomaviruses. *J Virol* 77:13125-35, 2003
130. Evander M, Frazer IH, Payne E, et al: Identification of the alpha6 integrin as a candidate receptor for papillomaviruses. *J Virol* 71:2449-56, 1997
131. Doorbar J: The papillomavirus life cycle. *J Clin Virol* 32 Suppl 1:S7-15, 2005
132. You J, Croyle JL, Nishimura A, et al: Interaction of the bovine papillomavirus E2 protein with Brd4 tethers the viral DNA to host mitotic chromosomes. *Cell* 117:349-60, 2004

Bibliography

133. Klimov E, Vinokourova S, Moisjak E, et al: Human papilloma viruses and cervical tumours: mapping of integration sites and analysis of adjacent cellular sequences. *BMC Cancer* 2:24, 2002
134. Matovina M, Sabol I, Grubisic G, et al: Identification of human papillomavirus type 16 integration sites in high-grade precancerous cervical lesions. *Gynecol Oncol* 113:120-7, 2009
135. Pett MR, Alazawi WO, Roberts I, et al: Acquisition of high-level chromosomal instability is associated with integration of human papillomavirus type 16 in cervical keratinocytes. *Cancer Res* 64:1359-68, 2004
136. Allen CT, Lewis JS, Jr., El-Mofty SK, et al: Human papillomavirus and oropharynx cancer: biology, detection and clinical implications. *Laryngoscope* 120:1756-72, 2010
137. Braakhuis BJ, Snijders PJ, Keune WJ, et al: Genetic patterns in head and neck cancers that contain or lack transcriptionally active human papillomavirus. *J Natl Cancer Inst* 96:998-1006, 2004
138. Fischer CA, Zlobec I, Green E, et al: Is the improved prognosis of p16 positive oropharyngeal squamous cell carcinoma dependent of the treatment modality? *Int J Cancer* 126:1256-62, 2010
139. Klussmann JP, Preuss SF, Speel EJ: [Human papillomavirus and cancer of the oropharynx. Molecular interaction and clinical implications]. *HNO* 57:113-22, 2009
140. Charfi L, Jouffroy T, de Cremoux P, et al: Two types of squamous cell carcinoma of the palatine tonsil characterized by distinct etiology, molecular features and outcome. *Cancer Lett* 260:72-8, 2008
141. Ang KK, Harris J, Wheeler R, et al: Human papillomavirus and survival of patients with oropharyngeal cancer. *N Engl J Med* 363:24-35, 2010
142. D'Souza G, Zhang HH, D'Souza WD, et al: Moderate predictive value of demographic and behavioral characteristics for a diagnosis of HPV16-positive and HPV16-negative head and neck cancer. *Oral Oncol* 46:100-4, 2010

Bibliography

143. Mehanna H, Beech T, Nicholson T, et al: Prevalence of human papillomavirus in oropharyngeal and nonoropharyngeal head and neck cancer--systematic review and meta-analysis of trends by time and region. *Head Neck* 35:747-55, 2013
144. Gillison ML, D'Souza G, Westra W, et al: Distinct risk factor profiles for human papillomavirus type 16-positive and human papillomavirus type 16-negative head and neck cancers. *J Natl Cancer Inst* 100:407-20, 2008
145. Evans M, Newcombe R, Fiander A, et al: Human Papillomavirus-associated oropharyngeal cancer: an observational study of diagnosis, prevalence and prognosis in a UK population. *BMC Cancer* 13:220, 2013
146. Snow AN, Laudadio J: Human papillomavirus detection in head and neck squamous cell carcinomas. *Adv Anat Pathol* 17:394-403, 2010
147. Robinson M, Sloan P, Shaw R: Refining the diagnosis of oropharyngeal squamous cell carcinoma using human papillomavirus testing. *Oral Oncol* 46:492-6, 2010
148. Wiest T, Schwarz E, Enders C, et al: Involvement of intact HPV16 E6/E7 gene expression in head and neck cancers with unaltered p53 status and perturbed pRb cell cycle control. *Oncogene* 21:1510-7, 2002
149. van Houten VM, Snijders PJ, van den Brekel MW, et al: Biological evidence that human papillomaviruses are etiologically involved in a subgroup of head and neck squamous cell carcinomas. *Int J Cancer* 93:232-5, 2001
150. Singhi AD, Westra WH: Comparison of human papillomavirus in situ hybridization and p16 immunohistochemistry in the detection of human papillomavirus-associated head and neck cancer based on a prospective clinical experience. *Cancer* 116:2166-73, 2010
151. Hall GL, Kademani D, Risk JM, et al: Tissue banking in head and neck cancer. *Oral Oncol* 44:109-15, 2008
152. Marur S, D'Souza G, Westra WH, et al: HPV-associated head and neck cancer: a virus-related cancer epidemic. *Lancet Oncol* 11:781-9, 2010

Bibliography

153. Bishop JA, Ma XJ, Wang H, et al: Detection of transcriptionally active high-risk HPV in patients with head and neck squamous cell carcinoma as visualized by a novel E6/E7 mRNA in situ hybridization method. *Am J Surg Pathol* 36:1874-82, 2012
154. Ukpo OC, Flanagan JJ, Ma XJ, et al: High-risk human papillomavirus E6/E7 mRNA detection by a novel in situ hybridization assay strongly correlates with p16 expression and patient outcomes in oropharyngeal squamous cell carcinoma. *Am J Surg Pathol* 35:1343-50, 2011
155. Moutasim K RM, Thavaraj S: Human papillomavirus testing in diagnostic head and neck histopathology. *DIAGNOSTIC HISTOPATHOLOGY* 21:77-84, 2015
156. Reimers N, Kasper HU, Weissenborn SJ, et al: Combined analysis of HPV-DNA, p16 and EGFR expression to predict prognosis in oropharyngeal cancer. *Int J Cancer* 120:1731-8, 2007
157. Smeets SJ, Hesselink AT, Speel EJ, et al: A novel algorithm for reliable detection of human papillomavirus in paraffin embedded head and neck cancer specimen. *Int J Cancer* 121:2465-72, 2007
158. Rietbergen MM, Leemans CR, Bloemena E, et al: Increasing prevalence rates of HPV attributable oropharyngeal squamous cell carcinomas in the Netherlands as assessed by a validated test algorithm. *Int J Cancer* 132:1565-71, 2013
159. Begum S, Cao D, Gillison M, et al: Tissue distribution of human papillomavirus 16 DNA integration in patients with tonsillar carcinoma. *Clin Cancer Res* 11:5694-9, 2005
160. Boscolo-Rizzo P, Del Mistro A, Bussu F, et al: New insights into human papillomavirus-associated head and neck squamous cell carcinoma. *Acta Otorhinolaryngol Ital* 33:77-87, 2013
161. Gillison ML: Human papillomavirus-associated head and neck cancer is a distinct epidemiologic, clinical, and molecular entity. *Semin Oncol* 31:744-54, 2004

Bibliography

162. D'Souza G, Kreimer AR, Viscidi R, et al: Case-control study of human papillomavirus and oropharyngeal cancer. *N Engl J Med* 356:1944-56, 2007
163. Chaturvedi AK, Engels EA, Anderson WF, et al: Incidence trends for human papillomavirus-related and -unrelated oral squamous cell carcinomas in the United States. *J Clin Oncol* 26:612-9, 2008
164. Benard VB, Johnson CJ, Thompson TD, et al: Examining the association between socioeconomic status and potential human papillomavirus-associated cancers. *Cancer* 113:2910-8, 2008
165. Ryerson AB, Peters ES, Coughlin SS, et al: Burden of potentially human papillomavirus-associated cancers of the oropharynx and oral cavity in the US, 1998-2003. *Cancer* 113:2901-9, 2008
166. Settle K, Posner MR, Schumaker LM, et al: Racial survival disparity in head and neck cancer results from low prevalence of human papillomavirus infection in black oropharyngeal cancer patients. *Cancer Prev Res (Phila)* 2:776-81, 2009
167. Begum S, Westra WH: Basaloid squamous cell carcinoma of the head and neck is a mixed variant that can be further resolved by HPV status. *Am J Surg Pathol* 32:1044-50, 2008
168. Wilczynski SP, Lin BT, Xie Y, et al: Detection of human papillomavirus DNA and oncoprotein overexpression are associated with distinct morphological patterns of tonsillar squamous cell carcinoma. *Am J Pathol* 152:145-56, 1998
169. Lechner M, Frampton GM, Fenton T, et al: Targeted next-generation sequencing of head and neck squamous cell carcinoma identifies novel genetic alterations in HPV+ and HPV- tumors. *Genome Med* 5:49, 2013
170. Seiwert TY, Zuo Z, Keck MK, et al: Integrative and comparative genomic analysis of HPV-positive and HPV-negative head and neck squamous cell carcinomas. *Clin Cancer Res* 21:632-41, 2015
171. Dahlgren L, Mellin H, Wangsa D, et al: Comparative genomic hybridization analysis of tonsillar cancer reveals a different pattern of

Bibliography

genomic imbalances in human papillomavirus-positive and -negative tumors. *Int J Cancer* 107:244-9, 2003

172. Mellin H, Friesland S, Lewensohn R, et al: Human papillomavirus (HPV) DNA in tonsillar cancer: clinical correlates, risk of relapse, and survival. *Int J Cancer* 89:300-4, 2000

173. Fakhry C, Westra WH, Li S, et al: Improved survival of patients with human papillomavirus-positive head and neck squamous cell carcinoma in a prospective clinical trial. *J Natl Cancer Inst* 100:261-9, 2008

174. Lindel K, Beer KT, Laissue J, et al: Human papillomavirus positive squamous cell carcinoma of the oropharynx: a radiosensitive subgroup of head and neck carcinoma. *Cancer* 92:805-13, 2001

175. O'Rourke MA, Ellison MV, Murray LJ, et al: Human papillomavirus related head and neck cancer survival: a systematic review and meta-analysis. *Oral Oncol* 48:1191-201, 2012

176. Hong AM, Dobbins TA, Lee CS, et al: Human papillomavirus predicts outcome in oropharyngeal cancer in patients treated primarily with surgery or radiation therapy. *Br J Cancer* 103:1510-7, 2010

177. Campisi G, Giovannelli L: Controversies surrounding human papilloma virus infection, head & neck vs oral cancer, implications for prophylaxis and treatment. *Head Neck Oncol* 1:8, 2009

178. Adelstein DJ, Ridge JA, Gillison ML, et al: Head and neck squamous cell cancer and the human papillomavirus: summary of a National Cancer Institute State of the Science Meeting, November 9-10, 2008, Washington, D.C. *Head Neck* 31:1393-422, 2009

179. Ziemann F, Arenz A, Preising S, et al: Increased sensitivity of HPV-positive head and neck cancer cell lines to x-irradiation +/- Cisplatin due to decreased expression of E6 and E7 oncoproteins and enhanced apoptosis. *Am J Cancer Res* 5:1017-31, 2015

180. Klussmann JP, Mooren JJ, Lehnen M, et al: Genetic signatures of HPV-related and unrelated oropharyngeal carcinoma and their prognostic implications. *Clin Cancer Res* 15:1779-86, 2009

181. Butz K, Shahabeddin L, Geisen C, et al: Functional p53 protein in human papillomavirus-positive cancer cells. *Oncogene* 10:927-36, 1995

Bibliography

182. Butz K, Geisen C, Ullmann A, et al: Cellular responses of HPV-positive cancer cells to genotoxic anti-cancer agents: repression of E6/E7-oncogene expression and induction of apoptosis. *Int J Cancer* 68:506-13, 1996
183. Westra WH, Taube JM, Poeta ML, et al: Inverse relationship between human papillomavirus-16 infection and disruptive p53 gene mutations in squamous cell carcinoma of the head and neck. *Clin Cancer Res* 14:366-9, 2008
184. Kimple RJ, Smith MA, Blitzer GC, et al: Enhanced radiation sensitivity in HPV-positive head and neck cancer. *Cancer Res* 73:4791-800, 2013
185. Arenz A, Ziemann F, Mayer C, et al: Increased radiosensitivity of HPV-positive head and neck cancer cell lines due to cell cycle dysregulation and induction of apoptosis. *Strahlenther Onkol* 190:839-46, 2014
186. Rieckmann T, Tribius S, Grob TJ, et al: HNSCC cell lines positive for HPV and p16 possess higher cellular radiosensitivity due to an impaired DSB repair capacity. *Radiother Oncol* 107:242-6, 2013
187. Dai Y, Grant S: New insights into checkpoint kinase 1 in the DNA damage response signaling network. *Clin Cancer Res* 16:376-83, 2010
188. Hong A, Dobbins T, Lee CS, et al: Relationships between epidermal growth factor receptor expression and human papillomavirus status as markers of prognosis in oropharyngeal cancer. *Eur J Cancer* 46:2088-96, 2010
189. Young RJ, Rischin D, Fisher R, et al: Relationship between epidermal growth factor receptor status, p16(INK4A), and outcome in head and neck squamous cell carcinoma. *Cancer Epidemiol Biomarkers Prev* 20:1230-7, 2011
190. P Oc, Rhys-Evans PH, Modjtahedi H, et al: The role of c-erbB receptors and ligands in head and neck squamous cell carcinoma. *Oral Oncol* 38:627-40, 2002

Bibliography

191. Huang SM, Harari PM: Epidermal growth factor receptor inhibition in cancer therapy: biology, rationale and preliminary clinical results. *Invest New Drugs* 17:259-69, 1999
192. Park JW, Nickel KP, Torres AD, et al: Human papillomavirus type 16 E7 oncoprotein causes a delay in repair of DNA damage. *Radiother Oncol* 113:337-44, 2014
193. Dok R, Kalev P, Van Limbergen EJ, et al: p16INK4a impairs homologous recombination-mediated DNA repair in human papillomavirus-positive head and neck tumors. *Cancer Res* 74:1739-51, 2014
194. Licitra L, Perrone F, Bossi P, et al: High-risk human papillomavirus affects prognosis in patients with surgically treated oropharyngeal squamous cell carcinoma. *J Clin Oncol* 24:5630-6, 2006
195. Braakhuis BJ, Tabor MP, Kummer JA, et al: A genetic explanation of Slaughter's concept of field cancerization: evidence and clinical implications. *Cancer Res* 63:1727-30, 2003
196. Slaughter DP, Southwick HW, Smejkal W: Field cancerization in oral stratified squamous epithelium; clinical implications of multicentric origin. *Cancer* 6:963-8, 1953
197. Rietbergen MM, Braakhuis BJ, Moukhtari N, et al: No evidence for active human papillomavirus (HPV) in fields surrounding HPV-positive oropharyngeal tumors. *J Oral Pathol Med* 43:137-42, 2014
198. McGovern SL, Williams MD, Weber RS, et al: Three synchronous HPV-associated squamous cell carcinomas of Waldeyer's ring: case report and comparison with Slaughter's model of field cancerization. *Head Neck* 32:1118-24, 2010
199. Xu CC, Biron VL, Puttagunta L, et al: HPV status and second primary tumours in oropharyngeal squamous cell carcinoma. *J Otolaryngol Head Neck Surg* 42:36, 2013
200. Lassen P, Eriksen JG, Hamilton-Dutoit S, et al: HPV-associated p16-expression and response to hypoxic modification of radiotherapy in head and neck cancer. *Radiother Oncol* 94:30-5, 2010

Bibliography

201. Hanns E, Job S, Coliat P, et al: Human Papillomavirus-related tumours of the oropharynx display a lower tumour hypoxia signature. *Oral Oncol* 51:848-56, 2015
202. Westra WH: The changing face of head and neck cancer in the 21st century: the impact of HPV on the epidemiology and pathology of oral cancer. *Head Neck Pathol* 3:78-81, 2009
203. Wansom D, Light E, Worden F, et al: Correlation of cellular immunity with human papillomavirus 16 status and outcome in patients with advanced oropharyngeal cancer. *Arch Otolaryngol Head Neck Surg* 136:1267-73, 2010
204. Wansom D, Light E, Thomas D, et al: Infiltrating lymphocytes and human papillomavirus-16--associated oropharyngeal cancer. *Laryngoscope* 122:121-7, 2012
205. Albers A, Abe K, Hunt J, et al: Antitumor activity of human papillomavirus type 16 E7-specific T cells against virally infected squamous cell carcinoma of the head and neck. *Cancer Res* 65:11146-55, 2005
206. Heusinkveld M, Goedemans R, Briet RJ, et al: Systemic and local human papillomavirus 16-specific T-cell immunity in patients with head and neck cancer. *Int J Cancer* 131:E74-85, 2012
207. Seiwert TY, Cohen EE: State-of-the-art management of locally advanced head and neck cancer. *Br J Cancer* 92:1341-8, 2005
208. Chin D, Boyle GM, Porceddu S, et al: Head and neck cancer: past, present and future. *Expert Rev Anticancer Ther* 6:1111-8, 2006
209. Jones AS, Fish B, Fenton JE, et al: The treatment of early laryngeal cancers (T1-T2 N0): surgery or irradiation? *Head Neck* 26:127-35, 2004
210. Brockstein B, Haraf DJ, Rademaker AW, et al: Patterns of failure, prognostic factors and survival in locoregionally advanced head and neck cancer treated with concomitant chemoradiotherapy: a 9-year, 337-patient, multi-institutional experience. *Ann Oncol* 15:1179-86, 2004
211. Argiris A, Karamouzis MV, Raben D, et al: Head and neck cancer. *Lancet* 371:1695-709, 2008

Bibliography

212. Leemans CR, Braakhuis BJ, Brakenhoff RH: The molecular biology of head and neck cancer. *Nat Rev Cancer* 11:9-22, 2011
213. Goodhead DT: Initial events in the cellular effects of ionizing radiations: clustered damage in DNA. *Int J Radiat Biol* 65:7-17, 1994
214. Moeller BJ, Richardson RA, Dewhirst MW: Hypoxia and radiotherapy: opportunities for improved outcomes in cancer treatment. *Cancer Metastasis Rev* 26:241-8, 2007
215. Lefebvre JL, Rolland F, Tessler M, et al: Phase 3 randomized trial on larynx preservation comparing sequential vs alternating chemotherapy and radiotherapy. *J Natl Cancer Inst* 101:142-52, 2009
216. Jennette KW, Lippard SJ, Vassiliades GA, et al: Metallointercalation reagents. 2-hydroxyethanethiolato(2,2',2'-terpyridine)-platinum(II) monocation binds strongly to DNA by intercalation. *Proc Natl Acad Sci U S A* 71:3839-43, 1974
217. Eisenberger M, Hornedo J, Silva H, et al: Carboplatin (NSC-241-240): an active platinum analog for the treatment of squamous-cell carcinoma of the head and neck. *J Clin Oncol* 4:1506-9, 1986
218. Pinto HA, Jacobs C: Chemotherapy for recurrent and metastatic head and neck cancer. *Hematol Oncol Clin North Am* 5:667-86, 1991
219. Airolidi M, Cortesina G, Giordano C, et al: Ifosfamide in the treatment of head and neck cancer. *Oncology* 65 Suppl 2:37-43, 2003
220. Pryor DI, Solomon B, Porceddu SV: The emerging era of personalized therapy in squamous cell carcinoma of the head and neck. *Asia Pac J Clin Oncol* 7:236-51, 2011
221. Howard JD, Lu B, Chung CH: Therapeutic targets in head and neck squamous cell carcinoma: identification, evaluation, and clinical translation. *Oral Oncol* 48:10-7, 2012
222. Prigent SA, Lemoine NR: The type 1 (EGFR-related) family of growth factor receptors and their ligands. *Prog Growth Factor Res* 4:1-24, 1992
223. Langer CJ: Targeted therapy in head and neck cancer: state of the art 2007 and review of clinical applications. *Cancer* 112:2635-45, 2008

Bibliography

224. Specenier P, Vermorken JB: Cetuximab in the treatment of squamous cell carcinoma of the head and neck. *Expert Rev Anticancer Ther* 11:511-24, 2011
225. Bonner JA, Harari PM, Giralt J, et al: Radiotherapy plus cetuximab for squamous-cell carcinoma of the head and neck. *N Engl J Med* 354:567-78, 2006
226. Balaban N, Moni J, Shannon M, et al: The effect of ionizing radiation on signal transduction: antibodies to EGF receptor sensitize A431 cells to radiation. *Biochim Biophys Acta* 1314:147-56, 1996
227. Harari PM, Huang SM: Head and neck cancer as a clinical model for molecular targeting of therapy: combining EGFR blockade with radiation. *Int J Radiat Oncol Biol Phys* 49:427-33, 2001
228. Feng FY, Lopez CA, Normolle DP, et al: Effect of epidermal growth factor receptor inhibitor class in the treatment of head and neck cancer with concurrent radiochemotherapy in vivo. *Clin Cancer Res* 13:2512-8, 2007
229. Wang S, El-Deiry WS: TRAIL and apoptosis induction by TNF-family death receptors. *Oncogene* 22:8628-33, 2003
230. Pukac L, Kanakaraj P, Humphreys R, et al: HGS-ETR1, a fully human TRAIL-receptor 1 monoclonal antibody, induces cell death in multiple tumour types in vitro and in vivo. *Br J Cancer* 92:1430-41, 2005
231. Wiley SR, Schooley K, Smolak PJ, et al: Identification and characterization of a new member of the TNF family that induces apoptosis. *Immunity* 3:673-82, 1995
232. Ashkenazi A: Targeting death and decoy receptors of the tumour-necrosis factor superfamily. *Nat Rev Cancer* 2:420-30, 2002
233. Chaudhary PM, Eby M, Jasmin A, et al: Death receptor 5, a new member of the TNFR family, and DR4 induce FADD-dependent apoptosis and activate the NF-kappaB pathway. *Immunity* 7:821-30, 1997
234. Ashkenazi A, Holland P, Eckhardt SG: Ligand-based targeting of apoptosis in cancer: the potential of recombinant human apoptosis ligand 2/Tumor necrosis factor-related apoptosis-inducing ligand (rhApo2L/TRAIL). *J Clin Oncol* 26:3621-30, 2008

Bibliography

235. Pan G, Ni J, Wei YF, et al: An antagonist decoy receptor and a death domain-containing receptor for TRAIL. *Science* 277:815-8, 1997
236. Sheridan JP, Marsters SA, Pitti RM, et al: Control of TRAIL-induced apoptosis by a family of signaling and decoy receptors. *Science* 277:818-21, 1997
237. Marsters SA, Sheridan JP, Pitti RM, et al: A novel receptor for Apo2L/TRAIL contains a truncated death domain. *Curr Biol* 7:1003-6, 1997
238. Emery JG, McDonnell P, Burke MB, et al: Osteoprotegerin is a receptor for the cytotoxic ligand TRAIL. *J Biol Chem* 273:14363-7, 1998
239. Griffith TS, Rauch CT, Smolak PJ, et al: Functional analysis of TRAIL receptors using monoclonal antibodies. *J Immunol* 162:2597-605, 1999
240. Tschopp J, Irmeler M, Thome M: Inhibition of fas death signals by FLIPs. *Curr Opin Immunol* 10:552-8, 1998
241. Yang Y, Fang S, Jensen JP, et al: Ubiquitin protein ligase activity of IAPs and their degradation in proteasomes in response to apoptotic stimuli. *Science* 288:874-7, 2000
242. Deveraux QL, Takahashi R, Salvesen GS, et al: X-linked IAP is a direct inhibitor of cell-death proteases. *Nature* 388:300-4, 1997
243. Filippova M, Parkhurst L, Duerksen-Hughes PJ: The human papillomavirus 16 E6 protein binds to Fas-associated death domain and protects cells from Fas-triggered apoptosis. *J Biol Chem* 279:25729-44, 2004
244. Garnett TO, Filippova M, Duerksen-Hughes PJ: Accelerated degradation of FADD and procaspase 8 in cells expressing human papilloma virus 16 E6 impairs TRAIL-mediated apoptosis. *Cell Death Differ* 13:1915-26, 2006
245. Kabsch K, Alonso A: The human papillomavirus type 16 E5 protein impairs TRAIL- and FasL-mediated apoptosis in HaCaT cells by different mechanisms. *J Virol* 76:12162-72, 2002
246. Chen AM, Li J, Beckett LA, et al: Differential response rates to irradiation among patients with human papillomavirus positive and negative oropharyngeal cancer. *Laryngoscope* 123:152-7, 2013

Bibliography

247. Lassen P, Eriksen JG, Hamilton-Dutoit S, et al: Effect of HPV-associated p16INK4A expression on response to radiotherapy and survival in squamous cell carcinoma of the head and neck. *J Clin Oncol* 27:1992-8, 2009
248. Machiels JP, Lambrecht M, Hanin FX, et al: Advances in the management of squamous cell carcinoma of the head and neck. *F1000Prime Rep* 6:44, 2014
249. Elrefaey S, Massaro MA, Chiocca S, et al: HPV in oropharyngeal cancer: the basics to know in clinical practice. *Acta Otorhinolaryngol Ital* 34:299-309, 2014
250. Haedicke J, Iftner T: Human papillomaviruses and cancer. *Radiother Oncol* 108:397-402, 2013
251. Bernier J, Domette C, Ozsahin M, et al: Postoperative irradiation with or without concomitant chemotherapy for locally advanced head and neck cancer. *N Engl J Med* 350:1945-52, 2004
252. Cooper JS, Pajak TF, Forastiere AA, et al: Postoperative concurrent radiotherapy and chemotherapy for high-risk squamous-cell carcinoma of the head and neck. *N Engl J Med* 350:1937-44, 2004
253. George M: Should patients with HPV-positive or negative tumors be treated differently? *Curr Oncol Rep* 16:384, 2014
254. Hamoir M, Ferlito A, Schmitz S, et al: The role of neck dissection in the setting of chemoradiation therapy for head and neck squamous cell carcinoma with advanced neck disease. *Oral Oncol* 48:203-10, 2012
255. Patel SN, Cohen MA, Givi B, et al: Salvage surgery for locally recurrent oropharyngeal cancer. *Head Neck*, 2015
256. Licitra L, Bernier J, Grandi C, et al: Cancer of the oropharynx. *Crit Rev Oncol Hematol* 41:107-22, 2002
257. ECOG: Paclitaxel, Cisplatin, and Cetuximab Followed By Cetuximab and Intensity-Modulated Radiation Therapy in Treating Patients With HPV-Associated Stage III or Stage IV Cancer of the Oropharynx That Can Be Removed By Surgery, 2010 [Last updated 12th July 2012]

Bibliography

258. RTOG: Radiation Therapy With Cisplatin or Cetuximab in Treating Patients With Oropharyngeal Cancer, 2011 [Last updated on 4th August 2014]
259. Mehanna H: De-ESCALaTE HPV: Determination of Epidermal growth factor receptor-inhibitor (cetuximab) versus Standard Chemotherapy (cisplatin) early And Late Toxicity Events in Human Papillomavirus-positive oropharyngeal squamous cell carcinoma: a randomised controlled trail, 2012. Doi: NCT01874171.
260. SKCCC: Treatment De-Intensification for Squamous Cell Carcinoma of the Oropharynx, 2009 [Last updated 18th June 2015]
261. TROG: Weekly Cetuximab/RT Versus Weekly Cisplatin/RT in HPV-Associated Oropharyngeal Squamous Cell Carcinoma (HPV Oropharynx), 2013 [Last updated on 17th August 2015]
262. Trial TQ: Reduced Dose Radiotherapy for HPV+ Oropharynx Cancer, 2012 [Last updated on 24th September 2015]
263. ADEPT: Adjuvant De-escalation, Extracapsular Spread, P16+, Transoral (ADEPT) Trial for Oropharynx Malignancy, 2013
264. 3311 E: Transoral Surgery Followed By Low-Dose or Standard-Dose Radiation Therapy With or Without Chemotherapy in Treating Patients With HPV Positive Stage III-IVA Oropharyngeal Cancer, 2013 [Last updated on 30th October 2014]
265. PATHOS: Post-operative Adjuvant Treatment for HPV-positive Tumours, 2014 [Last updated on 12th August 2014]
266. Masterson L, Moualed D, Liu ZW, et al: De-escalation treatment protocols for human papillomavirus-associated oropharyngeal squamous cell carcinoma: a systematic review and meta-analysis of current clinical trials. *Eur J Cancer* 50:2636-48, 2014
267. Rampias T, Sasaki C, Weinberger P, et al: E6 and e7 gene silencing and transformed phenotype of human papillomavirus 16-positive oropharyngeal cancer cells. *J Natl Cancer Inst* 101:412-23, 2009
268. Fung C, Grandis JR: Emerging drugs to treat squamous cell carcinomas of the head and neck. *Expert Opin Emerg Drugs* 15:355-73, 2010

Bibliography

269. Yuan CH, Filippova M, Tungteakkhun SS, et al: Small molecule inhibitors of the HPV16-E6 interaction with caspase 8. *Bioorg Med Chem Lett* 22:2125-9, 2012
270. Shahabi V, Maciag PC, Rivera S, et al: Live, attenuated strains of *Listeria* and *Salmonella* as vaccine vectors in cancer treatment. *Bioeng Bugs* 1:235-43, 2010
271. Ward MJ, Thirdborough SM, Mellows T, et al: Tumour-infiltrating lymphocytes predict for outcome in HPV-positive oropharyngeal cancer. *Br J Cancer* 110:489-500, 2014
272. Topalian SL, Hodi FS, Brahmer JR, et al: Safety, activity, and immune correlates of anti-PD-1 antibody in cancer. *N Engl J Med* 366:2443-54, 2012
273. Fife BT, Pauken KE: The role of the PD-1 pathway in autoimmunity and peripheral tolerance. *Ann N Y Acad Sci* 1217:45-59, 2011
274. Lyford-Pike S, Peng S, Young GD, et al: Evidence for a role of the PD-1:PD-L1 pathway in immune resistance of HPV-associated head and neck squamous cell carcinoma. *Cancer Res* 73:1733-41, 2013
275. Tanguy Y, Seiwert BB, Jared Weiss: A phase Ib study of MK-3475 in patients with human papillomavirus (HPV)-associated and non-HPV-associated head and neck (H/N) cancer. *Journal of Clinical Oncology*, , 2014 ASCO Annual Meeting Abstracts. 32, 2014
276. White JS, Weissfeld JL, Ragin CC, et al: The influence of clinical and demographic risk factors on the establishment of head and neck squamous cell carcinoma cell lines. *Oral Oncol* 43:701-12, 2007
277. Virgilio L, Shuster M, Gollin SM, et al: FHIT gene alterations in head and neck squamous cell carcinomas. *Proc Natl Acad Sci U S A* 93:9770-5, 1996
278. Telmer CA, An J, Malehorn DE, et al: Detection and assignment of TP53 mutations in tumor DNA using peptide mass signature genotyping. *Hum Mutat* 22:158-65, 2003
279. Ferris RL, Martinez I, Sirianni N, et al: Human papillomavirus-16 associated squamous cell carcinoma of the head and neck (SCCHN): a

Bibliography

natural disease model provides insights into viral carcinogenesis. *Eur J Cancer* 41:807-15, 2005

280. Ragin CC, Reshmi SC, Gollin SM: Mapping and analysis of HPV16 integration sites in a head and neck cancer cell line. *Int J Cancer* 110:701-9, 2004

281. Ballo H, Koldovsky P, Hoffmann T, et al: Establishment and characterization of four cell lines derived from human head and neck squamous cell carcinomas for an autologous tumor-fibroblast in vitro model. *Anticancer Res* 19:3827-36, 1999

282. Hauser U, Balz V, Carey TE, et al: Reliable detection of p53 aberrations in squamous cell carcinomas of the head and neck requires transcript analysis of the entire coding region. *Head Neck* 24:868-73, 2002

283. Steenbergen RD, Hermsen MA, Walboomers JM, et al: Integrated human papillomavirus type 16 and loss of heterozygosity at 11q22 and 18q21 in an oral carcinoma and its derivative cell line. *Cancer Res* 55:5465-71, 1995

284. Rubinstein LV, Shoemaker RH, Paull KD, et al: Comparison of in vitro anticancer-drug-screening data generated with a tetrazolium assay versus a protein assay against a diverse panel of human tumor cell lines. *J Natl Cancer Inst* 82:1113-8, 1990

285. Bradford MM: A rapid and sensitive method for the quantitation of microgram quantities of protein utilizing the principle of protein-dye binding. *Anal Biochem* 72:248-54, 1976

286. Schagger H: Tricine-SDS-PAGE. *Nat Protoc* 1:16-22, 2006

287. Bushman FD: Retroviral integration and human gene therapy. *J Clin Invest* 117:2083-6, 2007

288. Desfarges S, Ciuffi A: Retroviral integration site selection. *Viruses* 2:111-30, 2010

289. Cockrell AS, Kafri T: Gene delivery by lentivirus vectors. *Mol Biotechnol* 36:184-204, 2007

290. Brenner S, Malech HL: Current developments in the design of onco-retrovirus and lentivirus vector systems for hematopoietic cell gene therapy. *Biochim Biophys Acta* 1640:1-24, 2003

Bibliography

291. de Roda Husman AM, Walboomers JM, van den Brule AJ, et al: The use of general primers GP5 and GP6 elongated at their 3' ends with adjacent highly conserved sequences improves human papillomavirus detection by PCR. *J Gen Virol* 76 (Pt 4):1057-62, 1995
292. Remmerbach TW, Brinckmann UG, Hemprich A, et al: PCR detection of human papillomavirus of the mucosa: comparison between MY09/11 and GP5+/6+ primer sets. *J Clin Virol* 30:302-8, 2004
293. Konig F, Krekeler G, Honig JF, et al: Relation between human papillomavirus positivity and p16 expression in head and neck carcinomas--a tissue microarray study. *Anticancer Res* 27:283-8, 2007
294. Weinberger PM, Yu Z, Haffty BG, et al: Molecular classification identifies a subset of human papillomavirus--associated oropharyngeal cancers with favorable prognosis. *J Clin Oncol* 24:736-47, 2006
295. Franken NA, Rodermond HM, Stap J, et al: Clonogenic assay of cells in vitro. *Nat Protoc* 1:2315-9, 2006
296. Buch K, Peters T, Nawroth T, et al: Determination of cell survival after irradiation via clonogenic assay versus multiple MTT Assay--a comparative study. *Radiat Oncol* 7:1, 2012
297. Olthof NC, Huebbers CU, Kolligs J, et al: Viral load, gene expression and mapping of viral integration sites in HPV16-associated HNSCC cell lines. *Int J Cancer*, 2014
298. Langendijk JA, Psyrri A: The prognostic significance of p16 overexpression in oropharyngeal squamous cell carcinoma: implications for treatment strategies and future clinical studies. *Ann Oncol* 21:1931-4, 2010
299. Nagel R, Martens-de Kemp SR, Buijze M, et al: Treatment response of HPV-positive and HPV-negative head and neck squamous cell carcinoma cell lines. *Oral Oncol* 49:560-6, 2013
300. Gupta AK, Lee JH, Wilke WW, et al: Radiation response in two HPV-infected head-and-neck cancer cell lines in comparison to a non-HPV-infected cell line and relationship to signaling through AKT. *Int J Radiat Oncol Biol Phys* 74:928-33, 2009

Bibliography

301. Sorensen BS, Busk M, Olthof N, et al: Radiosensitivity and effect of hypoxia in HPV positive head and neck cancer cells. *Radiother Oncol* 108:500-5, 2013
302. Busch CJ, Kriegs M, Laban S, et al: HPV-positive HNSCC cell lines but not primary human fibroblasts are radiosensitized by the inhibition of Chk1. *Radiother Oncol* 108:495-9, 2013
303. Gubanov E, Brown B, Ivanov SV, et al: Downregulation of SMG-1 in HPV-positive head and neck squamous cell carcinoma due to promoter hypermethylation correlates with improved survival. *Clin Cancer Res* 18:1257-67, 2012
304. Hay N, Sonenberg N: Upstream and downstream of mTOR. *Genes Dev* 18:1926-45, 2004
305. Coppock JD, Wieking BG, Molinolo AA, et al: Improved clearance during treatment of HPV-positive head and neck cancer through mTOR inhibition. *Neoplasia* 15:620-30, 2013
306. Molinolo AA, Marsh C, El Dinali M, et al: mTOR as a molecular target in HPV-associated oral and cervical squamous carcinomas. *Clin Cancer Res* 18:2558-68, 2012
307. Yoshimura M, Itasaka S, Harada H, et al: Microenvironment and radiation therapy. *Biomed Res Int* 2013:685308, 2013
308. Toustrup K, Sorensen BS, Lassen P, et al: Gene expression classifier predicts for hypoxic modification of radiotherapy with nimorazole in squamous cell carcinomas of the head and neck. *Radiother Oncol* 102:122-9, 2012
309. Mortensen LS, Johansen J, Kallehauge J, et al: FAZA PET/CT hypoxia imaging in patients with squamous cell carcinoma of the head and neck treated with radiotherapy: results from the DAHANCA 24 trial. *Radiother Oncol* 105:14-20, 2012
310. Spanos WC, Nowicki P, Lee DW, et al: Immune response during therapy with cisplatin or radiation for human papillomavirus-related head and neck cancer. *Arch Otolaryngol Head Neck Surg* 135:1137-46, 2009

Bibliography

311. Kawakami H, Okamoto I, Terao K, et al: Human papillomavirus DNA and p16 expression in Japanese patients with oropharyngeal squamous cell carcinoma. *Cancer Med* 2:933-41, 2013
312. Chang-Liu CM, Woloschak GE: Effect of passage number on cellular response to DNA-damaging agents: cell survival and gene expression. *Cancer Lett* 113:77-86, 1997
313. Wenger SL, Senft JR, Sargent LM, et al: Comparison of established cell lines at different passages by karyotype and comparative genomic hybridization. *Biosci Rep* 24:631-9, 2004
314. Piersma SJ, Jordanova ES, van Poelgeest MI, et al: High number of intraepithelial CD8+ tumor-infiltrating lymphocytes is associated with the absence of lymph node metastases in patients with large early-stage cervical cancer. *Cancer Res* 67:354-61, 2007
315. Cohen SM, Lippard SJ: Cisplatin: from DNA damage to cancer chemotherapy. *Prog Nucleic Acid Res Mol Biol* 67:93-130, 2001
316. Chen Z, Ke LD, Yuan XH, et al: Correlation of cisplatin sensitivity with differential alteration of EGFR expression in head and neck cancer cells. *Anticancer Res* 20:899-902, 2000
317. Harris M, Wang XG, Jiang Z, et al: Radioimmunotherapy of experimental head and neck squamous cell carcinoma (HNSCC) with E6-specific antibody using a novel HPV-16 positive HNSCC cell line. *Head Neck Oncol* 3:9, 2011
318. Tang AL, Hauff SJ, Owen JH, et al: UM-SCC-104: a new human papillomavirus-16-positive cancer stem cell-containing head and neck squamous cell carcinoma cell line. *Head Neck* 34:1480-91, 2012
319. Lane DP: Cancer. p53, guardian of the genome. *Nature* 358:15-6, 1992
320. Ohnishi K, Ota I, Takahashi A, et al: Transfection of mutant p53 gene depresses X-ray- or CDDP-induced apoptosis in a human squamous cell carcinoma of the head and neck. *Apoptosis* 7:367-72, 2002
321. Butz K, Whitaker N, Denk C, et al: Induction of the p53-target gene GADD45 in HPV-positive cancer cells. *Oncogene* 18:2381-6, 1999

Bibliography

322. Huang H, Li CY, Little JB: Abrogation of P53 function by transfection of HPV16 E6 gene does not enhance resistance of human tumour cells to ionizing radiation. *Int J Radiat Biol* 70:151-60, 1996
323. el-Deiry WS, Tokino T, Velculescu VE, et al: WAF1, a potential mediator of p53 tumor suppression. *Cell* 75:817-25, 1993
324. Roninson IB: Oncogenic functions of tumour suppressor p21(Waf1/Cip1/Sdi1): association with cell senescence and tumour-promoting activities of stromal fibroblasts. *Cancer Lett* 179:1-14, 2002
325. Xiong Y, Hannon GJ, Zhang H, et al: p21 is a universal inhibitor of cyclin kinases. *Nature* 366:701-4, 1993
326. Crook T, Tidy JA, Vousden KH: Degradation of p53 can be targeted by HPV E6 sequences distinct from those required for p53 binding and trans-activation. *Cell* 67:547-56, 1991
327. Scheffner M, Werness BA, Huibregtse JM, et al: The E6 oncoprotein encoded by human papillomavirus types 16 and 18 promotes the degradation of p53. *Cell* 63:1129-36, 1990
328. Ha PK, Benoit NE, Yochem R, et al: A transcriptional progression model for head and neck cancer. *Clin Cancer Res* 9:3058-64, 2003
329. Psyrri A, DiMaio D: Human papillomavirus in cervical and head-and-neck cancer. *Nat Clin Pract Oncol* 5:24-31, 2008
330. Bradford CR, Zhu S, Wolf GT, et al: Overexpression of p53 predicts organ preservation using induction chemotherapy and radiation in patients with advanced laryngeal cancer. Department of Veterans Affairs Laryngeal Cancer Study Group. *Otolaryngol Head Neck Surg* 113:408-12, 1995
331. McKaig RG, Baric RS, Olshan AF: Human papillomavirus and head and neck cancer: epidemiology and molecular biology. *Head Neck* 20:250-65, 1998
332. Caicedo-Granados E, Lin R, Fujisawa C, et al: Wild-type p53 reactivation by small-molecule Minnelide in human papillomavirus (HPV)-positive head and neck squamous cell carcinoma. *Oral Oncol* 50:1149-56, 2014

Bibliography

333. Modur V, Thomas-Robbins K, Rao K: HPV and CSC in HNSCC cisplatin resistance. *Front Biosci (Elite Ed)* 7:58-66, 2015
334. Blitzer GC, Smith MA, Harris SL, et al: Review of the clinical and biologic aspects of human papillomavirus-positive squamous cell carcinomas of the head and neck. *Int J Radiat Oncol Biol Phys* 88:761-70, 2014
335. Kandoth C, McLellan MD, Vandin F, et al: Mutational landscape and significance across 12 major cancer types. *Nature* 502:333-9, 2013
336. Bernard X, Robinson P, Nomine Y, et al: Proteasomal degradation of p53 by human papillomavirus E6 oncoprotein relies on the structural integrity of p53 core domain. *PLoS One* 6:e25981, 2011
337. Califano J, van der Riet P, Westra W, et al: Genetic progression model for head and neck cancer: implications for field cancerization. *Cancer Res* 56:2488-92, 1996
338. Pyeon D, Newton MA, Lambert PF, et al: Fundamental differences in cell cycle deregulation in human papillomavirus-positive and human papillomavirus-negative head/neck and cervical cancers. *Cancer Res* 67:4605-19, 2007
339. Hall PA, Lane DP: p53 in tumour pathology: can we trust immunohistochemistry?--Revisited! *J Pathol* 172:1-4, 1994
340. Gannon JV, Greaves R, Iggo R, et al: Activating mutations in p53 produce a common conformational effect. A monoclonal antibody specific for the mutant form. *EMBO J* 9:1595-602, 1990
341. Buschmann T, Minamoto T, Wagle N, et al: Analysis of JNK, Mdm2 and p14(ARF) contribution to the regulation of mutant p53 stability. *J Mol Biol* 295:1009-21, 2000
342. Brachmann RK, Vidal M, Boeke JD: Dominant-negative p53 mutations selected in yeast hit cancer hot spots. *Proc Natl Acad Sci U S A* 93:4091-5, 1996
343. Sano D, Xie TX, Ow TJ, et al: Disruptive TP53 mutation is associated with aggressive disease characteristics in an orthotopic murine model of oral tongue cancer. *Clin Cancer Res* 17:6658-70, 2011

Bibliography

344. Wald AI, Hoskins EE, Wells SI, et al: Alteration of microRNA profiles in squamous cell carcinoma of the head and neck cell lines by human papillomavirus. *Head Neck* 33:504-12, 2011
345. Guihard S, Ramolu L, Macabre C, et al: The NEDD8 conjugation pathway regulates p53 transcriptional activity and head and neck cancer cell sensitivity to ionizing radiation. *Int J Oncol* 41:1531-40, 2012
346. Bossi G, Sacchi A: Restoration of wild-type p53 function in human cancer: relevance for tumor therapy. *Head Neck* 29:272-84, 2007
347. Scheffner M, Huibregtse JM, Vierstra RD, et al: The HPV-16 E6 and E6-AP complex functions as a ubiquitin-protein ligase in the ubiquitination of p53. *Cell* 75:495-505, 1993
348. Chocolatewala NM, Chaturvedi P: Role of human papilloma virus in the oral carcinogenesis: an Indian perspective. *J Cancer Res Ther* 5:71-7, 2009
349. Adhim Z, Otsuki N, Kitamoto J, et al: Gene silencing with siRNA targeting E6/E7 as a therapeutic intervention against head and neck cancer-containing HPV16 cell lines. *Acta Otolaryngol* 133:761-71, 2013
350. Li C, Johnson DE: Liberation of functional p53 by proteasome inhibition in human papilloma virus-positive head and neck squamous cell carcinoma cells promotes apoptosis and cell cycle arrest. *Cell Cycle* 12:923-34, 2013
351. Marullo R, Werner E, Zhang H, et al: HPV16 E6 and E7 proteins induce a chronic oxidative stress response via NOX2 that causes genomic instability and increased susceptibility to DNA damage in head and neck cancer cells. *Carcinogenesis* 36:1397-406, 2015
352. Scheffner M, Takahashi T, Huibregtse JM, et al: Interaction of the human papillomavirus type 16 E6 oncoprotein with wild-type and mutant human p53 proteins. *J Virol* 66:5100-5, 1992
353. Patel UA, Thakkar KH, Holloway N: Patient compliance to radiation for advanced head and neck cancer at a tertiary care county hospital. *Laryngoscope* 118:428-32, 2008

Bibliography

354. Mehra R, Ang KK, Burtneess B: Management of human papillomavirus-positive and human papillomavirus-negative head and neck cancer. *Semin Radiat Oncol* 22:194-7, 2012
355. Psyrri A, Sasaki C, Vassilakopoulou M, et al: Future directions in research, treatment and prevention of HPV-related squamous cell carcinoma of the head and neck. *Head Neck Pathol* 6 Suppl 1:S121-8, 2012
356. Wheeler S, Siwak DR, Chai R, et al: Tumor epidermal growth factor receptor and EGFR PY1068 are independent prognostic indicators for head and neck squamous cell carcinoma. *Clin Cancer Res* 18:2278-89, 2012
357. Psyrri A, Seiwert TY, Jimeno A: Molecular pathways in head and neck cancer: EGFR, PI3K, and more. *Am Soc Clin Oncol Educ Book*:246-55, 2013
358. Dorsey K, Agulnik M: Promising new molecular targeted therapies in head and neck cancer. *Drugs* 73:315-25, 2013
359. Purohit S, Bhise R, Lokanatha D, et al: Systemic therapy in head and neck cancer: changing paradigm. *Indian J Surg Oncol* 4:19-26, 2013
360. Falschlehner C, Ganten TM, Koschny R, et al: TRAIL and other TRAIL receptor agonists as novel cancer therapeutics. *Adv Exp Med Biol* 647:195-206, 2009
361. Herbst RS, Eckhardt SG, Kurzrock R, et al: Phase I dose-escalation study of recombinant human Apo2L/TRAIL, a dual proapoptotic receptor agonist, in patients with advanced cancer. *J Clin Oncol* 28:2839-46, 2010
362. Raulf N, El-Attar R, Kulms D, et al: Differential response of head and neck cancer cell lines to TRAIL or Smac mimetics is associated with the cellular levels and activity of caspase-8 and caspase-10. *Br J Cancer* 111:1955-64, 2014
363. Filippova M, Johnson MM, Bautista M, et al: The large and small isoforms of human papillomavirus type 16 E6 bind to and differentially affect procaspase 8 stability and activity. *J Virol* 81:4116-29, 2007
364. Tungteakkhun SS, Filippova M, Fodor N, et al: The full-length isoform of human papillomavirus 16 E6 and its splice variant E6* bind to

Bibliography

different sites on the procaspase 8 death effector domain. *J Virol* 84:1453-63, 2010

365. Mendelsohn J: Epidermal growth factor receptor inhibition by a monoclonal antibody as anticancer therapy. *Clin Cancer Res* 3:2703-7, 1997

366. Li S, Schmitz KR, Jeffrey PD, et al: Structural basis for inhibition of the epidermal growth factor receptor by cetuximab. *Cancer Cell* 7:301-11, 2005

367. 1308 E: A phase II trial of induction chemotherapy followed by cetuximab with low dose versus standard dose IMRT in patients with HPV-associated resectable squamous cell carcinoma of the oropharynx (OP), 2010

368. Pogorzelski M, Ting S, Gauler TC, et al: Impact of human papilloma virus infection on the response of head and neck cancers to anti-epidermal growth factor receptor antibody therapy. *Cell Death Dis* 5:e1091, 2014

369. Guster JD, Weissleder SV, Busch CJ, et al: The inhibition of PARP but not EGFR results in the radiosensitization of HPV/p16-positive HNSCC cell lines. *Radiother Oncol* 113:345-51, 2014

370. Kumar B, Cordell KG, Lee JS, et al: EGFR, p16, HPV Titer, Bcl-xL and p53, sex, and smoking as indicators of response to therapy and survival in oropharyngeal cancer. *J Clin Oncol* 26:3128-37, 2008

371. Kong CS, Narasimhan B, Cao H, et al: The relationship between human papillomavirus status and other molecular prognostic markers in head and neck squamous cell carcinomas. *Int J Radiat Oncol Biol Phys* 74:553-61, 2009

372. Al-Swiahb JN, Huang CC, Fang FM, et al: Prognostic impact of p16, p53, epidermal growth factor receptor, and human papillomavirus in oropharyngeal cancer in a betel nut-chewing area. *Arch Otolaryngol Head Neck Surg* 136:502-8, 2010

373. Won HS, Jung CK, Chun SH, et al: Difference in expression of EGFR, pAkt, and PTEN between oropharyngeal and oral cavity squamous cell carcinoma. *Oral Oncol* 48:985-90, 2012

Bibliography

374. Husain H, Psyrri A, Markovic A, et al: Nuclear epidermal growth factor receptor and p16 expression in head and neck squamous cell carcinoma. *Laryngoscope* 122:2762-8, 2012
375. Perrone F, Suardi S, Pastore E, et al: Molecular and cytogenetic subgroups of oropharyngeal squamous cell carcinoma. *Clin Cancer Res* 12:6643-51, 2006
376. Rampias T, Pectasides E, Prasad M, et al: Molecular profile of head and neck squamous cell carcinomas bearing p16 high phenotype. *Ann Oncol* 24:2124-31, 2013
377. Grandis JR, Zeng Q, Drenning SD, et al: Normalization of EGFR mRNA levels following restoration of wild-type p53 in a head and neck squamous cell carcinoma cell line. *Int J Oncol* 13:375-8, 1998
378. Chung CH, Ely K, McGavran L, et al: Increased epidermal growth factor receptor gene copy number is associated with poor prognosis in head and neck squamous cell carcinomas. *J Clin Oncol* 24:4170-6, 2006
379. Cohen EE, Lingen MW, Martin LE, et al: Response of some head and neck cancers to epidermal growth factor receptor tyrosine kinase inhibitors may be linked to mutation of ERBB2 rather than EGFR. *Clin Cancer Res* 11:8105-8, 2005
380. Licitra L, Storkel S, Kerr KM, et al: Predictive value of epidermal growth factor receptor expression for first-line chemotherapy plus cetuximab in patients with head and neck and colorectal cancer: analysis of data from the EXTREME and CRYSTAL studies. *Eur J Cancer* 49:1161-8, 2013
381. Vokes EE, Seiwert TY: EGFR-directed treatments in SCCHN. *Lancet Oncol* 14:672-3, 2013
382. Bullenkamp J, Raulf N, Ayaz B, et al: Bortezomib sensitises TRAIL-resistant HPV-positive head and neck cancer cells to TRAIL through a caspase-dependent, E6-independent mechanism. *Cell Death Dis* 5:e1489, 2014

Appendix- Publication arising during thesis

Bortezomib sensitises TRAIL-resistant HPV-positive head and neck cancer cells to TRAIL through a caspase-dependent, E6-independent mechanism

J Bullenkamp¹, N Raulf¹, B Ayaz², H Walczak³, D Kulms⁴, E Odell², S Thavaraj² and M Tavassoli^{1*}

Human papillomavirus (HPV) is causative for a new and increasing form of head and neck squamous cell carcinomas (HNSCCs). Although localised HPV-positive cancers have a favourable response to radio-chemotherapy (RT/CT), the impact of HPV in advanced or metastatic HNSCC remains to be defined and targeted therapeutics need to be tested for cancers resistant to RT/CT. To this end, we investigated the sensitivity of HPV-positive and -negative HNSCC cell lines to TRAIL (tumour necrosis factor-related apoptosis-inducing ligand), which induces tumour cell-specific apoptosis in various cancer types. A clear correlation was observed between HPV positivity and resistance to TRAIL compared with HPV-negative head and neck cancer cell lines. All TRAIL-resistant HPV-positive cell lines tested were sensitised to TRAIL-induced cell death by treatment with bortezomib, a clinically approved proteasome inhibitor. Bortezomib-mediated sensitisation to TRAIL was associated with enhanced activation of caspase-8, -9 and -3, elevated membrane expression levels of TRAIL-R2, cytochrome *c* release and G2M arrest. Knockdown of caspase-8 significantly blocked cell death induced by the combination therapy, whereas the BH3-only protein Bid was not required for induction of apoptosis. XIAP depletion increased the sensitivity of both HPV-positive and -negative cells to TRAIL alone or in combination with bortezomib. In contrast, restoration of p53 following E6 knockdown in HPV-positive cells had no effect on their sensitivity to either single or combination therapy, suggesting a p53-independent pathway for the observed response. In summary, bortezomib-mediated proteasome inhibition sensitises previously resistant HPV-positive HNSCC cells to TRAIL-induced cell death through a mechanism involving both the extrinsic and intrinsic pathways of apoptosis. The cooperative effect of these two targeted anticancer agents therefore represents a promising treatment strategy for RT/CT-resistant HPV-associated head and neck cancers. *Cell Death and Disease* (2014) 5, e1489; doi:10.1038/cddis.2014.455; published online 23 October 2014

Head and neck squamous cell carcinoma (HNSCC) represents the sixth most common cancer worldwide.¹ While the overall incidence of HNSCC, traditionally associated with tobacco or alcohol consumption, is declining, a subset of oropharyngeal cancers caused by infection with high-risk types of human papillomavirus (HPV) has risen significantly.^{2,3} Transformation upon HPV infection occurs mainly because of inactivation of the p53 and retinoblastoma tumour suppressor proteins mediated by the viral oncoproteins E6 and E7, respectively.⁴

HPV-positive (HPV⁺) cancers represent a distinct subset of HNSCC in terms of biology and clinical behaviour. In general, they are characterised by better overall survival and an improved response to conventional radio-chemotherapy (RT/CT) compared with HPV-negative (HPV⁻) cancers.^{5,6} To further minimise treatment-related toxicity without compromising outcome, there have been suggestions of treatment de-escalation in conjunction with targeted therapies.⁷

The novel anticancer agent TRAIL (tumour necrosis factor-related apoptosis-inducing ligand) selectively kills several

types of malignant cell lines with little effect on normal cells.⁸ Recombinant TRAIL or monoclonal antibodies targeting TRAIL receptors (TRAIL-Rs) are currently being tested in phase I/II clinical trials for patients with advanced tumours.^{9,10} TRAIL induces cell death by binding to TRAIL-R1 or TRAIL-R2, resulting in receptor oligomerisation and formation of the death-inducing signalling complex (DISC)¹¹ and activation of initiator caspase-8.¹² Caspase-8 directly activates effector caspase-3 to induce apoptosis through the type I pathway or cleaves the BH3-only protein Bid, generating tBid. This type II pathway involves an amplification loop through the intrinsic pathway of apoptosis characterised by cytochrome *c* release from the mitochondria, activation of initiator caspase-9 and ultimately caspase-3.¹³

Despite its tumour-selective activity, various cancer cell lines remain resistant to TRAIL, limiting the clinical potential of TRAIL-based monotherapies. Many recent studies focus on combination strategies with other agents to sensitise resistant cells to TRAIL.¹⁴ The proteasome inhibitor bortezomib is an FDA-approved drug for the treatment of multiple myeloma, but

¹Department of Molecular Oncology, King's College London, Guy's Campus, Hodgkin Building, London SE1 1UL, UK; ²Department of Oral Pathology, King's College London, Guy's Campus, Dental Institute, London SE1 9RT, UK; ³Centre for Cell Death, Cancer and Inflammation (CCCI), UCL Cancer Institute, 72 Huntley Street, London WC1E 6BT, UK and ⁴Experimental Dermatology, Department of Dermatology, TU Dresden, Dresden 01307, Germany

*Corresponding author: M Tavassoli, Department of Molecular Oncology, King's College London, Guy's Campus, Hodgkin Building, London SE1 1UL, UK. Tel: +44 0 20 7848 6120; Fax: +44 0 20 7848 6210; E-mail: mahvash.tavassoli@kcl.ac.uk

Abbreviations: TRAIL, tumour necrosis factor-related apoptosis-inducing ligand; HNSCC, head and neck squamous cell carcinoma; HPV^{+/−}, human papillomavirus positive/negative; RT/CT, radio-chemotherapy; TRAIL-R, TRAIL receptor; DISC, death-inducing signalling complex; nec-1, necrostatin-1

Received 7.7.14; revised 12.8.14; accepted 10.9.14; Edited by D Vucic

has shown only little single-agent activity in solid malignancies such as HNSCC while being effective in combination with other treatment options.^{15–17} Combining bortezomib with TRAIL-R agonists produced a synergistic cytotoxic effect in various types of cancers. Potential mechanisms underlying sensitisation to TRAIL-induced apoptosis include inhibition of NF- κ B signalling, stabilisation of BH3-only proteins, p53 or p21, upregulation of TRAIL-Rs and enhanced stability of caspase-8.^{18–26}

So far, little data is available on the therapeutic potential of TRAIL alone or in combination with bortezomib in HNSCC or other HPV⁺ related cancers. Treatment with the proteasome inhibitor MG132 sensitised TRAIL-resistant HPV⁺ cervical cancer cells to TRAIL through p53-dependent upregulation of TRAIL-Rs and inactivation of XIAP.²⁷ Overexpression of E6 was shown to protect colon cancer cells from death receptor-induced apoptosis by affecting the stability of the DISC, indicating a functional link between the presence of E6 and TRAIL signalling.²⁸

In this study, we tested the response of HPV⁺ and HPV⁻ HNSCC cells to treatment with TRAIL alone or combined with bortezomib, revealing a clear pattern of sensitivity to TRAIL depending on HPV status and a synergistic effect when combined with bortezomib. In addition, we identified some of the proteins and pathways involved in the response to TRAIL/bortezomib in HNSCCs.

Results

HPV-associated HNSCC cells are resistant to TRAIL. HPV⁺ HNSCCs generally display higher sensitivity to RT/CT than HPV⁻ cancers,⁶ but their response to targeted therapeutic agents remains largely unknown. We therefore investigated the cytotoxic effect of the tumour-selective apoptosis-inducing agent TRAIL in a panel of HPV⁺ and HPV⁻ HNSCC cell lines, demonstrating a link between HPV status and TRAIL sensitivity. Whereas treatment with increasing concentrations of recombinant TRAIL reduced the viability of HPV⁻ cells in a dose-dependent manner, all HPV⁺ cell lines tested remained resistant to TRAIL even at high concentrations (Figure 1a).

Bortezomib sensitises HPV⁺ HNSCC cells to TRAIL-induced cell death. The proteasome inhibitor bortezomib has been shown to sensitise cells to TRAIL in other types of cancer.²⁹ We therefore aimed to investigate whether concentrations of bortezomib with only low single-agent toxicity synergise with TRAIL in HPV⁺ HNSCC cells. The representative site-matched HNSCC cell lines 089 (HPV⁻) and 090 (HPV⁺), which demonstrated the highest difference in TRAIL sensitivity, were selected for further analysis. An initial dose-response assay revealed a similar response of 089 and 090 cells to treatment with bortezomib with an IC₅₀ value of ~2.5 ng/ml (Supplementary Figure 1). The combined effect of

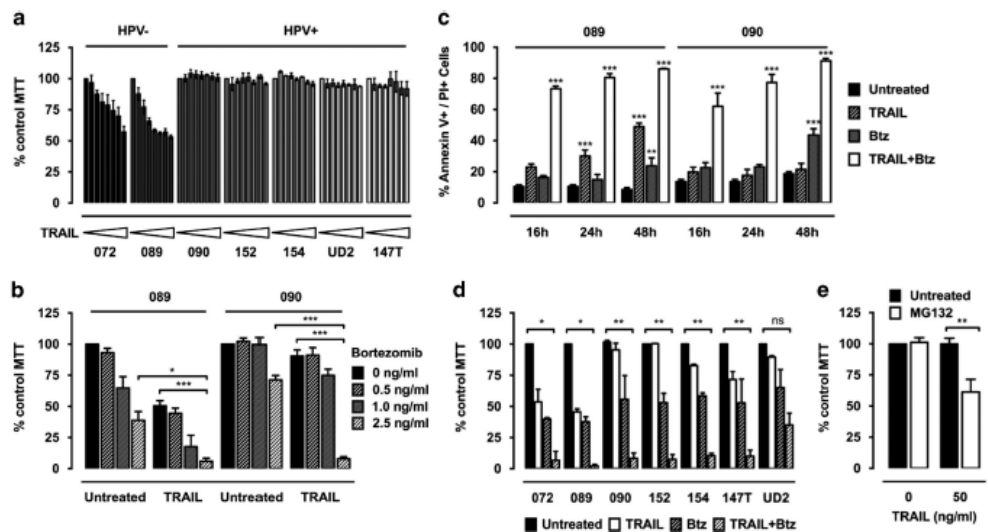


Figure 1 Sensitisation of HPV⁺ HNSCC cells to TRAIL by proteasome inhibition. (a) Seven HPV⁻ or HPV⁺ HNSCC cell lines were treated with increasing concentrations of TRAIL, up to 100 ng/ml for 72 h. Cell viability after treatment was analysed by 3-(4,5-dimethylthiazol-2-yl)-2,5-diphenyl tetrazolium bromide (MTT) assay of triplicate wells. Bars represent mean cell viability normalised to untreated control cells and error bars indicate S.E.M. of three independent experiments. (b) The 089 and 090 cells were treated with the indicated concentrations of TRAIL and/or bortezomib (Btz) for 48 h and analysed by MTT assay as before in four independent experiments. *P*-values were determined by two-way analysis of variance (ANOVA) (**P* < 0.05 and ****P* < 0.001). (c) The 089 and 090 cells were treated with 50 ng/ml TRAIL and 2.5 ng/ml Btz alone or in combination. Cells were collected at the indicated time points for Annexin V/PI staining and fluorescence-activated cell sorting (FACS) analysis. Bars indicate the mean percentage of dead cells defined as either Annexin V or PI positive and error bars indicate S.E.M. of three independent experiments. *P*-values were determined by two-way ANOVA (***P* < 0.01 and ****P* < 0.001). (d) Seven HNSCC cell lines were treated with single drugs or the combination of 50 ng/ml TRAIL and 2.5 ng/ml bortezomib for 48 h and analysed by MTT assay as before in three independent experiments. *P*-values were determined by two-way ANOVA (**P* < 0.05, ***P* < 0.01, ^{NS}*P* > 0.05). (e) The 090 cells were treated with 50 ng/ml TRAIL and 0.1 μ M MG132 for 48 h until MTT analysis as before in three independent experiments. *P*-values were determined by two-way ANOVA (***P* < 0.01)

both drugs was tested using 50 ng/ml TRAIL in combination with bortezomib at several concentrations below the IC_{50} value. Cotreatment with bortezomib sensitised HPV⁺ 090 cells to TRAIL-induced cell death, whereas bortezomib alone did not markedly impair cell viability (Figure 1b). This effect was highly synergistic with a combination index below 0.5 (data not shown). In addition, TRAIL-induced cell death in HPV⁺ 089 cells was further enhanced by bortezomib (Figure 1b).

The decrease in cell viability measured by MTT assays might also be because of bortezomib-induced cell cycle arrest reducing the number of viable cells. To determine whether combination treatment with TRAIL and bortezomib (TRAIL/bortezomib) triggers apoptosis in HNSCC cell lines, 089 and 090 cells were analysed by flow cytometry at the indicated time points (Figure 1c). Cell death, defined as positive staining for Annexin V or PI, was detected in both cell lines treated with TRAIL and bortezomib in combination. In contrast, TRAIL alone did not affect the viability of 090 cells but induced cell death in 089 cells, whereas bortezomib as a single drug displayed only slight toxicity in both cell lines.

A similar effect of bortezomib on TRAIL-induced cell death was also observed in a larger panel of HPV⁺ and HPV⁻ HNSCC cell lines. Cotreatment with TRAIL and bortezomib significantly reduced cell viability in all HPV⁺ cell lines compared with single treatments (Figure 1d). Overall, these results suggest that TRAIL-resistant HPV⁺ HNSCC cells become highly sensitive to TRAIL to a similar level as HPV⁻ cells when additionally treated with bortezomib.

To examine whether the sensitising effect of bortezomib is due to proteasome inhibition, another proteasome inhibitor,

MG132, was tested in combination with TRAIL. Similar to bortezomib, cotreatment with a subtoxic dose of MG132 sensitised HPV⁺ 090 cells to TRAIL-induced cell death (Figure 1e).

TRAIL and bortezomib combination treatment induces caspase-dependent cell death. In addition to apoptosis TRAIL has also been implicated in necroptotic cell death.³⁰ To analyse the type of cell death, 089 and 090 cells were pre-treated with the pancaspase inhibitor z-Vad-fmk (zVad) and/or the RIP1 kinase inhibitor necrostatin-1 (nec-1) followed by treatment with TRAIL/bortezomib. Pre-treatment with zVad significantly rescued both cell lines from TRAIL/bortezomib-induced cell death, increasing cell viability by ~30%. Further combination treatment with nec-1 provided significant additional protection by about 20%, which might indicate a necroptotic cell death induced by TRAIL/bortezomib in HNSCC cells (Figure 2a). These results were confirmed by Annexin V/PI staining after treatment of 089 and 090 cells with TRAIL/bortezomib plus zVad and/or nec-1. Addition of zVad alone or combined with nec-1 had a protective effect in both cell lines, reducing cell death by up to 40% (Figure 2b), confirming that TRAIL/bortezomib induce caspase-dependent cell death.

The activation of specific caspases in HPV⁺ 090 cells in response to the combination treatment was further analysed. Marked processing of caspase-3, generating the active 17 kDa fragment, and a slight reduction of procaspase-8 levels were only detected following treatment with TRAIL/bortezomib but not TRAIL alone (Figure 2c). Combination treatment but not individual drugs induced activation of

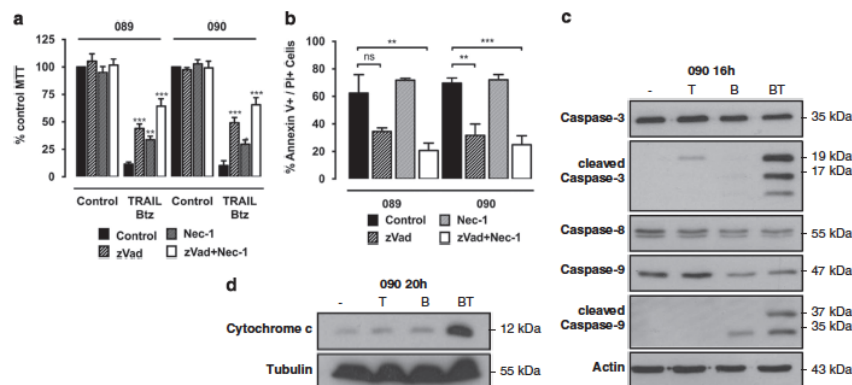


Figure 2 TRAIL and bortezomib cooperate to induce caspase-dependent apoptosis. (a) The 089 and 090 cells were treated with 50 ng/ml TRAIL and 2.5 ng/ml BTZ alone or in combination with the caspase inhibitor zVad (20 μ M) and/or the RIP1 kinase inhibitor nec-1 (50 μ M). Cell survival was measured 24 h later by 3-(4,5-dimethylthiazol-2-yl)-2,5-diphenyl tetrazolium bromide (MTT) analysis. Bars represent mean cell viability normalised to untreated control cells and error bars indicate S.E.M. of four independent experiments. P-values were determined by two-way ANOVA (* P < 0.05, ** P < 0.01 and *** P < 0.001). (b) Quantification of Annexin V and PI single- or double-positive populations in 089 and 090 cells treated with 50 ng/ml TRAIL and 2.5 ng/ml bortezomib combined with zVad and/or nec-1 as before. Bars represent the percentage of dead cells that were stained positive for Annexin V, PI or both and error bars indicate S.E.M. of three independent experiments. P-values were determined by one-way ANOVA (** P < 0.01 and *** P < 0.001). (c) Western blot analysis of caspase-3, -8 and -9 processing in 090 cells treated with TRAIL (T, 50 ng/ml) and bortezomib (B, 2.5 ng/ml) alone or in combination (BT) for 16 h. (d) Cytochrome c release was analysed by western blot analysis of cytosolic fractions from 090 cells treated with TRAIL (T, 50 ng/ml) and bortezomib (B, 2.5 ng/ml) alone or in combination (BT) for 20 h

caspase-9 as shown by the reduction in full-length caspase-9 levels and generation of the active 37 kDa fragment. This suggests activation of the intrinsic pathway of apoptosis, which is characterised by the release of cytochrome *c* from the mitochondria into the cytosol.³¹ Cytochrome *c* was detected in cytosolic fractions of O90 cells following combination treatment with TRAIL and bortezomib, hinting towards an involvement of the intrinsic pathway (Figure 2d).

Bortezomib-mediated sensitisation to TRAIL is associated with upregulation of TRAIL-R2 and requires caspase-8 but not Bid. Proteasome inhibition has previously been associated with increased transcription and membrane expression of TRAIL-R2.^{18,32} We therefore analysed the surface expression levels of TRAIL-Rs in O89 and O90 cells by flow cytometry. Measurement of basal receptor levels showed expression of TRAIL-R2 in both cell lines, whereas TRAIL-R1 was only detectable in O89 cells (Figure 3a and Supplementary Figure 2). Bortezomib treatment triggered a modest but significant increase in expression levels of TRAIL-R2 but not TRAIL-R1 in O90 cells. This might contribute to the increased TRAIL sensitivity of O90 cells; however, further

studies will be required to determine whether TRAIL-R upregulation is necessary for TRAIL sensitisation by bortezomib.

The major initiator caspase recruited to the activated TRAIL-R complex is caspase-8. Knockdown of caspase-8 in O89 and O90 cells (knockdown efficiency 80–100%) markedly reduced processing of caspase-3 in response to the combination treatment (Figure 3b). Moreover, it significantly increased cell survival in both cell lines following treatment with TRAIL/bortezomib by ~40% compared with control cells (Figures 3c and d and Supplementary Figure 3). The remaining cytotoxic effect could be due to residual levels of caspase-8 or activation of other initiator caspases compensating for caspase-8 deficiency.

The truncated form of Bid, tBid, links death receptor activation to the intrinsic pathway and is stabilised by proteasome inhibition, representing a potential mechanism for sensitisation to TRAIL by bortezomib.²⁵ The effect of Bid depletion on the sensitivity to TRAIL/bortezomib was studied using stable O89 and O90 Bid shRNA cells (knockdown efficiency 70%; Figure 3e). No significant difference in the response to TRAIL and/or bortezomib was observed between

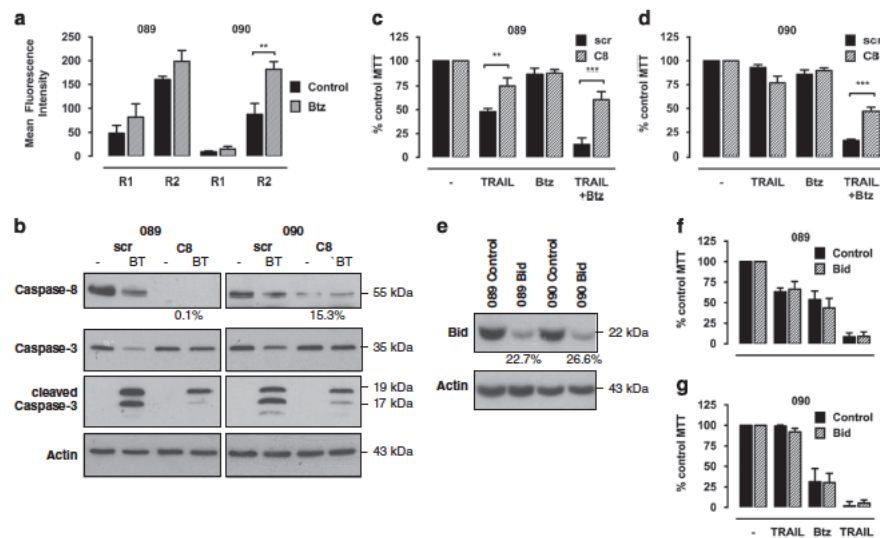


Figure 3 Bortezomib-induced sensitisation involves upregulation of DR5 and is mediated by caspase-8 but not Bid. (a) The O89 and O90 cells were treated with 2.5 ng/ml bortezomib (Btz) for 20 h. The surface expression of TRAIL-Rs was assessed by flow cytometry following staining with monoclonal antibodies for TRAIL-R1 (DR4) or TRAIL-R2 (DR5) and a secondary anti-mouse fluorescein isothiocyanate (FITC)-coupled antibody. Bars represent mean fluorescence intensity of FITC corrected for staining with a nonspecific isotype control and error bars indicate S.E.M. of three independent experiments. *P*-values were determined by one-way analysis of variance (ANOVA) (***P* < 0.01). (b) Stable inducible O89 and O90 caspase-8 (C8) and scrambled control (scr) short hairpin RNA (shRNA) cells were generated by lentiviral infection and shRNAs were induced with 1 µg/ml doxycycline for 24 h. Caspase-3 and -8 levels following treatment with 50 ng/ml TRAIL and 2.5 ng/ml bortezomib (BT) for 16 h were assessed by western blot analysis compared with respective control cells. The efficiency of caspase-8 knockdown was calculated using ImageJ software normalised to β-actin. Blots were cut and combined at the indicated line. (c and d) Cell viability of O89 (c) and O90 (d) C8 and scr shRNA cells after induction with 1 µg/ml doxycycline in the presence of 50 ng/ml TRAIL and/or 1 ng/ml Btz was analysed by 3-(4,5-dimethylthiazol-2-yl)-2,5-diphenyl tetrazolium bromide (MTT) assay after 48 h of treatment. Bars represent mean cell viability normalised to untreated control cells and error bars indicate S.E.M. of three independent experiments. *P*-values were determined by two-way ANOVA comparing C8 shRNA with corresponding control cells (***P* < 0.01 and ****P* < 0.001). (e) Stable Bid and non-silencing control shRNA O89 and O90 cells were generated by lentiviral infection. The efficiency of Bid knockdown in both cell lines was assessed by western blot analysis compared with respective control cells and calculated using ImageJ software normalised to β-actin. (f and g) Cell viability of O89 (f) and O90 (g) Bid and control shRNA cells in the presence of 50 ng/ml TRAIL and/or 1 ng/ml Btz as indicated was analysed by MTT analysis after 48 h. Bars represent mean cell viability normalised to untreated control cells and error bars indicate S.E.M. of three independent experiments

Bid knockdown and control cells (Figures 3f and g), indicating that bortezomib-induced sensitisation to TRAIL occurs independently of Bid.

XIAP depletion increases cell death in response to TRAIL alone and in combination with bortezomib. The anti-apoptotic protein XIAP prevents caspase-3 activation and its inhibition has been linked to increased sensitivity to TRAIL.^{33,34} Stable knockdown of XIAP in O90 cells (knockdown efficiency 70%) resulted in enhanced caspase-3 activation in response to bortezomib alone or in combination with TRAIL, as evident by increased caspase-3 processing and cleavage of PARP, but did not markedly affect caspase-3 activation following treatment with TRAIL alone at this time point (Figure 4b). In contrast, stable O89 XIAP knockdown cells (knockdown efficiency 80%) showed increased processing and activity of caspase-3 in response to the combination treatment as well as TRAIL alone.

XIAP knockdown reduced the survival of O89 cells in response to TRAIL to a similar level as obtained in combination with bortezomib, but did not affect their sensitivity to bortezomib alone (Figure 4c). Importantly, TRAIL-resistant O90 cells were significantly sensitised to TRAIL following XIAP knockdown, which reduced cell viability in response to TRAIL alone by ~30% (Figure 4d). In both cell lines, depletion of XIAP significantly enhanced cell death after combination treatment with TRAIL and bortezomib at all concentrations tested.

Bortezomib-induced p53 stabilisation in HPV⁺ cells is not the main mechanism for TRAIL sensitisation. In HPV⁺ tumours, p53 is kept inactive through E6-mediated proteaso-

mal degradation,³⁵ whereas HPV⁻ HNSCCs often contain inactivating p53 mutations, resulting in a stabilised but non-functional protein. Bortezomib treatment of HPV⁺ HNSCC cell lines has previously been associated with p53 stabilisation and induction of p53-dependent cell cycle arrest and apoptosis.³⁶ Here we show that bortezomib induces restoration of p53 and induction of the p53 target protein p21 in all HPV⁺ cell lines tested with the exception of 147 T cells that already showed a marked basal p53 expression (Figure 5a). By contrast, HPV⁻ O89 and O72 cells, which contain mutated p53,³⁷ showed no further increase in p53 protein levels and only a minimal induction of p21 in O72 cells.

To test the importance of p53 for the response of HPV⁺ cells to TRAIL/bortezomib, stable E6 shRNA O90 cells were generated. Western blot analysis showed almost ninefold increased levels of p53 in E6 knockdown cells compared with control cells, indicating reduced degradation of p53 after E6 depletion. E6 shRNA and control cells were subsequently treated with TRAIL alone or in combination with bortezomib for analysis of cell viability, but showed no significant difference in the response to either drug (Figures 5c and d). These results suggest that TRAIL resistance in O90 cells is not because of the presence and activity of E6 and that p53 restoration is insufficient to sensitise cells to TRAIL.

P21 represents a major mediator of p53-induced cell cycle arrest in the G0/G1 phase in response to DNA-damaging agents and other cellular stresses.³⁸ Flow cytometry-based cell cycle analysis of bortezomib-treated HNSCC cells showed a strong G2/M arrest of up to 50% in all cell lines and a small increase in the sub-G1 population, indicating apoptotic cells (Figure 5e). The extent of G2/M arrest was

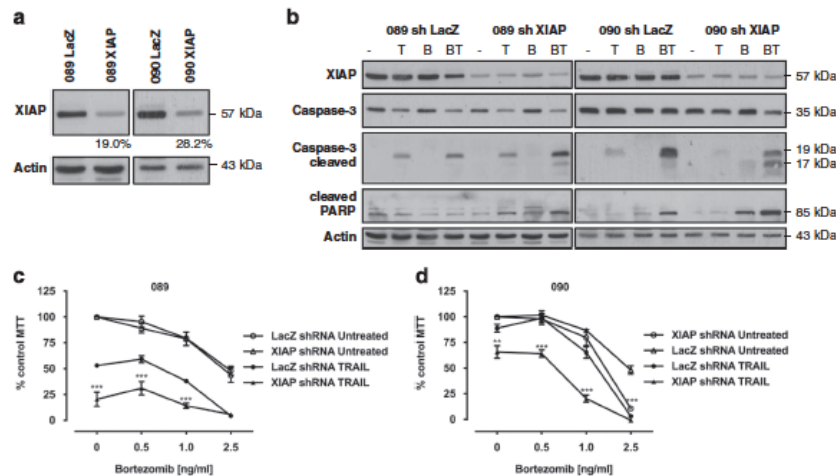


Figure 4 XIAP depletion enhances sensitivity of HPV⁺ cells to TRAIL alone or combined with bortezomib. (a) Stable XIAP and LacZ control shRNA O89 and O90 cells were generated by lentiviral infection. The efficiency of XIAP knockdown in both cell lines was assessed by western blot analysis compared with respective control cells and calculated using ImageJ software normalised to β -actin. Blots were cut and combined at the indicated line. (b) Stable O89 and O90 XIAP and LacZ short hairpin RNA (shRNA) cells were treated for 16 h with 50 ng/ml TRAIL alone (T), 2.5 ng/ml bortezomib (B) or both combined (BT). Protein levels of XIAP, caspase-3 and cleaved poly ADP ribose polymerase (PARP) were analysed by immunoblotting. (c and d) Cell viability of O89 (c) and O90 (d) XIAP and LacZ shRNA cells in the presence of 50 ng/ml TRAIL in combination with increasing bortezomib concentrations as indicated was analysed by 3-(4,5-dimethylthiazol-2-yl)-2,5-diphenyl tetrazolium bromide (MTT) assay after 48 h. Bars represent mean cell viability normalised to untreated control cells and error bars indicate S.E.M. of four independent experiments. *P*-values were determined by two-way ANOVA comparing XIAP shRNA with corresponding LacZ control cells (***P* < 0.01 and *** *P* < 0.001).

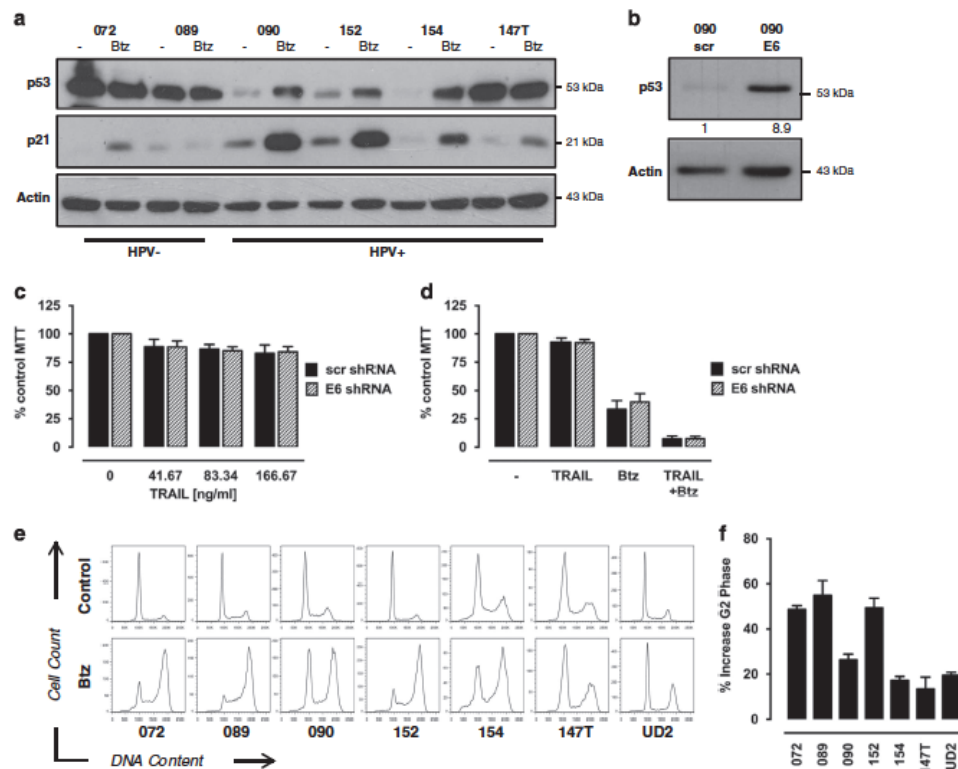


Figure 5 Role of p53 and E6 for bortezomib-mediated sensitisation to TRAIL. (a) The expression of p53 and p21 was detected by western blot analysis in six HNSCC cell lines after 16 h of treatment with 2.5 ng/ml bortezomib (Btz). (b) Stable E6 and scrambled control (scr) short hairpin RNA (shRNA) 090 cells were generated by lentiviral infection. E6 knockdown was confirmed by western blot analysis detecting p53 expression levels calculated using ImageJ software normalised to β -actin. (c) Cell viability of 090 E6 and scr shRNA cells treated with the indicated concentrations of TRAIL for 48 h was analysed by 3-(4,5-dimethylthiazol-2-yl)-2,5-diphenyl tetrazolium bromide (MTT) assay of triplicate wells. Bars represent mean cell viability normalised to untreated control cells and error bars indicate S.E.M. of five independent experiments. (d) Cell viability of 090 E6 and scr shRNA cells in the presence of 50 ng/ml TRAIL alone or in combination with 2.5 ng/ml Btz was analysed by MTT assay after 48 h as before in five independent experiments. (e) Seven HNSCC cell lines were treated with 2.5 ng/ml Btz for 24 h before cell cycle analysis by flow cytometry. Representative histograms indicating cells in the respective cell cycle phases are shown. (f) Bars represent increase of the percentage of cells in the G2/M phase following treatment with 2.5 ng/ml bortezomib for 24 h compared with untreated control cells and error bars indicate S.E.M. of three independent experiments

more pronounced in HPV⁻ cells compared with HPV⁺ cells (Figure 5f), which might reflect their generally faster cellular proliferation rate (data not shown). However, the importance of this bortezomib-induced G2/M arrest for TRAIL-induced cell death in HNSCC cells requires further investigation.

Discussion

HPV⁺ HNSCCs are characterised by improved overall and disease-specific survival compared with site- and age-matched controls.⁵ However, HPV status does not currently influence management of the disease and existing treatment modalities are associated with severe side effects. It is therefore necessary to investigate the impact of dose de-escalation and novel targeted therapeutic agents in this group of patients with the aim of maintaining efficacy while minimising toxicity. One such novel tumour-selective agent is

TRAIL, and despite early promising result in other cancers,⁸ little is known about its effectiveness in HNSCC.

In contrast to the site-matched HPV⁻ cell lines tested here, HPV⁺ HNSCC cells were found to be highly resistant to TRAIL when used as a single agent even at high concentrations. There was no clear association between TRAIL resistance in HPV⁺ cells and endogenous levels of anti- or proapoptotic proteins such as TRAIL-Rs, caspase-3/-8 or XIAP (data not shown). However, expression profiling of a larger panel of regulatory proteins of apoptosis in a cohort of HPV⁺ and HPV⁻ HNSCC samples remains necessary to identify differentially expressed proteins that contribute to the distinct response pattern described here. From a clinical perspective, our data suggest that TRAIL is unlikely to be efficacious as a single modality treatment option for the management of HPV⁺ head and neck cancers.

The function of many proteins involved in death receptor signalling and apoptosis induction is regulated by

ubiquitination and subsequent proteasomal degradation.³⁹ In various other TRAIL-resistant cancer cells, including cell lines derived from squamous cell carcinomas, inhibition of proteasomal activity resulted in enhanced sensitivity to TRAIL-induced cell death.^{22,23} Here we show that combination treatment with recombinant TRAIL and low doses of the clinically approved proteasome inhibitor bortezomib displays synergistic cytotoxicity in all HPV⁺ HNSCC cell lines tested. While bortezomib treatment alone showed only a slight effect on the activation of apoptotic pathways, bortezomib markedly enhanced TRAIL-induced apoptosis in HNSCC cells, accompanied by increased processing of caspase-3, -8 and -9. A recent study demonstrated increased activity of recombinant TRAIL in patient-derived ovarian carcinoma cells when combined with bortezomib, while primary hepatocytes remained resistant, indicating low toxicity of the combination treatment in normal cells.⁴⁰ The combined cytotoxic effect of bortezomib and TRAIL in both HPV⁺ and HPV⁻ cell lines suggests a promising novel therapeutic approach for the effective and selective killing of HNSCCs.

A number of preclinical studies in other types of cancer have identified mechanisms underlying the sensitisation of cancer cells to TRAIL by bortezomib. These include increased expression of TRAIL-Rs,^{21,32} enhanced activation of caspase-8,²⁶ stabilisation of BH3-only proteins,^{19,25} inactivation of XIAP^{27,34} or induction of p53 or p21.^{20,27} Based on these studies, we aimed to investigate pathways that contributed to the increased sensitivity of HNSCC cells to TRAIL when combined with bortezomib.

Consistent with other studies, bortezomib treatment of HPV⁺ cells was associated with elevated membrane expression levels of TRAIL-R2.^{18,32} While this modest increase is unlikely to be the sole mechanism for the observed synergy, it may contribute to TRAIL sensitivity because of an increased number of receptors on the cell surface and therefore a higher degree of caspase-8 activation. Procasase-8 levels were slightly reduced in HPV⁺ cells following combination treatment with TRAIL and bortezomib, suggesting enhanced activation of caspase-8 compared with single treatments. Moreover, bortezomib might also stabilise the active caspase-8 fragment to enhance its activity as suggested by recent reports that provided evidence for its regulation through ubiquitination and degradation.⁴¹ Depletion of caspase-8 resulted in markedly reduced processing of caspase-3 and provided significant protection against TRAIL/bortezomib in both HPV⁺ and HPV⁻ cells. Nevertheless, ~50% of cells remained sensitive to combination treatment with TRAIL/bortezomib in the absence of caspase-8, which might indicate a role for another initiator caspase such as caspase-10.

TRAIL and bortezomib in combination triggered cytochrome *c* release and activation of caspase-9, indicating induction of the mitochondrial pathway of apoptosis. The stability of the truncated form of the BH3-only protein Bid, which triggers the permeabilisation of the mitochondrial membrane after cleavage by active caspase-8, is regulated by proteasomal degradation.⁴² In glioblastoma cells, bortezomib-mediated stabilisation of tBid was shown to facilitate TRAIL-induced cell death by amplifying apoptosis through the mitochondrial pathway.^{24,25} In HNSCC cells, depletion of Bid had no effect on the cytotoxicity of TRAIL and bortezomib, suggesting that

bortezomib-mediated sensitisation of HPV⁺ cells to TRAIL is independent of Bid and that TRAIL-induced apoptosis is mediated through the type I pathway. Activation of the intrinsic apoptotic pathway in response to the combination treatment, as evident by cytochrome *c* release and cleavage of caspase-9, potentially represents a parallel cellular process triggered by bortezomib but is unlikely to be the decisive mechanism of cell death.¹⁸

XIAP prevents the activation of caspase-3 and -9 at different levels, including inhibition of substrate binding and proteasomal degradation of processed caspase-3 forms.⁴³ Downregulation or inhibition of XIAP has been proposed as a mechanism of bortezomib-induced sensitisation to TRAIL in different cancer models.^{34,44,45} In our system, depletion of XIAP partially sensitised HPV⁺ cells to TRAIL and significantly enhanced the synergistic effect of bortezomib. Similar data were obtained in HPV⁺ cervical cancer cells in which XIAP downregulation increased TRAIL-induced apoptosis, in particular when combined with MG132.²⁷ Moreover, the sensitising effect of proteasome inhibition to TRAIL in lymphoma cells with acquired TRAIL resistance could be partially reproduced by knockdown of XIAP.⁴⁶ These findings suggest that XIAP partially accounts for the resistance of HPV⁺ cells to TRAIL as a single treatment. In addition to cytochrome *c*, several other factors are released into the cytosol upon activation of the mitochondrial pathway of apoptosis, including Smac/DIABLO that neutralises the activity of XIAP.⁴⁷ Bortezomib-induced permeabilisation of the outer mitochondrial membrane might therefore result in reduced activity of XIAP to facilitate the full processing of caspase-3 in response to TRAIL stimulation and induction of apoptosis in HPV⁺ cells.

In contrast to many other HNSCCs, HPV-associated tumours retain wild-type p53 that is inactivated by proteasomal degradation through E6 and AP.³⁵ Restoration of p53 expression following proteasome inhibition or E6 downregulation was shown to trigger cell cycle arrest and apoptosis in HPV⁺ HNSCC cells.^{4,36} In addition, sensitisation of HPV⁺ cervical cancer cells to TRAIL by proteasome inhibition involved upregulation of p53.^{27,48} Induction of p53 after treatment with chemotherapeutic agents can increase TRAIL sensitivity because of the upregulation of death receptors DR4 and DR5.⁴⁹ Although we observed bortezomib-induced stabilisation of p53 in all HPV⁺ cell lines tested, increased levels of p53 following depletion of E6 were insufficient to sensitise cells to TRAIL. Similar results were obtained previously in HPV-associated cervical cancer cells where transient downregulation of E6 did not confer sensitivity to death receptor-mediated apoptosis.⁴⁸ Our data therefore do not support a role for the E6 oncoprotein in causing TRAIL resistance. Additionally, stabilisation of p53 by bortezomib is unlikely to be responsible for sensitisation to TRAIL.

A recent study suggests that TRAIL can exert enhanced cytotoxic activity in cells arrested in G1 or G2 phase.⁵⁰ Here, bortezomib alone induced clear G2/M arrest in all HPV⁺ and HPV⁻ HNSCC cell lines, which might contribute to their increased sensitivity to TRAIL. While these data point to a potential role for bortezomib-mediated cell cycle arrest, the precise mechanism of sensitisation to TRAIL remains to be determined in future studies.



In conclusion, this study shows that the combination of TRAIL and bortezomib efficiently induces apoptosis through both the death receptor and mitochondrial pathway in TRAIL-resistant HPV⁺ HNSCC cells and enhances TRAIL-mediated cell death in HPV⁻ cells. This combination treatment might therefore represent a novel therapeutic option for drug-resistant HPV⁺ head and neck cancers. However, further investigations, including a larger panel of cell lines and *in vivo* studies, are required to warrant future clinical application of these compounds for the treatment of head and neck cancer patients.

Materials and Methods

Cell lines and reagents. Five HPV⁺ and two HPV⁻ cell lines were obtained from various sources and tested for their respective HPV status (Supplementary Table 1). The HPV⁺ cell lines UPCI:SCC089 (089) and UPCI:SCC072 (072), as well as the HPV⁻ cell lines UPCI:SCC090 (090), UPCI:SCC152 (152) and UPCI:SCC154 (154), were a gift from Professor Susanne Gollin, University of Pittsburgh (Pittsburgh, PA, USA). The HPV⁺ cell lines UD-SCC2 (UD2) and VU147-T (147 T) were provided by Professor Henning Bier, University of Munich (München, Germany) and Professor Renske Steenberg, VU University Amsterdam (Amsterdam, The Netherlands), respectively. All UPCI cell lines and UD-SCC2 cells were cultured in MEM with Earle's salts supplemented with 10% FBS, 2 mM L-glutamine, 100 µg/ml gentamicin and 1 × MEM non-essential amino acids. VU147-T cells were cultured in DMEM high glucose supplemented with 10% FBS, 50 µg/ml streptomycin, 100 µg/ml penicillin and 1 mM sodium pyruvate (all cell culture reagents were obtained from PAA Laboratories, Pasching, Austria).

Recombinant human isoleucine zipper trimerised TRAIL was provided by Professor Henning Walczak, University College London (London, UK). The pancaspase inhibitor zVad was purchased from Promega (Southampton, UK), the proteasome inhibitor MG132 from Sigma-Aldrich (Poole, UK) and nec-1 from StressMarq (Victoria, BC, Canada). Bortezomib was obtained through the Guy's Hospital Pharmacy (London, UK).

MTT cell viability assay. Cells were seeded in 96-well plates at a density of 10^4 cells per well and treated with TRAIL and/or bortezomib after 24 h. For inhibitor studies, cells were pre-treated for 1 h with 20 µM zVad and 50 µM nec-1 was included in the treatment. At the indicated times, 20 µl MTT reagent (5 mg/ml; Calbiochem, Watford, UK) was added, followed by incubation for 2–3 h and addition of 150 µl MTT solubilisation solution (50% dimethylformamide, 0.2% glacial acetic acid, 20 mM HCl, 10% SDS). After incubation overnight, the OD₅₅₀ was measured on a LT-4000 microplate reader (Labtech, Uckfield, UK).

Statistical analysis of the results from at least three independent experiments as indicated was performed using GraphPad Prism 6 software (Graphpad Software Inc., La Jolla, CA, USA) and one- or two-way ANOVA as appropriate and specified. Drug synergy was determined using CompuSyn software (ComboSyn Inc., Paramus, NJ, USA) according to the Chou-Talalay method.⁵¹

Western blot analysis. Cells were trypsinised, washed in PBS and resuspended in lysis buffer (2 mM MgCl₂, 25 mM HEPES, 2 mM EGTA, 0.1% Triton X-100) including protease inhibitors. After 30 min incubation on ice, protein lysates were obtained by centrifugation for 15 min at 16 000 × g. Forty to sixty micrograms of protein was used for further immunoblot analysis as described previously.⁵²

Cytosolic fractions were isolated as described previously.⁵³ Briefly, cells of four confluent 15 cm plates were harvested for each condition, cells were washed two times with PBS and resuspended 1:1 in ice-cold lysis buffer (10 mM Tris, pH 7.5, 1 mM EGTA, 200 mM sucrose, plus protease inhibitor cocktail). After 30 min incubation, cells were lysed using a 26 G syringe until ~60% of cells were Trypan blue positive. Several centrifugation steps were performed at 700 to 1200 × g for 5 min at 4 °C to remove intact cells. The supernatant was centrifuged at 16 000 × g for 30 min at 4 °C to obtain the cytosolic/ER fraction of which 100 µg was used for immunoblot analysis.

Antibodies used for immunoblotting were: β-actin, tubulin (Sigma-Aldrich), caspase-3, caspase-9, PARP, Bid, p21 (Cell Signalling, Danvers, MA, USA), caspase-8 (Enzo Life Sciences, Exeter, UK), XIAP (BD Transduction Laboratories, Oxford, UK), cytochrome c (Abcam, Cambridge, UK) and p53 (Novocastra, Leica Biosystems, Milton Keynes, UK). Secondary HRP-coupled anti-rabbit and anti-mouse antibodies were obtained from GE Healthcare (Chalfont St. Giles, UK) and

Sigma-Aldrich, respectively. The relative expression levels of proteins were normalised to β-actin using ImageJ software (NIH, Bethesda, MD, USA).

Flow cytometry. Cells were cultured on 24-well plates at a density of 5×10^4 cells per well and treated with the indicated drugs the next day. Cells were collected at the specific time points by trypsinisation. Apoptosis was quantified by staining with Annexin V-FITC (BD Pharmingen, Oxford, UK) and propidium iodide (PI; Sigma-Aldrich). For cell cycle analysis, cells were fixed in 70% ethanol at -20 °C and stained with DNA staining solution containing PI and RNase A (Sigma-Aldrich) for 30 min. All data were acquired on a BD FACSCanto II cytometer (Beckton-Dickinson, Oxford, UK) and analysed using FlowJo software (Tree Star Inc., Ashland, OR, USA).

For measurement of death receptor expression cells were cultured on 6-well plates at a density of 3×10^5 cells per well and treated with bortezomib the next day. Cells were collected by scraping in PBS and centrifuged for 5 min at 1000 × g and 4 °C. Cell pellets were incubated with primary antibodies HS101 (TRAIL-R1, provided by Professor Henning Walczak, University College London, London, UK) and HS201 (TRAIL-R2) or an isotype control (mouse IgG; Sigma-Aldrich) at a concentration of 10 µg/ml for 30 min on ice. Following washing with ice-cold FACS buffer (4% FBS in PBS), a secondary anti-mouse FITC-coupled antibody (Sigma-Aldrich) was added and cells were incubated for 20 min on ice. Samples were centrifuged for 2 min at 800 × g and the pellet was resuspended in FACS buffer before acquisition of data on a BD FACSCanto II flow cytometer.

Lentiviral shRNA knockdown. Lentiviral vectors were produced in HEK293T cells transfected with the second-generation packaging plasmid pCMVΔ8.91 and plasmid pMDG encoding VSV-G-pseudotyped envelope, as well as the construct of interest by calcium phosphate precipitation. At 24, 36 and 48 h after transfection, viral supernatants were harvested, filtered through a 0.45 µm filter and stored at -70 °C supplemented with 5 µg/ml polybrene. After transduction of target cells with the lentivirus, infected cells were selected in the presence of appropriate antibiotics.

A mixture of five Bid shRNA constructs including a non-silencing control shRNA were kindly provided by Professor Simone Fulda, University Hospital Frankfurt (Frankfurt am Main, Germany) (Supplementary Table 2). The XIAP shRNA as well as LacZ shRNA constructs were obtained from Professor Hamid Kashkar, University of Cologne (Cologne, Germany).⁵⁴ Inducible caspase-8 and respective scrambled shRNA vectors were provided by Professor Pascal Meier, Institute of Cancer Research (London, UK) (Supplementary Table 2). The constructs for E6 and corresponding scrambled control shRNA were purchased from Santa Cruz (Heidelberg, Germany; sc-156008).

Conflict of Interest

The authors declare no conflict of interest.

Acknowledgements. JB is funded by a studentship awarded by the Rosetrees Trust and student support from the Dental Institute, King's College London. NR is funded by Rosetrees Trust. BA is receiving financial support from the Commonwealth Scholarship Commission in the UK. We thank Dr. Silvia von Karstedt, University College London, for many helpful discussions and advice during the course of these studies.

- Jemal A, Bray F, Center MM, Ferlay J, Ward E, Forman D. Global cancer statistics. *CA Cancer J Clin* 2011; 61: 69–90.
- Chaturvedi AK, Engels EA, Pfeiffer RM, Hernandez BY, Xiao W, Kim E et al. Human papillomavirus and rising oropharyngeal cancer incidence in the United States. *J Clin Oncol* 2011; 29: 4294–4301.
- Suh Y, Amelio I, Guerrero Urbano T, Tavassoli M. Clinical update on cancer: molecular oncology of head and neck cancer. *Cell Death Dis* 2014; 5: e1018.
- Rampias T, Sasaki C, Weinberger P, Psyrri A. E6 and e7 gene silencing and transformed phenotype of human papillomavirus 16-positive oropharyngeal cancer cells. *J Natl Cancer Inst* 2009; 101: 412–423.
- Dayyani F, Etzyl CJ, Liu M, Ho CH, Lippman SM, Tsao AS. Meta-analysis of the impact of human papillomavirus (HPV) on cancer risk and overall survival in head and neck squamous cell carcinomas (HNSCC). *Head Neck Oncol* 2010; 2: 15.
- Gupta AK, Lee JH, Wilke WW, Quon H, Smith G, Matly A et al. Radiation response in two HPV-infected head-and-neck cancer cell lines in comparison to a non-HPV-infected cell line and relationship to signaling through AKT. *Int J Radiat Oncol Biol Phys* 2009; 74: 928–933.
- Kimple RJ, Hazari PM. Is radiation dose reduction the right answer for HPV-positive head and neck cancer? *Oral Oncol* 2014; 50: 560–564.
- Falschlehner C, Garten TM, Koschny R, Schaefer U, Walczak H. TRAIL and other TRAIL receptor agonists as novel cancer therapeutics. *Adv Exp Med Biol* 2009; 647: 195–206.

9. Herbst RS, Eckhardt SG, Kurzrock R, Ebbinghaus S, O'Dwyer PJ, Gordon MS et al. Phase I dose-escalation study of recombinant human Apo2L/TRAIL, a dual proapoptotic receptor agonist, in patients with advanced cancer. *J Clin Oncol* 2010; 28: 2839–2846.
10. Younes A, Vose JM, Zelenetz AD, Smith MR, Burris HA, Ansell SM et al. A phase 1b/2 trial of mapatumumab in patients with relapsed/refractory non-Hodgkin's lymphoma. *Br J Cancer* 2010; 103: 1783–1787.
11. Wang S, El-Deiry WS. TRAIL and apoptosis induction by TNF-family death receptors. *Oncogene* 2003; 22: 8628–8633.
12. Juo P, Woo MS, Kuo CJ, Signorelli P, Blemann HP, Hamun YA et al. FADD is required for multiple signaling events downstream of the receptor Fas. *Cell Growth Differ* 1999; 10: 797–804.
13. Li H, Zhu H, Xu CJ, Yuan J. Cleavage of BID by caspase 8 mediates the mitochondrial damage in the Fas pathway of apoptosis. *Cell* 1998; 94: 491–501.
14. Hellwig CT, Rehm M. TRAIL signaling and synergy mechanisms used in TRAIL-based combination therapies. *Mol Cancer Ther* 2012; 11: 3–13.
15. Richardson PG, Mitsiades C, Hideshima T, Anderson KC. Bortezomib: proteasome inhibition as an effective anticancer therapy. *Annu Rev Med* 2006; 57: 33–47.
16. Kubicek GJ, Axelrod RS, Machay M, Ahn PH, Anne PR, Fogh S et al. Phase I trial using the proteasome inhibitor bortezomib and concurrent chemoradiotherapy for head-and-neck malignancies. *Int J Radiat Oncol Biol Phys* 2012; 83: 1192–1197.
17. Van Waas C, Chang AA, Lebowitz PF, Druzgal CH, Chen Z, Elsayed YA et al. Inhibition of nuclear factor-kappaB and target genes during combined therapy with proteasome inhibitor bortezomib and reirradiation in patients with recurrent head-and-neck squamous cell carcinoma. *Int J Radiat Oncol Biol Phys* 2005; 63: 1400–1412.
18. Johnson TR, Stone K, Nikrad M, Yeh T, Zong WX, Thompson CB et al. The proteasome inhibitor PS-341 overcomes TRAIL resistance in Bax and caspase 9-negative or Bcl-xL overexpressing cells. *Oncogene* 2003; 22: 4953–4963.
19. Nikrad M, Johnson T, Puthalath H, Coultas L, Adams J, Kraft AS. The proteasome inhibitor bortezomib sensitizes cells to killing by death receptor ligand TRAIL via Bcl-2 only proteins Bim and Bim. *Mol Cancer Ther* 2005; 4: 443–449.
20. Lashinger LM, Zhu K, Williams SA, Shrader M, Dinney CP, McConkey DJ. Bortezomib abolishes tumor necrosis factor-related apoptosis-inducing ligand resistance via a p21-dependent mechanism in human bladder and prostate cancer cells. *Cancer Res* 2005; 65: 4902–4908.
21. Chen JJ, Chou CW, Chang YF, Chen CC. Proteasome inhibitors enhance TRAIL-induced apoptosis through the intrinsic regulation of DR5: involvement of NF-kappa B and reactive oxygen species-mediated p53 activation. *J Immunol* 2008; 180: 8030–8039.
22. Yoshida S, Wase M, Kuthara S, Uchida M, Kurihara Y, Watanabe H et al. Proteasome inhibitor sensitizes oral squamous cell carcinoma cells to TRAIL-mediated apoptosis. *Oncol Rep* 2011; 25: 645–652.
23. Seki N, Toh U, Sayers TJ, Fujii T, Miyagi M, Akagi Y et al. Bortezomib sensitizes human esophageal squamous cell carcinoma cells to TRAIL-mediated apoptosis via activation of both extrinsic and intrinsic apoptosis pathways. *Mol Cancer Ther* 2010; 9: 1842–1851.
24. Naumann I, Kappler R, von Schweinitz D, Debatin KM, Fulda S. Bortezomib primes neuroblastoma cells for TRAIL-induced apoptosis by linking the death receptor to the mitochondrial pathway. *Clin Cancer Res* 2011; 17: 3204–3218.
25. Unterkircher T, Cristofanon S, Vallanki SH, Nonnenmacher L, Karpel-Masler G, Wirtz CR et al. Bortezomib primes glioblastoma, including glioblastoma stem cells, for TRAIL by increasing Bcl2 stability and mitochondrial apoptosis. *Clin Cancer Res* 2011; 17: 4019–4030.
26. Brooks AD, Jacobsen KM, Li W, Shanker A, Sayers TJ. Bortezomib sensitizes human renal cell carcinomas to TRAIL apoptosis through increased activation of caspase-8 in the death-inducing signaling complex. *Mol Cancer Res* 2010; 8: 729–738.
27. Hougardy BM, Maduro JH, van der Zee AG, de Groot DJ, van den Heuvel FA, de Vries EG et al. Proteasome inhibitor MG132 sensitizes HPV-positive human cervical cancer cells to TRAIL-induced apoptosis. *Int J Cancer* 2006; 118: 1892–1900.
28. Garnett TO, Filippova M, Duerksen-Hughes PJ. Accelerated degradation of FADD and procaspase 8 in cells expressing human papilloma virus 16 E6 impairs TRAIL-mediated apoptosis. *Cell Death Differ* 2006; 13: 1915–1926.
29. de Wilt LH, Kroon J, Jansen G, de Jong S, Peters GJ, Kruijt FA. Bortezomib and TRAIL: a perfect match for apoptotic elimination of tumour cells? *Crit Rev Oncol Hematol* 2013; 85: 363–372.
30. Jouan-Lanhouet S, Arshad MI, Piquet-Pallorce C, Martin-Chouly C, Le Moigne-Muller G, Van Herreweghe F et al. TRAIL induces necroptosis involving RIPK1/RIPK3-dependent PARP-1 activation. *Cell Death Differ* 2012; 19: 2003–2014.
31. van Gurp M, Fesjens N, van Loo G, Saellens X, Vandenabeele P. Mitochondrial intermembrane proteins in cell death. *Biochem Biophys Res Commun* 2003; 304: 487–497.
32. Seol DW. p53-independent up-regulation of a TRAIL receptor DR5 by proteasome inhibitors: a mechanism for proteasome inhibitor-enhanced TRAIL-induced apoptosis. *Biochem Biophys Res Commun* 2011; 416: 222–225.
33. Cummins JM, Kohli M, Rago C, Kinzler KW, Vogelstein B, Burz F. X-linked inhibitor of apoptosis protein (XIAP) is a nonredundant modulator of tumor necrosis factor-related apoptosis-inducing ligand (TRAIL)-mediated apoptosis in human cancer cells. *Cancer Res* 2004; 64: 3006–3008.
34. Gillissen B, Richter A, Richter A, Overkamp T, Essmann F, Hemmati PG et al. Targeted therapy of the XIAP/proteasome pathway overcomes TRAIL-resistance in carcinoma by switching apoptosis signaling to a Bax/Bak-independent type I mode. *Cell Death Dis* 2013; 4: e643.
35. Scheffner M, Werner BA, Hubregtse JM, Levine AJ, Howley PM. The E6 oncoprotein encoded by human papillomavirus types 16 and 18 promotes the degradation of p53. *Cell* 1990; 63: 1129–1136.
36. Li C, Johnson DE. Liberation of functional p53 by proteasome inhibition in human papilloma virus-positive head and neck squamous cell carcinoma cells promotes apoptosis and cell cycle arrest. *Cell Cycle* 2013; 12: 923–934.
37. White JS, Weissfeld JL, Ragin CC, Rossie KM, Martin CL, Shuster M et al. The influence of clinical and demographic risk factors on the establishment of head and neck squamous cell carcinoma cell lines. *Otol Oncol* 2007; 43: 701–712.
38. Waldman T, Kinzler KW, Vogelstein B. P21 is necessary for the p53-mediated G1 arrest in human cancer cells. *Cancer Res* 1995; 55: 5187–5190.
39. Zhang HG, Wang J, Yang X, Hsu HC, Mount JD. Regulation of apoptosis proteins in cancer cells by ubiquitin. *Oncogene* 2004; 23: 2009–2015.
40. Tuthill MH, Montinaro A, Zimgrabe J, Prieske K, Draber P, Prieske S et al. TRAIL-R2-specific antibodies and recombinant TRAIL can synergize to kill cancer cells. *Oncogene* 2014; e-pub ahead of print 9 June 2014; doi:10.1038/onc.2014.156.
41. Gonzalez F, Lawrence D, Yang B, Yee S, Pitt R, Marsters S et al. TRAF2 sets a threshold for intrinsic apoptosis by tagging caspase-8 with a ubiquitin shutoff timer. *Mol Cell* 2012; 48: 888–899.
42. Breitschopf K, Zeiser AM, Dimmeler S. Ubiquitin-mediated degradation of the proapoptotic active form of bcl-2. A functional consequence on apoptosis induction. *J Biol Chem* 2000; 275: 21648–21652.
43. Deveraux QL, Takahashi R, Salvesen GS, Reed JC. X-linked IAP is a direct inhibitor of cell-death proteases. *Nature* 1997; 388: 300–304.
44. Thayaprasingham B, Kunz A, Peters N, Kulms D. Sensitization of melanoma cells to TRAIL by UVB-induced and NF-kappaB-mediated downregulation of XIAP. *Oncogene* 2009; 28: 345–362.
45. van Dijk M, Halpin-McCormick A, Sessler T, Samali A, Szeged E. Resistance to TRAIL in non-transformed cells is due to multiple redundant pathways. *Cell Death Dis* 2013; 4: e702.
46. Menke C, Bin L, Thorburn J, Behbakht K, Ford HL, Thorburn A. Distinct TRAIL resistance mechanisms can be overcome by proteasome inhibition but not generally by synergizing agents. *Cancer Res* 2011; 71: 1883–1892.
47. Du C, Fang M, Li Y, Li L, Wang X, Smac, a mitochondrial protein that promotes cytochrome c-dependent caspase activation by eliminating IAP inhibition. *Cell* 2000; 102: 33–42.
48. Tan S, Hougardy BM, Meersma GJ, Schaap B, de Vries EG, van der Zee AG et al. Human papilloma virus 16 E6 RNA interference enhances cisplatin and death receptor-mediated apoptosis in human cervical carcinoma cells. *Mol Pharmacol* 2012; 81: 701–709.
49. Wu GS, Burns TF, McDonald ER III, Meng RD, Kao G, Muschel R et al. Induction of the TRAIL receptor KILLER/DR5 in p53-dependent apoptosis but not growth arrest. *Oncogene* 1999; 18: 6411–6418.
50. Ehrhardt H, Wachter F, Grunert M, Jeremias I. Cell cycle-arrested tumor cells exhibit increased sensitivity towards TRAIL-induced apoptosis. *Cell Death Dis* 2013; 4: e661.
51. Chou TC, Talalay P. Quantitative analysis of dose-effect relationships: the combined effects of multiple drugs or enzyme inhibitors. *Adv Enzyme Regul* 1984; 22: 27–55.
52. Bullenkamp J, Cole D, Malik F, Akhatabi H, Kulasekararaj A, Odell EW et al. Human Gyrovirus Apoptin shows a similar subcellular distribution pattern and apoptosis induction as the chicken anaemia virus derived VP3/Apoptin. *Cell Death Dis* 2012; 3: e296.
53. Frezza C, Cipolat S, Scorrano L. Organelle isolation: functional mitochondria from mouse liver, muscle and cultured fibroblasts. *Nat Protoc* 2007; 2: 287–295.
54. Kashkar H, Seeger JM, Hombach A, Deggerich A, Yazdanpanah B, Utermohlen O et al. XIAP targeting sensitizes Hodgkin lymphoma cells for cytotoxic T-cell attack. *Blood* 2006; 108: 3434–3440.



Cell Death and Disease is an open-access journal published by **Nature Publishing Group**. This work is licensed under a Creative Commons Attribution 4.0 International Licence. The images or other third party material in this article are included in the article's Creative Commons licence, unless indicated otherwise in the credit line; if the material is not included under the Creative Commons licence, users will need to obtain permission from the licence holder to reproduce the material. To view a copy of this licence, visit <http://creativecommons.org/licenses/by/4.0>

Supplementary Information accompanies this paper on Cell Death and Disease website (<http://www.nature.com/cddis>)